The University of Nottingham

UNITED KINGDOM · CHINA · MALAYSIA

The School of Geographical Science

Self-Adaptive Fire Evacuation by Using Self-Designed 3D Indoor Positioning System

By

Jingjing YAN BSc MSc (Hon)

Thesis submitted to the University of Nottingham for the degree of Doctor of Philosophy

September 2019

ABSTRACT

The efficiency of indoor fire evacuation plays an important role for survival improvement and the development of smart fire evacuation system can help solve this problem. An ideal intelligent indoor fire evacuation system must consider users' physical features and provide a customized evacuation route based on their positions. Meanwhile, it should be able to track the real-time environmental conditions in internal networks in indoor environments. In other words, this type of fire evacuation system should be able to react immediately to the environmental changes in indoor area and provide real-time and valid navigation at any time during movements, avoiding panic/stampede and congestions in exits. This kind of system will be of great importance in future application for human safety. It requires the guidance service to be able to provide current user locations and provide a nearest available exit based on this information, integrated with fire expansion information. It is highly possible under the quick development with the improvement of indoor positioning technologies. The research presented in this thesis has developed a novel 3D positioning system in order to provide solutions for user localization and navigation during fire evacuation and the effect with and without support of navigation will be assessed based on the results of simulation.

This study will first provide a review of popular indoor positioning technologies and select possible techniques based on the demands of flexible localizations with satisfied accuracy and low cost with few infrastructures. Pedestrian Dead Reckoning (PDR) and visual tracking are then selected as promising candidates to be combined for 2D positioning and tracking. The applications of the corresponding algorithms for the selected positioning technologies have been chosen based on the comparison of the accuracy and the easiness of operations in the review as well. It will then provide a self-designed system with the integrations of the above selected techniques for horizontal positioning of each floor, within the testing environment located inside a four-floor building of University of Nottingham Ningbo China (UNNC). This 2D passive vision-aided PDR positioning system proposed by this study can achieve an average positioning accuracy of 0.08m on a single floor with less impact of occlusion, which is higher than the systems using similar sensors

while using a simpler algorithm, fewer sensors and quicker computation. It has also been tested under the situation with severe occlusions in the selected building. Its accuracy (0.16m) is still comparable to the other studies with less occlusion, which has shown the reliability and stability of the performances for the algorithms while still keeping the advantages of fewer sensor requirement (low-cost) and better sensor accessibility (user-friendly). The system is then further developed into a 3D version with the ability for floor identification by using a smartphone-based barometer. It also achieved a comparable accuracy of height estimation (0.5m) to other studies using the barometers while using fewer sensor and simpler computation. The accuracy of the floor detection is around 98%. The above achieved accuracy in both horizontal and vertical directions are better than the required accuracy targeted by several emergency services, including the Federal Communications Commission (FCC). The above designed tracking system as well as the applied algorithms for sub-systems is the major theoretical contribution of this research.

The system can also be applied for speed and inter-personal distance measurement, when tracking the movement of the pedestrians. These measured parameters can be applied into the simulation of the indoor fire evacuation process with the support from the smartphone-based navigation system by using a social-force based agent-based model, with the integration of a simplified fire expansion model. Moreover, the PDR based action recognition can also provide good support for posture recognition and localization reporting of people for later rescue. With the establishment of the simulation model, this study is able to discover the bottlenecks inside the selected building under normal conditions. Moreover, it is able to compare the efficiency of two evacuation strategies, i.e. nearest exits and random walking. These two strategies can represent the indoor evacuation with and without the support of the navigation system. According to the results, the evacuation with the support of navigation system (nearest exits) is more efficient with higher survival rate, shorter average evacuation time, and shorter average evacuation distance. With the above experiments and simulations, this study has achieved an initial success of developing an indoor evacuation navigation system, with promising results.

RESEARCH OUTPUTS

The following peer reviewed publications are the research outputs linked to the investigation process of this thesis, which mainly focus on the development of the indoor positioning system with the combination of the PDR and visual tracking.

Journal Paper

YAN, J., HE, G., BASIRI, A. & HANCOCK, C. 2019. 3D Passive-Vision-Aided Pedestrian Dead Reckoning for Indoor Positioning. *IEEE Trans. on Instrumentation and Measurement*, 1370-1386.

Conference Papers

YANG, Y., HANCOCK, C., KAPOGIANNIS, G., JIN, R., DE LIGT, H., **YAN, J.**, CHEN, C. & LI, C. Integrating Indoor Positioning Techniques with Mobile Laser Scanner to Create Indoor Laser Scanning Models. FIG Congress, 2019. Hanoi, Vietnam.

YAN, J., HE, G., BASIRI, A. & HANCOCK, C. Vision-aided indoor pedestrian dead reckoning. IEEE International Instrumentation & Measurement Technology Conference, 2018. Houston, USA. IEEE, 1-6.

CHEN, C., TANG, L., HANCOCK, C. M., **YAN, J.**, DE LIGT, H. & ZHANG, P. 2D-based indoor mobile laser scanning for construction digital mapping application. FIG Congress, May 6-11, 2018. Istanbul, Turkey.

YAN, J., HE, G., BASIRI, A. & HANCOCK, C. Indoor pedestrian dead reckoning calibration by visual tracking and map information. Ubiquitous Positioning, Indoor Navigation and Location-Based Services (UPINLBS), 2018. IEEE, 40-49.

YAN, J., HE, G. & HANCOCK, C. Low-cost vision-based positioning system. Adjunct Proceedings of the 14th International Conference on Location Based Services, 2018. ETH Zurich, 44-49.

YAN, J., HE, G. & HANCOCK, C. Vision-aided indoor pedestrian tracking system. Proceedings of International Conference on Indoor Positioning and Indoor Navigation (IPIN), 2017, Sapporo, Japan.

ACKNOWLEDGEMENTS

Firstly, I would like to thank my supervisors, Dr Gengen He and Dr Anahid Basiri for their wisdom, patience and guidance during my entire PhD study. They have provided many meaningful feedback to my work as well as various opportunities for me to freely explore my own interests during my research. I have also been encouraged to enter different research conferences and communicate with other researchers in the similar fields with inspirations for my own work. I have enjoyed the entire process of this journey to the final achievement of PhD with their generous support.

I would like to thank the Head of Civil Engineering, Dr Craig Hancock, who has provided his expertise of helping me through some of the barriers of pedestrian dead reckoning.

I would like to thank the Head of the Geographical Science, Dr Odette Paramor, who has also helped me through various problems during my PhD life besides the academic research.

Special thanks to my colleague Fei Yang, who has helped me with the experiments of video recording and processing for deep learning based pedestrian detection from the videos.

I would like to appreciate the financial support from the International Doctoral Innovation Centre, Ningbo Education Bureau, Ningbo Science and Technology Bureau, and the University of Nottingham. This work was also supported by the UK Engineering and Physical Sciences Re-search Council [grant number EP/L015463/1].

CONTENTS

LIST OF FIGURES

LIST OF ABBREVIATIONS

Abbreviations	Full Name
ABM	Agent-Based Model
APE	Absolute Positioning Error
ASET	Available Safe Egress Time
AVINS	Active Vision-aided Inertial Sensing System
BB	Bounding Box
BLE	Bluetooth with Low Energy
CA	Cellular Automata
CCD	Charged Couple Device
CDF	Cumulative Distribution Function
CFD	Computational Fluid Dynamics
CNN	Convolutional Neutral Network
FC Layer	Fully-Connected Layer
FCC	Federal Communications Commission
FDS	Fire Dynamics Simulation
GAN	Generative Adversarial Network
GIS	Geographic Information system
GNSS	Global Navigation Satellite System
GNM	Geometric Network Model
IBC	International Building Code
ID	Inter-person Distance
IMU	Inertial Measurement Unit
INS	Inertial Navigation System
IR	Infrared
LBS	Location-Based Service
LoS	Line-of-Sight
MAE	Mean Average Error
MEMS	Micro Electro-Mechanical Systems
NFC	Near Field Communication
NFPA	National Fire Protection Association
OPS	Optical Positioning System

Abbreviations	Full Name
OSHA	Occupational Safety and Health Administration
PDR	Pedestrian Dead Reckoning
PMB	Sir Peters Mansfield Building
PVINS	Passive Vision-aided Inertial Sensing System
QR-Code	Quick-Response Barcode
R-CNN	Region-Based-Convolutional Neural Network
RF	Radio Frequency
RFID	Radio Frequency Identification Services
RMSE	Root-Mean Square Error
ROI	Region of Interest
RP	Region Proposals
RPE	Relative Positioning Error
RPN	Region Proposal-based Network
RSET	Required Safe Egress Time
RSS	Received Signal Strength
SF	Social Force
SPM	Spatial Pyramid Matching
SPP-net	Spatial Pyramid Pooling Network
SS	Selective Search
SVM	Support Vector Machine
SW	Stoop Walking
TKSW	Trunk-and-Knee-flexion Stoop Walking
TSW	Trunk-flexion-only Stoop Walking
ToA	Time of Arrival
ToF	Time-of-Flight
UNNC	University of Nottingham Ningbo China
UW	Upright Walking
UWB	Ultra-Wide Band
VINS	Vision-aided Inertial System
VOS	Visual-Optical Spectrum
WLAN	Wireless Local Area Network

Chapter 1. INTRODUCTION

1.1. BACKGROUND

Fire safety is always an important social topic and the efficiency for evacuation is of great interest in future research to improve the percentage of survival. Fire has been and always will be a significant threat to life and property and psychological well-being, thus it is an important part of the human society and livelihood in terms of planning, construction, response and mitigation. According to the data of 2015 provided by Fire Service Bureau in China, there were 346701 incidents of fire event being reported, which causes more than 1899 deaths, 1213 injuries and 4358.95 million RMB in estimated damages. Fire occurring in indoor area especially at residential area is most common with 113871 reported events, contributing to 32.84% of all fire incidents and leading to 1319 deaths (69.46% of all), 637 injuries (52.51% of all) and 664.86 million RMB in estimated loss (15.25% of all) (Fire-Service-Bureau, 2017). In order to limit the loss of life and property during fire, many policies had been applied such as firefighting by fire brigade, insurance, regulations for building establishment, fire evacuation education, indoor material and product usage controlling, and building design (Xin and Huang, 2013).

Fire results from a complex chain of chemical reactions, where a flammable material (fuel) mixes with oxygen in air and is subsequently oxidized in an exothermic process. When encountering the flammable materials under high temperature, an ignition will appear, and a fire will be initialized (Artim, 1999, Thompson, 2016). The persistence of a fire event is affected by multiple indoor system factors: building and its functions, building material construction and contents, fire initial ignition, fire growth, smoke expansion, the response from fire department, or evacuation behaviours by human (Purser and Bensilum, 2001, Yung and Benichou, 2003). The risk of a fire event can be analysed in three fire aspects, which are the environment for fire event, fire automatic repression and human behaviours (Xin and Huang, 2013). Since the beginning of 20th century, the building evacuation studies have focused on learning about human movements in building connection parts such as corridors, stairs and doors (Bryan, 2002b, O Connor, 2005, Kobes et al., 2010a) and figuring out technological solutions concentrated on architectural design (Kobes et al., 2010a, Kuligowski, 2016). Until the end of 20th century, the research focus has started shifting to human behaviour aspect. An ORST (Occupant Response Shelter Escape Time) model was introduced as a theoretical method to describe how people respond in fire evacuation with different attributes located in different positions in indoor area. It also implies that the availability of facilities will affect the evacuation as well, which is depended on fire characteristics (fire location, fire range and smoke expansion) and building characteristics (e.g. conditions of facilities) (Sime, 1999, Sime, 2001, Kobes et al., 2010a, Tang and Ren, 2012, Atila et al., 2013). In addition, the human responses at the individual level also vary with changing environment (Gwynne et al., 2001, Kobes et al., 2010b).

The change of environmental factors is mainly determined by the specific situation of fire event, which can be divided into several stages, depending on whether there is new intake of oxygen (Fig.1.1a) (Artim, 1999, Thompson, 2016). This study is more interested in the period before early decay without further introduction from new-coming air caused by the entry of firefighters. The fire expansion during this period follows a near-linearly growing pattern which is relatively easily to be simulated in a temporal-spatial approach, and it will be later described in Chapter 5. The other reason of focusing on this period is because in this phase, the evacuation of the occupants inside the building is more self-dependent without the help from the fire department (Purser and Bensilum, 2001, Pires, 2005, Kobes et al., 2010a). This has raised the importance of the study of human behaviours during this period, in terms of survival. The study of human behaviour during this specific stage can help understand human responses under fire emergencies, improve the safety design of buildings, and increase the efficiency, communication systems, as well as pre-event training for evacuation (Kuligowski, 2016).

The human response/indoor evacuation can be roughly divided into three main periods: pre-alarm, pre-evacuation and movement/evacuation period (Fig.1.1b) (Purser and Bensilum, 2001, Ronchi and Nilsson, 2013, Kinateder et al., 2014, Kuligowski, 2016). The pre-alarm phase lasts from the ignition of fire to the initiation of alarm and/or the indoor occupants realize the cues of fire event (Purser and Bensilum, 2001, Kuligowski, 2016). The fire characteristics is very dependent on the specific stage of fire development. The period selected by this study includes the ignition and growing before early decay. The incipient/ignition stage is when the fuel contacts the fuel source. The fire during this period grows slowly and organically, which varies from some minutes to several hours depending on the inflammable material properties, fire positions, building structures and amount of available oxygen. Smoke also develops during this phase from light to moderate level. In order to the study the mechanism of the fire expansion affected by multiple environmental factors in reality and validate the simulation model, some of the previous studies have tried to do some empirical studies of the fire expansion by setting up a mock-up experiment with the same scale of the pre-recorded fire event (Grosshandler et al., 2005, Bryner et al., 2007, Galea et al., 2008). However, the setup of a fire in reality is of high risk and requires high professional expertise to control, making it a non-ideal option to experimentally test the expansion of fire. The utilization of the experimental data from previous studies within a simulated computational model is rather more feasible and this approach is deployed in this study.

During the growth period of fire, the human behaviours include the pre-evacuation phase and movement phase. The pre-evacuation period starts after the initiation of ignition until people starts evacuation movements while the movement period estimates the time during current location to safety (Purser and Bensilum, 2001, Kuligowski et al., 2010, Kinateder et al., 2014, Kuligowski, 2016). In addition, the pre-evacuation period can be further divided into two phases as risk perception/evacuation decision phase and protective action initialization phase (Purser and Bensilum, 2001, Pires, 2005, Kobes et al., 2010b, Ronchi and Nilsson, 2013, Kinateder et al., 2014, Kuligowski, 2016).

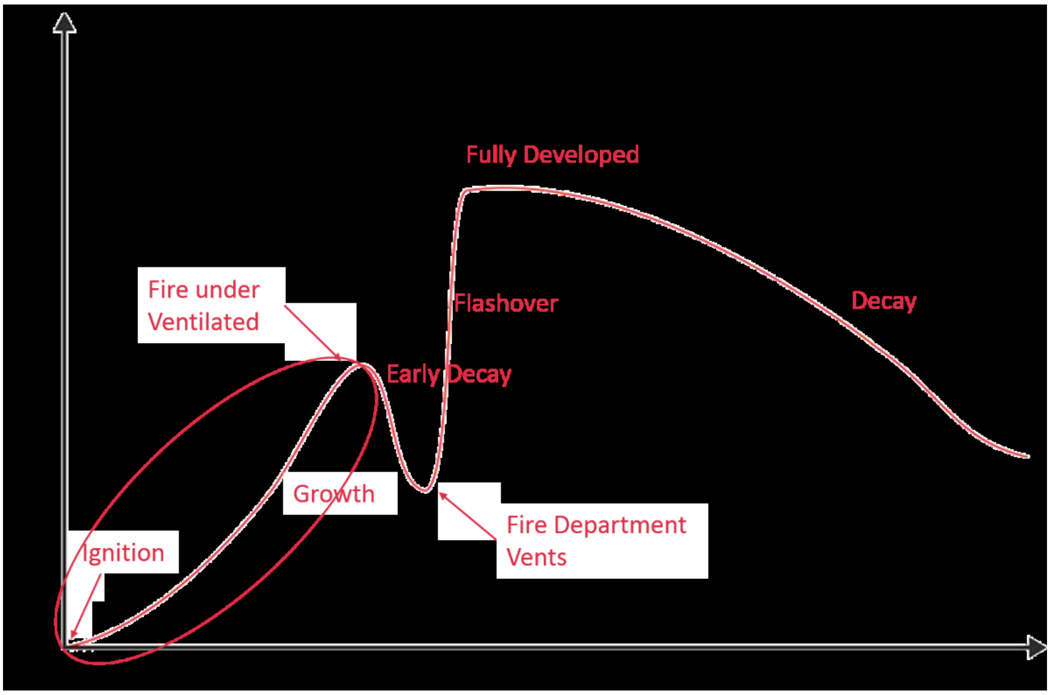

(a)

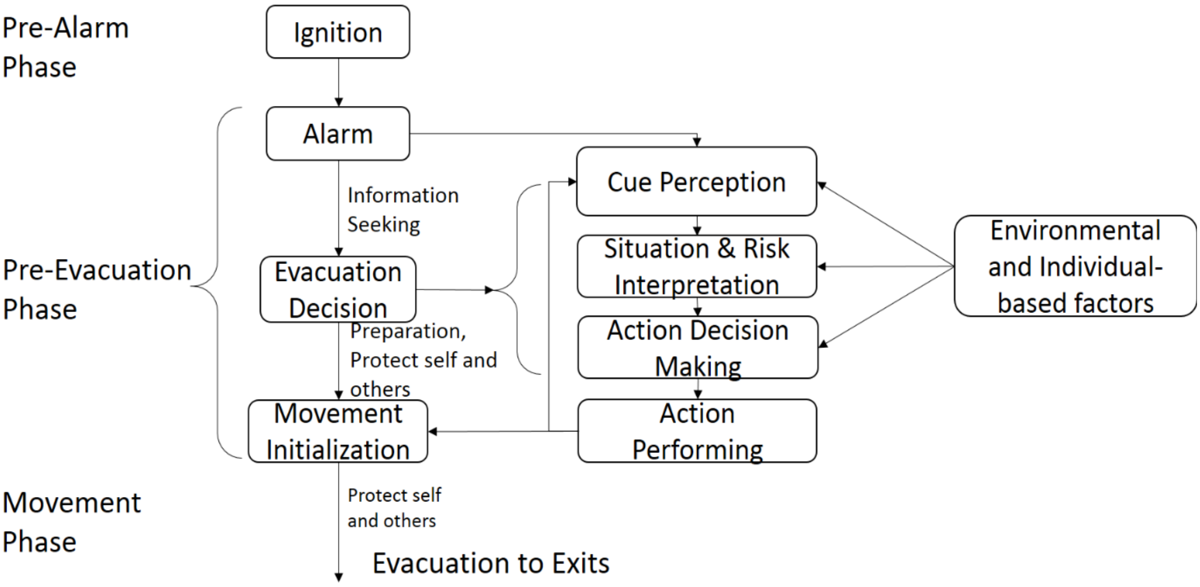

(b)

Fig.1.1. The development of the fire (a) and the overall process for indoor evacuation including three main phases: pre-alarm, pre-evacuation, and movement periods with sub phases (b) (Artim, 1999, Purser and Bensilum, 2001, Pires, 2005, Josh, 2010, Kobes et al., 2010b, Ronchi and Nilsson, 2013, Kinateder et al., 2014, Kuligowski, 2016, Thompson, 2016).

As people's behaviours/actions are performed based on the decision making process instead of random choice or a stimulated response to the environmental change during indoor fire emergencies (Kuligowski, 2009), a decision making phase first appears following pre-alarm phase before taking any actions (Kuligowski, 2009, Kinateder et al., 2014, Kuligowski, 2016). Previous researches have shown that the behavioural process of human responses during decision making phase starts from perception of certain cues of fire for later interpretation of facing situations and risks, and finally to decision making of actions before the beginning of protective actions (Purser and Bensilum, 2001, Bryan, 2002a, Kuligowski, 2009, Kuligowski, 2016). The decision making process is potentially depended on the risk perception by human and can also be affected by multiple factors such as the building functions, the components of egress facilities, and the strategies of evacuation (Kuligowski, 2009, Ronchi and Nilsson, 2013). The protective actions are supposed to be collecting personal belongings, alerting others for evacuation preparation, shutting down machinery, and other actions allowing for self and other protection (Purser and Bensilum, 2001, Kuligowski, 2016). The time it takes to arrive at a decision correlates with the higher rate of deaths and injuries during the fire event, especially in residential and hotel buildings (Purser and Bensilum, 2001), making this period more influential on survival than the movement period (Proulx, 2001, Bryan, 2002b, Kobes et al., 2010b). This study focuses on both phases and simulated in a non-fire setting way such scenarios in a selected building at UNNC. This study also includes a survey of the students who daily study and move inside this building and collect their answers about their pre-evacuation responses. From their responses, this research is able to classify various behaviours and validly estimate the pre-evacuation period of people.

During evacuation/movement phase, the first priority of indoor evacuation will be evacuation acceleration as humans under fire emergency situation will act in panic, leading to congestion and confluence at exits and stairs, or other drastic behaviours such as crushing and trampling (Hajibabai et al., 2007, He et al., 2013, Mohan et al., 2016). Meanwhile, decision making during the movement of people under a fire event is also time consuming by floor plan discovery and escape route formulation. These two factors can both cause the loss of lives (Kuligowski, 2016, Mohan et al., 2016). A intelligent fire evacuation system should cut down the time of decision making by monitoring the status of building and provide safest evacuation plan by using automatic fire perception and route prediction based on location positioning system (Mohan et al., 2016).

The understanding of the indoor evacuation process will help to establish the egress model to estimate the evacuation time for evacuation, which is an efficient way for life safety level evaluation (Kuligowski, 2009, Kuligowski et al., 2010, Kuligowski, 2016), and reduce the experiment expense under different situations (Pelechano and Malkawi, 2008, Guo, 2010, Tang and Ren, 2012). With the established egress model, the Available/Required Safe Egress Time (ASET/RSET), which is the required time for indoor evacuation, can be then determined (Purser and Bensilum, 2001, Proulx, 2008, Kuligowski, 2009). They are also depend on various features of process for occupant evacuation, such as fire detection, alert notification, occupant response to alert in pre-evacuation period, the profile of occupants (e.g. age, physical and intelligent ability, awake state and crowd density), decision based pre-evacuation behaviours (e.g. information seeking, personal belongings collection, exit choosing and other protective activities), evacuation movements (e.g. pathfinding, moving to an exit and crowd flow), evacuation route design, exit numbers and width, as well as the heat and smoke exposure impacts on psychological and physical aspects during evacuation (Purser and Bensilum, 2001, Tang and Ren, 2012, Ortakci et al., 2016). This study will apply an Agent-Based Model (ABM) to help investigate the evacuation process of pedestrian movements inside the selected building, with the calculation of ASET/RSET.

To provide the information which is required for ASET/RSET calculation and evacuation simulation (e.g. pedestrian speed and inter-person distance), the development of a low-cost, highly available, intuitive and user friendly smart tracking system can provide a suitable solution. It is also helpful in the real localization of the users inside the building for future applications. <u>This study will investigate whether the integration of the smartphone-based Pedestrian Dead Reckoning (PDR), visual tracking and height estimation can provide a relatively satisfactory solution of 3D localization for navigation services to support fire evacuation, with the considerations of cost, accessibility, and</u>

accuracy. It is also the central focus of this research, which is regarded as the major theoretical contribution of this study as the developed novel system can accurately track pedestrians' locations and identify walking postures during evacuation for risk assessment and provide visible indoor spatial information to the occupants. With the above achieved functions by the developed indoor 3D tracking system, it is also interested in whether the application of such system can help to improve the efficiency of fire evacuation, by comparing the simulation results of two strategies with and without the support of this system based on the selected parameters, e.g. survival rate, evacuation time and evacuation distance. In future, the established system is not only for evacuation purposes but also for the building management and other applications related with location-based services.

1.2. Motivations and Objectives of the Study

1.2.1. Motivations

1.2.1.1. The Requirement of A Self-Designed Indoor Positioning System

In Section 1.1, it has indicated the physical reason of focusing on the period before the involvement of firefighters during fire development. This period can be easily simulated by a temporal-spatial model for evacuation survival analysis, as there is no new supplement of air, with less introduction of variations of the fire expansion process. Meanwhile, it is also the period when the firefighters have not arrived at the scene, and all the occupants should try to evacuate in the shortest time to the outside for survival based on individual mobility and decision making (Purser and Bensilum, 2001, Pires, 2005, Kobes et al., 2010a), regardless the degree of familiarity to the indoor environment. Therefore, the tracking of the occupants' physical locations is relatively important, regardless before and after the initialization of the rescue (Kobes et al., 2010b, Sha et al., 2006). Before the involvement of firefighters, the user positions are correlated with the navigation service which is very location-based, while during the rescue process, the realization of the user positions can assist the localization of potential victims. The application of indoor location positioning systems can help detect the positions of people in a large indoor area with complicated internal structure and lead them to the nearest safe exits by using technologies such as Wi-Fi network, Bluetooth beacons, LED lights, magnetic fields and UWB (Ultra-Wide Band) (Mohan et al., 2016), in order to avoid the psychological stresses caused by confusion. However, the understanding of the impacts from the user locations is still very limited, and this study only focuses on whether indoor navigation will improve efficiency of the fire evacuation. This has raised the importance of providing a supportive method of guiding the user to the outside, especially within an unfamiliar indoor environment.

The feedback of having this LBS-based navigation support during fire evacuation from both the rescue departments and occupants themselves has also been considered during the formation of this research. According to the previous official reports from Fire Service Bureau in China (Fire-Service-Bureau, 2017), it has encouraged a more efficient way of individual evacuations before the arrival of fire brigades and insisted on the importance of daily training of fire drills, which aims to reduce the overall evacuation time and to improve the survival rate. Meanwhile, they are interested in having the constantly accessible position information of evacuees (Rantakokko et al., 2007, Rantakokko et al., 2010) if they are still inside the building after the arrival of fire brigades, in order to improve the efficiency of rescue and reduce the risks for firefighters by having a shorter stay in the fire scene (Sha et al., 2006). The occupants' attitude of having navigation services during the evacuation process is also of great importance as they are direct users and beneficiaries. Before this research, a general survey question about the willingness to have guidance service for evacuation assistance has been conducted among the students and staffs of different departments inside the UNNC, and the responses from the majority are positive. With the above positive attitudes from both fire department and occupants, this research has raised the interest of establishing an intelligent navigation system to assist the evacuation process.

According to previous studies, an effective intelligent fire emergency simulation system should ideally satisfy six requirements (Cutter, 2003, Zlatanova and Holweg, 2004):

a) Representation of physical and human process in dynamic and multi-

dimensions;

b) *Update of spatial data collection and information integration for users;*
c) *Interoperation between integrated data from multiple sources and semantic/data discovery with the support of CAD models or 3D* Geographic Information system (*GIS);*
d) *Integration of dynamic geospatial data and spatial-temporal data analysis and modelling for planning and decision making;*
e) *Instant provision of updated information to users via mobile and wireless communications;*
f) *3D visualization on multiple equipment.*

Meanwhile, it also requires several critical functions such as 3D geo-location positioning, analysis of network connectivity, occupant flow, 3D topology, and indoor navigation (Miller and Shaw, 2001, Lee and Zlatanova, 2008). The 3D location is provided by location-aware devices to identify location information of site of disaster (e.g. fire scene), occupants, area of congestion, and isolated zones in indoor area, which requires the integration with sensor networks (Jensen et al., 2009). The analysis of network connectivity will be applied to identify isolated networks or zones blocked by congestion or fire without any exit node connecting to the destination node. The occupant flow analysis is also regarded as evacuation model to update movements of occupant and impedances of flow by estimation of flow rate and dynamic capacities of corridors and staircases. The 3D topology, which is usually represented by 3D GNM for internal building structures (Lee, 2004b), is used to figure out the locations of congestions in network. The navigation function will then seek feasible routes without dangers in multi-layer format and provide the navigation guidance to the users (Lee and Zlatanova, 2008).

The application of GIS can help integrate the sub modules of fire evacuation system as well as effectively managing and integrating spatial data of 3D topological and geometric features of internal building structure (Lee, 2007, Tang and Ren, 2012, Atila et al., 2013). This can help to provide a comprehensive description of indoor fire features and support intelligent decision making to guide the user to safety (Tang and Ren, 2012, Atila et al., 2013). The previous study of GIERS (GIS-based Intelligent Emergency

Response Systems) pointed out that the 3D GIS had the potential to improve the speed of emergency response in multi-level structures in urban space. By representing the internal multi-layer building with 3D GIS extended from conventional 2D GIS, the overall speed of rescue operations can be significantly improved (Kwan and Lee, 2005, Lee, 2007, Lee and Zlatanova, 2008). As the response for decision making is time critical (Lee and Zlatanova, 2008) and the uncertainty of indoor route can lead to the longer response delay (Kwan and Lee, 2005), the above discovery has motivated the development of intelligent emergency systems (i.e. Intelligent Building Evacuation system-IBE system) in complex indoor area with the application of 3D GIS integrated with Intelligent Transportation System (Meijers et al., 2005). A hybrid data model will be consisted of a 3D geometric model, a graph model and a 3D city model. The 3D geometric model represents the 3D solid features of 3D polygonal faces in an enclosed boundary, the 3D graph model is used to represent the topological relationships among these solid features, and the 3D city models support 3D visualization of the information in real view (Lee, 2007, Lee and Zlatanova, 2008). This study adopts this idea during the development of an indoor positioning system, and it assigns the 3D geographical information to its acquired positioning results. Meanwhile, it conducts the simulation in a 3D GIS-based indoor environment and enables the 3D visualization during the application.

Moreover, there are many other factors requiring considerations during the design of the positioning system, which can improve the robustness and accessibility of the system:

1) As the designed system will be applied to the fire scene for the growth stage, it is supposed to be highly tolerated to the harsh environmental conditions (e.g. high temperature and humidity).
2) The tracking gear should not rely on bulky antennas with exposed cables, and its weight should not be over 1kg.
3) The energy efficiency of system utilization should also be considered, and it should be able to work properly more 24 hours.
4) The representation of the positioning results should be easily understood by the evacuees during the evacuation process.

5) In order to improve the flexibility of the operations, there should be no requirement for pre-installations of the system in the environment.
6) Moreover, the cost of the system should also be at a low level, in order to achieve wider market.
7) The integration of other data, such as the monitoring of physiological status should also be considered, in order to have a more thorough assessment of the current status of occupants (Rantakokko et al., 2007, Rantakokko et al., 2010).

This study has also considered these factors during the selection of candidates for the positioning technologies and the design of the algorithm for data utilization. It also has involved posture recognition, in order to check the physiological status of people, which is considered as a threatening risk of fall (Campbell, 2013, Ferraz and Saba, 2017) and requires higher energy consumption for movement (Morrissey et al., 1985, Davis, 2011a, Grasso et al., 2000, Cao et al., 2014, Hora and Sladek, 2014, Kluger et al., 2014, Cao et al., 2018).

1.2.1.2. The Requirement of An ABM-Based Simulation

The conduction of a real navigation-supported fire drill is also of great risk and high cost (Fahy, 2005, Jain and Mclean, 2008, Kady and Davis, 2009a). Thus, this research decides to have experiments only on the positioning but doing simulations on fire evacuations. According to the previous studies, the current evacuation approaches, which can be divided into two types as crowd movement simulation models and 3D network models, are not sufficient with corresponding disadvantages (Jun and Kim, 2009, Vanclooster et al., 2010). The crowd movement simulation models are developed for emergency situation prediction and building interior planning design safety evaluations (Vanclooster et al., 2010, Atila et al., 2013). For evacuation aspect, the modification of model simulators is very common in for protection provision such as fire safety ranking (Zhao et al., 2004). Typical examples are agent-based models (Hajibabai et al., 2007) and cellular automata (CA) models (Park et al., 2007, Jun and Kim, 2009). They are more concentrated on the user related factors and behaviours with the consideration of individuality and occupant profile but lack of crowd interaction (Pelechano and Malkawi, 2008) and comprehensive semantic spatial data, leading to complicated and unclear calculations which will make the reality modelling uncertain and difficult (Vanclooster et al., 2010, Atila et al., 2013). According to the review of 26 egress models by NIST, the limitations of these models are the lacking of available actual evacuation database (Kuligowski et al., 2010, Averill, 2011). This study will apply the measured parameters into the simulation model based on the survey and experimental data collected by a self-designed 3D indoor positioning system, in order to improve the reality of the model.

The other popular class is network modelling based approach, which divides the indoor area into nodes and arcs to represent the egress components and the linkage between different components separately (Kuligowski et al., 2005, CFPA, 2009, Kuligowski et al., 2010). It mainly focuses on modifying Dijkstra's 2D shortest routing algorithm to 3D with weights from distance or time (Lee, 2001, Karas et al., 2006, Musliman et al., 2008, Vanclooster et al., 2010, Atila et al., 2013), based on using a graph network model (Gilliéron et al., 2004, Karas et al., 2006, Jun et al., 2009) and achieving 3D visualization by CityGML (Kolbe, 2009). Common options of networks used for research are "Node Relation Structures (NRS), Geometric Network Model (GNM), and coarse networks" (Lee, 2001, 2007, Kuligowski et al., 2010). However, other impedance factors, especially from human aspect for emergency situations, are still lacking approaches to integrate them into routing process (Pu and Zlatanova, 2005), and it is more focused on distance calculation of paths (Meijers et al., 2005, Lee, 2007, Lee and Zlatanova, 2008). In order to solve this problem, this study applies a hybrid ABM with the integration of the Social-Force (SF) model, which can better describe the human factors in the simulation, as these two methods are previously inadequate for route planning due to the missing of real connection to the real world (Jun and Kim, 2009, Vanclooster et al., 2010). Besides, there are multiple questions should be determined initially, e.g. usage domain of algorithm (for evacuation response or for risk management), user number (one route for many users or various routes for one user) and types as well as their related behaviours (Vanclooster et al., 2010). This study tries to provide a more comprehensive solution with the considerations of these factors, during the establishment of an ABM-based evacuation model.

Moreover, there is no complete assessment of how indoor positioning technologies can be applied to help improve the efficiency of indoor fire evacuation (Niu, 2014, Sime, 2001, Kobes et al., 2010b). The previous studies usually provide a conceptive design of integrating different positioning technologies together and the way of how they are supposed to work during the evacuation process (Inoue et al., 2008, Chittaro and Nadalutti, 2008, Chittaro and Nadalutti, 2009, Szwedko et al., 2009, Chu, 2010). This study attempts to provide a more comprehensive solution to this problem. It first develops a low-cost, accessible and relatively accurate indoor positioning system. Then, it utilizes the measured parameters based on the application of this system for evacuation simulation under different evacuation strategies with and without navigation guidance, in order to provide a relatively realistic assessment of efficiency improvement. Meanwhile, as human behaviours based on decision making process also play an important role in indoor fire evacuation, it is also necessary to monitor humans' actions during movement period while tracking their trajectories. The action recognition here in this study refers more specifically to human posture recognition during their movement and the interested postures are roughly divided into three groups as up-straight walking, and stoop walking with and without the flexion of the knee. The reason of focusing on these specific postures will be further explained in Chapter 5. In a long term, the applications of simulation results from collected user data with the assistance of the positioning system in the indoor environment can help architects and urban planners to identify possible bottlenecks in buildings and improve future structure design. It can also help emergency managers, e.g. university marshal, to compare different evacuation strategies during evacuations (Bakar et al., 2017, Mahmood et al., 2017, Trivedi and Rao, 2018).

Moreover, the pathfinding also requires multiple spatial and cognitive capabilities based on occupants' perception and prior knowledge, e.g., indoor familiarity, psychological stress (Graham and Roberts, 2000, O Connor, 2005, Kobes et al., 2010b, Kobes et al., 2010a) and user attitudes to the navigation support. These factors are also worth of considerations during the fire evacuation simulation. However, they are not able to be integrated into the ABM-based simulation in this study and thus are individually discussed for future improvements.

1.2.2. Aims and Objectives

This study aims to investigate whether the application of a self-developed intelligent indoor navigation system with acceptable positioning accuracy can help to improve the efficiency of an indoor fire evacuation process, based on the results of ABM-based simulation. It focuses on the period before the arrival of firefighters, during which the evacuation movements are entirely dependent on self-decision and mobility (Purser and Bensilum, 2001, Pires, 2005, Sha et al., 2006, Kobes et al., 2010a). The hypothesis of this study is that the evacuation process aided by navigation is more efficient than the evacuation process without navigation assistance.

The accuracy of provided occupant locations, especially for the real-time positions, is of great importance to the fire scene for emergency management, enabling a reliable real-time monitoring. Meanwhile, the route planning also requires accurate occupant locations (Sha et al., 2006, Rantakokko et al., 2007, Rantakokko et al., 2010, Deng et al., 2013, Li et al., 2014). According to FCC, the required accuracy for the fire emergency is 50m in horizontal direction and 3m at vertical direction (FCC, 2015). The current best positioning accuracy achieved by the Commercial Mobile Radio Service (CRMS) reported in FCC was 5~10 m (FCC, 2015). Other studies have proposed more stringent standards to fit the requirements of the firefighters, i.e. 1m for horizontal accuracy of room identification and 2m for vertical accuracy of floor differentiation (Rantakokko et al., 2007, Rantakokko et al., 2010). In order to provide a more accurate solution of user locations, which can both benefit the effectiveness of route planning for the occupants and the efficiency of victim identification by the fire brigades, the accuracy is required to be at a relatively high level. Therefore, this study aims to provide a 3D positioning system to satisfy the higher proposed standards for fire evacuation scenario. The system should also be able to provide automatic estimations of uncertainty with the detected positions.

To achieve this goal, the entire project is divided into four parts as:

1) The development of a novel 3D indoor positioning system, which enables constant indoor pedestrian tracking with low cost, high accessibility and relatively high accuracy;
2) The recognition of different walking posture based on the processing of the collected data from the designed 3D indoor tracking system;
3) The establishment of an ABM-based fire evacuation model based on data collected by the 3D indoor tracking system, whose results can be used for evacuation efficiency comparison;
4) The investigation of potential cognition factors, which can also have effects on the evacuation process but have not been applied into the ABM-based fire evacuation model.

1.2.2.1. Design of A 3D Indoor Positioning System

To design a 3D indoor positioning system achieving the above requirements, a few objectives are required to be realized in the following order:

1) Selection of suitable positioning methods from the current indoor positioning technologies which can satisfy the requirements of lower cost, higher accessibility and accuracy;
2) Development of corresponding algorithms to utilize the data provided by sub-systems from selected positioning candidates, enabling them to work independently with the assumption of unavailability of either of one sub-system during the operation;
3) Design of a comprehensive solution for data integration from sub-systems to enable them work cooperatively with the absolute 2D positioning information for seamless indoor-outdoor transition;
4) Provide a solution for the integration of the height estimation and floor identification to the 2D system to provide 3D positions;

1.2.2.2. Walking Posture Recognition

1) Experimental measurements for user velocity and inter-person distances in a four-floor building under both emergency and non-emergency scenarios, which can later be fed to the ABM-based simulation;

2) Posture recognition based on measured user velocity and step length of different genders by data processing, i.e. upright walking and stoop-walking with and without knee flexion;

1.2.2.3. Intelligent Indoor Evacuation Simulation

The evacuation with the support of the navigation system can be regarded as the evacuation strategy based on 'nearest exit', while the evacuation process with no navigation is regarded as 'random walking'. The application of the ABM-based evacuation simulation aims to demonstrate that the evacuation process aided by navigation is more efficient than the evacuation process without navigation assistance, based on the measured user parameters from self-designed 3D indoor positioning system. To achieve the above purpose, the following objectives are realized in order:

1) Establishment of an SF-based ABM for pedestrian movements in a GIS-based simulation environment;
2) Establishment of a spatial-temporal-based fire expansion model;
3) Conduction of ABM-based evacuation simulation under the scenarios before and after the triggering of the fire alarm with 10 times;
4) Analysis of the simulation results based on the comparison of survival rate, the average and Maximum RSET within the ASET, the maximum velocity before and after the alarm, and the mean evacuation distances of using two different evacuation strategies with and without navigation support;

1.2.2.4. Investigation of Potential Cognition Factors

This study has some partial investigations on cognition factors based on the prior knowledge of the occupants. It has conducted a survey of user responses among students who daily work inside the selected test site under virtual scenarios, focusing on questions on the three aspects:

1) The level of Indoor familiarity of the test building, including the familiarity to the exits, risky places, and satisfaction degree of the indoor signs;
2) Psychological stress when walking with bending postures, on the aspects of difficulty sensation, nervousness and awareness of speed reduction;

3) Attitudes to the smartphone-based navigation services during fire evacuation; decision making under extreme cases and calming factors after trapping.

With the acquired results, this study can achieve the first stage of developing a personalized intelligent indoor navigation system for fire evacuation, with supportive evidences from simulations.

1.3. Structure of the Thesis

The chapters for this study are organized as follows. Chapter 1 introduces the background, motivation, objectives and the original contributions of this study, i.e. the development of an intelligent indoor navigation system to improve the efficiency of indoor fire evacuation with advantages of low-cost, flexible and accessible configuration, easy operation, highly accurate and reliable performance and user friendly application.

Chapter 2 will first provide some existing examples of integrated systems for fire evacuation and navigation for future inspiration. A review of these systems can help gain better understanding of how an efficient intelligent indoor evacuation system should be while addressing the current limitations of these systems. As the previous designs of intelligent indoor evacuation systems are quite limited on their accessibility, the system will then review the current technologies of indoor positioning, in order to find out proper positioning candidates who satisfy the requirements of low-cost, high accuracy and high accessibility. It particularly focuses on Pedestrian Dead Reckoning (PDR) and visual tracking technologies as the priorities of positioning technology selections. The reason for choosing these two technologies is due to their higher flexibility of application, lower cost for establishment and relatively satisfactory accuracy with better user experience. The detailed comparisons can be found in Chapter 2 and it will also compare the algorithms of applying these two technologies, in order to find solutions with better accuracies and simpler applications.

Chapter 3 will delineate the process of designing a novel 2D indoor positioning system with the integration of the PDR and visual tracking technologies (2D PVINS). The chapter starts with the investigation of utilization of the sub-systems, i.e. Smartphone-based PDR and Surveillance-based Visual Tracking, in order to develop the corresponding novel algorithms for these sub-systems to work independently with relatively satisfactory accuracy. The processing of the visual data starts from using a single camera, and then proceeds to investigate a novel algorithm to transfer from multiple-cameras, which will help for the later development of a multi-camera-based PVINS. Then, the transformation of the relative positioning information from the sub-systems to the GIS-based absolute positioning information is considered as the preparation stage for data integration of the two sub-systems. The visual data is used to calibrate the PDR results in the visible areas, with relatively high accuracy. This study has developed and compared two different approaches of data integration and it has determined a more effective approach with higher relative accuracy. The test of the accuracy of the established 2D PVINS system is executed on the fourth floor of a four-floor building. With the development of the system and algorithms, the system is gradually able to handle the 2D user tracking from using a single camera to four cameras, and the coverage area is enlarged to the entire floor with a relatively higher accuracy (0.08m) than other studies using similar or alternative foot-mounted systems. This newly designed system is also highly tolerate to the existence of occlusions, which is later tested in Chapter 4 as more than half of the tested path is not covered by the cameras. The achieved accuracy (0.16m) is also comparable to the previous studies with lower amount of occlusions. The robustness of the designed system is also tested on both Android-based and iOS-based smartphones, comparing to the Android-only systems in previous studies.

Chapter 4 will further develop that novel system into a 3D version, with the integration of the smartphone-based barometer. It first develops a novel algorithm of using a single smartphone-based barometer with relatively acceptable accuracy of height estimation (0.5m) and floor identification compared to the previous studies either using similar sensors or alternative sensors. The development of this algorithm starts from the fingerprint-based pressure-height transformation model. The results acquired from this method is not satisfactory according to the validation process as the environmental factors can affect the measurements of each time and using one value to represent one floor is not sufficient. Thus, this study prescribes to use a certain range to represent the corresponding floor. This study has proposed two methods as average-based and linearity-based detection. From the comparison of these two results, this study has demonstrated the advantages of integrating these two approaches, with the pronounced ability to transparently identify even transition areas between different floors. To further improve the accuracy of using a single smartphone-based barometer, this study chooses to use two smartphone-based apps for self-calibration.

After the integration with the previously developed 2D PVINS, the accuracy of the system after the initial trial in the same four-floor building is comparable to those foot-mounted systems with more precise sensor suites. This has provided the evidence for the effectiveness of the designed novel system, with the advantages of being low-cost, user friendly and highly accurate. The developed system is able to track the user movement inside the entire building at this stage with a relatively comparable accuracy to other 3D positioning systems, compliant to the requirements by the Federal Communications Commission (FCC) for fire emergency with 50m horizontal accuracy and 3m vertical accuracy (FCC, 2015). This system will help derive accurate measurements of the velocity and inter-person distance under different postures, which is demonstrated in Chapter 5 as important parameters used in the ABM-based fire evacuation simulation. The acquired data can also be used for different stoop-walking postures and up-walking by analysing the acquired speed and step-length data, also explained in Chapter 5.

Chapter 5 will first design a novel hybrid ABM-based system for indoor fire evacuation simulation for the selected building with four floors before and after fire alarm with lower risk and cost. The developed system is integrated with a self-designed simplified fire expansion model, in order to improve the reality of the ABM-based simulation, which is usually not included in the previous studies using ABM. Moreover, it is operated in a GIS-based environment with continuous pedestrian movements. The designed simulation model is able to identify the bottlenecks inside the building, which can provide valuable insights for later building design. Meanwhile, it compared the evacuation strategies with and without the support of the navigation system as designed above by simulating the evacuation process with the guidance as the nearest-exits while the one without guidance support is regarded as random walking. The hypothesis that navigation can help to improve evacuation efficiency is supported by the comparison of the survival rate, the average and maximum evacuation RSET and the average evacuation distance for survivals. The results also suggest the width and distributions of the exits can be important factors for user selections of the evacuation routes and efficiency.

In addition to the above testing of physical feasibility of the designed navigation system for indoor fire evacuation, Chapter 6 presents an investigation of the potential cognition factors of pedestrians' fire response performance based on the survey data. These cognition factors should be considered as they are not included in the default simulation model described in Chapter 5 while being important for decision making process in real life situations. *The survey is taken among the indoor occupants with a median age of 22 in the same building for physical experiments, under a virtual situation of using bending posture during evacuation.* The cognition factors can be divided into three aspects as **indoor familiarity** (spatial cognition), **psychological stress**, and **decision making for different situations**. For indoor familiarity, the study is interested in familiarity to exits and risky places as well as the satisfaction degree of the current indoor sign installation. <u>The acquired results is gender-dependent to some extent and the familiarity to the indoor exits and the risky places are positively correlated with satisfaction degree of the current installation of the indoor signs.</u> The integration of the height factor with the other two indoor familiarity factors can improve the degree of the indoor sign satisfaction. For psychological stress, this study concentrates on the situated cognition of moving difficulty, nervousness, and speed reduction when using a bending posture during the fire evacuation to avoid smoke inhalation. The results are also gender-dependent and this study has tested the hypothesis that the growing indoor spatial cognition can help ease the psychological hardness and nervousness. However, it only becomes self-evident upon reaching a certain threshold. When integrating the effects from indoor familiarity and the other two psychological factors, the correlation to the sensation of deceleration can be strengthened. This study has also investigated the participants' attitude to the navigation support during evacuation under different situations and the results are quite encouraging with the majority of the participants has shown positive attitudes. For the corresponding decision time of the selected extreme cases, it is case-dependent to some extent and is worth future considerations when designing a personalized smartphone-based app. Moreover, it has provided an additional hypothetical case of being trapped inside the building and discovered three previously non-prioritized calming factors, which is a) the distance to the nearest firefighters, b) the current fire conditions of in the surrounding environment, and c) the locations of all firefighters. All these mentioned cognition factors can be considered in future design of navigation support for indoor fire evacuations.

Chapter 7 will summarize all the findings mentioned in the previous chapters and give some suggestions on future works.

1.4. Original Contributions

The following contributions to the fields of 3D indoor Passive Vision-aided PDR, posture recognition, ABM-based simulation, and cognition factor of fire response performances can be derived from this study.

1) A novel algorithm for smartphone-based PDR positioning with automatic step-length calibration and turning detection;
2) A modified Faster R-CNN based passive visual tracking, with simple implementation, high accuracy, and real-time detection;
3) A novel algorithm for multi-scene shifting for visual tracking, assisted by the automatic PDR turning detection;
4) A novel algorithm for depth information transformation from image space to heading information;
5) A novel data fusion method based on the comparison of two proposed candidates, with simpler operation and higher effectiveness, achieving higher accuracy than other 2D positioning systems (PVINS and foot-mounted systems) under similar less-occlusion situations, and more than

20% 2D accuracy improvement for severe occlusion-affected areas than previous 2D PVINSs;

6) A novel algorithm for height/floor estimation with more detailed floor-level division using single embedded barometer in a smartphone;
7) The acquired results with absolute coordinates to be directly used in outdoor systems;
8) The application on both Android-running and iOS-running smartphones with better robustness than previous Android-only systems;
9) The recognition of upright walking, bending with and without knee flexions from PDR data based on pattern identification;
10) A novel design of a hybrid ABM-based pedestrian evacuation model in a four-floor building with experimental results of parameter settings, with the visualizations in both 2D and 3D;
11) A novel design of simplified temporal-spatial model of fire expansion;
12) The correlation investigation of cognition factors based on survey data among indoor familiarity, psychological stress and decision making under virtual situations.

Chapter 2. LITERATURE REVIEW

2.1. PREVIOUS STUDIES OF INTEGRATED FIRE EMERGENCY SYSTEM DESIGN AND PROTOTYPE

In the previous studies, there are many of them focusing on the design of a multi-sensor based intelligent fire emergency system with the functions of human positioning and tracking, human flow monitoring and route planning during the evacuation process. According to a previous study which has proposed a conceptual framework of an intelligent fire emergency system, it suggests that this kind of system should be able to represent the 3D building topography with floors and their related rooms, while localizing pedestrians with indoor positioning technologies, e.g. Wi-Fi or Radio Frequency Identification Services (RFID). It should also be able to present the network connectivity of internal structure and track the moving target with relative precise positions (Becker et al., 2009). Moreover, there are also some more aspects need to be considered for the evacuation system, such as the resistance to heat and humidity, the power issue, portability of devices, and multi-layered positioning and navigation system (Scholz et al., 2010).

The current developed systems of intelligent fire evacuation can be divided into two categories based on the user group as for firefighters and for individual victims. However, the researches of the latter are relatively limited comparing to those of the former (Bastos et al., 2015). Therefore, this study aims to provide a potential solution to enrich the victim-oriented category. Nevertheless, it is still worth taking some advantages from the design of firefighter-oriented systems. Thus, the following sections will have a short review of the current systems both for firefighters and individual users and find out their limitations, which need considerations for the system design in this study.

2.1.1. For Firefighters (Rescue) Aspect

For the intelligent fire emergency system designed for the firefighters, it is established to support indoor navigation for corresponding scenes such as damage mitigation and survivor recue (i.e. ingress routing) (Niu, 2014). The requirements for an appropriate working system for firefighters can be divided into three aspects. First, the system should be able to handle different data processing requirements at end-users and in network. Second, the device manipulation should be easily adaptive and configurable. Finally, the sensed information should be stored at the related landmark nodes and it should allow the later evaluation for future system optimization (Scholz et al., 2010). These requirements are also applicable to victim-oriented systems, except the data processing and storage are better to be conducted at the processing centre.

Previous works of firefighter-oriented systems have experienced several updates with increasing flexibility, from WearIT@Work (Boronowsky et al., 2005, Ramirez et al., 2009), LifeNet (Klann, 2009), Siren (Jiang et al., 2004), to the most current Landmark Nodes System (Scholz et al., 2010). According to the designs of these systems, it can be found out that they are more focused on integration of surrounding context information to human-centred navigational practices based on cognition than precise localizations (Ramirez et al., 2009). This is slightly different from the focus for the victims mentioned in Section 1.2.2, as the localization accuracy is relatively important for victim-oriented systems. However, it is also worth considering the surrounding information during evacuation, i.e. fire expansion in this study, as it will affect the user safety during evacuation and finally affect their decision making of evacuation route selection.

However, all these systems are designed for the firefighters with professional experiences (Klann, 2009, Scholz et al., 2010), which may not be suitable to be used for evacuees as the mechanism of pedestrian evacuation can be different from that of rescue process, and the utilization of these systems may require some special training to deal with the professional operations. Moreover, they all require specific set of the sensor system pre-installed in the environment and heavy equipment attached to the users, making them have a higher cost for installation and configuration as well as less accessibility and lower user-friendliness daily applications. The evacuation support for user aspect needs a different setup, and this will be discussed in the next section.

2.1.2. For Individual User (Victim) Aspect

The system for fire victims to escape from hazardous building (i.e. egress routing), should have short-time localization as the long-time response will significantly decrease the chance for survival. According to the previous experience of fire emergency, the first 10 minutes are of great importance for self-evacuation (Niu, 2014) based on the estimation of fire expansion. This will be further described in fire dynamics model in Chapter 5.

The previous studies for the victim-oriented indoor evacuation system are usually smartphone-based, and the common indoor positioning technologies are Bluetooth Low Energy (BLE) -based (Sashima et al., 2006, Inoue et al., 2008) and RFID-based (Chittaro and Nadalutti, 2008, Chittaro and Nadalutti, 2009). However, the functioning of the BLE/RFID tags installed in the building environment will be affected by the environmental factors such as temperature, smoke, or power supply during the fire disaster. Some later studies have tried to overcome this problem by integrating RFID with Quick-Response Barcode (QR-Code) (Szwedko et al., 2009) or Near Field Communication (NFC) (Chu, 2010). However, the QR/NFC tags require pre-installations inside the building for positioning (Chu, 2010), which may increase the cost of system configuration. Moreover, the energy consumption for intensive BLE/RFID reading by the mobile reading can also be a problem. Thus, this kind of system is less feasible being used in the real applications.

All the above-mentioned systems require the pre-installations of specific sensors inside the indoor area, which are of relative high-cost as the precision of the user locations is highly dependent on the number of available BLE/RFID tags. Moreover, they also require specific hardware for data transmission as well as regular management for both positioning and data transmission devices. This will also lead to an increasing cost of using these systems and lower the accessibility of system applications. Moreover, the energy consumption can also be a problem for specific data reading, which should be considered in the design of the positioning system.

Thus, this study will carefully consider the positioning technologies applied for the victim-oriented intelligent navigation system, which requires no pre-installation of specific indoor infrastructure and no specific user device for application while achieving satisfactory level of positioning accuracy. This will be discussed in the following section of selecting appropriate positioning approaches for the fire evacuation based on the comparison of current popular indoor positioning technologies. Moreover, the energy consumption for user positioning is supposed to be lower than the previous systems in order to achieve long-term functioning. The effects from the environmental aspects should also be noticed, which is regarded as the environmental tolerance to the fire scene as one of the major challenge for system design for the fire evacuation. These problems will be discussed during the design of the proposed positioning system in this study in Chapter 3 and 4.

2.2. Indoor Positioning Technologies

Currently, people spend large amount of time in indoor area, such as residential buildings, shopping malls, large transport infrastructures (Klepeis et al., 2001, Jensen et al., 2009). Meanwhile, they are more easily getting lost in indoor area comparing to in the outdoor environments, which may partially due to the increasing difficulty of landmark recognition in indoor space (Huang et al., 2009). With further development of urbanization, the indoor structures of architectures especially the public facilities, are becoming increasingly complicated and large. It has raised difficulties for the exploration of indoor environment (Pu and Zlatanova, 2005, Jensen et al., 2009). Meanwhile, human-induced disasters, such as fires and the terrorist attacks (e.g. Sep,11th attacks at World Trade Centre in USA in 2001, March 11th Madrid train in 2004 and July 7th London bombing in 2005) often occur on these indoor micro-spatial environments with multi-level structure in urban areas (Kwan and Lee, 2005, Lee and Zlatanova, 2008). For fire evacuation, there will be additional problems caused by human psychological conditions as people will get anxious and react in an impulsive way when looking for an exit. Moreover, the movement of people during evacuation will also be affected by the familiarity of floor plan and the pressure from the neighbours when moving in a crowd, which will intensify the complications when retrieving appropriate routes for evacuation (Vanclooster et al., 2010, He et al., 2013, Mohan et al., 2016). A reliable indoor navigation system can help mitigate the above situation by providing accurate positioning and guidance information to the occupants.

However, the current widely used outdoor positioning system, i.e. Global Positioning System (GPS) which uses Global Navigation Satellite System (GNSS) signals for accurate position acquisition with geographic coordinate generation (Van Diggelen and Abraham, 2001, Rehrl et al., 2005, Misra and Enge, 2006, Kjærgaard et al., 2010, Martin et al., 2010, Niu, 2014, GSA, 2015), is not available in the indoor area. This is due to two reasons: the relatively low accuracy of GPS for indoor positioning and improper functioning of GPS in indoor area. As the indoor structure is more compressed than outdoor space and the accuracy of GPS is above 10 meters, this will raise difficulties for target positioning in the transition zone between outdoor and indoor areas. The improper functioning of GNSS is due to the low penetration capability of Radio Frequency (RF) signals through construction materials and the multipath propagation caused by signal reflection, scattering and diffraction, which has limited the application of GNSS system in indoor area (Van Diggelen and Abraham, 2001, Jiang et al., 2010, Kjærgaard et al., 2010, Niu, 2014). In addition, GPS will become unavailable even in outdoor area, especially in the area surrounded by the high buildings, which can also block the satellite signals (Kourogi et al., 2006, Jiang et al., 2010, Niu, 2014). This has raised the demand of alternative indoor positioning technologies to provide more precise position information for Location-Based Services (LBSs) and analysis of human movements and activity patterns inside the buildings (Lee, 2004a).

In order to overcome the above mentioned problems, many solutions have been proposed to provide accurate and constant positioning for indoor LBSs (Lee and Zlatanova, 2008, Filonenko et al., 2010). These indoor positioning systems can automatically detect the positions of indoor objects, such as products in warehouses, medical staffs or equipment in one hospital, or firefighters at the action scene (Liu et al., 2007). The popularization of smart devices also affects the usage of LBSs (Yun et al., 2013), as they play increasingly important roles in people's communication, positioning, and information gaining (Butler, 2011).

The current solutions for indoor positioning can be divided into two groups as infrastructure-based and infrastructure-free approaches (Elloumi et al., 2016, Basiri et al., 2017). Infrastructure-based methods require pre-installations of transmitters or pre-training of databases, including Wi-Fi, BLE, RFID, and UWB. Therefore, these kinds of methods are usually with the disadvantages of relative high-cost, lower flexibility, more time consuming and higher sensitivity to the environmental factors, such as multipath propagation, noise, and interference (Inoue et al., 2008, Bonenberg et al., 2010, Sun et al., 2014, Tian et al., 2015, Elloumi et al., 2016). On the other hand, the approaches from the other group seem to be more promising in future market, with higher flexibility in operation and lower cost in infrastructure installation (Dong-Si and Mourikis, 2012). In addition, the advancement in manufacturing of Inertial Measurement Units (IMU) of Micro Electro-Mechanical Systems (MEMS) and cameras of Charged Couple Device (CCD), which are common sensors used for the latter two classes, has also led to products with lower price, less energy consumption, smaller size and higher precision (Fuchs et al., 2011, Harle, 2013, Racko et al., 2016, Basiri et al., 2017, Tardif et al., 2010, Mourikis and Roumeliotis, 2007). These advantages becomes more prominent with the ubiquity of IMU sensors in smartphones and surveillance cameras in public building areas, leading to the wider applications in indoor scenarios in daily life (Dong-Si and Mourikis, 2012). However, there is still no ideal solution which satisfies the requirements of accuracy, availability, continuity, and reliability when comparing with GPS for outdoor positioning (Filonenko et al., 2010, Maghdid et al., 2016) and thus more investigations are required. One solution for this can be multi-sensor fusion, i.e. the integration of different sensors to provide an integrated solution for indoor positioning (Panahandeh and Jansson, 2014, Vu et al., 2012). This requires the selection of suitable candidates, which can satisfy the requirements of working inside the fire scene mentioned in **Section 1.2.1.1**.

2.2.1. Selection of Indoor Positioning Technologies for Fire Evacuation

The suitability of indoor positioning technologies for fire routing should be considered in three aspects: accuracy, cost of installation, and the user experience (Niu, 2014). The detailed analysis is listed in Table 2.2.1. Among all reviewed technologies, the PDR system is a special localization system due to its dependence and requiring absolute estimated position, however, its high availability in smartphones without other infrastructures has made it a competitive candidate in future indoor positioning for fire emergency. According to a previous research on the priority ranking of suitable indoor positioning technologies for different applications, the PDR assisted by GNSS is the top one option (10.43%) for safety and security applications (8.74% for second selection Wi-Fi), which mainly aimed at providing emergency services seamlessly at indoor and outdoor area with the advantages of instant response, relative high accuracy (less than tens of meters), very high reliability and continuity, low energy consumption, reasonable or low price for equipment and system installation. Meanwhile, it also take the third position for most suitable technology for indoor navigation and tracking (13.3%) (Basiri et al., 2017), making this technology with great advantage to be applied in the establishment of intelligent indoor fire evacuation system. In this study, the PDR is selected as one of the important sub-systems for indoor positioning due to the above-mentioned reasons. Meanwhile, the GIS-based maps will help provide absolute positioning information and is beneficial to the indoor-outdoor transition.

PDR systems or Inertial Navigation Systems (INSs), which are regarded as dead-reckoning-based systems for pedestrians (Harle, 2013), can provide the relative user positions, orientation and velocity in indoor area by using triad accelerometers and gyroscopes for step detection and heading estimation (Woodman, 2007, Rajagopal, 2008, Abdulrahim et al., 2011, Lin et al., 2012, Griesbach et al., 2014, Link et al., 2011). This kind of systems can be divided into several groups depending on the implementation locations of IMU sensors on the human body as foot-mounted (Hung and Suh, 2013, He et al., 2015a), hand-held (Parnian and Golnaraghi, 2010, Racko et al., 2016), backpack (Hide et al., 2010a, Hide et al., 2010b, Liu et al., 2010), in-pocket (Steinhoff and Schiele, 2010) or head-mounted (Azimi et al., 2012, Sadda et al., 2013, He et al., 2015a).

This study will focus on the hand-held smartphone-based PDR. This is because smartphones have been integrated into routine and spaces of daily life (Bentley et al., 2015) and the sensors needed for PDR are already embedded in smartphones. Smartphone-based LBS services have been widely used by people around the world (Bao et al., 2015, Bentley et al., 2015). It is estimated that current active 74% of smartphone owners are active LBS users (Duggan and Smith, 2013) and the downloading of positioning related apps is proposed to reach 7.5 billion in 2019 (GSA, 2015). Thus any positioning system which is based on smartphones, can address some of the challenges of indoor LBS and bring more mass market opportunities.

In addition, their affordable prices makes the less-infrastructure-dependent positioning system more feasible to implement (Elloumi et al., 2016). The common operating systems for smartphones, i.e. iOS and Android, have been both used for PDR based position estimation in previous studies (Kang et al., 2012, Tian et al., 2015, Sun et al., 2014, Elloumi et al., 2016, Racko et al., 2016, Torres-Sospedra et al., 2017, Zampella et al., 2017, Faragher et al., 2012, Liu et al., 2012a, Liu et al., 2012b), although with a higher tendency towards the Android running devices, which may due to its lower price than iOS based system and is dominant in current smartphone market. This study will have experiments on both smartphone-based operation systems in order to improve the robustness of the designed positioning system for the fire scene. The reason of using hand-held posture is due to that the evacuees need to check their current positions regularly, which are usually presented on the screen of the smartphone.

However, the bias drift, which will accumulate with time, is still regarded as the major disadvantage of IMU sensors, and this drawback is exaggerated for sensors on smartphones with lower precision, and the typical positioning errors for smartphones may exceed 100m in 1 minute (Zhang et al., 2011b, Sabatini and Genovese, 2014, Woodman, 2007). This leads to errors in long-term PDR-alone positioning, and thus external positioning information is required for position calibration and absolute localization (Abdulrahim et al., 2011, Harle, 2013, Panahandeh and Jansson, 2014, Pinchin et al., 2012b, Vu et al., 2012).

Many studies have searched for a potential external positioning system to calibrate the performance of PDR. In recent researches, approximately two-thirds of multi-sensor systems are inertial systems calibrated by external systems, and their common calibration choices are Received Signal Strength (RSS), Time-of-Flight (ToF), and map matching (Adler et al., 2015). For the external positioning system to assist PDR positioning, this study chooses Optical Positioning System (OPS), which is under-represented in previous studies (Adler et al., 2015). Unlike Bluetooth and RFID which need the installation of infrastructures and tag wearing, the infrastructures for surveillance data have already been installed in most of indoor environments, which are much easier and more flexible for application. Wi-Fi is another good solution as a supplement to PDR data, however, the database for Wi-Fi fingerprints needs to be update regularly, requiring large amount of labour works. The surveillance system does not have the similar problem, which can save much effort and is more convenient for practical. Thus, the surveillance-based visual tracking is applied in this study, in order to calibrate the PDR positioning results.

The recent quick improvement of OPS's service quality with increasing availability in the form of surveillance cameras has promoted the development of many pedestrian based applications, including indoor pedestrian navigation (Mautz and Tilch, 2011, Elloumi et al., 2016). The introduction of OPS in hybrid positioning process can also enrich information from visual data by object detection (Mourikis and Roumeliotis, 2007, Mautz and Tilch, 2011). There are two conventional methods for object detection, i.e. optical flow and feature extraction (Panahandeh and Jansson, 2014), has been explored widely. Optical flow, although with higher accuracy, needs more computation power and may require precise conditions of lighting and precise equipment. In addition, it assumes that between-frame motions are small and limited enough to be ignored (Griesbach et al., 2014), which might not be true in real-world applications and scenarios. Feature-based methods extract landmark features in images for positioning, can provide solutions in many indoor scenarios with relatively low computation power (Panahandeh and Jansson, 2014). However, the performance of OPS can be easily impacted by occlusion in the ambient, which is common inside the buildings, and generally indoors, as the Line-of-Sight (LoS) between camera and targets is essential for OPS (Hartmann et al., 2010, He et al., 2015a). This remains to be one of the challenges to track people through occlusion (Roy et al., 2015), though many studies have tried to predict the pedestrian's positions by using Kalman filters (Yuan et al., 2013, Mirabi and Javadi, 2012, De Villiers et al., 2012) or assuming the moving velocity of pedestrian does not change (Yan et al., 2013, Hua et al., 2014). However, these methods are problematic as the moving pattern of pedestrian will change before and after occlusion and thus it is hard to use algorithms for prediction. Therefore, it is better have another independent tracking system for constant tracking of user positions (i.e. PDR in this study) while the OPS can help to calibrate the positioning results in the LoS areas.

In **Section 2.2.3**, it will have a review over the current visual tracking technologies and how it applied in real time tracking. Meanwhile, it will also compare these approaches, in order to give an optimal option to be applied in the further development of vision-aided PDR in this study.

TABLE 2.2.1
THE ANALYSIS OF INDOOR POSITIONING TECHNOLOGIES IN FIRE EMERGENCY

Positioning Technology	Independence	Data Rate	Accuracy	Cost for Users	Cost of the Infrastructure	User Experience
GNSS	√	~1Hz	4~7m	£1~£100	Already existed, no additional cost	Not available in indoor area
PseudoLite	√	~1Hz	3~7m	~£5000 for Locata Receiver	~£100,000 per transmitter (Depending on specific indoor deployment)	Good for Experiments
IR	√	~50Hz	10cm~6m	~£1 (marker)	~£1 (marker)	Good for Experiments
Ultrasonic/Sound	√	1Hz~tens of Hz	1cm ~1m	£10~£300	£10~£100 per node	Suitable for special users such as disabled people or fire responders with high precision
Wi-Fi (Fingerprinting)	√	0.2Hz, 0.25 Hz, 3 Hz,	2~4m	Existed Smartphones	~£20 per Wireless AP (at least 2 APs, depending on specific indoor deployment)	Optimal for Evacuees but only for Android-based devices
Wi-Fi (ToA)	√	1~10Hz	1.7~10m	>£5	~£20 per Wireless AP (at least 2 APs, depending on specific indoor deployment)	Optimal for Evacuees but only for Android-based devices
RFID (Passive)	√	20Hz, 80Hz	15~50cm	>£10 per tag	>£1000 per reader	Suitable for special cases (problems with tag using)
RFID (Active)	√	0.2Hz, 0.5Hz	1~3m	~£300 interrogator, >£500 M220 reader	>£10 per tag (Depending on specific indoor deployment)	Suitable for special cases (problems with tag using)
Bluetooth	√	0.2Hz, 1Hz, 2Hz, 30Hz	2~5m	~£5 receiver/ Existed on smartphones	£5–£30 per tag	Optimal for Evacuees due to availability in smartphones
UWB	√	10Hz~25Hz	15cm~1m	£60 (for ubisense tag IP63 slim) ~1000 Lab Equipment	Expensive lab equipment	Good for Experiments
PDR/INS	×	~1KHz	Depends on external system	Low/ Existed Smartphones	Depends on external system	Optimal for Evacuees

2.2.2. Problems of Current Smartphone-Based Navigation Systems

According to Section 2.2.1, the smartphone-based PDR is one of the selected candidates for the positioning system proposed in this study, and the navigation services are also supposed to be provided on a smartphone-based platform. However, there are some limitations of current smartphone-based navigation systems need to be realized during the system operation, especially for the data representation to the users. Although this study will not do real testing of navigation services, it still needs to consider these limitations during the positioning system design and simulation process.

In general, a smartphone-based multimodal navigation system can be divided into two modules. One module will allow the online mobile access to the database of multimodal routes for route calculation between any given starting points and destinations. The provided result will contain segmented journey plan with different transportation and related time estimation. The other module will provide an offline service for guiding under both outdoor and indoor situations (Rehrl et al., 2005).

Early studies for smartphone-based navigation applications could be divided into three categories: testing systems for pedestrian navigation, positioning techniques under both outdoor and indoor environment, as well as pathfinding ideal models. The navigation and pathfinding process for human is based on interaction between human and environment, especially the spatial cognition by human (Darken et al., 1998).

For example, the REAL project has developed a resource-adaptive hybrid navigation, which is composed of Infrared (IR) sensing for passive localization and Augmented Reality (AR) technology for active location sensing to deal with indoor and outdoor situations respectively. Its indoor navigation system is based on IR transmitters installed on ceilings while the outdoor system is a GPS-based positioning system. In addition, the system takes the users' specific request besides the navigation into considerations to develop optimal solution. The route description is based on both output devices' capability of presentation and input sensor information's quality (Baus et al., 2002). In a later project called NAVIO focuses on the information aspect of pedestrian navigation services of indoor and outdoor area, which satisfies users' request and supports users' decision making. This system has integrated appropriate sensor data for positioning, develops routes based on specific context and user requirements, and enables the multimedia communication for user guidance. In addition, it also tried to solve the challenges of real-time user location tracking, 3D presentation of user location with high precision, and seamless transition between outdoor and indoor environments (Gartner et al., 2004, Retscher and Thienelt, 2004). The project LoL@ also provides the map-based visualization of user guidance on smartphones (Rehrl et al., 2005). Some other previous studies, which focus on the applications in the environment inside the mass transit facilities, have divided the wayfinding into two cognitive spaces, i.e. Network Space and Scene Space. The Network Space describes the public transportation network and can be represented by map and timetables, while the Scene Space is regarded as settings at nodes of public transport system such as transfer facilities and infrastructures, usually is modelled by schematic geometry based on hierarchical cognitive schema and partial orders (Rüetschi and Timpf, 2004a, Rüetschi and Timpf, 2004b). According to the design of these systems, it has raised the importance of user context and geographical information presentation to the users during the process of navigation besides providing accurate user locations.

However, the current smartphone-based pedestrian navigation is still far from maturity when comparing to the navigation systems for vehicles. In fact, the current so-called available pedestrian navigation system is based on the slightly modified car navigation system. It is very problematic due to the different requirements between two groups of users and conceptual mistakes (Rehrl et al., 2005).

First, the route calculation of pedestrian navigation system should be based on the pedestrian walking network. However, the common solutions for outdoor pedestrian navigation still use the street network, which is more suitable for vehicles rather than foot-travellers Second, the current design of pedestrian navigation system cannot satisfy constantly changing user context. It may due to unreliable and user-location dependent sensor readings for pedestrian navigation system as well as various requirements from users for information and guidance under different situations. Third, the current pedestrian navigation system is only available for outdoor environments. However, pedestrians will come across different types of buildings in urban area and it is necessary for pedestrian navigation system to be seamlessly applied to both indoor and outdoor area as well as transition regions (Baus et al., 2002, Rehrl et al., 2005).

In order to overcome these drawbacks, this study will apply its own GIS-based indoor maps and path network during navigation simulation, while providing reliable and accurate indoor user locations. To limit the user context under certain conditions, it focus on the application for a specific scenario of the fire evacuations, which is before the arrival of the fire brigades. In addition, it should also work properly when transferring from indoor to the outdoor environment, which also requires a uniform geographical coordinate of data presentation for both indoor and outdoor system. Moreover, the majority of the user-related parameters will be measured in experiments, which can help to improve the effectivity and reliability of the simulations.

2.2.3. Selection of Visual Tracking Algorithms

The pedestrian tracking in large indoor area is of great importance to be solved in computer vision (Dollar et al., 2012), as it enables applications related with security and indoor navigation and route guidance (Jensen et al., 2009). As the surveillance camera system can provide real-time data and has been widely available, this kind of video data has become a new data source to be applied with GIS commercial platforms for multiple scenarios (Collins et al., 2000, Pai et al., 2004, Haritaoglu et al., 2010, Zhou et al., 2016).

Many approaches have been developed recently and the classification of tracking technologies can be divided into several categories based on different criteria, such as number of used cameras, type of cameras (e.g. grayscale or colour, static or moving, mono or stereo), number of targets, speed and resolution of camera, the style of applied situation, coverage area and camera locations (Petrushin et al., 2006, Zhou et al., 2016). *This study will more focus on the fixed camera systems for visual tracking as surveillance* *tracking.*

2.2.3.1. Conventional Methods of Localization Based on Fixed Camera System

The fixed visual systems can track people with multi-cameras by establishing a camera network such as CCTVs to cover the space and produce an intelligent system to detect user (Piscataway, 2000, Torres-Solis et al., 2010). The user location can be traced through video streams by comparing patterns in image sequences based on visual odometry (Basiri et al., 2017). In this way, the location of the targeted people will be estimated based on its position within the captured image and the fixed position of camera and once its salient feature is recognized by the system. Most of previous studies are focused on the target tracking limited in the view of a single camera, only a few studies proposed suitable solutions for indoor tracking of people with continuous moving in a complete scenario (Torres-Solis et al., 2010).

The cameras used for pedestrian tracking can be divided into stereos and non-stereos. The accuracy of the stereo-camera-based system can reach 10 cm for localization. However, its high cost is an unneglectable disadvantage as it requires the installation of many cameras to cover the occlusion and corner area of indoor environment (Mourikis and Roumeliotis, 2007). Other than using stereo cameras, other studies using non stereo cameras with image processing techniques for people localization. Many studies have established Multiple Camera Indoor Surveillance (MCIS) system to track the pedestrian movements, and their accuracy can reach 0.15m (Petrushin et al., 2006, Wang and Wang, 2007, Munoz-Salinas et al., 2009, Torres-Solis et al., 2010). These methods are all based on the conventional methods of pedestrian tracking with certain model application for human identification.

The conventional methods of passive pedestrian detection are based on figure-ground segmentation of video data (Moeslund et al., 2006, Enzweiler and Gavrila, 2008, Dollar et al., 2012, Tsai et al., 2016, Zhou et al., 2016). Many previous studies have utilized background subtraction for foreground detection to identify people in the images. After detecting human in each image, the next step is to transfer the human position in image space to other coordinate systems (e.g. Zhou et al., 2016, Tsai et al., 2016). However, feature based methods will be limited on its applications on different environments as their parameters needs to be modified regularly based on prior domain knowledge to extract certain features with a relatively low accuracy. Deep learning based methods can overcome these problems based on less domain knowledge with direct input of image and improve the flexibility of algorithm application by using low-dimension feature vectors with non-maximum suppression classification and sharing features among all classes. Moreover, the parameters applied in conventional approaches needs manual selection, which may increase the amounts of the labour works while decreasing the flexibility of applications. This will also be overcome by applying the deep-learning based methods as their parameters will be automatically extracted during the processing (Girshick et al., 2014, He et al., 2014, Girshick, 2015, Ren et al., 2015)

The following section will compare some of the current deep learning based methods, in order to provide an optimal selection with relatively high accuracy. *Based on the results acquired from the comparison, This study will then utilize an optimal deep-learning based methods for human detection.*

2.2.3.2. Deep Learning Based Pedestrian Detection

This study has compared the current popular deep-learning based pedestrian detection, mainly focusing on their detection accuracy and detection efficiency (Table 2.2.3.2). As the result from the visual tracking is supposed to calibrate the smartphone-based PDR, the algorithm applied for this study should be able to achieve relatively higher accuracy and real-time detection, while not requiring high storage and long processing time. Based on the comparison results in Table 2.2.3.2, it can be found out that the Faster R-CNN is an optimal choice which almost satisfies the above requirements.

However, according to the provided detection accuracy, it may not be accurate enough due to multi-output of 20 different classes. In this study, it is not necessary to output 20 different classes but only two classes as human and non-human. This may help to improve the pedestrian detection accuracy, and more details will be given in Chapter 3.

TABLE 2.2.3.2

THE COMPARISON OF POPULAR DEEP-LEARNING-BASED PEDESTRIAN DETECTION ALGORITHMS

Algorithm	CNN	R-CNN	SPP-net	Fast R-CNN	Faster R-CNN
Related Studies	AlexNet (Krizhevsky et al., 2012); Overfeat (Sermanet et al., 2013a, Chatfield et al., 2014); ZF-5 (Zeiler and Fergus, 2014); GoogLeNet (Szegedy et al., 2015)	Girshick et al. (2014)	He et al. (2014)	Girshick (2015)	(Ren et al., 2015)
Major Features of structures	Sliding Window +CNN-based object detection (Sermanet et al., 2013b) SVM-based classification;	RP generation; SS+CNN-based object detection; (Gu et al., 2009, Carreira and Sminchisescu, 2012, Uijlings et al., 2013); BB Regression (Girshick et al., 2014, He et al., 2014, Girshick, 2015, Ren et al., 2015); Updating weights of CNN layers; SVM-based classification;	RP generation; Shared feature maps; Arbitrary-size input images (Sivic and Zisserman, 2003, He et al., 2014); SPM–based feature extraction (Grauman and Darrell, 2005, Lazebnik et al., 2006); BB Regression; SVM-based classification;	RP generation; Shared feature maps; Updating weights of CNN layers; Arbitrary-size input images; ROI-based feature extraction; Softmax-based classification; Share features during training;	RPN (Long et al., 2015) + Fast R-CNN
Training Database	Unsupervised pre-training + Supervised fine tuning	ILSVRC2012 + PASCAL VOC 2007 (Fine-tuned pre-training)	PASCAL VOC 2007	PASCAL VOC 2007	MS COCO + PASCAL VOC 2007 + PASCAL VOC 2012
20-Class Detection Accuracy (%)	58.7	66	63.1	66.9	78.8
Limitations on Detection Efficiency	Limited applications for image classification; Fixed-sized input images (Krizhevsky et al., 2012, Zeiler and Fergus, 2014, Donahue et al., 2014, Girshick et al., 2014)	Repetitive feature extraction; Fixed-sized input images; High feature storage requirement (Girshick, 2015) Long training and testing process	Fixed weights of CNN layers; High feature storage requirement; Relatively long training and testing process;	Quicker training and testing process but not real-time detection	Live streaming for online detection

2.3. PREVIOUS STUDIES OF INTEGRATIONS OF PDR AND VISUAL TRACKING

The fusion of PDR and visual tracking, also known as the Vision-aided Inertial System (VINS), is expected to benefit from the advantages of both two positioning systems, providing the localization service with higher overall accuracy, continuity, accessibility and reliability (Vu et al., 2012, Griesbach et al., 2014, Jiang and Yin, 2015, Jiang and Yin, 2017, Zhang and Zhou, 2018). The OPS can be used to calibrate drift accumulation with its higher accuracy, while PDR can solve the discontinuity problem of OPS caused by occlusion in LoS due to its ability to provide relatively accurate results in short time intervals (Jiang and Yin, 2015, Jiang and Yin, 2017, Zhang and Zhou, 2018).

Based on the way of system deployment, the VINSs can be divided into two classes: the Active VINSs (AVINSs) and the Passive VINSs.

2.3.1. AVINSs

The AVINSs have been used extensively in many applications and researches, as it can provide 3D location information and orientation estimation for motion tracking. Some of the potential applications are concentrated in the field of robotic mapping and Simultaneous Localization and Mapping (SLAM), and unmanned vehicle system (Panahandeh and Jansson, 2014, Lin et al., 2012, Hardegger et al., 2015). In previous studies, the common implementation of system for these applications is to attach a monocular/stereo camera and an IMU sensor on a fixed platform, which uses feature extraction by camera and motion estimation by inertial sensor. The motion parameters can also be deduced by image processing from video data based on scene flow and features (Tardif et al., 2010, Dong-Si and Mourikis, 2012, Vu et al., 2012, Hide et al., 2010b, Hide et al., 2010a), which makes the fusion of sensor data to be plausible. The fusion of inertial and visual data is based on egomotion heading estimation (Li et al., 2013b). The methods used to achieve that can be divided into three groups: (a) slowing the sample rate of IMU data (Skog et al., 2010), (b) using Particle Filter (PF) (e.g. Ramanandan et al., 2012, Dong-Si and Mourikis, 2012), and (c) applying Kalman Filters (KF) (Song et al., 2011, Griesbach et al., 2014) and its extensions such as Extended Kalman Filters (EKF) (Tardif et al., 2010, He et al., 2015a) and Unscented Kalman Filters (UKF) (Panahandeh and Jansson, 2014). The latter two approaches are more widely used in current research articles of indoor mapping with better performance. One previous study has developed a system named as VISrec, which uses a dual-track system to combine the IMU data and optical measurements in a loosely-coupled way. The pose estimation by camera based on feature detection and matching could help to limit the drift caused by IMU, while the pose prediction by inertial sensor could also constrain the searching area for feature tracking (Vu et al., 2012). However, this kind of system is built on the robot, it is not suitable for human to use during movement.

Meanwhile, the current smartphones equipped with rich sensor suite, which could help to create more opportunities for low-cost indoor localization, providing with the processing capability in real-time and high-accuracy pose estimation (Li et al., 2013b). Some of AVINSs have utilized the embedded cameras and IMU sensors in smartphones for indoor localization (Hide et al., 2010b, Hide et al., 2010a, Li et al., 2013b). The built-in cameras were used to film the ground, in order to estimate cameras' relative position and orientation based on ground-plane feature matching. Meanwhile, IMU sensors were used for step detection and heading estimation (Hide et al., 2010b, Hide et al., 2010a, Li et al., 2013b). *However, this approach is not fully practical, particularly for commercial applications, as the video recording by embedded camera is energy consuming and cannot support long durations for indoor localization.*

2.3.2. PVINSs

Instead, this study uses surveillance cameras for pedestrian detection while using inertial sensors in smartphones (Yan et al., 2018b, Yan et al., 2018a). This method is regarded as PVINS. Other than AVINS, the sensors in this kind of system are distributed on different platforms and further data transformation is needed before sensing integration. Some of the recent studies also utilize this idea and regard this method as passive-vision-aided active inertial navigation (Jiang and Yin, 2015, Jiang and Yin, 2017, Zhang and Zhou, 2018). These studies integrate the pedestrian-detection-based visual results from a single surveillance camera and PDR results from the embedded IMU sensors in the smartphone to continuously track 2D user movements horizontally in either indoor or outdoor environments.

The studies conducted by Missouri University (Jiang and Yin, 2015, Jiang and Yin, 2017) tracks user in the visible area by self-trained SVM-based detector and the visual tracking results from the filming view are warped to a top-down view by using four corresponding pairs. For PDR positioning, it is based on speed vector with fixed step length and moving direction, by using accelerometer, gyroscope and magnetometer. The positioning results are required to be transferred from world coordinate (relative positioning) into image coordinate for trajectory matching. They are matched by checking whether the distance between these two trajectories are within a certain threshold in each sliding window by applying the similarity matrix. This requires the updating of similarity matrix in the sliding window, and may cause some difficulty in computation. Meanwhile, the image warping to the top-down view also requires the whole filming scene to be fixed, and be covered inside the visible area of the camera. This may require some more computation when shifting to a second camera as the warping matrix needs to be re-calculated. In addition, it requires an additional time period to determine whether pedestrian detection is still working by checking the frames in this duration, which may also cause lag errors in detection. Moreover, it still exists in a relative coordinate and did not provide a solution to connect with real geographical coordinates. In this study, the cameras are facing directly to the corridors and the user positions will be estimated based on depth information and its horizontal coordinates are proportional to the real width of the corridor. In addition, the integration of visual positioning to PDR is only based on time stamp similarity and only the heading information from visual tracking is used for PDR calibration instead of positions. Therefore, <u>the system does not need to calculate these matrices and can freely shift from one camera to another as a multi-camera system.</u> Moreover, as this study applied deep-learning methods for pedestrian detection, <u>it does not need self-training detectors and self-updating of scales as the detectors are already available resources and can automatically</u>

update the size of detection selection, which can save some manual work. It can also achieve nearly real-time detection and respond immediately when no pedestrian is detected. Therefore, it will introduce less delay-detection errors to the system.

Another study conducted by Shanghai Technology University (Zhang and Zhou, 2018) tried to combine the two systems by matching the gait features from both visual and PDR system. The system installs the camera to view the whole scene, which is the whole room in this specific case, and use foreground segmentation for pedestrian detection with no occlusion. The detected user feet position will be on the extension cord of two points: the top point of foreground mask and the gravity centre of bounding box (BB), and the length between feet point and top point of foreground mask is proportional to the height of BB. The occlusion in this study is defined as the condition that the pedestrian is only partially detected, and the feet point of that situation is regarded as the mid-point of the bottom boundary detected by Convolutional Neural Network (CNN). For the gait feature extraction from visual data, it is achieved by finding the repeating pattern of higher proportion of the lower body in BBs After combining step state, step frequency and heading, the gait features from two systems with the largest matching rate will be integrated for 2D positioning. This method can improve feet position accuracies in no-occlusion areas with a more complicated algorithm. However, it also increases the responding time of system as it needs more computation steps and the foreground segmentation method cannot be processed as quickly as deep-learning method does. Moreover, this algorithm cannot be applied in the area with occlusion, which has also limited the accuracy of the system when people are too close to the camera and the feet points cannot be treated as the bottom mid-points as they are no longer on the ground. In this study, the camera is installed to face towards the walking direction of user, and thus the system does not need to separately treat the calculation of feet positions and they can all be treated as the mid-points of bottom boundaries of BBs Moreover, it removes those BBs when no entire human bodies can be viewed in the frames. Comparing the matching algorithms, the method in (Zhang and Zhou, 2018) needs gait feature extraction before integrating visual tracking and PDR data together, leading to an increase of the computation complexity for the application. In this study, the system only needs the similarity checking of time stamps from two sub-systems as it is a continuous process, which is simpler to achieve. Moreover, none of the above-mentioned studies have provided with a solution to integrate the positioning results with the real geographical coordinates, i.e. the global mapping system. The system proposed by this study has achieved that and provide opportunities for further application of seamless indoor-outdoor transition. This study also compares the performances between two types of common models of smartphones, other than the previous studies that they only use Android-running smartphones, which has improved the system robustness for different kinds of smartphones.

Previous studies have also proved that the combination of floor plan as environmental constraints, supported by the application of PF (Pinchin et al., 2012a, Pinchin et al., 2012b, Hardegger et al., 2015) or certain activities at road networks (Zhou et al., 2015), can help to improve the accuracy of indoor positioning. This study also takes this constraint into account to estimate the positioning solutions, though without using of previous mentioned methods. Instead, it is processed by geo-referencing in order to provide absolute position information to the results, which needs less computation power.

2.4. FLOOR DETECTION

The above sections have introduced the selections of positioning technologies and how they may work cooperatively in previous studies. However, in a multi-floor indoor environment, the system also needs to handle the situation of walking up or downstairs. Therefore, this system needs to provide 3D positioning information or at least 2.5D information about which floor the user is currently on, and it is useful for various LBSs (Tanigawa et al., 2008, Shen et al., 2015, Ye et al., 2016). Common examples are floor localization during fire emergency, floor map chosen in a shopping mall for, and navigation in multi-floor car park (Li et al., 2013a, Ye et al., 2016, Shen et al., 2015). For the situation of fire evacuation, the floor detection is of great importance as it will determine the original display of floor map to the users and it will also help the firefighters to identify the floor locations of trapped people for later rescue.

2.4.1. Floor Detection by RSS-Based Wireless Positioning

In past decades, the majority of floor localization methods are based on RSS-fingerprint-based wireless positioning (Shen et al., 2015, Wu et al., 2013, Ye et al., 2016), by Wi-Fi (LaMarca et al., 2005, Wang et al., 2012, Yang et al., 2012, Alzantot and Youssef, 2013) or Global System for Mobile Communications (GSM) (Otsason et al., 2005, Varshavsky et al., 2007). The main idea is to create a radio map for the entire indoor environment, establish the relationship between physical locations and corresponded RSS fingerprints. The user locations can then be estimated by comparing measured RSS to references on map (Varshavsky et al., 2007, Ye et al., 2012, Shen et al., 2015, Ye et al., 2016).

One of the main drawbacks of this kind of method is its poor scalability due to requirement of labour-intensive and time-consuming site surveying and training process (Ye et al., 2012, Shen et al., 2015, Ye et al., 2016). In addition, the low accuracy is another major disadvantage of all RSS-fingerprint based methods (Shen et al., 2015, Ye et al., 2016). For example, the identification accuracy of SkyLoc is only 73% in all samples, which is not satisfactory for real applications. This is mainly due to RSS are sensitive to interruptions between transmitters and receivers caused by obstacles, such as walls and floors (Shen et al., 2011, Xia et al., 2015). The multipath effects also impact the RSS based vertical localization. These errors may be tolerated when moving in horizontal directions but will be significant when doing vertical movements, leading to false floor identification (Xia et al., 2015). This will lead to wrong floor plan selection, which is quite important for indoor LBSs (Xia et al., 2015) and the acceptable accuracy for height measurement for good floor detection should be less than 3m (Li et al., 2013a).

Later studies have tried to improve the accuracy of floor detection by Wi-Fi-based methods. Some of them tried to improve the algorithms of using Wi-Fi RSS fingerprints. One study develops an RSS identification (RSSI) method, which uses Bayesian Graphical Model to process Wi-Fi fingerprints and achieves an accuracy of 2.3m (Al-Ahmadi et al., 2010). Another study improves the algorithm by applying K-Nearest Neighbour (KNN) and group variance algorithms for multi-floor detection, and achieves sub-meter accuracy (Alsehly et al., 2011), though this accuracy is only available in ideal conditions. Besides, the Wi-Fi RSSI based methods are still very problematic in practical with high computational complexity, intensive database access, complicated training procedures, and heavy burden of data transfer (Bai et al., 2013). Some other studies tried to use other kinds of electromagnetic signals such as Bluetooth and RFID. These methods usually require pre-installation of transmitters/tags in indoor environment for floor correction and the signal receivers/readers are carried by user. Their precision thus will be limited by the density of installed tags, which is of high cost for real practical applications and a pre-calibration of system calibration is also required (Ting et al., 2011, Bai et al., 2013, Kim et al., 2017). In order to overcome these problems, a smartphone-based barometer is integrated to provide height/floor information.

2.4.2. Floor Detection by Embedded Barometer in Smartphone

With the development of available embedded smartphone sensors, the applications of infrastructure-less methods are becoming more popular in floor localization (Constandache et al., 2010a, Constandache et al., 2010b, Ofstad et al., 2008, Ye et al., 2012). However, the application of smartphone-based IMU sensors to provide 3D positions will raise the problem of increasing bias in vertical direction (Ye et al., 2012, Zhang et al., 2012, Ye et al., 2016). This is due to the introduction of nonlinearity caused by accelerometer rotation during measurements. The error will grow quadratically with time accumulation and it cannot handled by standard EKF (Zhang et al., 2011b, Zhang et al., 2012). Therefore, the fusion of other sensor data is necessary to stabilize the height tracking by fixed beacons or data training (Constandache et al., 2010a, Zhang et al., 2011b, Sabatini and Genovese, 2014). The former one will have additional cost for installation as mentioned above, and the latter one needs high-cost data training process (Ye et al., 2016). Although some of the later studies tried to cut down the training effort by application of crowdsourcing (Alzantot and Youssef, 2012, Wang et al., 2012), a reliable detection is still user-specific and sample-dependent, which needs relatively high energy consumption (Wang et al., 2012, Ye et al., 2016).

Using a barometer may be a good alternative solution (Ebner et al., 2015). First, it has been widely used at outdoors for altitude measurements (Li et al., 2013a, Xia et al., 2015), as it is low in energy cost (Wang et al., 2006, Muralidharan et al., 2014, Xia et al., 2015, Ye et al., 2016) and requires no additional installations. A barometer altimeter allows height estimation based on air pressure above the given reference level, which is usually sea level (Li et al., 2013a, Sabatini and Genovese, 2014, Shen et al., 2015, Xia et al., 2015). It could be used to track floor level of user inside building with the provision of building information (known heights of various floor) or relative height between floors with initial level (Wang et al., 2006, Bai et al., 2013, Li et al., 2013a, Muralidharan et al., 2014).

Second, there are more smartphones has embedded pressure sensors such as Galaxy Nexus 4, Galaxy S3, Samsung S4, iPhone 6, Xiaomi Mi2, and their more recent versions, with the availability of smaller-size, higher accuracy and cheaper barometers in portable smart devices (Muralidharan et al., 2014, Ebner et al., 2015, Jeon et al., 2015, Shen et al., 2015, Xia et al., 2015, Ye et al., 2016). Together with corresponded software for data fusion, the portable-sensor-assisted methods have drawn more attentions in the field of providing 3D information (Sabatini and Genovese, 2014, Shen et al., 2015, Xia et al., 2015, Ye et al., 2016). One recent research has studied the performance of floor changing detection by mobile-embedded barometer and has found it performs with higher accuracy on one-floor change detection than that only uses accelerometer as well as with higher tolerance to perturbations of simultaneously using other functions of smartphones such as making phone calls and playing games (Ye et al., 2012, Muralidharan et al., 2014). However, this study does not solve the problem of exact floor identification (Ye et al., 2016) and indicates that a single barometer can only be used as relative changes of floor/height other than absolute height (Muralidharan et al., 2014, Sabatini and Genovese, 2014, Xia et al., 2015, Ye et al., 2016). This is because that the pressure information acquired by single barometer is very noisy and keeps changing over time. It can be easily affected by multiple factors, such as temperature, humidity, and even opening and closing of windows or doors. On the other hand, the relative changes of pressure between floors are less various and can be regarded as a constant value (Li et al., 2013a, Muralidharan et al., 2014, Sabatini and Genovese, 2014, Ebner et al., 2015, Xia et al., 2015, Ye et al., 2016, Kim et al., 2017). In order to solve that problem, a pioneering project called B-Loc has used multiple pressure sensors on each floor, in order to create a map of barometer fingerprints with time stamps for real time projection, which achieves about 98% accuracy of floor identification after testing in a 10-floor building (Ye et al., 2016). However, it is still limited as it requires real time samples for reference (Shen et al., 2015). A later study has reduced the number of barometers by using one reference device and one carrying device for exact floor identification (Kim et al., 2017). This study is also developed based on this idea for self-calibration but uses a different algorithm, which will be introduced later in Chapter 4.

Previous studies has also proved that MEMS barometer can be integrated with IMU sensors, which is known as baro-IMU for indoor navigation systems (Tanigawa et al., 2008, Zhang et al., 2012, Flores and Farcy, 2014, Sabatini and Genovese, 2014, Lin et al., 2015), It can improve the accuracy of providing height information than using only MEMS-based accelerometers while keeping tracking horizontal user positions (Ye et al., 2012, Muralidharan et al., 2014). By using this method, the positioning errors from horizontal and vertical directions are treated separately. For example, one previous study has loosely coupled these two types of data with self-designed hardware under experimental conditions. Its height estimation has achieved a Root Mean Square Error (RMSE) in a range between 0.05m and 0.68m with simple motions (Sabatini and Genovese, 2014). A later study applied this approach with smartphone sensors to help guide the blind in subway stations and commercial centres with longer distance, achieving decimetre-level accuracy on height estimation (Flores and

Farcy, 2014). However, many studies more concentrate on improving the 2D positioning accuracy by enhanced PDR algorithm, rather than focusing on the vertical height error. They just collect the pressure data of each floor as fingerprints and treat the between-floor height as constant, with a pre-calibrated pressure sensor by GNSS signals (Lin et al., 2015, Shin et al., 2014). The typical vertical error is approximately 2m (Lin et al., 2015), and the detection accuracy is still unknown as they do not provide any results about whether the floor detection can be performed accurately and in time. This may be explained by that the requirement for floor detection by barometer is not very high in the real-world applications, as the height difference between floors is relatively significant. This study will introduce the transition levels of floors which is usually neglected by previous studies (Tanigawa et al., 2008, Zhang et al., 2012, Flores and Farcy, 2014, Sabatini and Genovese, 2014, Shin et al., 2014, Lin et al., 2015). Therefore, the accuracy of height estimation is becoming more important as more detailed changes are needed. Some studies set up a referential device to improve the height estimation. They have achieved better mean accuracy at about 0.15m (Kim et al., 2017).

This study also adheres to the idea of providing height information for indoor tracking. However, it only uses a single device but different data collection tools to set up referential measurements. In addition, as the barometer can only help improve the performance in the 3rd dimension (Ebner et al., 2015), it still needs an external positioning system for calibration in the horizontal direction, which corresponds to the 2D PVINS in this study mentioned in Chapter 3. The major challenge for 3D indoor positioning is to achieve high precision while using low-cost and user friendly setups (Niu, 2014). The former two requirements have been addressed somewhat by the previous studies (Foxlin, 2005, Zhang et al., 2015), while satisfying the user experience remains a problem to be overcome. This study contributes a solution with relatively high accuracy while using low-cost and user friendly sensors, such as surveillance cameras and smartphone-based PDR as well as a smartphone-based barometer. It also provides a novel design of a 3D indoor tracking system with the integration of passive multi-scene

OPS, and active PDR and altimetry estimation, supported by auto-shifting georeferenced maps. It is the first time to use only these three sub-systems for 3D localization simultaneously and collaboratively.

2.5. Posture Applied for Fire Evacuation Process

The posture can be an important factor, as people during the fire evacuation may not always be able to keep upright poses. The harmful environmental factors during a fire, such as heat, smoke, and burning gases, may require human to use atypical postures other than upright walking (UW) for survival (Cao et al., 2014, Muhdi et al., 2006, Nagai et al., 2006, Kady and Davis, 2009a). In order to quickly evacuate from the threatening environment with no impediment of breathing, people need to seek for a safe and fast-moving manner. According to Occupational Safety and Health Administration (OSHA), the breathing zone requires to be at least 10 inch radius around the nose and mouth of pedestrian (OSHA, 2015). Thus, when under the condition that the atmosphere is becoming 'Immediately Dangerous to Life or Health (IDLH), the evacuees are required to lower their body in order to make their breathing zone secured (Cao et al., 2014).

The National Fire Protection Association (NFPA) suggested people to use crawling postures during severe fire evacuation in order to move under smoke and avoid inhaling toxic gases (Davis, 2011b, Gallagher et al., 2011, NFPA and Coté, 2015). In addition, it also helps to improve the vision of evacuees for route searching when staying under smoke (Cao et al., 2018). However, many previous studies have drawn a conclusion that crawling using knees and hands could cause significant reduction of moving velocity compared to the UW. They have proved that the reduction of the speed of using crawling than that of using erection posture varied from 36.8% to 66.7% (Gupta and Yadav, 2004, Muhdi et al., 2006, Nagai et al., 2006, Kady and Davis, 2009a, Gallagher et al., 2010, Cao et al., 2014, Cao et al., 2018), and the average speed for crawling is in a range between 0.5m/s to 0.86m/s (Morrissey et al., 1985, Muhdi et al., 2006, Nagai et al., 2006, Kady and Davis, 2009a, Kady and Davis, 2009b, Gallagher et al., 2010, Gallagher et al., 2011, Cao et al., 2014, Cao et al., 2018). Meanwhile, the speed reduction of the stoop-walking (SW) is much less than that for crawling. The maximum reduction (24%) appears when the pedestrians are required to move under conditions of low height (<1.2 m) (Gallagher et al., 2010), bending more than 70% of the self-stature (Morrissey et al., 1985). For the other studies which do not require the users to severely bend during the movement, the reduction of the speed from that of UW is in a range of 4.66% to 11% (Cao et al., 2018, Cao et al., 2014), and the average speed is between 1.01m/s to 1.84m/s depending on different body size and experimental conditions (Gallagher et al., 2010, Gallagher et al., 2011, Cao et al., 2014, Cao et al., 2018).

Moreover, the flexion of trunk and/or knee require more muscle energy expenditure than using a upright posture for walking (Morrissey et al., 1985, Davis, 2011a, Grasso et al., 2000, Cao et al., 2014, Hora and Sladek, 2014, Kluger et al., 2014, Cao et al., 2018). Previous studies has proved that by comparing the relative physiological indicators of using crawling and UW, i.e. the average heart rates (HR), oxygen consumption rates (VO_2), and ventilation rate (V_E). They have approved that the crawling posture requires a significantly larger amount of these physiological demands than using the UW posture, with more metabolic energy consumption in a range of 73% to 375% (Morrissey et al., 1985, Gallagher et al., 2011, Davis, 2011a, Cao et al., 2014, Cao et al., 2018). The situation of using SW is more diverse, depending on the specific degree of flexion. Some of the previous studies have tested the corresponding metabolic cost of using different degrees of the stooping/bending (Morrissey, 1980, Morrissey et al., 1985, Cao et al., 2014, Cao et al., 2018). According to the results, they have suggested that amount of energy consumption grows with the increasing degree of the trunk flexion (stooping) (Table 2.6.1). The 70% SW seems to be a boundary for bending without losing more than twice of the energy required by the UW-based movement, and it is the maximum safe energy loss for pedestrians according to previous studies (Morrissey, 1980, Morrissey et al., 1985, Cao et al., 2014, Cao et al., 2018).

TABLE 2.6.1
RELATIVE INCREASE OF ENERGY CONSUMPTIONS UNDER DIFFERENT SW POSTURES COMPARING TO UW POSTURE

Degree of Bending (%)	Relative Increase of Energy Consumption (%)
90	13.3~19.4
80	19.6~43
70	33.3~90.8
60	60~275
50 (Crawling)	73~375

A recent study has an empirical test of the longest distance that human can struggle to pass using a posture of UW, SW and crawling. It has shown that human can suffer from fatigue when using crawling to move through a long distance (91.44m), and the available average maximum distance is about 45.8m~52.6m while using the SW (80%~90% SW) and UW postures, this problem does not occur (Cao et al., 2018). Comparing to the enforced distance (76.2m) from International Building Code (IBC) for building with sprinkler system (ICC, 2015), the survival rate for people using crawling posture will be at a relatively low level (4.17%~16.67%) (Cao et al., 2018). These facts make the crawling posture not the best option for evacuation movement as it requires more metabolic costs and leads to lower moving speed (Muhdi et al., 2006, Gallagher et al., 2011). Meanwhile, the SW with relatively lower height reduction seems to be more plausible during evacuation. Thus, this study is interested in applying SW postures with the maximum available bending (70% SW) at the boundary of safe energy consumption, in order to enable the long-term movements of pedestrians during the evacuation process. Moreover, as the selected postures will suffer more velocity reduction within the safe requirement, it can also be used to estimate the extremes of the survival time and rate of indoor pedestrians.

However, the increasing level of stooping may increase the risk of falls (Campbell, 2013, Ferraz and Saba, 2017). Falls are regarded as the second leading factor of world-wide accidental injuries or deaths (He et al., 2012, Pannurat et al., 2014, Burns et al., 2016). Previous studies have proved that the forward leaning posture will be an important factor to fall risk and the risk will grow with the degree of forward bending (Brauer et al., 2000, Brown, 2017). This may be due to the change of the Centre of Mass (COM) motion in vertical and mediolateral (ML) direction (Brauer et al., 2000, Orendurff et al., 2004). Normally, the pedestrians will spontaneously adopt knee flexion during movements (Brauer et al., 2000). In order to investigate the riskiest case at the falling boundary, this study will mainly focus on using the different SW postures by using trunk-only flexion or trunk + knee flexion, with the maximum available height reduction (30%) for evacuation. It will also investigate the preferred SW type of different genders based on the results gathering from the survey data. It will first apply the velocity and step-length measurement based on the method provided in Chapter 3 and 4. These data will then be fed into the designed evacuation model to simulate the fire evacuation process, in order to estimate the evacuation time and survival rate by using a mixture of these SWs under different evacuation strategies.

2.6. ABM FOR CROWD EVACUATIONS DURING FIRE EMERGENCY

As the fire evacuation cannot be practiced in reality due to the high risk, this study will use simulations to testify the efficiency of the evacuation strategies with and without the support of the smartphone-based navigation. In this study, it has chosen ABM for evacuation process simulation due to its two characteristics. First, it can provide simulations of crowd behaviours under emergency condition in a ‘bottom-up’ structure based on the individual-level behaviours and the interactions between individuals as well as their surrounding environment (Borshchev and Filippov, 2004, Goldstone and Janssen, 2005, Schut, 2010, Wagner and Agrawal, 2014, Vermuyten et al., 2016). Second, it has been widely used in various situations (Santos and Aguirre, 2004, Braun et al., 2005, Pan et al., 2007, Zheng et al., 2009, Jiang et al., 2014), with higher flexibility to handle different setups. The advantages of choosing ABM to simulate autonomous agents with heterogeneous evacuation behaviours in a virtual building environment can be divided into three aspects (Borshchev and Filippov, 2004, Wagner and Agrawal, 2014):

a) high capability of representing highly complicated activities;

b) low requirement of prior knowledge of internal crowd effects for system implementation;
c) easy establishment with parameters in a microscopic (local) scale instead of in a macroscopic (global) scale.

Moreover, the research interests of using this kind of model for emergency planning and preparation is also growing with the existence of various application scenarios (Jain and Mclean, 2008, Wagner and Agrawal, 2014, Zhou et al., 2010, Pluchino et al., 2015, Picascia and Yorkesmith, 2016, Perez et al., 2017, Trivedi and Rao, 2018) in order to help reduce the fatal results in the public areas (Zhou et al., 2010, Mahmood et al., 2017).

The previous studies of applying ABM for crowd evacuations can be categorized into four types based on different purposes, among them the evacuation planning for the pedestrian facilities is of the most interests. The majority of the studies for this purpose are interested in planning for the buildings (Braun et al., 2005, Massaguer et al., 2006, Pan et al., 2006, Pelechano and Badler, 2006, Pan et al., 2007, Camillen et al., 2009, Okaya and Takahashi, 2011, Ha and Lykotrafitis, 2012) or large rooms with several exits (Bonomi et al., 2009, He and Zhao, 2010, Yamamoto, 2013), aiming to provide a solution that all people inside the facilities can evacuate to the outside quickly and safely. These studies usually use the evacuation time as an important indicator to evaluate the quality of the proposed evacuation plan. The common approaches are to calculate the average and the maximum evacuation time of all evacuees, and the latter is more popular as it can help to improve the survival rate during planning (Vermuyten et al., 2016). Other studies are also interested in the number of the survivors in Available Safe Egress Time (ASET) (Proulx, 2008, Opasanon and Miller-Hooks, 2009, Spearpoint and Xiang, 2011, Kasereka et al., 2018). This study will focus on both the number of survivors within the determined ASET and calculate the average Required Safe Egress Time (RSET) for the survivals.

The fire disaster is a special case in ABM-based studies, which usually uses a hybrid ABM integrates with other microscopic simulation methods (e.g. CA and

SF) to investigate the evacuation processes under different scenarios. The ABM + CA approach is more suitable to model evacuations in a discrete manner and fixed ID between individuals with fire data (Filippoupolitis et al., 2008, Shi et al., 2009a, Tang and Ren, 2008, Tang and Ren, 2012). Other studies have introduced more complicated conditions, such as the introduction of the changing spatial accessibility (Gwynne et al., 2001, Galea et al., 2008), the application of different occupant characteristics (Uehara and Tomomatsu, 2003, Kasereka et al., 2018), and the integration of these techniques (Wagner and Agrawal, 2014, Tan et al., 2015). However, the results acquired by these methods will be limited by the setup of the cell size of CA, as it can affect the maximum pedestrian density and flow rates (Lord et al., 2005, Pelechano and Malkawi, 2008). In order to avoid this problem, another study simplified the fire spread as a spatial-temporal model but keep the GIS-based building geometry with the considerations of different behaviours (Niu and Song, 2016). This study also takes this idea in order to integrate the fire expansion model into the crowd evacuation process.

One the other hand, the ABM + SF model is good at modelling evacuations in a continuous manner and the changing ID between individuals and surrounding environment without fire data (Zheng et al., 2009, Vermuyten et al., 2016). Previous studies have used it to describe self-organizing crowd phenomena, such as blocks (Lin et al., 2006), queuing and mass behaviours (Braun et al., 2005, Pelechano et al., 2007), correlating with psychological/panic effects, as the psychological effects can act as a force to alter the velocity (Helbing et al., 2000, Zheng et al., 2009, Vermuyten et al., 2016). Other studies have been interested in using it to identify possible bottlenecks in building design and compare different evacuation strategies during evacuations (Bakar et al., 2017, Mahmood et al., 2017, Trivedi and Rao, 2018). This method has removed the effects from the cell size configurations as the setup of the moving speed and ID can be acquired from the previous empirical studies of pedestrian flow based on the fundamental diagram (Seyfried et al., 2005, Daamen and Hoogendoorn, 2007, Chattaraj et al., 2009) and the interactions between human and environment described by SF model is more realistic (Yang et al., 2013, Vermuyten et al., 2016). However, the fire data is usually ignored in this method as the expansion of fire is better described in mesh-based method.

This study will take the idea in (Niu and Song, 2016) to have a simplified spatial-temporal model of fire expansion. Meanwhile, it will integrate with a hybrid ABM+SF model to describe crowd evacuations with self-measured speed and ID, in order to compare the number of survivors in ASET of using a mixture of SW postures with different evacuation strategies during evacuations and identify possible bottlenecks in the building.

Chapter 3. 2D Vision-aided Indoor Pedestrian Dead Reckoning

3.1. Introduction

This study proposes a hybrid system for indoor positioning which should be able to fulfil the above-mentioned conditions in **Section 1.2.1**. In this chapter, it will present the partial design of the entire system, which is able to satisfy the positioning purpose in horizontal direction. *The inertial sensors and cameras are attached on independent platforms, with the support of the georeferenced digital floor map. The video data is taken from several static surveillance cameras while the inertial data is taken from smartphones held by the users. It does not require any additional installation with complete surveillance system and available inertial data collection from smartphone.* Other than using landmark-based image matching for localization and camera orientation estimation, this study uses deep-learning-based object detection for pedestrian positioning, with the prior information of camera locations inside the building (Yan et al., 2018c, Yan et al., 2018b, Yan et al., 2018a). The estimated 2D paths from smartphone-based PDR and visual tracking both need to be firstly processed by coordinate transformation based on the real geographical information. The visual data is then used to calibrate PDR in visible areas by heading correction with similar time stamps (Yan et al., 2018a). This system is tested on two types of smartphones for ubiquity checking and has developed from partial tracking to whole floor tracking.

3.2. Design and Development of the System

The designed system is divided into two parts with one major positioning system as smartphone-based PDR and a supporting system as visual tracking system (Fig.3.2). During the operation, the smartphone-based PDR system keeps actively tracking the movements of user while the visual system only provides user positions in the visible areas by pedestrian detection, shifting from one camera to another. During the movement, the smartphones with either Android or iOS operation system, are held horizontally and pointing forward. Their accelerations and the angular velocities are collected simultaneously. The former is used for step detection and step length estimation while the latter is applied for calibrating heading estimation. The integration of these data can help calculate relative 2D PDR positions.

Meanwhile, the video recording is triggered since the user starts moving. Once entering the LoS area of each camera and a significant change is detected from the estimated PDR headings, the 2D visual positions will be calculated based on BBs' positions by pedestrian detection and the estimated depth information in corresponding frames. The 2D visual headings are determined by visual positions in every two consecutive frames (Yan et al., 2018a).

The positioning result by the visual tracking has a relatively high density due to its sampling frequency. This may not be close to the walking mechanism of pedestrians and it will require a larger space of data storage. Meanwhile, the visual tracking data from the surveillance system may raise some issues related to the privacy. In this case, they may not be very appropriate to serve as the positioning guidance but to serve as supportive information to calibrate smartphone-based PDR. Therefore, this study only keeps the positioning results of calibrated smartphone-based PDR, and the visual tracking results will be removed after data processing. The data fusion process can then be treated as the calibration of positioning results from smartphone-based PDR by visual tracking results.

This study has tested two methods: a) time-synchronization-based position replacement (Yan et al., 2018b), and b) using synthesized results from calibrated headings and PDR step lengths. The latter one is selected for later system accomplishment. This is because heading calibration responds better to the real-world scenarios based on the conclusions in (Yan et al., 2018a), thus it can provide better synthesized position estimation. Before 2D calibration, both results from PDR and visual tracking are supposed to be transformed into the same spatial reference system, i.e. geo-coordinate transformation. It is beneficial for further development of seamless indoor-outdoor positioning by sharing same coordinate system. To achieve that, the corresponding floor plans will help to provide absolute positioning information in World Geodetic System (WGS) 1984. These maps are pre-stored in the system and will be integrated into the 2D PVINS results by automatic selection based on the results of floor detection. The system in 2D PVINS aspect provides a calibrated 2D path in an absolute coordinate system at each epoch, i.e. the corresponding time stamps of each step (Yan et al., 2018b, Yan et al., 2018c).

The experiments during this research keep improving from (a) only using camera for visual tracking as a trial; (b) using one camera and a smartphone running Android system and integrating data by position-replacement; (c) using two types of smartphones as Android and iOS to check whether the operating systems could be a barrier for application; (d) comparing with newly developed method called heading calibration and finding out the latter one is better option; and (e) using multiple cameras for single floor tracking. The overall design of system also evolves at the same time as listed below in Fig.3.2. During this process, the whole system is also becoming more robust as the data fusion process is becoming closer to the real scenarios and it can handle more cameras to track user's movement on an entire floor. However, this chapter only focuses on the applications on single user and have not been developed into a multi-user tracking system. Considering the special case of tracking multiple people during fire emergency, it can treat multi-people group into one people as they will all move towards the same direction.

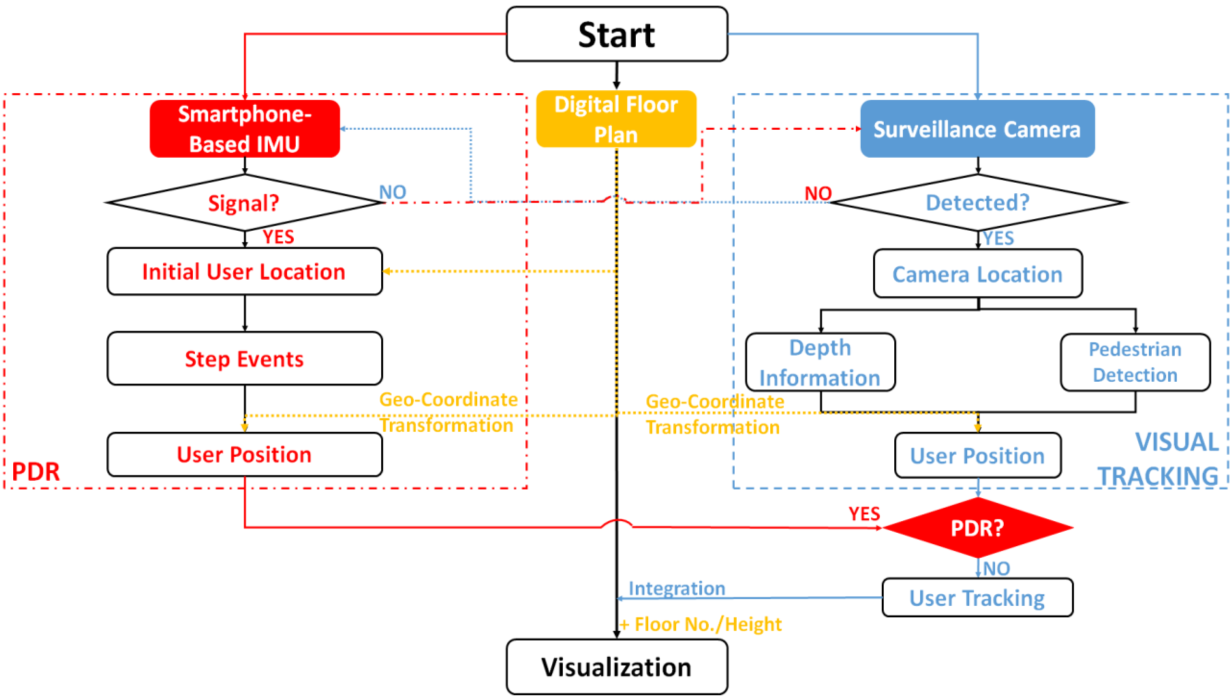

(a) Trial on visual tracking (first version of system design)

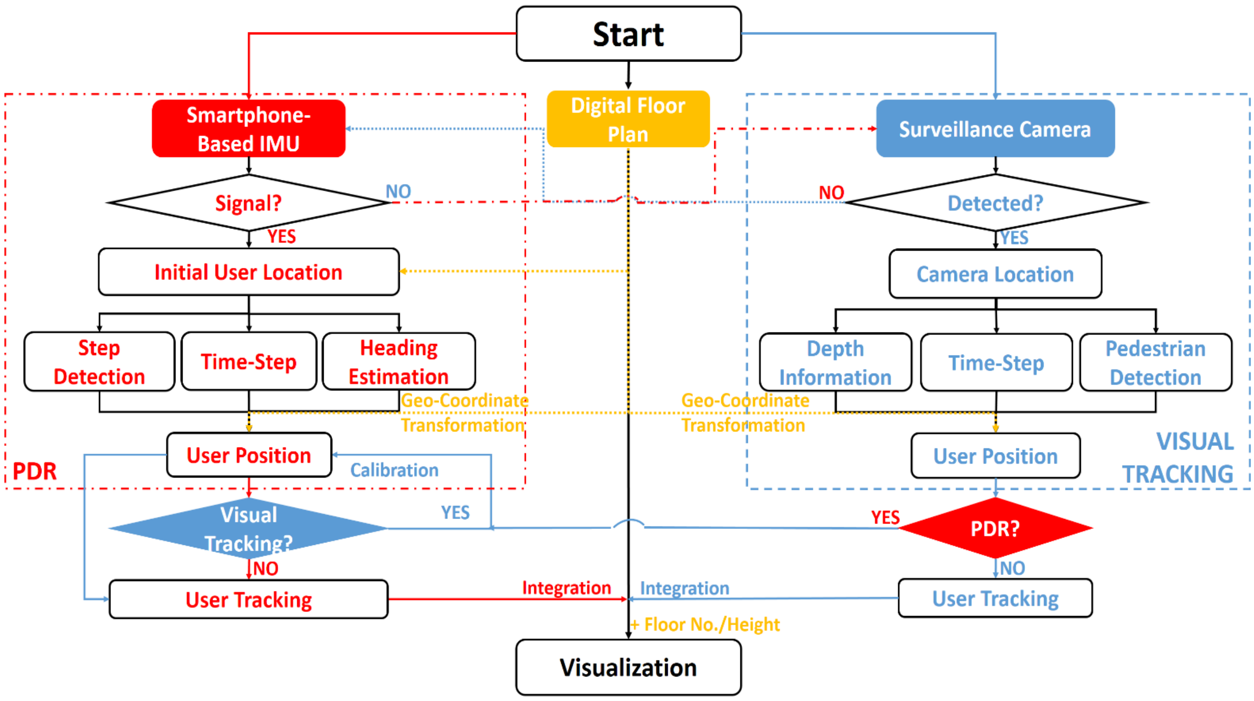

(b) Integration with Android-phone-based IMU (Second Version)

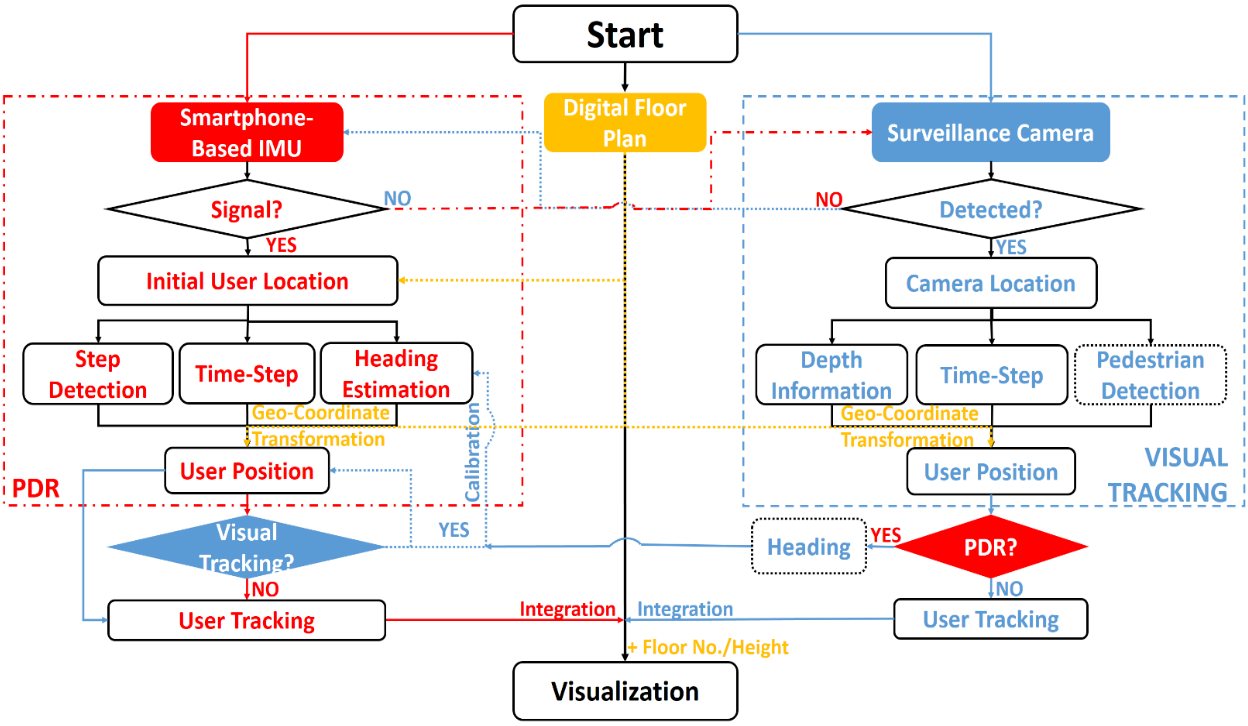

(c) Calibration methods comparison and feasibility checking between two types of smartphones (Third Version)

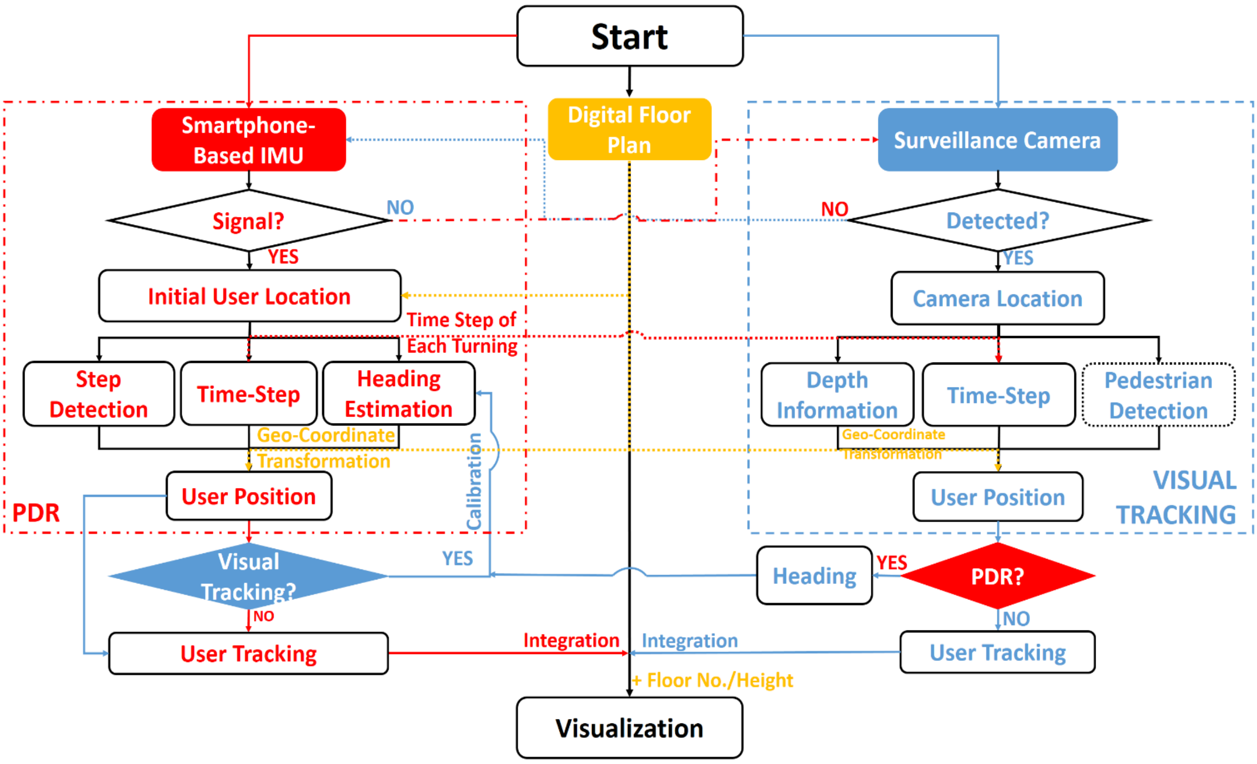

(d) Using multiple cameras for single floor checking (Fourth Version)

Fig.2.2. The development of system design for vision-aided PDR system (a) - (d).

3.3. SMARTPHONE-BASED PDR

The inertial position estimation in this study is built upon Step-and-Heading System (SHS), which uses 2D description of pedestrian strides as length and heading. The proposed inertial positioning proceeds as follows: (1) step detection, (2) step length estimation, (3) heading estimation, and (4) position estimation. The system also transforms its coordinate from the body frame to the global frame (Torres-Sospedra et al., 2017, Zampella et al., 2017, Harle, 2013, Yan et al., 2018a, Yan et al., 2019).

3.3.1. Step Detection

The step detection is based on gait cycle detection, which recognises gait cycles by searching for repetitive data patterns. Before the measurements, the smartphones are required to remain stationary for a period (52s) in order to stabilize the accelerometers and gyroscopes, removing potential noise from unexpected vibrations. The measurements from the accelerometers are first filtered using a low-pass filter with frequency condition as a function of the accelerometer's sampling rate (Racko et al., 2016).Then, the motion accelerations with respect to time taken in three axes as $a_x(t), a_y(t),$ and $a_y(t)$ needs to be synthesized together. This is due to distribution of vertical signals, which mainly contribute to step peaks, may appear in all axes based on the current device's altitude and orientation (Kang et al., 2012, Yan et al., 2018a). While may not be always true, but the projection to the horizontal axis can be done. In addition, the training of evacuation may include such recommendation to the users. Having assumed the horizontal grip, the step detection is only related to the relative synthesized motion accelerations in the vertical direction $a^*(t)$ and its magnitude can be calculated as in (3.3.1):

$$|a^*(t)| = \sqrt{(a_x(t))^2 + (a_y(t))^2 + (a_z(t))^2} - g \qquad (3.3.1)$$

where g is the earth's gravity, requiring to be removed from the vertical motion component. The synthetic motion's magnitude $|a^*(t)|$ is then needed to be processed by applying a pre-settled threshold to identify different features of a gait cycle in each sliding window as one acceleration, two static and one deceleration phase. The length of the window is determined by the frequency of the accelerations (Goyal et al., 2011, Yan et al., 2018a, Yan et al., 2018b). After that, a zero-crossing approach is then applied to detect different cycles i (Goyal et al., 2011, Yan et al., 2018b). Examples of the detected steps after acceleration processing by Android and iPhone are represented in Fig.3.3.1.

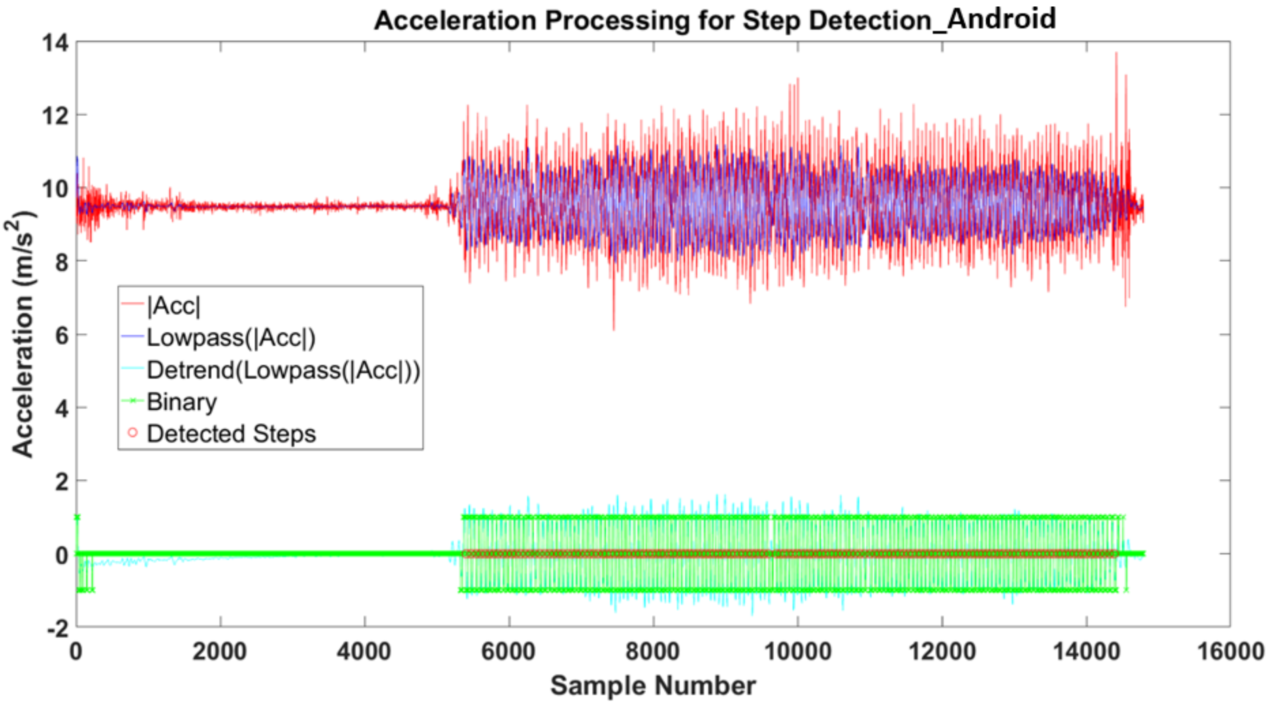

(a)

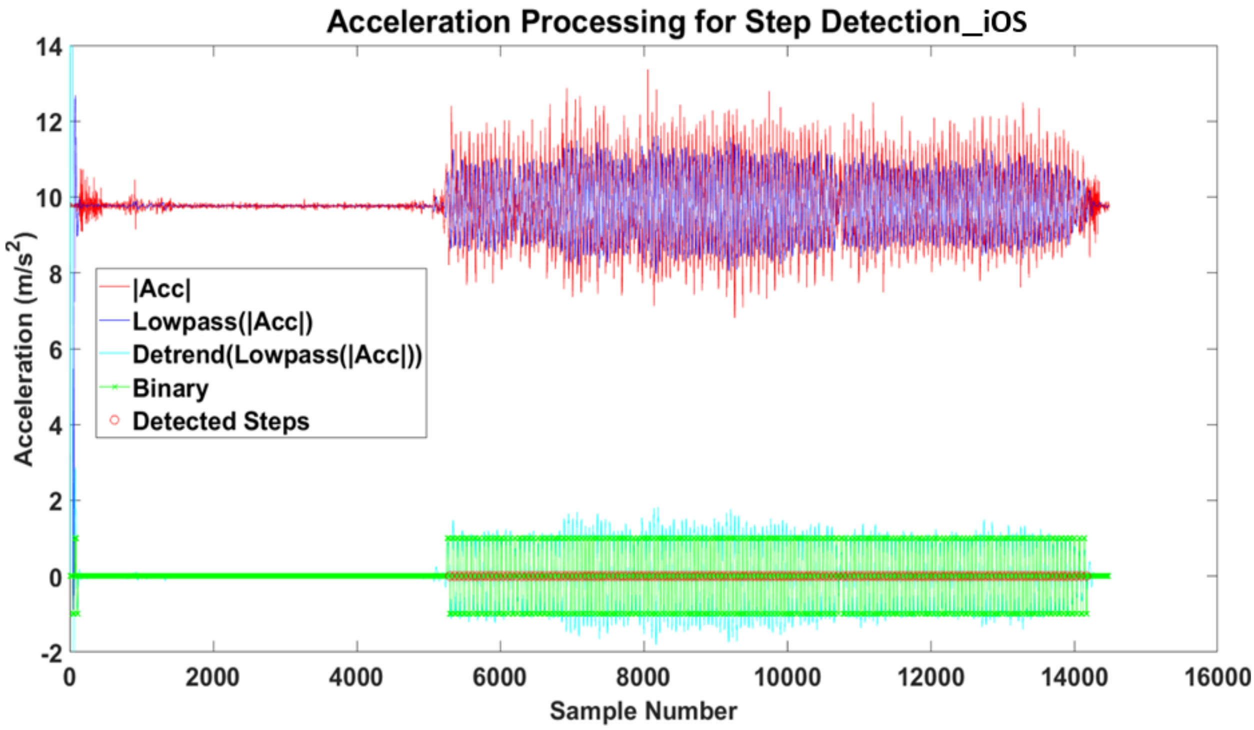

(b)

Fig.3.3.1. Examples of the processed synthetic accelerations and detected steps by Android (a) and iOS (b).

The detected steps will be compared to the existing step counting app in the smartphones as well as the actually counted step number, in order to evaluate the performance of the algorithm.

3.3.2. Step Length Estimation

Step length estimation is based on Weinberg's algorithm as demonstrated in formula (3.3.2), which uses a non-linear model with value of maximum ($|a^*{}_{max}(i)|$) and minimum ($|a^*{}_{min}(i)|$) of synthetic accelerations' magnitude of each step event (Weinberg, 2002, Yan et al., 2018b, Yan et al., 2019).

$$SL_i = \sqrt[4]{|a^*{}_{max}(i)| - |a^*{}_{min}(i)|} * k \ (i = 1,2, \dots, n) \tag{3.3.2}$$

where SL_i is the step length of the i^{th} step and k is an empirical value of penalty for estimation (Zampella et al., 2017, Yan et al., 2018b). In the initial stage, the step length has not been calibrated, which is one of the error source for PDR as this study uses a fixed k for coefficient of step length estimation. According to the previous studies, normal stride length can be within the range from 0.95m to 1.5m (Danion et al., 2003, Mason et al., 2005, Huang et al., 2010b), and k is then determined by the ratio between processed results of accelerations and assumed walking step length in 1.22m. It can be modified into a real-time value which is determined by the ratio between estimated distance and real distance of the walking path. This problem is addressed in later development of system, and the step length can be calibrated by a ratio η which is determined by the sum of estimated step length (i.e. the estimated length of the walking path) and the measured length of referential walking path D_{Real}, as the pedestrians are walking in a straight direction.

$$SL'_i = \eta * SL_i , \eta = \frac{\sum_{i=1}^{n} SL_i}{D_{Real}} \ (i = 1,2, \dots, n) \tag{3.3.3}$$

3.3.3. Heading Estimation

Each step's orientation is relative by its corresponding angular velocity changes in the body frame of the smartphone $X_B - Y_B - Z_B$, which can be measured by the embedded three-axis gyroscope in smartphone as ω_x^t, ω_y^t and ω_z^t (Fig 3.3.3.1).

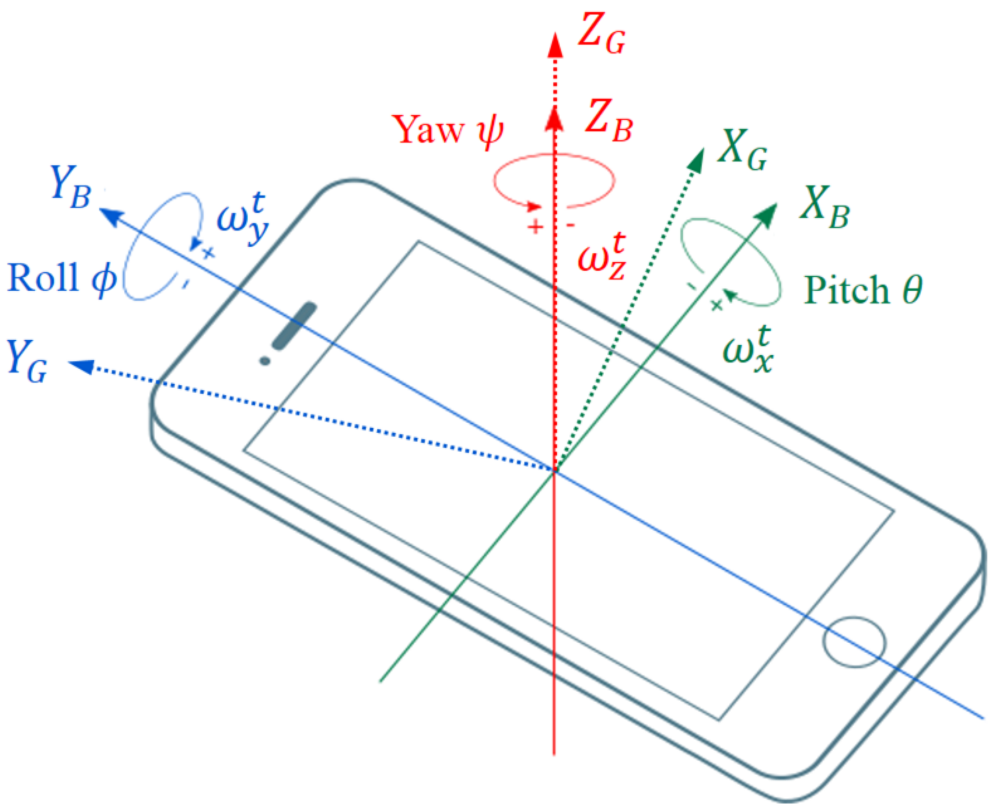

Fig.3.3.3.1. The smartphone frame in $X_B - Y_B - Z_B$, and the local ground frame in $X_G - Y_G - Z_G$.

The collected angular velocity will first be processed to remove the bias, which is calculated based on the mean value of the collected data during the stationary phase before movement. The changes of heading in smartphone frame from current stage to the next stage within certain duration Δt can be described as (3.4.4):

$$\Omega = \begin{pmatrix} 0 & -\omega_z^t \Delta t & \omega_y^t \\ \omega_z^t \Delta t & 0 & -\omega_x^t \Delta t \\ -\omega_y^t \Delta t & \omega_x^t \Delta t & 0 \end{pmatrix} \tag{3.3.4}$$

The next step is to transfer that change from body frame to the local ground frame $X_G - Y_G - Z_G$ by using a 3×3 rotation matrix as:

$$R(t + \Delta t) = R(t) * \exp(\Omega) \tag{3.4.5}$$

where $R(t)$ is the rotation matrix of the current stage and the $R(t + \Delta t)$ for the next stage. The local ground frame $X_G - Y_G - Z_G$ here refers to the frame of 2D CAD floor plans without geographical transformations and the starting point of the trajectory is treated as $(0, 0)$ of the local ground frame and the initial heading is supposed to be along X_G axis. When in the initial stage, the rotation matrix can be represented in $R(0)$, which can be described by rotations happened in three axes as $R_x(0), R_y(0), R_z(0)$. The transformation process is described in (3.4.6) -(3.4.9):

$$R_x(0) = \begin{pmatrix} 1 & 0 & 0 \\ 0 & \cos(\phi(0)) & -\sin(\phi(0)) \\ 0 & \sin(\phi(0)) & \cos(\phi(0)) \end{pmatrix} \tag{3.3.6}$$

$$R_y(0) = \begin{pmatrix} \cos(\theta(0)) & 0 & \sin(\theta(0)) \\ 0 & 1 & 0 \\ -\sin(\theta(0)) & 0 & \cos(\theta(0)) \end{pmatrix} \tag{3.3.7}$$

$$R_z(0) = \begin{pmatrix} \cos(\psi(0)) & -\sin(\psi(0)) & 0 \\ \sin(\psi(0)) & \cos(\psi(0)) & 0 \\ 0 & 0 & 1 \end{pmatrix} \tag{3.3.8}$$

$$R(0) = R_z(0)R_y(0)R_x(0) \tag{3.3.9}$$

where $R_x(0), R_y(0),$ and $R_z(0)$ are sub rotation matrix consist of roll $\phi(0)$, pitch $\theta(0)$ and yaw $\psi(0)$ directions of body frame respectively. The overall rotation matrix $R(0)$ is determined by the integration of these three components. The initial states of roll $\phi(0)$ and pitch $\theta(0)$ angles are determined by average changes of initial accelerations in corresponding directions and the initial yaw $\psi(0)$ will be zero (Yan et al., 2018a). The next step is to find corresponding Euler angles from calculated rotation matrices $R(t)$ from angular velocity changes. In this study, as the smartphone is held in a relatively stable condition by user's hand, pointing to the walking direction, the heading i.e. $\psi(i)$ of each step is only the results of changes in yaw direction (Racko et al., 2016, Zampella et al., 2017, Yan et al., 2018a) and can be calculated as in (3.3.10) based on the previous detected step events i:

$$\psi(i) = \arctan\left(R_{2,1}(i), R_{1,1}(i)\right)\ (i = 1,2,\ldots,n) \tag{3.3.10}$$

This is because that the rotation matrix $R(t)$ can rewritten as:

$$R(t) = R_z(t)R_y(t)R_x(t) \tag{3.3.11}$$

$$= \begin{bmatrix} \cos(\theta(t))\cos(\psi(t)) & \sin(\phi(0))\sin(\theta(t))\cos(\psi(t)) - \cos(\phi(t))\sin(\psi(t)) & \cos(\phi(t))\sin(\theta(t))\cos(\psi(t)) + \sin(\phi(t))\sin(\psi(t)) \\ \cos(\theta(t))\sin(\psi(t)) & \sin(\phi(0))\sin(\theta(t))\sin(\psi(t)) + \cos(\phi(t))\cos(\psi(t)) & \cos(\phi(t))\sin(\theta(t))\sin(\psi(t)) - \sin(\phi(t))\cos(\psi(t)) \\ -\sin(\theta(0)) & \sin(\phi(0))\cos(\theta(0)) & \cos(\phi(0))\cos(\theta(0)) \end{bmatrix}$$

This equation can be also be represented as:

$$R(t) = \begin{bmatrix} R_{1,1}(t) & R_{1,2}(t) & R_{1,3}(t) \\ R_{2,1}(t) & R_{2,2}(t) & R_{2,3}(t) \\ R_{3,1}(t) & R_{3,2}(t) & R_{3,3}(t) \end{bmatrix} \tag{3.3.12}$$

According to this equation, it can be found out that:

$$\tan\big(\psi(t)\big) = \frac{R_{2,1}(t)}{R_{1,1}(t)} \tag{3.3.13}$$

The accuracy of the estimated headings is depended on the precision of the accelerometers and gyroscopes of the smartphones. This is because the initial state of the heading is depended on accelerations and the following states are depended on the measurement from the angular velocities. The noise from the heading measurement will be provided and be compared with the accuracy of the rotation provided by the map.

As the path in this study is more complicated than in previous works (Yan et al., 2018b, Yan et al., 2018a), the acquired headings $\psi(i)$ is processed for automatic turning detection by finding the sudden changes of average values with a certain threshold applied (Fig.3.3.3.2), which can be later used for matching with visual tracking for 2D position calibration. Previous study has tried to extract features from both magnetometer and gyroscopes for heading direction classification by applying Principal Component Analysis (PCA) algorithm (Shin et al., 2014). However, it will increase the complexity of computation introduce some unexpected errors during detection, and reduce the variety of heading directions by using classification. The method used in this study tries to simplify the computation process by only using gyroscope. It smooths down these unexpected changes in headings by averaging while providing more options for heading directions. In the provided example, about 2 corners are detected and their average delay of detection is one step.

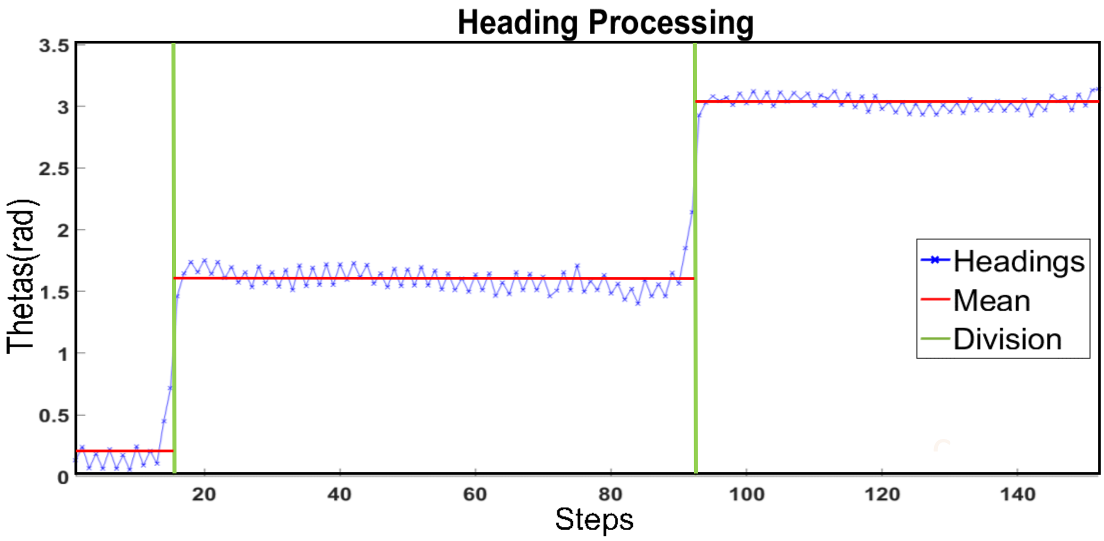

Fig.3.3.3.2. An example of turning detection by heading processing.

3.3.4. Position Estimation and Error Measurement

The user position P_i is then calculated by combination of corresponded estimated step length SL_i with estimated heading $\psi(i)$ and the location of previous step:

$$P_i = \begin{bmatrix} P_{E_i} \\ P_{N_i} \end{bmatrix} = \begin{bmatrix} P_{E_{i-1}} + SL'_i * \sin(\psi(i)) \\ P_{N_{i-1}} + SL'_i * \cos(\psi(i)) \end{bmatrix} \quad (3.3.11)$$

where P_{E_i} and P_{N_i} represent the eastern and northern position components in the local ground frame separately (Racko et al., 2016, Zampella et al., 2017, Yan et al., 2018a). Before the calculation of position error, the estimated positions need to be transformed into a real geographic system as the reference positions are measured in this way (Yan et al., 2018a). The Absolute Positioning Error APE_i is then defined as the distance between the estimated position $P(t(i))$ and reference position $R_f(t(g))$ in each trial, based on finding the closest time stamps as there are some errors between the number of detected steps and the actually counted steps by users. Then the Root Mean Squared Error (RMSE) is calculated as the average of all E_i based on the number of detected step points n in each individual test and the Mean Average Error (MAE) is the average value of these RMSEs based on the number of repeated experiments N. Meanwhile, the Relative Positioning Error RPE_i is the difference between the estimated position $P(t(i))$ in a single test and the average value of that position after N repeated experiments. Then precision of the system is determined by the mean of RPE_i based on the number of the detected steps.

$$APE_i = \lim_{(t(g)-t(i))\to 0} \left\| P(t(i)) - R_f(t(g)) \right\|, \quad (3.3.12)$$

$$RMSE_m = \frac{1}{n} \sum_i^n E_i \ (i = 1,2, \dots n) \quad (3.3.13)$$

$$MAE = \frac{1}{N} \sum_i^N RMSE_m \ (m = 1,2, \dots N) \quad (3.3.14)$$

$$RPE_i = \left\| P(t(i)) - \frac{1}{N} \sum_i^N P(t(i))_m \right\| (m = 1,2, \dots N) \quad (3.3.15)$$

$$Precision = \frac{1}{n} \sum_i^n RPE_i \ (i = 1,2, \dots, n) \quad (3.3.16)$$

With the above process, the positions of user during movement can be tracked by smartphone-based PDR, with the provision of the initial user position. This is because that the PDR system can only provide relative positioning information. Meanwhile, as the drifts of PDR system will accumulated with time, the next section is to introduce the highly accurate OPS to provide additional information for calibration.

3.4. PEDESTRIAN DETECTION BASED VISUAL TRACKING

3.4.1. Pedestrian Detection

This research uses Faster R-CNN for pedestrian detection (Fig.3.4.1.1). It is based on 3-layer Regional Proposal Network (RPN) and 5-layer Region-Based CNNs (R-CNNs), and is one of the state-of-art methods for deep learning with higher accuracy and real-time processing (Ren et al., 2015, Yan et al., 2018c, Yan et al., 2018b, Yan et al., 2018a). The RPN is used for recognizing the potential object areas (ROIs). The ROIs are processed by Pooling for BB prediction with a detector based on VGG-16 model (Ren et al., 2015) and the results are passed to Full-Connected layers for later Softmax classification to differentiate all classes. This study simplifies the original 20 classes into two: ‘human’ and ‘non-human’. Meanwhile, the BB regression is used to improve the detection accuracy. Some of the later studies have tried to increase the robustness of Faster R-CNN by improving the performance of detecting partial human bodies (Cai and Tan, 2016), however, this study mainly focuses on the detection of whole human body and thus still uses Faster R-CNN. Faster R-CNN requires a minimum of manual inputs as almost the whole process is atomized while providing a relatively high flexibility and ubiquity, in comparison with the traditional feature-based methods (Girshick et al., 2014, He et al., 2014, Girshick, 2015, Ren et al., 2015).

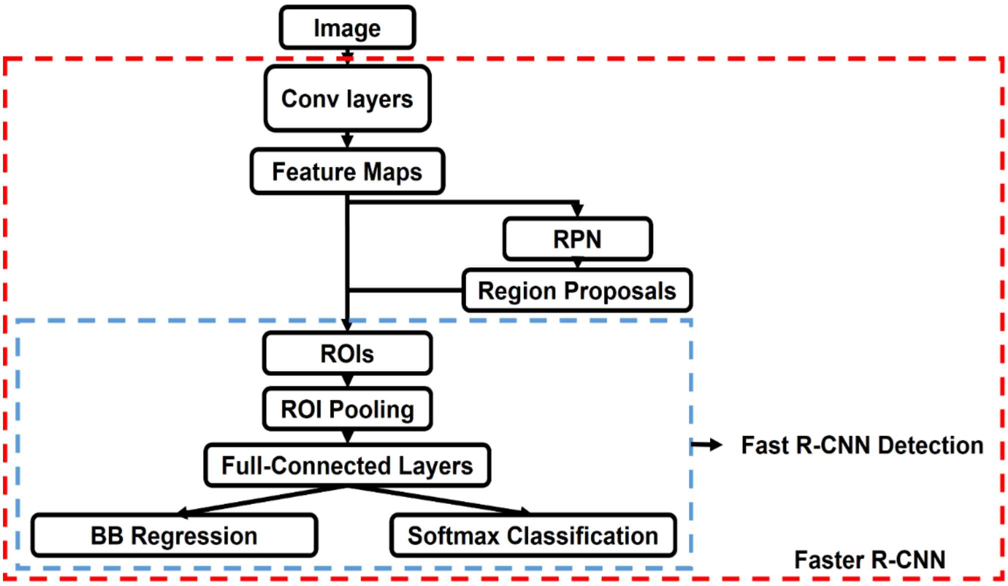

Fig.3.4.1.1. Framework of Faster R-CNN.

In this study, a pre-trained human detector is used, by using database from MS COCO and PASCAL VOC 2007 + 2012. The cameras are located on different floors and the cameras are facing nearly orthogonal to the corridors. As the resolution of camera is too low for facial recognition, there is no risk of personal information releasing. Before the operation, the acquired video data need be divided into frames for later processing as the Faster R-CNN algorithm only works for individual images. These frames will be uploaded to the system by streaming. After being processed by Faster R-CNN, the BBs are extracted from these frames and the corresponding frame numbers are also recorded for later time stamps acquisition. As the size of these BBs will be automatically adjusted to the size of human in the frames and the cameras are facing nearly orthogonal to the corridor, the gravity centre of filming user is therefore assumed to be at the centre of BBs. Then the middle points of the bottom boundaries of the BBs are then regarded as the lowest points of the users or potentially user's mobility aid as the camera facing directly to user (Ren et al., 2015, Yan et al., 2018c, Yan et al., 2018b, Yan et al., 2018a). In previous studies, it usually needs to compute the highest possibility of pedestrian in confidence map or find the projection of gravity centre in foreground detection for pedestrian localization (Jiang and Yin, 2015, Jiang and Yin, 2017, Zhang and Zhou, 2018), which may cause more computation power. These points can be constructed into the entire user path (Fig.3.4.1.2), which can be used for position-replacement-based data fusion, and their coordinates can be determined by the horizontal coordinates (x_i^1, x_i^2) of the BBs in frames, which needs to be transferred to the real distance by the width of the BBs and the width of each frame, and the depth information D'_i which is derived from pinhole model. These points can be constructed into the entire user path (Fig.3.5.1b). Although this study only uses one user, Faster R-CNN has the potential to handle multiple users for pedestrian detection. However, the overlapping of people in camera will be a big challenge at that time. Meanwhile, the relatively long filming distance in the beginning between targeted user and corresponded camera will also cause the problem of missing detection of user (Yan et al., 2018c, Yan et al., 2018b).

Fig.3.4.1.2. An example of extracted BB from frame (left) and entire user path (right), where (x_i^1, y_i^1) represents the upper left of BB, and (x_i^2, y_i^2) reprents the lower right of BB.

For multi-camera system, this process only functions with both a sudden change of PDR's headings (i.e. corner turning) and average ratio n of height and width of extracted BBs ($n = 2.5$ in this study) (Fig. 3.4.1.3). If only partial of human body is extracted by one BB, it will be removed as the lowest position cannot represent foot position. This helps to remove some incorrect measurements of pedestrian detection caused by long filming distance (Yan et al., 2018c, Yan et al., 2018b, Yan et al., 2018a) and makes sure the entire body of human is maintained in each BB for useful foot positions. The heading information is then determined by every two consecutive frames.

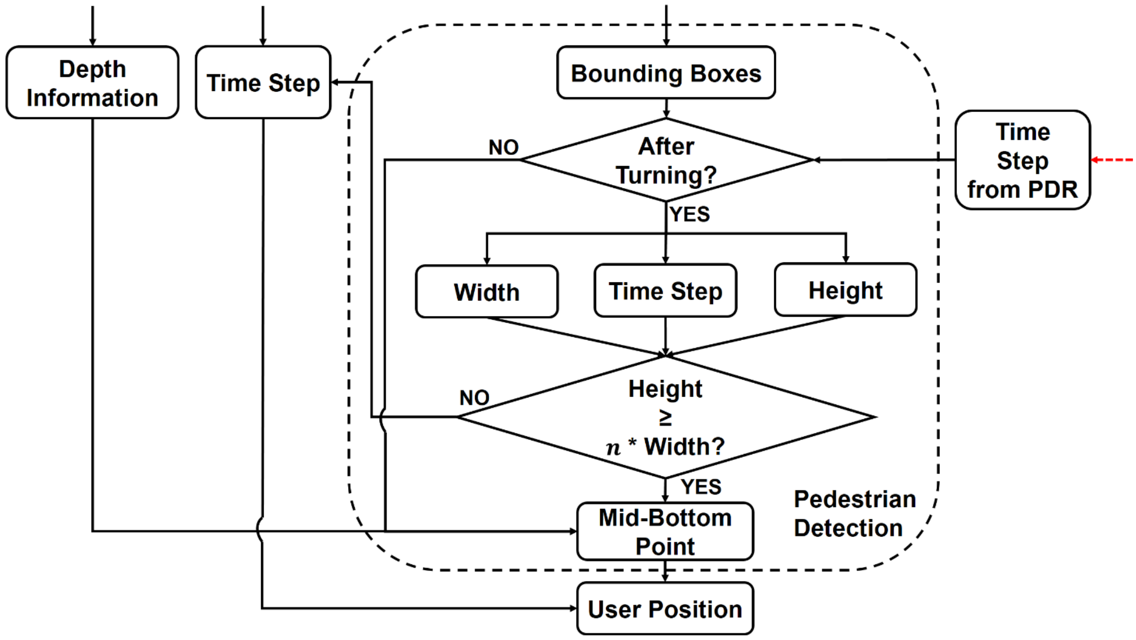

Fig.3.4.1.3. The shift of visual tracking from one camera to another in multi-camera system.

3.4.2. Person Localization

As the view of the camera is facing directly to the corridor, the coordinate system for the user position in the image space $X_C - Y_C - Z_C$ is based on the top-down projection of the camera scene (Fig. 3.4.2.1) and it treats the boundary locating the furthest point detected by camera as $Y_C = 0$.

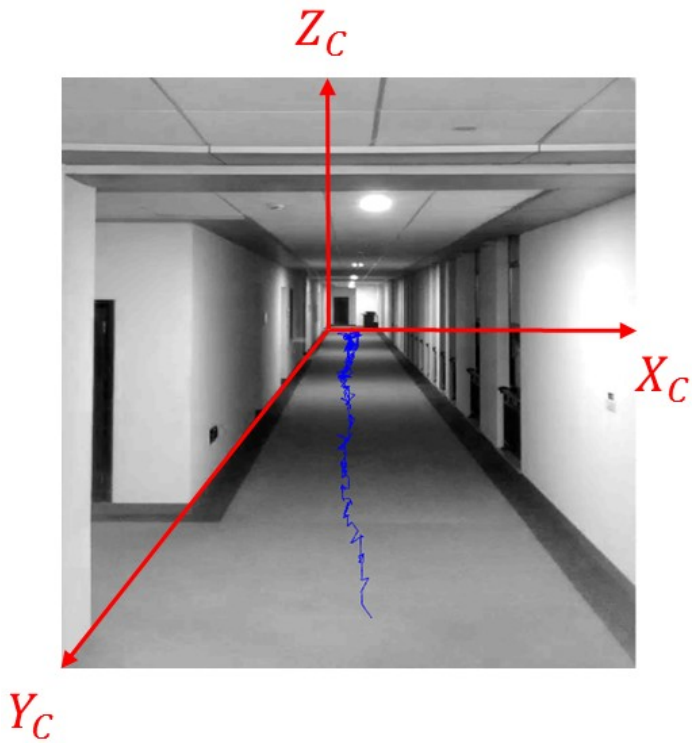

Fig.3.4.2.1. The coordinate system of pedestrian locations in camera scene.

The coordinates of the user in each frame can then be represented as $(X_i, D'_1 - D'_i)$, where X_i is related to the ratio of width of frames and corridor:

$$\frac{\frac{(x_i^1+x_i^2)}{2}}{X_i} = \alpha * \frac{W_F}{W_{Corr}}, \alpha = \frac{\sqrt{(x_i^2)^2-(x_i^1)^2}}{W'_{Corr}} \ (i = 1,2,\dots,n) \quad (3.4.2.1)$$

where (x_i^1, x_i^2) is the horizontal coordinates of the upper left and lower right corner of the BBs, W_F is the frame width, W'_{Corr} is the relative corridor width on the user position in frame, and W_{Corr} is the width of the corridor, which will be provided later by integrating map information. α is the ratio between corridor width on frame and in reality and this value is very close to 0.5 in this study. The depth information D'_i is driven from the distance D_i between user and camera in i^{th} frame. The common way for depth information acquisition is based on using stereo cameras or having additional sensors. For the former, it usually apply a method called synthetic stereo vision, which will estimate depth information by filming same scene from different locations by the same camera with known baseline. However, the main limitations of this method is that the baseline determination requires complementary techniques, which cannot be directly derived from the video data alone. For the latter, the using of additional sensors can simplify the process of acquiring depth of the objects as this distance can be directly measured. However, this will increase the cost of information acquisition as the common sensors to achieve that goal is laser scanners and range cameras (Mautz and Tilch, 2011), and they are much expensive than using algorithms. This study will not use either of these two methods, instead it will use a pinhole camera model (Dollar et al., 2012) as in (3.4.2.2), which is simple for operation and calculation:

$$\frac{h_i}{f} = \frac{H_p}{D_i} \ (i = 1,2,\dots,n) \quad (3.4.2.2)$$

where h_i represents the pixel height of human in ith frame extracted from video, H_P is the real height of person, D_i denotes the real distance of human to camera at ith position and f is the focal pixel length. During practice, f is determined by the pixel height of first frame as the initial distance to camera can be pre-determined according to map information by setting the starting point of human movement. With known height of participant and its pixel height extracted 1st frame, the focal pixel length of camera is then determined. The following D_i is proportional to h_i and a series of relative distances of human to camera are then estimated from the above information. The real depth information D'_i is then can be determined by the formula below:

$$|D'_i| = \sqrt{(D_i)^2 - (H_C - H_P)^2} \quad (3.4.2.3)$$

where the H_C represents the height of the camera which is 3m in this study, and H_P represents the height of the person. The first depth gathered from the calculation D'_1 can be calibrated by the real length of corridor, which will be provided by the map information and the ratio γ will be applied to the calculation of $|D'_i|$:

$$|D'_1|^* = \gamma * |D'_1| \quad (3.4.2.4)$$

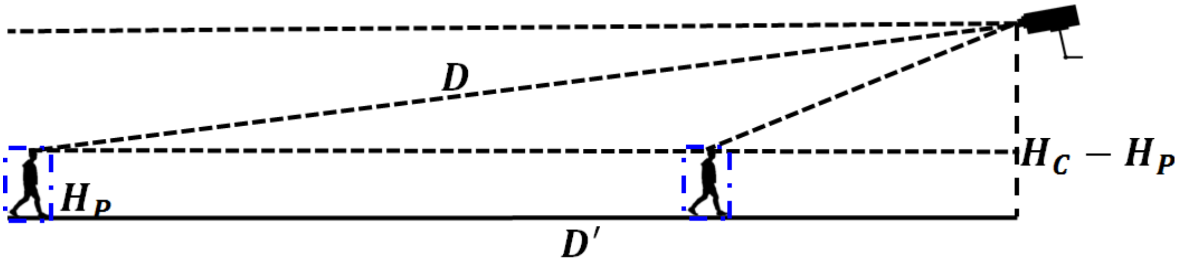

Fig.3.4.2.2. The filming mechanism of camera for depth information calculation.

The heading information $\varphi(i)$ is subsequently determined by step points from every two consecutive frames as $(X_i, D'_1 - \gamma * D'_i)$ and $(X_{i+1}, D'_1 - \gamma * D'_{i+1})$ (Yan et al., 2018c, Yan et al., 2018b, Yan et al., 2018a, Yan et al., 2019):

$$\varphi(i) = \arctan_2((X_i, D'_1 - \gamma * D'_i), (X_i, D'_1 - \gamma * D'_{i+1}) \quad (3.4.2.5)$$

3.5. Integration with Floor Plan

Before the calibration phase, both results achieved from smartphone-based PDR and also camera-based visual tracking need to be projected into the same coordinate system provided by map information, i.e. geo-coordinate transformation. The way to achieve that is by applying rotation M, scaling β, and translation δ:

$$\begin{bmatrix} x_R \\ y_R \end{bmatrix} = M \begin{bmatrix} x_r \\ y_r \end{bmatrix} * \beta + \delta \quad (3.5.1)$$

where (x_R, y_R) are the coordinates from real global geographical coordinate system while (x_r, y_r) are from the corresponding local coordinate frames, which can be (P_{E_i}, P_{N_i}) from PDR and $(X_i, D'_1 - \gamma * D'_i)$ from visual tracking systems. In this study, the two sets of the user positions in different local coordinate frames share the same rotation M, and translation δ, while only the visual-based user positions in the local ground coordinates requires the scaling as its positions are estimated based on the video frames, which may require the calibration from the absolute coordinates. The rotation M, scaling β, and translation δ can be determined during the process of geo-referencing by finding four pairs of points between 2D CAD-based floor maps and footprint of the selected building in absolute outdoor positioning system.

The reason of choosing CAD-based 2D image floor plan as the reference for the geo-referencing in this study is due to its high accessibility and low-cost in the indoor environments. The absolute positions with some simplified semantic representations of indoor building information are then created by importing those images into ArcGIS (Fig.3.5). The digitized floor plans are georeferenced into WGS84 UTM 51N coordinate system with the prior building height information for 3D positioning. The use of WGS84 will help to develop a seamless transition between indoor and outdoor environments. This is particularly helpful as it is a widely used Spatial Reference System (SRS) for GPS and many other similar systems for outdoor positioning (Yan et al., 2018c, Yan et al., 2018b, Yan et al., 2018a).

(a) (b)

Fig.3.5. An example of transferring image floor plan (a) to georeferenced digital floor plan (b).

The accuracy of the georeferenced maps is verified by the blueprints of the floor plans, which have real distances of the indoor structures. This study has compared the distances of major corridors in each floor between the provided data in the blueprints with those measured from the digitalized maps, in order to evaluate the accuracy of the acquired maps. The average difference between the distances provided by the blueprints and those measured from the maps is 0.06m. However, as all the PDR and visual tracking results are geo-transformed based on the same georeferenced floor plans, this difference will be inherited and will not affect their relative positions.

After that, the maps are posted back to the web map in order to check whether they match with the outdoor GPS system in WGS84 UTM 51N. The reason of comparing with the coordinates from referential data provided by the web map instead of real measurements by Differential GPS is due to that the web map is also used by the fire brigades for navigation. Meanwhile, it is better to share the coordinate consistency by using the outdoor system with similar precision for a relatively seamless transition, instead of introducing additional noise caused by different approaches of coordinate measurements. This study has selected the four corners of the buildings as the referential pairs to compare the measured coordinates based on the georeferenced maps with the provided data from the web map. The acquired average difference between the georeferenced maps and the referential data in the web map is 0.03m. This drift should be noticed when evaluating the accuracy of the indoor-outdoor transition in the future.

3.6. Calibration of Smartphone-Based PDR

The calibration of the smartphone-based PDR can also be regarded as the process of data integration as the smartphone-based PDR is the major positioning system, and its positioning mechanism is closer to the way of pedestrian walking. Meanwhile, the positioning density of visual tracking is relatively higher, which will cause the problem of positioning data storage as the visual tracking data is supposed to be deleted after being processed at the data centre. Earlier researches (Mautz and Tilch, 2011, Elloumi et al., 2016, Mourikis and Roumeliotis, 2007) suggest that visual positioning is more accurate than PDR in LoS areas. Thus, this study uses the visual positioning solutions to calibrate the drift for PDR-based positioning. This research introduces two approaches for PDR calibration, both supported by visual tracking with map information. The comparison between these two methods will be later discussed in result analysis, in order to pick up a better option for data fusion of multi-camera system.

3.6.1. Position Replacement Based Data Integration

The first approach is to directly replace the PDR positioning results with the visual tracking results based on time synchronization. As both PDR and visual tracking results have recorded time stamps, their results with similar time stamps can then be matched together by replacing results from PDR positioning with vision-based tracking. The time stamps of PDR are deduced from the detected step events and the related time stamps from the accelerometer readings, while that of the videos are inferred from the frame number and filming frequency.

$$P\big(t(i)\big) = \lim_{(t(j)-t(i))\to 0} \big(X_{t(j)}, D'_1 - \gamma * D'_i\big) \tag{3.6.1}$$

where $t(i)$ is the time step from the i^{th} step event, and $t(j)$ is the time step from j^{th} frame.This method has the advantage of simple implementation and decreased computation cost (Yan et al., 2018a, Yan et al., 2018b), although the synchronization could cause some issues in some scenarios.

3.6.2. Heading Calibration Based Data Integration

In reality, however, the time stamps of two positioning systems cannot be perfectly matched, and a more realistic situation is that the time stamp of current detected step from PDR is between two successive detected positions from frames with similar time stamps. This leads to the development of a second method, i.e. heading calibration. The heading calibration method is closer to the real-time simulation as it replaces the PDR's heading $\psi(t(i))$ of each step by the direction determined by two consecutive frames based on similar time steps.

$$\psi'\big(t(i)\big) = \lim_{(t(j)-t(i))\to 0} \mathrm{arctan}_2(\big(X_{t(j)}, D'_1 - \gamma * D'_{t(j)}\big), \big(X_{t(j)}, D'_1 - \gamma * D'_{t(j)+1}\big) \tag{3.6.2}$$

where $t(i)$ is the time step from the i^{th} step event, $t(j)$ and $t(j+1)$ are the time steps from j^{th} and its following frames. The calibrated headings are subsequently used with the previous estimated step lengths to re-calculate user positions. The 2D user positions will be recalculated based on the integration of these calibrated headings and pre-calibrated step length SL'_i (Yan et al., 2018a, Yan et al., 2019).

$$P(t(i)) = \begin{bmatrix} P_{E_{t(i)}} \\ P_{N_{t(i)}} \end{bmatrix} = \begin{bmatrix} P_{E_{t(i-1)}} + SL'_{t(i)} * \sin\left(\psi'(t(i))\right) \\ P_{N_{t(i-1)}} + SL'_{t(i)} * \cos\left(\psi'(t(i))\right) \end{bmatrix} \qquad (3.6.3)$$

With this process, PDR and OPS are integrated together to provide a 2D path, with synthesized headings from PDR and OPS, and calibrated step length from PDR. This method requires a slightly difficult implementation and a more computational power when dealing with a large amount of data. Therefore, the scalability of the system could be an issue, however, this is not the case in this study (Yan et al., 2018a).

3.7. Experimental Set Up for During Research

3.7.1. Study Area

The test site in this study is located at the 4th floor of PMB building at UNNC. The reference map is a digitized floor plan of experimental site by using ArcGIS 10.3, with simple semantic representations of indoor structures. All data are transferred to a desktop by wireless network for post-processing by MATLAB. As the experiments have tested the different number of cameras for user tracking, there are three sets of trajectories with different structures designed for the corresponding tests. Along the designed walking path, some distinctive markers with an inter-distance of 0.63m are marked on the ground to guide the users to follow these markers during movements. The user is asked to step over these marked referential points as strictly as possible, and the time stamp of each step point will be recorded at the same time. When passing the corners, the user does not need to turn exactly 90°, but to turn comfortably and naturally. Each set of the experiment is then run for 10 times with the same target pedestrian, and the results are presented with one selected example and the average performances. The existing indoor surveillance cameras are all facing directly to the corresponding corridors with the targeted user in the centre of the frame, and they are installed at a height of 3m to the floor of each level inside the test building.

3.7.1.1. Test of the Using Single Camera

The test of using single camera is conducted on a walking path with an entire length of 51.66m, including one 90° turning (Fig.3.7.1.1). The counted number of the step markers is 83 for this walking trajectory. The entire time used for walking along this path is about 52s under a normal walking speed about 1.0 m/s. The location of the camera is at the ceiling in front of the Room 416, facing to the corridor. The steps within the trajectory which is invisible by camera is 15 and those in the visible area of the camera is 68.

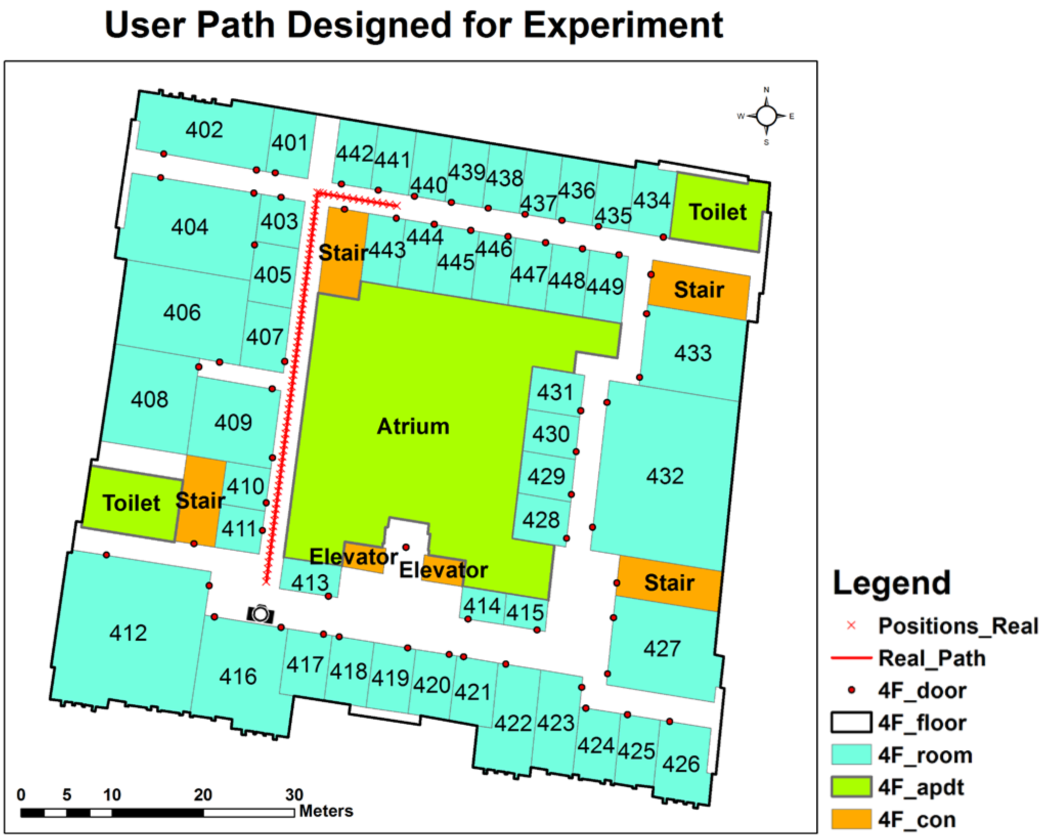

Fig.3.7.1.1. The walking trajectory for the designed system with one camera.

3.7.1.2. Test of the Using Two Cameras

The test of using two cameras is conducted on a walking path with an entire length of 89.46 m, including two 90° turnings (Fig.3.7.1.2). For this walking path, the counted number of steps is 143 and the entire walking time is about 89s, still under a similar walking speed about 1.0 m/s. The locations of the cameras are at the ceiling in front of the Room 416 (Camera #1) and Room 427 (Camera #2), facing directly to the corridors. The steps within the trajectory which is invisible by cameras is 15. For the footprints in the visible areas of cameras, there are 71 steps within the scene of Camera #1 and 57 steps within the scene of Camera #2.

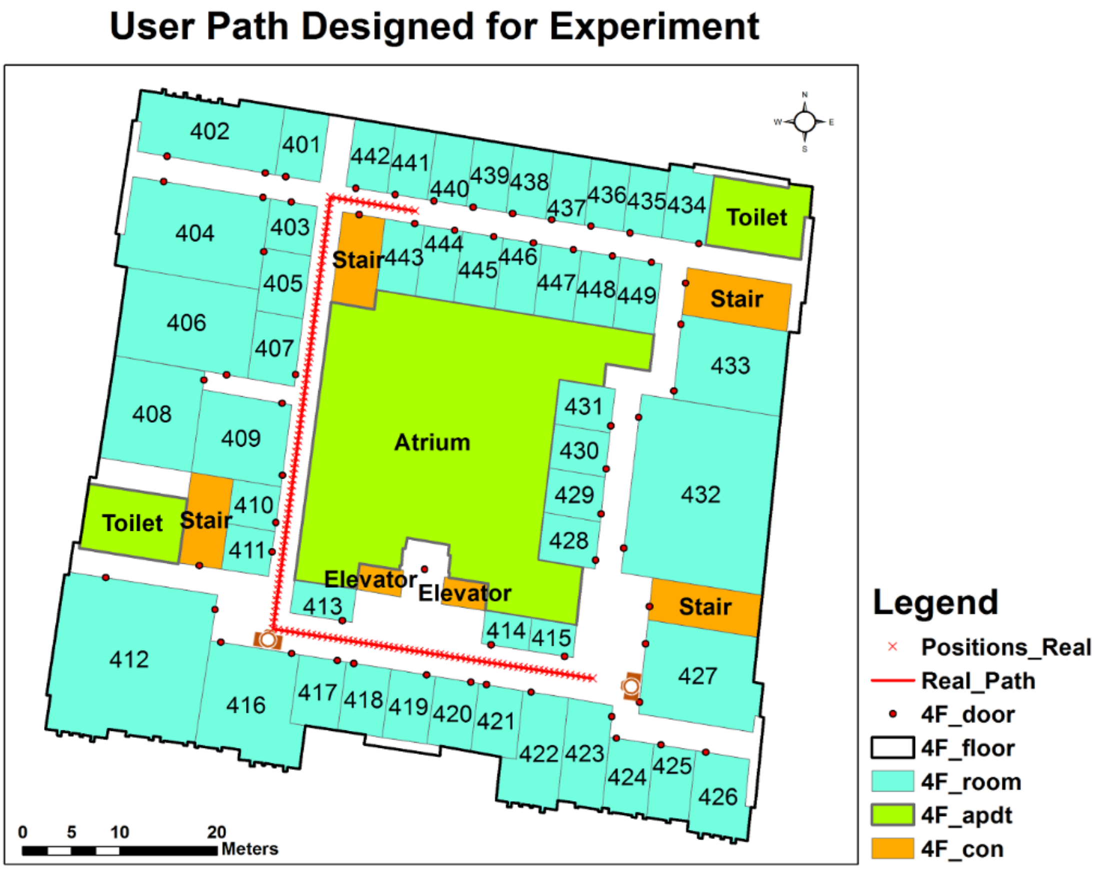

Fig.3.7.1.2. The walking trajectory for the designed system with two cameras.

3.7.1.3. Test of the Using Four Cameras

The test of using four cameras is conducted on a walking path with an entire length of 170.73 m, including six 90° turnings (Fig.3.7.1.2). For this walking path, the counted number of steps is 272 and the entire walking time is about 171s, still under a similar walking speed about 1.0 m/s. The locations of the cameras are at the ceiling in front of the Room 416 (Camera #1), Room 427 (Camera #2), Room 433 (Camera #3), and Room 434 (Camera #4), facing directly to the corresponding corridors. For the steps in the invisible areas of cameras starting from Room 433 to Room 434, its walking trajectory can be described as 6 steps with two turnings and 21 steps for the last straight walking. For the footprints in the visible areas of cameras, there are 71 steps in the scene of Camera #1, 57 steps in the scene of Camera #2, 50 steps in the scene of Camera #3, and 65 steps in the scene of Camera #4.

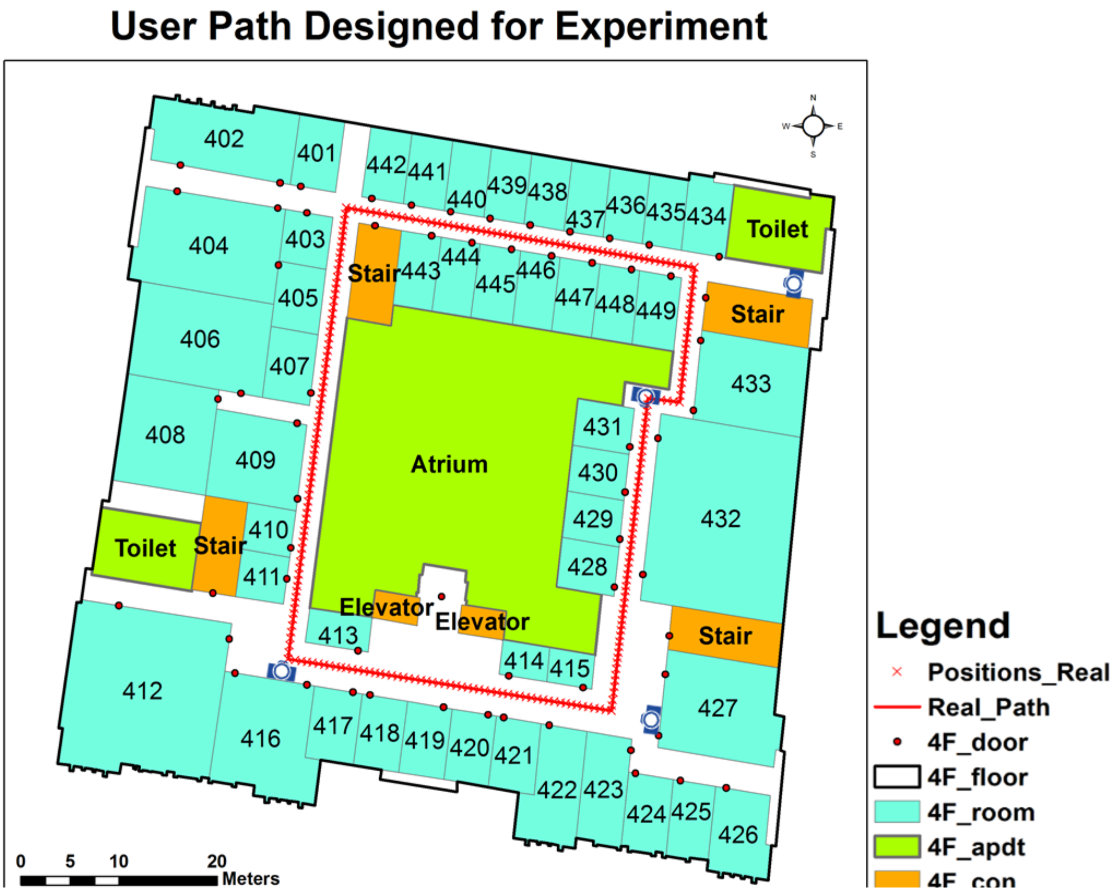

Fig.3.7.1.3. The walking trajectory for the designed system with four cameras.

3.7.2. Equipment

For smartphone-based PDR system, the smartphone model selected for Android system is Huawei MT7-TL00, and that for iOS system is iPhone 7 Plus. The operating systems of the smartphones applied in this experiment are in Android 6 and iOS 11 respectively.

Before the formal trials of different walking trajectories, this study has tried two different data collection apps, i.e. GetSensorData (Zampella et al., 2017) and MATLAB Mobile. However, the former is only applicable on the Android-based systems while the latter can work with both kinds of smartphone-based operation systems. In order to remove the noise caused by different apps of data collection, this study chooses to use MATLAB mobile for both types of smartphones in the formal trials.

All collected data are post-processed in MATLAB after being uploaded to the desktop, which is assumed to be the data processing centre for future applications. The sampling frequency for two smartphones are all first settled to be 100 Hz and then are reduced to 50 Hz, and this will not significantly affect the positioning accuracy but can improve the efficiency of computation. During the experiment, both smartphones are held stably and horizontally, pointing to the heading direction along the walking trajectory. The method of smartphone-based positioning has already been described in **Section 3.3**. For the visual tracking system, the resolution of camera is 680×540, vertical FOV is 27°, and thus the pixel length for the camera is about 1.05×10^3 per inch. The frame frequency is 16 frames per second. Cameras start filming simultaneously with the initialization of smartphone-based PDR.

3.8. RESULTS AND ANALYSIS

3.8.1. Visual Tracking

Before the evaluating the positioning accuracy of the visual tracking system, the detection accuracy should first be investigated as it will affect the later positioning results as additional noise. It is essential to check whether the pedestrian detection by each camera is functioning properly under a similar detection accuracy. After processing all video data by Faster R-CNN of cameras at different locations, the average detection accuracy of them is at 99.7% and the lowest detection accuracy appears at Camera #1 as it has the longest corridor for detection with more potential errors (99.4%) (Table 3.8.1). As their detection accuracy is nearly 100%, it suggests that the pedestrian detection performances of all cameras are acceptable for further processing of positioning.

TABLE 3.8.1
PEDESTRAIN DETECTION ACCURACY OF CAMERAS AT DIFFERENT LOCATIONS

Cameras	Camera #1	Camera #2	Camera #3	Camera #4
Detection Accuracy (%)	99.4	99.8	99.9	99.6

As results of visual tracking have denser positioning points than the provided by referential points due to higher data frequency, one referential point may have multiple corresponding visual tracking points with similar time stamps. Thus, it may be difficult to evaluate the accuracy of these positioning points by matching them to specific referential step points. The solution in this study is to find a pair of consecutive referential step points with closer time stamps to the visual tracking points. Then, it will compare the differences between the partial trajectory formed by the selected pair of step points and the visually tracked points within this time interval. The following sections of accuracy calculation all follow this method, and the corresponding specific details are provided below.

3.8.1.1. For Single Camera

The mean estimated accuracy (RMSE) of the single-camera-based visual tracking based on the above method is 0.06m of the selected sample in Fig. 3.8.1.1 and the MAE after 10 experiments remains a similar value (Table 3.8.1.1). The extracted visual tracking points construct a path that match well with the reference path. However, these points are not evenly distributed (Fig.3.8.1.1). In the beginning, the positioning points are quite dense while toward the end, the positioning points start to become sparser. There are two reasons for this phenomenon. First, as mentioned previously in **Section 3.4.1**, the target is too far away to be detected by the camera, leading to mistakes in the pedestrian detection. Second, as the depth information is calculated based on a pinhole model which mainly relies on the pixel height h_i changes in frames, this also affects the results when calculating the distance. In the initial stage, the changes of h_i are trivial, this leads to the dense distribution of positioning points, while in the ending part, the changes of h_i are becoming more significant (Yan et al., 2018a, Yan et al., 2018b) and thus leading to the distribution of positioning becoming more scattered.

TABLE 3.8.1.1
RMSE, MAE AND PRECISION OF USING SINGLE CAMERA

Cameras	Camera #1
RMSE in the Presented Example (m)	0.06
MAE of 10 Experiments (m)	0.06
Precision (m)	0.02

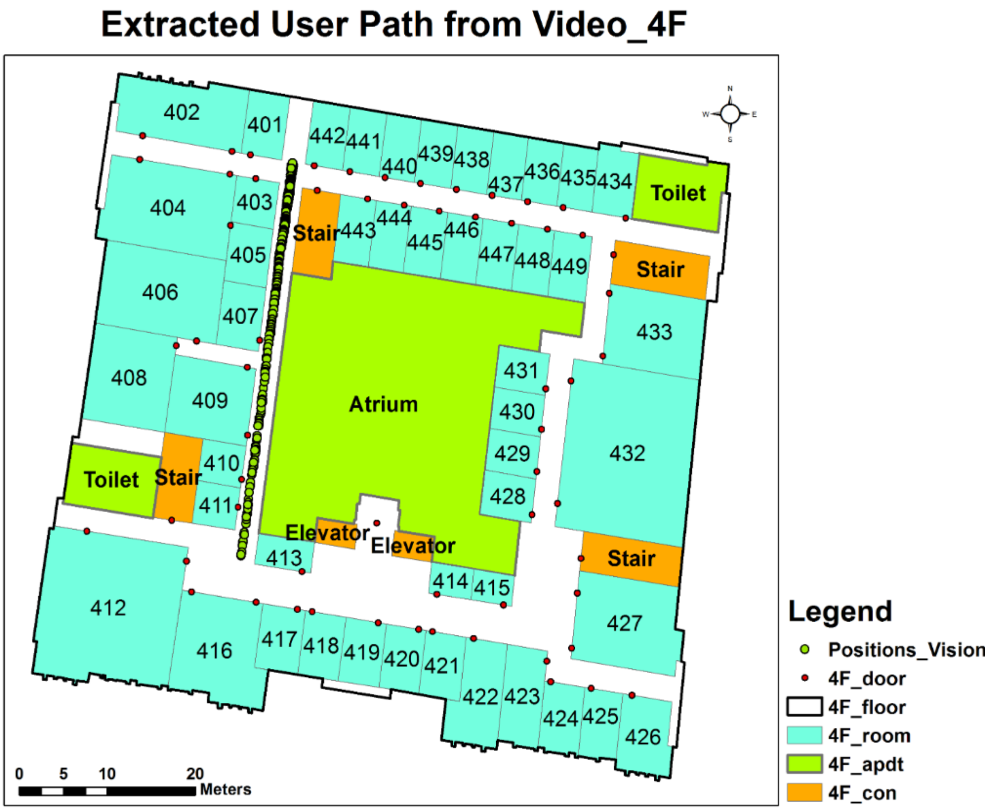

Fig.3.8.1.1. An example of using only one camera for visual tracking.

3.8.1.2. For Two Camera

The RMSE of visual tracking results is 0.06m for Camera#1 and 0.04m for Camera #2 respectively and the synthesised RMSE of the two-camera-based system by using the above method is 0.05m and the MAE for 10 experiments also remains a similar value (Table 3.8.1.2). This time two partial paths are obtained from visual tracking results, matching well with the designed path in corresponded parts. Both two paths have the problems of uneven distribution of position points as results of using single camera due to same reasons. In addition, there are some missing points when shifting from first camera to second as there are no entire detected human bodies in frames and they are deliberately removed by the designed algorithm (Fig.3.8.1.2).

TABLE 3.8.1.2
RMSE, MAE AND PRECISION OF USING TWO CAMERAS

Cameras	Camera #1	Camera #2
RMSE in the Presented Example	0.06	0.04
Synthesized MAE After 10 Experiments (m)	0.05	0.05
Precision (m)	0.02	0.01

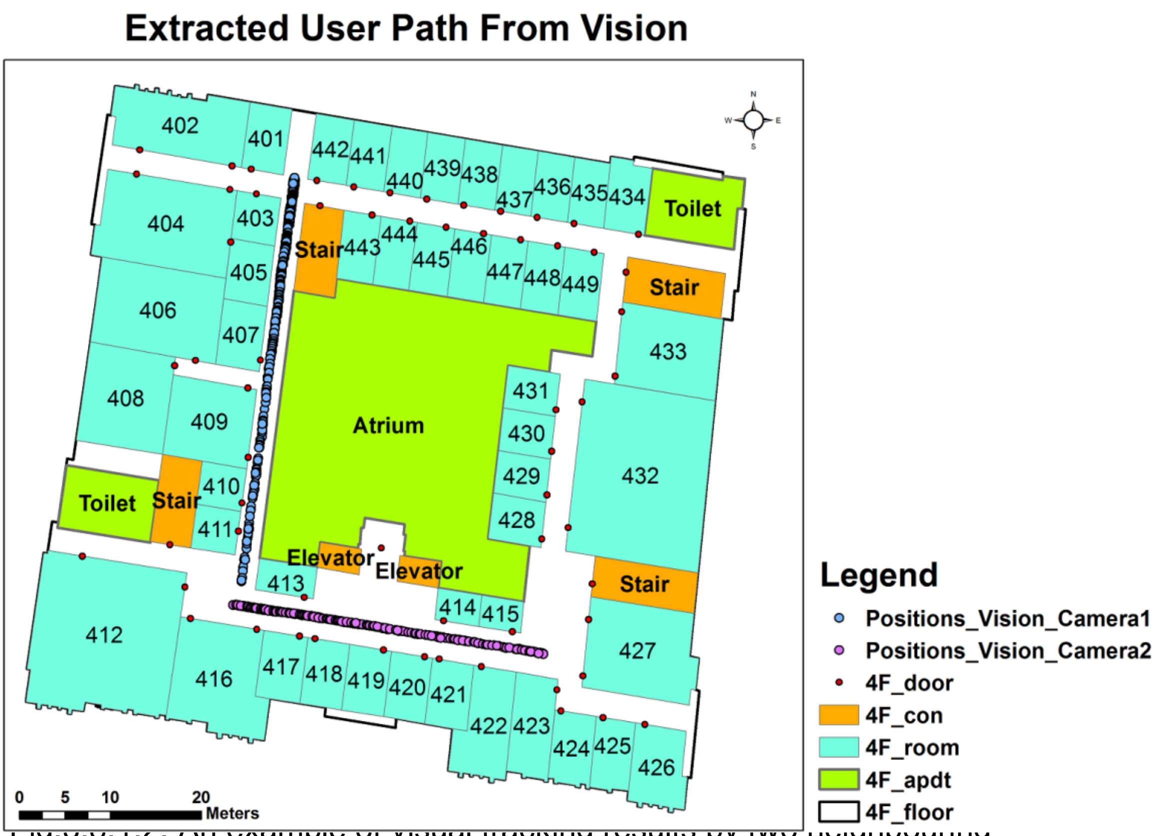

Fig.3.8.1.2: An example of visual tracking results by two neighbouring cameras.

3.8.1.3. For Four Camera

The RMSE of visual tracking results is 0.06m for Camera#1, 0.04m for Camera #2, 0.03m for Camera #3, and 0.04m for Camera #4 respectively. The synthesised RMSE of the four-camera-based system by using the above method is 0.04m and the MAE for 10 experiments also remains a similar value (Table 3.8.1.3). As the mechanism is similar to that of using two cameras for the whole floor tracking, thus, the problem of uneven distributed positioning points is also inherited. This time, the cameras only cover partial of the tracking area due to the original installed infrastructures (Fig.3.8.1.3), and the rest of the user movements need to be compensated by PDR.

TABLE 3.8.1.3
RMSE, MAE AND PRECISION OF USING FOUR CAMERAS

Cameras	Camera #1	Camera #2	Camera #3	Camera #4
RMSE in the Presented Example	0.06	0.04	0.03	0.04
Synthesized MAE After 10 Experiments (m)	0.04	0.04	0.04	0.04
Precision (m)	0.02	0.01	0.01	0.01

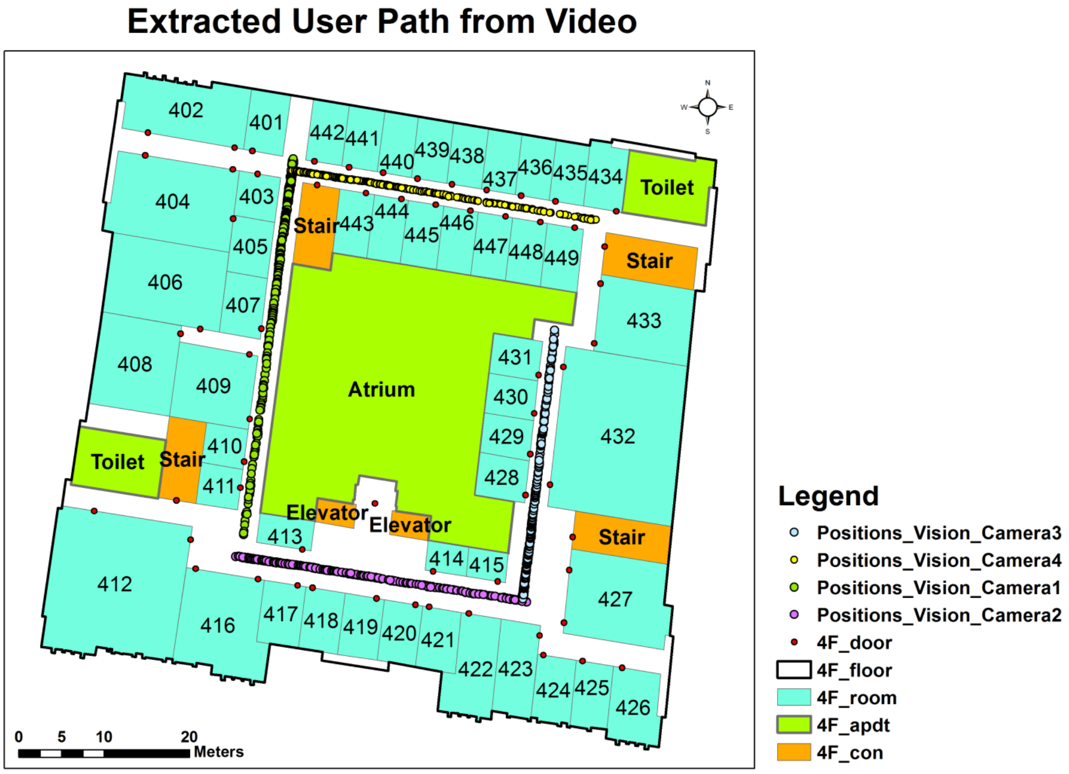

Fig.3.8.1.3. An example of visual tracking results by four cameras for entire floor.

3.8.1.4. Disadvantages of Directly Applying Visual tracking for PDR Calibration

As mentioned earlier in the accuracy calculation for visual tracking, the filming frequency cannot match with the step frequency and the detected target positions are always in the middle of a step but cannot identify the starting and ending points of each step event.

Meanwhile, the previous visual gait detection (Jiang and Yin, 2015, Jiang and Yin, 2017, Zhang and Zhou, 2018) is not suitable for this study as:

a) This study does not apply foreground masks, which is quite labour intensive and responds slowly, but using a pinhole model for distance estimation;
b) The filming frequency is lower than previous studies;
c) The ratio between IMU sampling frequency and filming frequency is not in integer.

This makes the results from visual positioning more time-domain based rather than gait-based, and these data are not suitable to be directly used for calibrating the PDR positioning in visible areas, though it has posiitoning

MAEs within 0.04~0.06m and precisions within 0.01~0.02m. However, this will not affect the headings between steps and these information can be later applied for PDR calibration.

3.8.2. Smartphone-Based PDR

As this study has applied the embedded sensors in the smartphones to provide the user positions, it may have a larger bias than commercial foot-mounted IMU sensors (Harle, 2013). The specific parameters of accelerations and gyroscopes of the selected smartphone models can be found in Table 3.8.2.

TABLE 3.8.2
RMSEs of Smartphone-Based IMUs of Seleced Smartphone Model

	X	Y	Z
HUAWEI Mate7			
Acceleration (m/s^2)	0.013	0.014	0.022
Gyroscope (rad/s)	0.0048	0.0032	0.0043
iPhone 7Plus			
Acceleration (m/s^2)	0.016	0.015	0.024
Gyroscope (rad/s)	0.0032	0.0034	0.0028

According to the above results, it can be found out that the accelerometers of the iPhone 7Plus have larger noise than that of the HUAWEI Mate7, which may be due to the higher sensitivity of the accelerometers in iPhone 7Plus. Meanwhile, the gyroscope from HUAWEI Mate7 has more noise than that of the iPhone 7Plus. This noise may also affect the results acquired by applying the designed PDR algorithms of different smartphone models. The following section will have an investigation of potential effects of this noise from accelerometers on the step detection and step length calculation as well as from gyroscopes on the heading estimation. This can help to evaluate the effectiveness of proposed PDR algorithm and the heading calibration algorithm respectively.

3.8.2.1. Tests on Different Types of Smartphones before Visual Integration

This specific experiment is conducted on the trajectory with similar setups to that of applying the single camera, repeating for 10 times. For the effects of noise from the accelerometers, it is evaluated by comparing the results from the true measurements to those with and without applying the corresponding PDR algorithm before visual calibration. The specific results can be found in Table 3.8.2.1.1 and Table 3.8.2.1.2.

According to the acquired results, it can be found that the application of the proposed step detection algorithm can improve the accuracy of detected steps than using the embedded apps inside the smartphones (Table 3.8.2.1.1). This has suggested the effectiveness of the proposed algorithm on the aspect of step detection. Meanwhile, the results also show that iPhone 7Plus has better accuracy of step detection with and without the processing by the applied PDR algorithm than that of HUAWEI Mate7. This may be due to the higher sensitivity of the accelerometers in iPhone 7Plus than that in HUAWEI Mate7. It can also be viewed from Fig.3.3.1 as its acceleration changes are more significant than Android phone.

TABLE 3.8.2.1.1

MEAN ERROR OF DETECTED STEPS WITH AND WITHOUT ALGORITHM PROCESSING

Smartphone Model	HUAWEI Mate7	iPhone 7Plus
Counted Steps	83	83
Mean Estimated Steps with Embedded Step Counting App	77	79
Mean Error (%)	7.23	4.82
Mean Estimated Steps with Applying Proposed Algorithm	81	84
Mean Error (%)	2.41	-1.20

For the step length estimation, it can be found that before being processed by the calibration method mentioned in Section 3.3.2, the step lengths estimated based on the data from HUAWEI Mate7 have a slightly better average performance than those by iPhone 7Plus (Table 3.8.2.1.2). This may be due to the higher noise of accelerometers in iPhone 7Plus (Table 3.8.2), leading to the accumulations of step length error in the selected examples (Fig 3.8.2.1). This can be mitigated by the introduction of step length calibration as MAEs of step length estimation from the both types of smartphone models have been significantly improved based on the results in Table 3.8.2.1.2. Moreover, their average performances have reached a similar level, which can help to remove the effects caused by the different precision of the accelerometers in corresponding types of smartphones. However, as the noise of accelerometers from iPhone 7Plus is slightly larger than that of HUAWEI Mate7 due to its higher sensitivity, HUAWEI Mate7 has a slightly better average performance of step length estimation than iPhone 7Plus in this experiment.

TABLE 3.8.2.1.2

MAEs of Step Length Estimation with and without Algorithm Processing

Smartphone Model	HUAWEI Mate7	iPhone 7Plus
Measured Step Length (m)	0.63	0.63
Mean Step Length without Step Length Calibration	0.81	0.82
MAE (m)	0.18	0.19
Mean Step Length with Step Length Calibration	0.64	0.65
MAE (m)	0.01	0.02
Improvement of MAE (%)	94.4%	89.5%

For effects of noise from the gyroscopes, it is evaluated by comparing the results between those acquired by the application of corresponding PDR algorithm before calibration and those measured from the referential points on the georeferenced maps. According to the acquired PDR results, it can be visualized that they have suffered from bias drift, which is especially severe after turning the corner in the presented example (Fig.3.8.2.1).

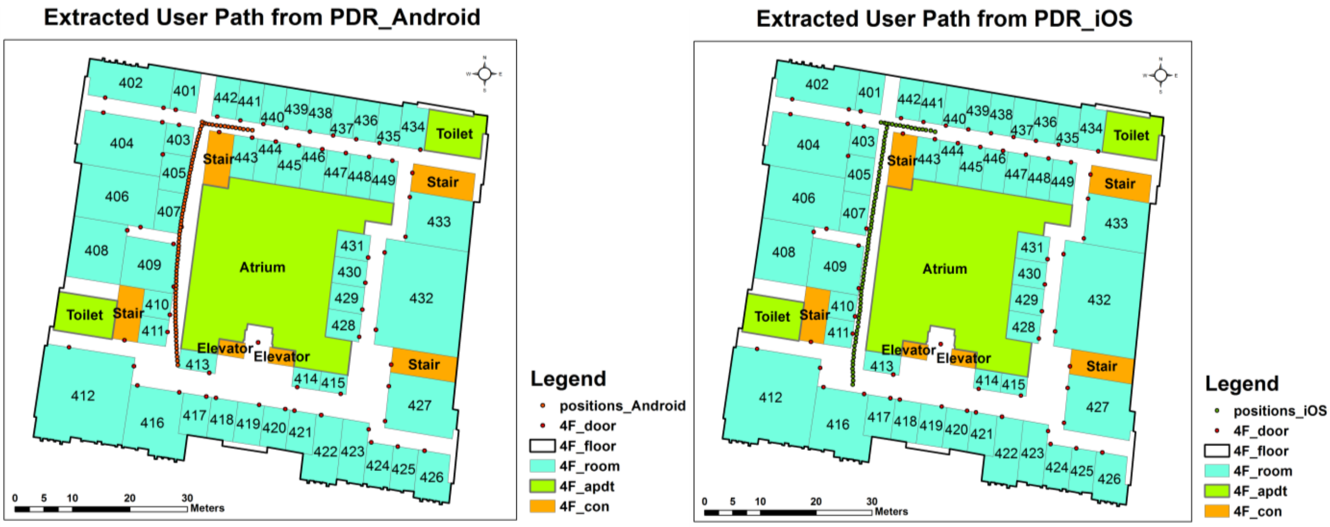

(a) (b)

Fig.3.8.2.1. Examples of smartphone-based PDR before calibration by Android (a) and iOS (b).

When comparing the accumulated errors of the heading between the two selected smartphone models, it can be found that HUAWEI Mate7 has more drifts than iPhone 7Plus (Table 3.8.2.1.3), which is caused by the higher noise of gyroscope in HUAWEI Mate7 than that in iPhone 7Plus (Table 3.8.2). This phenomenon will be more severe with the accumulation of time when walking on longer paths, especially for using HUAWEI Mate7. The introduction of calibration from the visual tracking may help to mitigate this problem by reducing the effects of noise from the gyroscopes.

TABLE 3.8.2.1.3
MAEs OF HEADING ESTIMATION WITH ALGORITHM PROCESSING

Smartphone Model	HUAWEI Mate7	iPhone 7Plus
MAE of Synthesized Angular Velocity before Calibration(rad/s)	0.004	0.003
MAE of Heading Estimation before Calibration(rad)	0.208	0.156

The RMSE of the acquired positioning results based on PDR processing is 0.83m (Android) and 1.05m (iOS) respectively, in the presented example (Fig.3.8.2.1). According to the MAEs after 10 repeated experiments, the average positioning performances of both two types of smartphone models are similar, with 0.82m for Android and 0.83m for iOS respectively. This may be due to the larger variations of the positioning performances by iPhone 7Plus, which is particularly caused by the noise from the accelerometers, leading to larger errors in the precision of the results. Meanwhile, it can also be found that the positioning accuracy of HUAWEI Mate7 is more affected by the noise from the gyroscopes. According to the results, it has a slightly higher accuracy on step length estimation (Table 3.8.2.1.2) and comparable accuracy on step detection (Table 3.8.2.1.1). However, it still has comparable MAE and precision for the positioning results to those from iPhone 7Plus (Table 3.8.2.1.3).

TABLE 3.8.2.1.3
ACCURACY AND PRECISION OF POSITIONING BY SMARTPHONE-BASED PDR

Smartphone Model	HUAWEI Mate7	iPhone 7Plus
RMSE in the Presented Example	0.83	1.01
MAE of 10 Experiments(m)	0.82	0.83
Precision (m)	0.15	0.18

3.8.2.2. Selection of Better Calibration Method without Step Length Calibration by Using Single Camera

The comparison of two calibration methods is based on calibrated PDR results on both Android and iOS platforms by using one camera and the results are summarized in Table 3.8.2.2.1 and 3.8.2.2.2. In order to remove the effects from the step length calibration, this comparison does not include this process in the positioning estimation.

The position-replacement method directly replaces the PDR results by vision-based tracking positions based on finding the closest time stamps. Comparing its results to those of pre-calibration, this method provides a better solution than using PDR-only tracking system as it takes the advantage of accurate positioning by OPS in LoS area. Moreover, the ending positioning point of calibrated PDR matches with that of the referential path (Fig.3.8.2.2.1). Thus, it can provide a correct starting point for the following tracking if a second camera is introduced into the current system.

The RMSEs for selected examples from two smartphones reach the similar level, which are 0.73m (Android) and 0.75m (iOS) respectively, suggesting this method is able to handle the positioning calibration regardless of the smartphone models by removing the effects of the noise from the embedded gyroscopes. The MAEs of the positioning do not change significantly after repeating 10 times (Table 3.8.2.2.1) with slightly lower variations (Table 3.8.2.2.2). This may be explained by two reasons. First, the pinhole effect from depth estimation can affect the step length estimation in the visual tracking, leading to the uneven distribution of step points. Second, the different sampling frequency of two positioning system can affect the time synchronization of the positioning results. The application of this method also introduces these errors to calibrated results by direct position replacement (Yan et al., 2018a). However, it should be noticed that the variations caused by the larger noise of the accelerometers in the iOS-based smartphone have been slightly mitigated as the position replacement can help to smooth its effects on step length estimations.

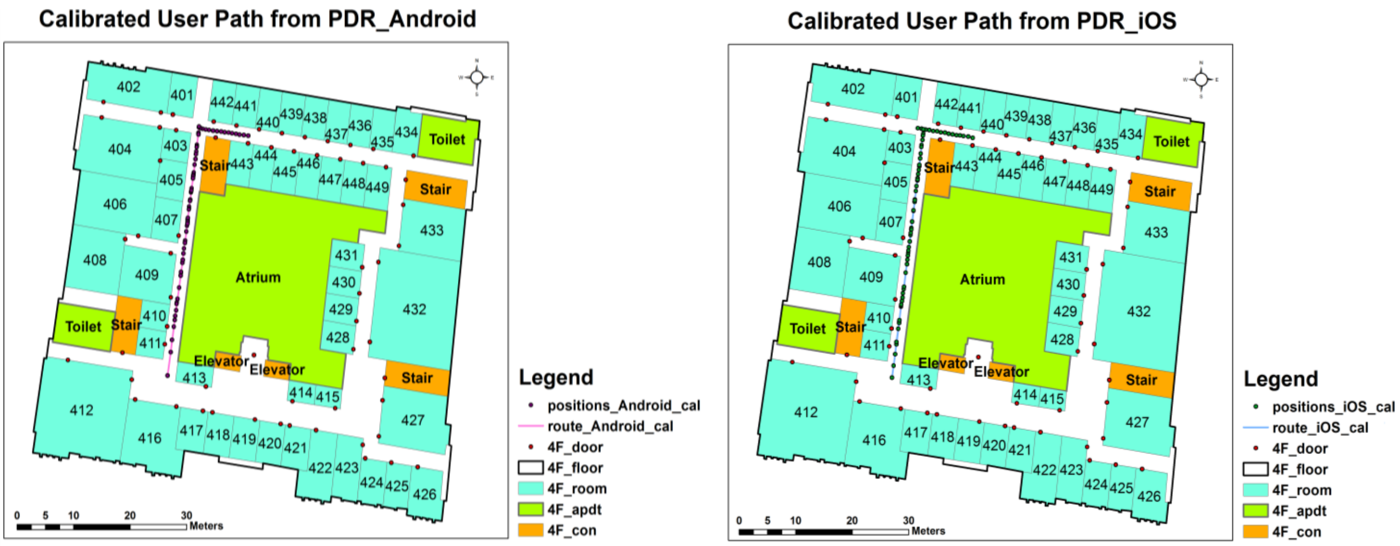

(a) (b)

Fig.3.8.2.2.1. Examples of calibrated smartphone-based PDR by position replacement method by Android (a) and iOS (b).

The heading calibrations only introduce the replacements of heading estimated from the visual tracking results, while keep the walking mechanism of pedestrian similar as that used for marking referential points. Comparing to the results of using the former method, the heading calibration is more accurate as the uneven distribution effect caused by pinhole model has been mitigated by only calibrating the orientations but keeping original step lengths for position estimation. Meanwhile, it still takes the merits of the previous position-replacing-based hybrid system on removing the effects of the noise from the embedded gyroscopes.

This also leads to lower RMSEs than using the former method in selected examples as 0.51m (Android) and 0.56m (iOS) (Fig.3.8.2.2.2). After repeating for 10 times, their MAEs are also better than using the previous method while having similar values for both types of the smartphones (Table 3.8.2.2.1), with much better precisions than using the former method (Table 3.8.2.2). This may be because this method has mitigated the effects caused by the time synchronization to find the corresponding referential points. However, according to Table 3.8.2.2.2, the positioning precision of the iOS-based smartphone by using this method is still not as good as that of the Android-based system. This is due to that it has slightly larger noise from the accelerometers, which can affect the step length estimation and this has not been overcome by using heading calibration only at the current section. This can be improved by the later introduction of step length calibration. Moreover, it also has the potential to be adjusted to online calibrations. The heading information acquired from every two consecutive frames can be directly used for real time PDR heading calibrations other than post-processing. However, it has the problem that the ending point may not be perfectly matched with that of the referential path as there are still some errors in the step-length estimation process (Yan et al., 2018a).

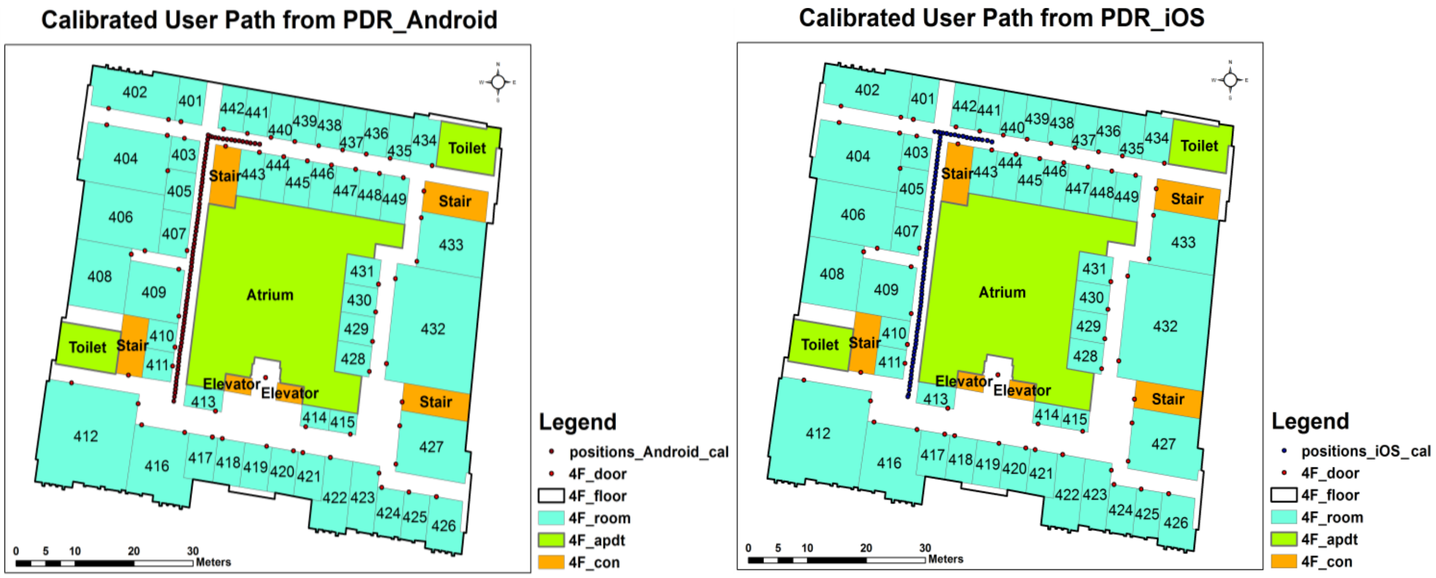

(a) (b)

Fig.3.8.2.2.2. Examples of calibrated smartphone-based PDR by heading calibration method by Android and iOS.

When checking their Cumulative Distribution Function (CDF) of errors for selected samples, the advantage of using second method, i.e. heading calibration, becomes more prominent as it has more points with lower errors compared to the original data and position-replacement method. In addition, it also helps to reduce the maximum positioning error as showed on the CDF distribution. On the other hand, the position-replacement method seems to have more variations, though it has more positioning points with lower errors than the original, leading to lower RMSE. Some of points introduce more errors as it has wider distribution of error range and the maximum error of the positioning point is also larger than the original data, due to the pinhole effects of directly using visual tracking results (Fig.3.8.2.2.3).

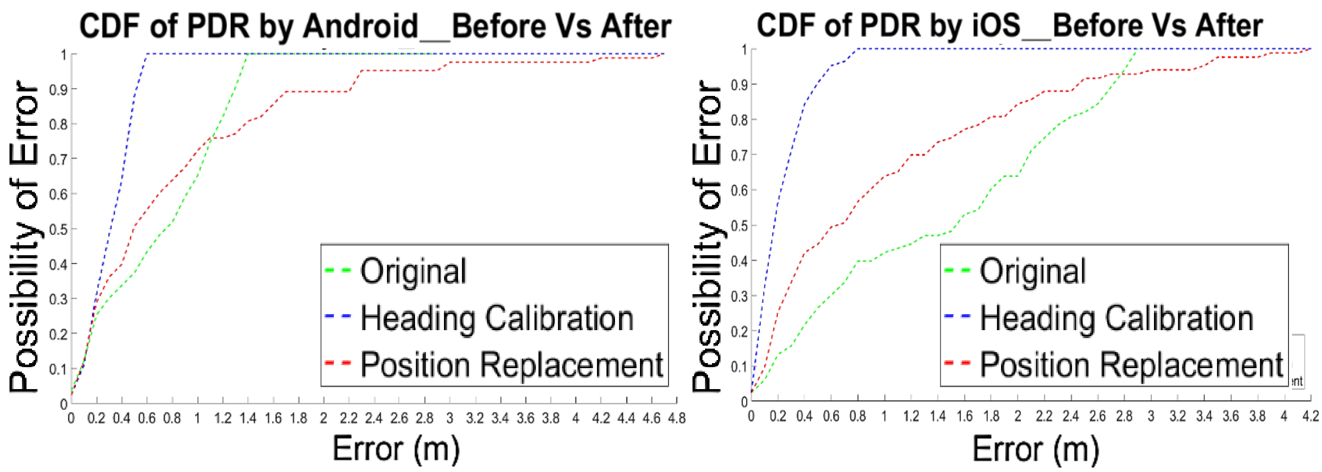

(a) (b)

Fig.3.8.2.2.3. Examples of CDF of smartphone-based PDR by Android and iOS before and after calibration. (The original in green, the position replacement in red and the heading calibration in blue).

TABLE 3.8.2.2.1
MAEs OF TWO SMARTPHONE-BASED PDR BEFORE AND AFTER VISUAL CALIBRATION

		Device	
Mean Location Accuracy (MAE)		Huawei Mate7	iPhone 7Plus
Pre-Calibration		0.82 m	0.83 m
Post-Calibration (Without Step Length Calibration)	Position Replacement	0.73 m	0.73 m
	Improvement	10.9%	12.0%
	Heading Calibration	0.51 m	0.52 m
	Improvement	37.8%	37.3%

TABLE 3.8.2.2.2
PRECISION OF TWO SMARTPHONE-BASED PDR BEFORE AND AFTER VISUAL CALIBRATION

		Device	
Precision		Huawei Mate7	iPhone 7Plus
Pre-Calibration		0.15 m	0.18 m
Post-Calibration (Without Step Length Calibration)	Position Replacement	0.13	0.14
	Improvement	13.3%	22.2%
	Heading Calibration	0.07	0.08
	Improvement	53.3%	61.1%

In all, the hybrid system has higher accuracy than the PDR-only system by reducing the noise from the embedded gyroscopes, regardless of using either position-replacing-based or heading-correction-based calibration (Table

3.8.2.2.1). The heading-calibration-based approach is more accurate in this study with better MAE, as it maintains the walking mechanism of pedestrians, while mitigating the errors from the time stamp synchronization of finding corresponding referential marked step points. In addition, the results indicate that the design of hybrid system can handle both types of smartphone models by achieving similar level of accuracy after calibration. As both types of the smartphones are common models in the market, it suggests that this system has the potential to become a ubiquitous solution for indoor positioning. However, the results in this section only depend on using a fixed k for coefficient of step length SL_i estimation without the considerations of removing noise caused by the accelerometers. This can be modified and improved into a more case-dependent value which is determined by the ratio η between estimated distance and real distance of designed walking trajectory for the experiment. This processing will be included in the following experiments with multi-cameras.

3.8.2.3. The System with the Integration of Two Cameras

By applying the approaches in Section 3.4.1, the data integration of multiple cameras has become plausible for the system. The referential walking path with the marked step points of this experiment is presented in Section 3.7.1.2. In the selected example, the iOS platform has detected the correct number of steps while the Android system only has detected 141 steps. After repeating 10 times, both types of the smartphones have the similar problem of missing step detection as in the previous single-camera experiments. Both the iOS-based and the Android-based smartphones tended to detect 1~2 fewer steps (Table 3.8.2.3.1). Currently, there is no proper solution for this problem for this kind error caused by the noise from the embedded accelerometers.

TABLE 3.8.2.3.1

MEAN ACCURACY OF STEP DETECTION BY USING TWO SMARTPHONE MODELS

Smartphone Model	Counted Steps	HUAWEI Mate7	iPhone 7Plus
Detected Steps	143	141	142
Mean Accuracy	100%	98.6%	99.3%

According to previous results, heading calibration, which replaces each step's heading acquired from PDR by orientation decided by two consecutive frames with similar time steps, is more accurate than position replacement method. In the following experiments, the user position will be re-calculated based on the integration of these calibrated headings and it will also introduce the calibrated step length SL'_i after applying η as mentioned in **Section 3.3.2**. This can also help to improve the final accuracy of system by mitigating the errors from step length estimation, which are caused by the noise from the embedded accelerometers.

In the selected examples before calibration, the RMSE of positioning is 0.22m by using iPhone and 0.52m by using HUAWEI Mate7, respectively. After repeating 10 times along the same walking trajectory, the MAEs of these two specific smartphone models are similar at about 0.3m (Table 3.8.2.3.2). This may be due to the introduction of step length calibration, which can help to reduce the errors caused by the noise from the embedded accelerometers. Together with the better performances of the step detection from iPhone 7Plus, the pre-calibration MAE of iOS-based smartphone is slightly better than that of the Android-based smartphone. This can also explain the better pre-calibration performances of the precision of both types of smartphone models.

After calibrating the heading information, the RMSE of selected examples has reached 0.21m (Android) and 0.16m (iOS) (Fig.3.8.2.3) respectively. The MAE after taking 10 repeated experiments has reached about 0.14±0.01m, with more than 50% improvement. Meanwhile, as it has reduced the errors caused by the noise from the embedded gyroscopes, the precisions of positioning for both types of the smartphones have also been improved (Table 3.8.2.3.2).

TABLE 3.8.2.3.2

MAE AND PRECISION OF STEP DETECTION BY USING TWO SMARTPHONE MODELS BEFORE AND AFTER VISUAL CALIBRATION

Smartphone Model	HUAWEI Mate7	iPhone 7Plus
MAE Before Visual Calibration (m)	0.31	0.29
MAE After Visual Calibration (m)	0.15	0.13
Improvement	53.3%	51.7%
Precision Before Visual Calibration (m)	0.11	0.12
Precision After Visual Calibration (m)	0.06	0.05
Improvement	45.5%	58.3%

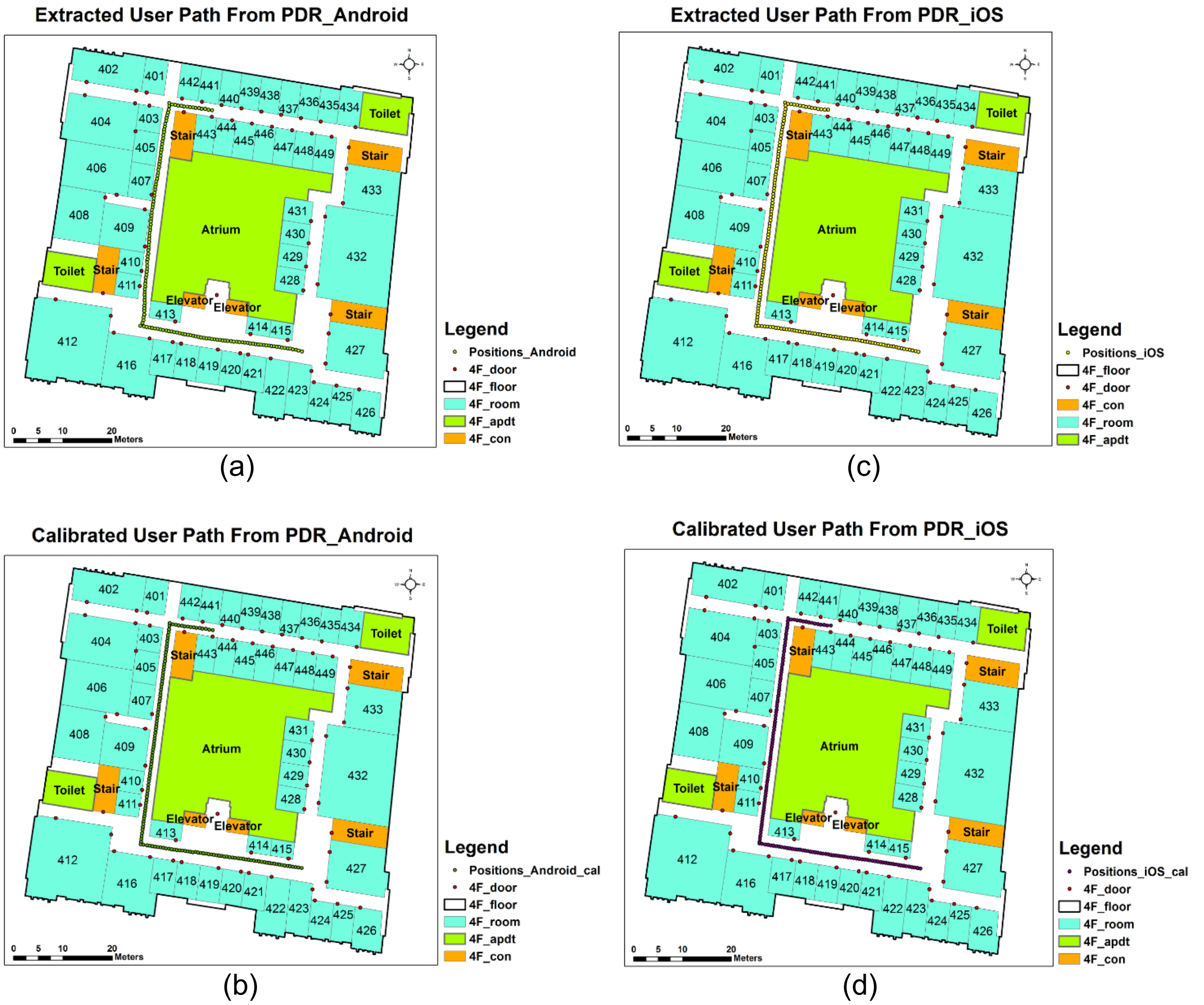

Fig.3.8.2.3. The comparison of pre-calibration and post-calibration of PDR using two cameras on Android (a)-(b) and iOS (c)-(d).

3.8.2.4. The System with the Integration of Four Cameras

Based on the results acquired from the previous experiment, the user tracking along the entire floor becomes plausible with the same mechanism. This time, four cameras are used for heading calibrations. The referential walking trajectory with the marked step points of this experiment is presented in Section 3.7.1.3 for later comparison with estimated positioning results. Both iOS and Android systems have detected the correct number of steps in the presented examples. For their MAEs after 10 experiments, the missing detection of steps still exits as the noise from the embedded accelerometers cannot be overcome by the proposed step detection algorithm and they will grow simultaneously with the increasing trajectory length (Table 3.8.2.4.1). In addition, the unstable connection of the Wi-Fi during the experiments can also cause the interruption of the data transfer for positioning estimation.

TABLE 3.8.2.4.1

MEAN ACCURACY OF STEP DETECTION BY USING TWO SMARTPHONE MODELS

Smartphone Model	Counted Steps	HUAWEI Mate7	iPhone 7Plus
Detected Steps	272	268	269
Mean Accuracy	100%	98.5%	99.2%

The positioning results of calibrated user positions from both types of phones match well with the reference path and reach similar level of accuracy, with RMSEs of 0.15 m (Android) and 0.12 m (iOS) in the presented example (Fig.3.8.2.4). The MAEs of two types of smartphones after calibration is at about 0.11 m with more than 60% improvement than the pre-calibrated results. This is related with the increasing proportion of visible areas with more introduction of visual calibration. Their precision after calibration is about 0.07 m with an improvement in the range of 54.5% to 66.7%, which is still related with the miss detection of the step events as the detection accuracy is better by using iPhone 7Plus (Table 3.8.2.4.2).

TABLE 3.8.2.4.2

MAE AND PRECISION OF STEP DETECTION BY USING TWO SMARTPHONE MODELS BEFORE AND AFTER VISUAL CALIBRATION

Smartphone Model	HUAWEI Mate7	iPhone 7Plus
MAE Before Visual Calibration (m)	0.31	0.29
MAE After Visual Calibration (m)	0.12	0.10
Improvement	61.3%	65.5%
Precision Before Visual Calibration (m)	0.12	0.11
Precision After Visual Calibration (m)	0.08	0.06
Improvement	54.5%	66.7%

This experiment has shown that the proposed hybrid system is available for single user tracking on the entire floor regardless of smartphone models, by achieving similar level of MAEs after calibration. This suggests that the proposed system has the potential to become a ubiquitous solution for indoor positioning. In addition, as this system utilizes the existing indoor infrastructures and user devices, it can achieve a low-cost solution without the installation of the additional sensors. Moreover, it also has the potential to be adjusted by online calibrations, as the heading information acquired from every two consecutive frames can be directly used in real time PDR heading calibrations for position estimation, other than post processing. However, the application of this system is based on the assumption of existence of a complete surveillance system and the designed system is more suitable to be applied to public indoor space.

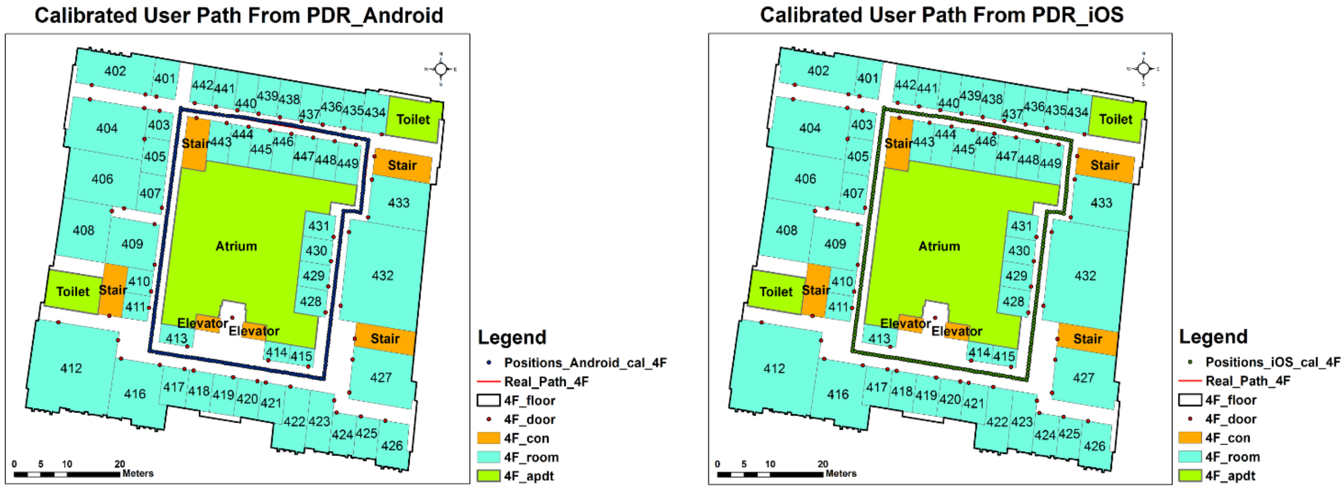

(a) (b)

Fig.3.8.2.4: The calibrated smartphone-based PDR for whole floor tracking.

3.8.2.5. 2D System Validation

The above experiments described in **Section 3.8.1.1** to **3.8.2.4** is based on the data of a single user. In order to validate the robustness of the designed 2D system, more variations of participants have been introduced with similar experimental setups as using two cameras, which can be found in **Table 5.2.3.1.2** of Section **5.2.3.1.1** in Chapter 5 with more females and males involved in the experiments. In addition, this study also has involved a group of the same number of males and females who are unfamiliar to the selected building, i.e. PMB, to participate in the experiment. The acquired results have both achieved similar accuracy and precision as listed in Table 3.8.2.3.2. This has suggested a relatively stable performance of the designed 2D system with various users.

In addition, the similar 2D experimental setups have also been tested in at a specific floor with similar structure in another building at UNNC, which is used for 3D building model establishment by matching the measured 2D trajectory to the corresponding 2D Laser Scanning (Chen et al., 2018, Yang et al., 2019). According to the achieved accuracy (Yang et al., 2019), the distribution of positioning error is also similar as that descried in the CDF in this study (Fig. 3.8.2.2.3), with a maximum value of RMSE at 0.81m (0.8m in this study). This has suggested the reliability of the application of the designed 2D system under various environments.

3.8.2.6. The Comparison to Other PVINS with Similar Setups

The details of the approaches for two similar studies conducted before have already been described in Chapter 2. Comparing with the study conducted by Shanghai Technology University (Zhang and Zhou, 2018), the best performance of RMSE of their proposed PVINS can achieve an accuracy of 0.08m, with all positioning areas are in the view of camera. However, the minimum RMSE achieved in this study is still comparable to that, even with less visible areas (90.04%). The other study conducted by Missouri University (Jiang and Yin, 2015, Jiang and Yin, 2017) has a minimum RMSE of 0.5m, with a maximum improvement of 22.6%, summarizing from four tests. This is lower than the results achieved in this study with a minimum RMSE at 0.08m and the corresponding maximum improvement of 65.5% (Table 3.8.2.3.2). This may be due to that this study has more visible areas, which has more effect from the visual tracking calibration. Meanwhile, the designed path as ground truth has a similar rectangular shape of walking trajectory as applied in the previous studies. This means the proposed system is comparable to other studies under similar conditions of environmental complexity. Meanwhile, it has slightly more turnings than those in the previous studies, which may introduce more noise from the gyroscopes when in the invisible areas.

Moreover, the ending points of both calibrated paths match well with the entrance of building, which can keep tracking user trajectory and later be directly shifted to the outdoor positioning system with available GPS signals. This system also has been tested on two types of smartphones while the previous studies mainly focus on Android-based systems. However, the system proposed by this study cannot provide gait-feature based visual tracking as in (Jiang and Yin (2015), Jiang and Yin (2017), and Zhang and Zhou (2018)), which makes the visual tracking results not fully compatible with step event mechanism of PDR. It makes this system more single-directional calibration based, i.e. calibrating PDR by visual tracking not calibrating visual tracking by PDR.

TABLE 3.8.2.3.2

POSITIONING ACCURACY COMPARISON BETWEEN OHTER STUDIES USING PVINS

Reference	(Jiang and Yin, 2015, Jiang and Yin, 2017)	(Zhang and Zhou, 2018)	This Study
FPS	30	20	17
Visible Area	>50	100	90.04
Device	Samsung Galaxy S4	Huawei Honor8	Huawei Mate7, iPhone 7Plus
Turnings	4	3	6
Best RMSE (m)	0.50	0.08	0.08
Maximum Improvement (%)	22.6	56.5	65.5
Calibration	Bi-directional	Bi-directional	Single-directional

3.9. SUMMARY

Findings from this chapter contributes the design of a hybrid system for 2D multi-camera PVINS supported by the digital map information in WGS 1984 on distributed platforms, with a relatively high accuracy of 0.07%. The accuracy is better than required accuracy targeted by several emergency services, including the Federal Communications Commission (FCC) (50m). It is even significantly higher than the best performances provided by the Commercial Mobile Radio Service (CRMS) reported in FCC (5~10 m) (FCC, 2015). Both sub-systems can work independently with the support of digital map information. The accuracy of inertial system in the visible areas can be improved by additional visual tracking information while the PDR data can reversely compensate the visual data in the invisible areas. This hypothesis has been proved in this experiment as the accuracy of calibrated results from both smartphones has been significantly improved and achieved similar levels. Its algorithm for pedestrian detection, i.e. Faster R-CNN, can be directly implemented without training by utilizing online resources while achieving real-time detection with high detection accuracy.

Meanwhile, it first introduces a novel algorithm for automatic scene-shifting integrated with PDR's automatic turning recognition. Meanwhile, it also finds out a simple but effective novel algorithm to integrate PDR and visual tracking systems. It first puts forward two kinds of calibration algorithms: the direct position replacement and the heading calibration. By comparing the calibrated results, it finds out that the latter one is more accurate than the former one as it follows the mechanism of PDR with the maintenance of step event detection. It has also achieved similar accuracy as previous 2D PVINS under similar conditions of environmental occlusion and complexity, but with simpler implementation. This system has also been tested on two common smartphone operating systems in search for a potentially ubiquitous solution. It also has the potential to be a low-cost solution as it does not need additional installation of sensors but only utilizing available sensors from user and indoor environment. Moreover, the acquired results with absolute world coordinates can be directly used in outdoor systems and visualized in corresponding floor plan. However, the acquisition of surveillance data may be a limitation as it will raise the issue of personal privacy and this time a permission is pre-applied for data downloading. In the next chapter, this system will be developed into a more comprehensive arrangement with the ability to track the entire movement of a single user in the building with multiple floors as this study only tests on a single floor. The smartphone-based PDR system will be further tested on staircase-walking with the support of a barometer for height detection, in order to automatically change to related floor plan.

Chapter 4. 3D VISION-AIDED INDOOR PEDESTRIAN DEAD RECKONING WITH BAROMETER

4.1. INTRODUCTION

In previous chapter, it shows the proposed designed system works well on single floor positioning, in other words, in horizontal directions. The 3D PVINS designed in this study is developed based on the 2D multi-camera PVINS mentioned in the previous chapter, to continuously track user movements inside the buildings with surveillance cameras with known-locations and user-held smartphones, supported by auto-shifted corresponding digital floor maps. However, the previous 2D PVINS more focuses on providing positions in horizontal directions (Yan et al., 2018c, Yan et al., 2018b, Yan et al., 2018a). In order to enrich the information of the third dimension, the smartphone-embedded barometer will also be integrated in this study for floor detection. This chapter will provide a novel design of a low-cost 3D indoor tracking system and the prototype will be tested in a four-floor building by using two types of smartphones, running both of the most widely used operating systems of iOS and Android separately. Moreover, the environmental conditions will have higher proportions of occlusion areas than in previous experiments mentioned in Chapter 3, which is limited by the currently installed surveillance cameras in the indoor area. This may also help to further test the robustness of designed system under extreme occlusive conditions, which is closer to the real scenarios in the fire evacuations.

4.2. SYSTEM DESIGN

The proposed system is designed and developed based on the previous 2D vision-aided PDR (Yan et al., 2018c, Yan et al., 2018b, Yan et al., 2018a) to the 3D version (Fig.4.2). During the operation, the smartphone-based PDR keeps actively tracking the user movement, while the OPS only functions in the LoS areas, shifting from one scene to another. During the movement, the smartphones are held horizontally and pointing forward. The accelerations and the angular velocities are collected simultaneously. The former is used for step detection and step length estimation while the latter is applied for heading estimation. The integration of these data can help calculate relative 2D PDR positions. Meanwhile, the video recording is triggered since the user starts moving. Once entering the LoS area of each camera and a significant change is detected from the estimated PDR headings, the 2D visual positions will be calculated based on BBs' positions by pedestrian detection and the estimated depth information in corresponding frames. Meanwhile, the 3D information of the corresponding functioning camera will also be reported to the main system, which will help to calibrate the floor detection. The 2D visual headings are determined by visual positions in every two consecutive frames (Yan et al., 2018a). They will later be used for 2D PDR heading calibration based on similar time stamps. For data fusion, this study replaces previous time-synchronization-based position replacement in (Yan et al., 2018b) by using synthesized results from calibrated headings and PDR step lengths. This is because heading calibration responses better to the real-world scenarios based on the conclusions in (Yan et al., 2018a) mentioned in previous chapter, thus it can provide better synthesized position estimation.

Before 2D calibration, the 2D results from PDR and visual tracking should both be transformed into real geographical coordinates, i.e. geo-coordinate transformation. It is beneficial for further development of seamless indoor-outdoor positioning (Yan et al., 2018b, Yan et al., 2018a). To achieve that, the corresponding floor plans will help to provide absolute positioning information. These maps are pre-stored in the system and will be integrated into the 2D PVINS results by automatic selection based on the results of floor detection. The system in 2D PVINS aspect is providing a calibrated 2D path in an absolute coordinate system at each epoch, i.e. the corresponding time stamps of each step. This 2D path will later be integrated with the estimated height and floor information by finding the similar time stamps.

For 3D information, the system uses the smartphone-based barometer to continuously identify the current floor of the user during movements. Before the start of operation, the barometer needs a self-calibration. This is done by comparing and adjusting the two readings acquired from two smartphone apps installed on the very same smartphone. One is chosen as the 'standard' pressure, and the other is calibrated measurement for the same reading. The calibrated measurements are then processed for height estimation and floor detection. This process will be discussed in more details in the following sections. This chapter has tested different algorithms and investigated a relatively optimal solution. With the 3D locations of cameras already stored in the system, the calibration results for the floor detection can also be improved.

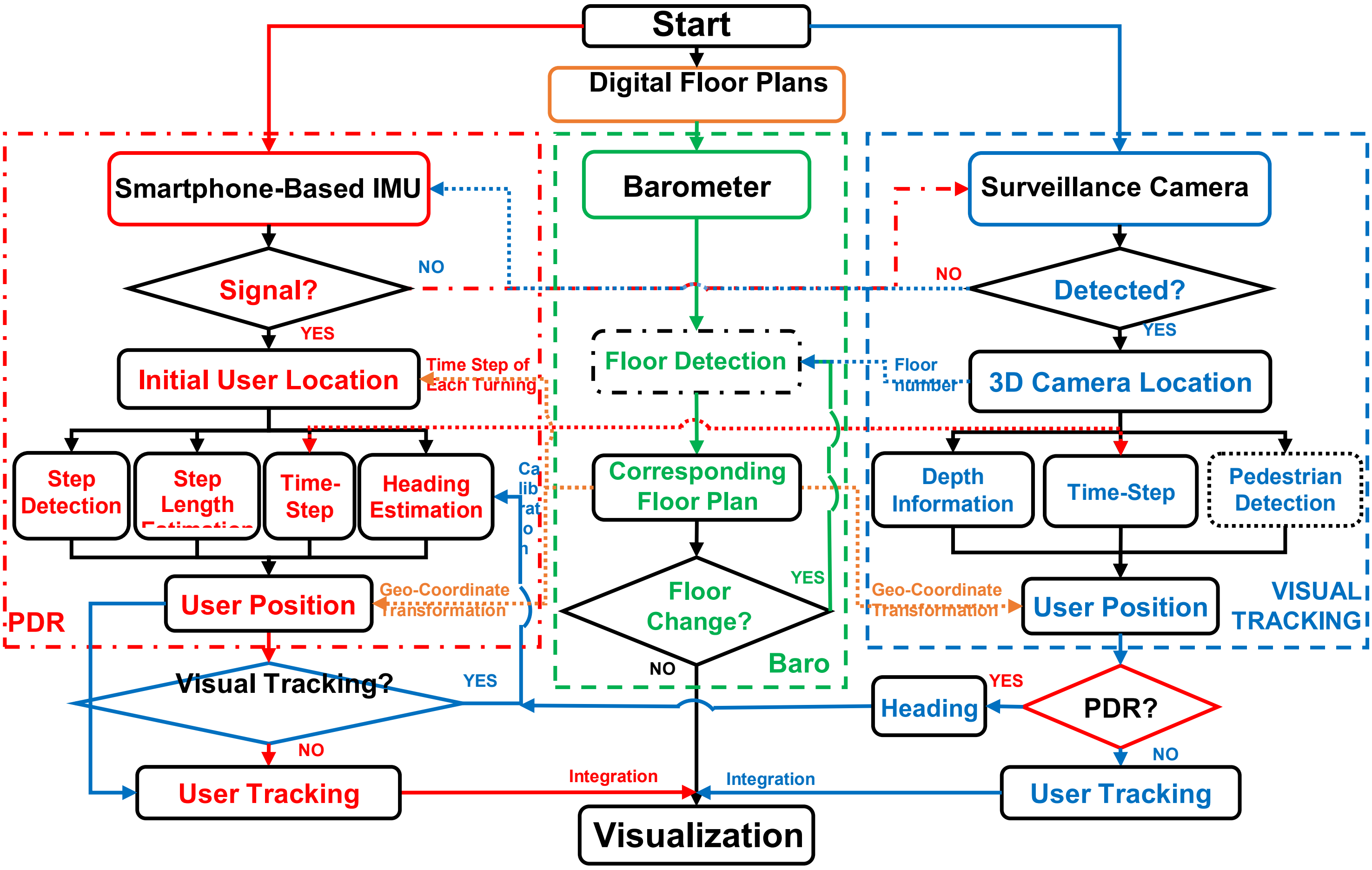

Fig.4.2. The architecture of the proposed system (PDR, Visual, Barometer, and digital floor plans are represented in red, blue, green and orange, respectively). The pedestrian detection and the PDR in dash-boxes have been described in Chapter 3, the floor detection is described in the following).

Having distinguished the floors, the results will be integrated with 2D PVINS with a minimum difference of time stamps. The final 3D path will be presented in a 2D form on each floor with the corresponding georeferenced floor plan for visualization.

4.3. PRESSURE-HEIGHT MODEL FOR FLOOR DETECTION

4.3.1. Pressure-Height Model

A barometer altimeter allows height estimation based on air pressure above the given reference level, which is by default sea level (Li et al., 2013a, Sabatini and Genovese, 2014, Shen et al., 2015, Xia et al., 2015). According to a recent document of Pressure Reduction Formula by World Meteorological Organization's (WMO) Commission for Instruments and Methods of Observation (CIMO), the change of pressure ΔP is proportional to the change of height/altitude Δh, regarding the gas density ρ and gravity g as constant:

$$\Delta P = -\rho g \Delta h \tag{4.3.1.1}$$

It can be rewritten as:

$$= -\frac{P}{R_s T} g.\Delta h \tag{4.3.1.2}$$

whereas R_s is the specific gas content, and it is usually treated as a constant under dry air condition in R_d. The formula can be then be transformed into

$$P = P_0 \times \left(\frac{T}{T_0}\right)^{\frac{g}{R_d \Gamma}} \; (\Gamma = -\frac{\Delta T}{\Delta h}) \tag{4.3.1.3}$$

whereas P_0 is the sea-level pressure, P is the air pressure of the current level, Γ is the temperature lapse rate, and T is the current temperature (K) while T_0 is the standard temperature at sea level. Γ is usually regarded as a constant, which is a negative ratio between height and temperature. As the relationship between current T and T_0 can be described as:

$$T_0 = T + \Gamma \times \Delta h \tag{4.3.1.4}$$

The formula (4.3) can then be transferred into:

$$\begin{aligned} P &= P_0 \times \left(\frac{T}{T + \Gamma \times \Delta h}\right)^{\frac{g}{R_d \Gamma}} \\ &= P_0 \times \left(1 - \frac{\Gamma \times \Delta h}{T + \Gamma \times \Delta h}\right)^{-\frac{g}{R_d \Gamma}} \end{aligned} \tag{4.3.1.5}$$

The common setups for these parameters are listed in Table 4.3.1.

TABLE 4.3.1

COMMON PARAMETERS FOR HEIGHT-PRESSURE MODEL

Parameter	Description	Value
P_0	Standard Atmospheric Pressure	101.325 kPa
Γ	Temperature Lapse Rate	0.0065 K/m
g	Gravitational Acceleration	9.80665 m/s^2
R_d	Specific Gas Content of Dry Air	287.04 J/kg/K

With the applications of these parameters, the height information can be extracted based on the specific formula below:

$$h = \frac{((\frac{P_0}{P})^{\frac{1}{5.257}} - 1) \times T}{0.0065} \tag{4.3.1.6}$$

The temperature T is supposed to be the indoor temperature of corridors, open space, and staircases other than room temperature. With this formula, the next step is to determine how to transfer that information for floor detection.

4.3.2. Directly Applying Height-Pressure Model

The first developed method is based on the idea of fingerprinting but in a simplified version, which is to establish a height database for the whole building, and it can later be used as reference data for floor localization (Li et al., 2013a, Muralidharan et al., 2014, Sabatini and Genovese, 2014, Ebner et al., 2015, Xia et al., 2015, Ye et al., 2016, Kim et al., 2017). During the operation, the barometer of the smartphone keeps reading pressure measurements while the user is moving down from 4th floor to the 1st floor, by using 'Barograph' app. In order to collect more data for later validation, user moved around each floor during the whole process when going down. After transferring the pressure to height information, the average heights information is used to detect the changes of floors and the mean value for each floor is kept for the referential heights for later floor detection. These results are then validated by a reverse process walking upstairs, in order to see whether the absolute referential height information can still be used for floor detection. The sampling frequency of pressure reading is one reading per second and the indoor conditions for these two experiments are controlled for temperature (all set to be 20°C), humidity, and walking speed, with negleagible range of flucturation. In the trial, it also tried to detect the transition areas, which are the staircase areas between every two floors and are usually negelected in previous studies (Muralidharan et al., 2014, Sabatini and Genovese, 2014, Xia et al., 2015, Ye et al., 2016, Kim et al., 2017). They can be detected by following certain movement patterns. During the movement from one floor to another in this experiment, the user needs to pass two staircases and a linkage area between them based on the structure of staircases used in the experimental area in this research. This needs to be treated as a whole process in floor detection. The approach to detect these areas is regarding the values between the means of each floor to be the whole transition areas. For special cases in this research of height change, the transition area between floors requires to pass three different means of heights (Fig.4.3.2.1).

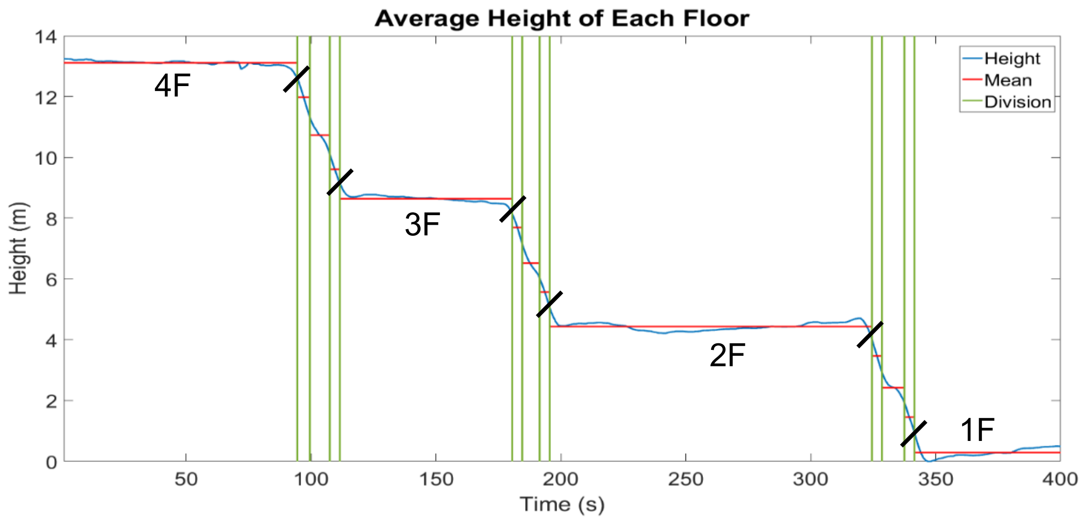

(a)

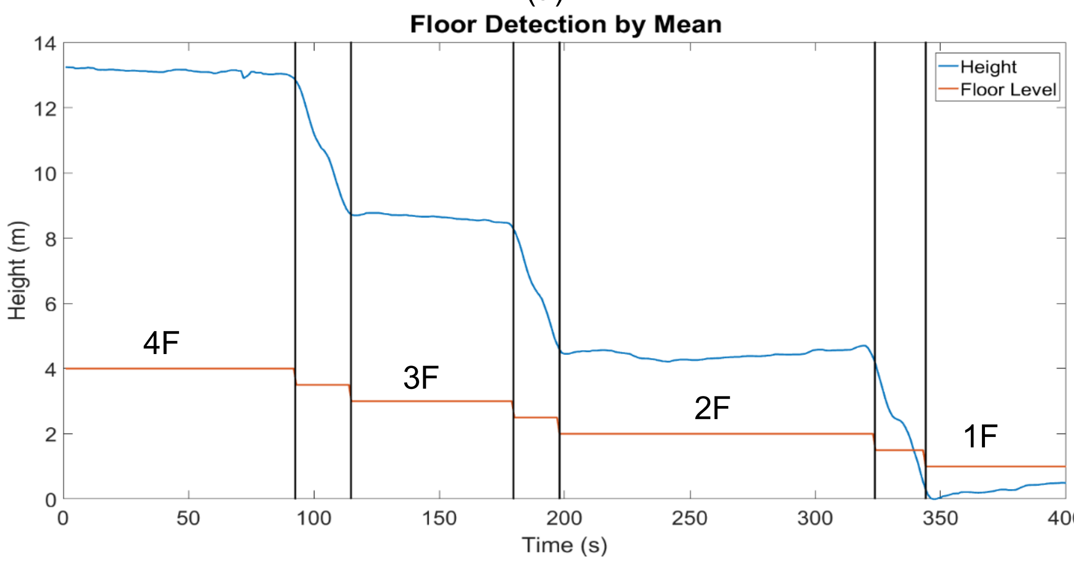

(b)

Fig.4.3.2.1: The processing of absolute height information collected in trial (The values between the black sections are treated as transition areas) (a) and the results of detected floors (b).

According to the result in Fig.4.3.2.1a, it has shown that the average height of each floor cannot represents the whole floor. In other words, the transferred height information from the pressure data varies with time. Thus*, using only* *one certain value, which also has been used in many studies before (Muralidharan et al., 2014, Sabatini and Genovese, 2014, Xia et al., 2015), is not suitable to describe the whole single floor. Instead, a range maybe more suitable to describe a single layer as the values fluctuates around the mean.* In order to improve that situation, the height ranges are settled for floor detection based on their means as well as maximum and minimum values in every intervals. It has also suggested that the average value may not be sufficient at identifying the initial several steps of changing heights when walking downstairs, though it works well on distinguishing different floors with significant height changes (Fig.4.3.2.1b). This may be also due to relatively high variations of collected height information in each layer. Meanwhile, the averaging method smoothes the changes of values and when a real change of floor level appears, it will slow the response of detection, causing errors in the results.

When turning to the validation process, the reference data does not work well on validation process and the absolute height information measured during test is not very appropriate to be used for real-time floor localization (Fig.4.3.2.2). First, it fails to detect the ground level but treats the whole level as the transition area between ground and second floor. In addition, the second and third floor are mistakenly detected in the places where there should be transition areas between first-to-second floor and second-to-third floor and these transition areas are falsely detected as well. The fourth level are detected earlier than it should be. When comparing their accuracies, the referential height information does not seem to reach similar level (72.8%) as that of the previous training period for reference data (97.5%). *These problems may be due to the high variation of pressure data over time, even under similar environmental conditions (Ye et al., 2016, Kim et al., 2017). The uncalibrated barometer sensor could be another possible reason* as it will also introduce some errors into the model when transferring pressure data to height. In addition, this method also increases the burden for data storage as these barometer data needs a long-period of data collection to deal with different situations (e.g. different weather conditions). However, the real-time measurements may still be different, even with these information (Shen et al., 2015, Ye et al., 2016).

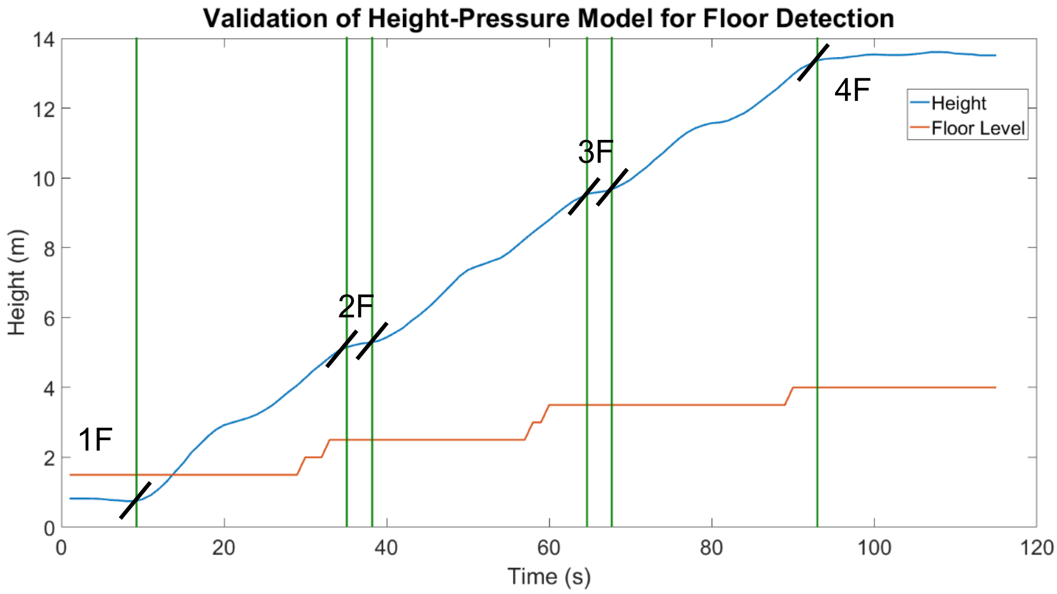

Fig.4.3.2.2. The validation process of floor detection based on the collected reference data (the correct floor identifications are marked out in black).

Another validation experiment also proves the above findings as the absolute height references cannot work for the data collected two weeks later as the pressure reading has changed significantly, which is taken under a raining condition with relatively higher humidity but still under similar temperature condition. In this validation experiment, the pressure measured from the ground floor has increased to 101.86 kPa rather than 101.32 kPa in the reference database, leading the whole transferred height to be significantly decreased if still using standard atmospheric pressure as ground level pressure. Indeed, this value P_0 needs to be replaced by the real-time readings instead of a fixed theoretical value to increase the accuracy of the pressure-height model. Moreover, as the historical dataset cannot always represent the real scenarios, the floor localization should not be based on the collected absolute height information.

Considering these mentioned problems, <u>a more robust floor localization method should be developed for floor detection, which should be more flexible to deal with the real-time measurements, have low requirement of data storage, have higher accuracy and more stable performance of floor detection while not requiring not much complicated computation and less affected by the environmental factors.</u> The using of only pressure-height model is not sufficient for those purposes and therefore, a more comprehensive algorithm is required to solve these problems.

4.4. UPGRADING OF FLOOR LOCALIZATION METHOD

In order to overcome the above problems, a more sophisticated algorithm is developed to improve the accuracy of floor detection. This method will not use the absolute height information for floor identification, instead, it will utilize a hypothesis that the changes in pressure between different floors can be treated as constant values (Li et al., 2013a, Muralidharan et al., 2014, Sabatini and Genovese, 2014, Ebner et al., 2015, Xia et al., 2015, Ye et al., 2016, Kim et al., 2017), and the floor localization problem can be treated as floor change detection with the identification of the initial level of user. It will try to detect the number of changes of floor levels based on the real-time measurements with the identification of initial level. This makes every measurement independent with each other and will not be affected by the environmental effects (Ye et al., 2016, Kim et al., 2017). However, in this study, it should be treated as a certain range instead of a persistent value to deal with variations of each floor, based on the abovementioned findings. The following sections will focus on how to determine the height ranges for different level and to recognize the time stamps of floor changes in time.

4.4.1. Absolute Height to Relative Height

The height range determination for different levels will be based on the application of relative height information, which is based on the plausibility of previous hypothesis that height differences between every two floors are constant levels. In order to test that hypothesis, a comparison of the relative height changes is taken based on two random datasets collected under different environmental conditions with different temperatures (Fig.4.4.1.1).

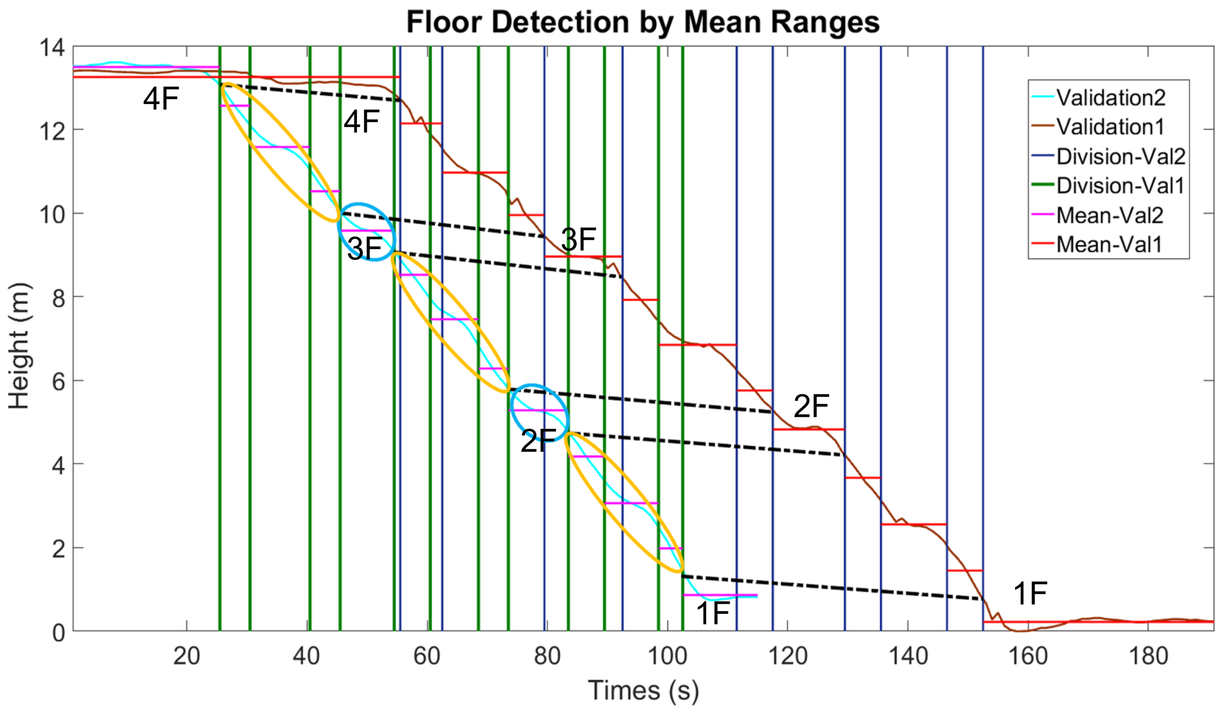

Fig.4.4.1.1. The comparison of absolute height changes based on two datasets collected under different environmental conditions (yellow circles for transition areas and blue circles for each floor).

It has found out that the intervals between every two neighbouring floors which are also treated as the transition areas of different levels, are relatively remained at similar levels although these intervals may vary with each other. For example, the height change from fourth floor to third floor of two tests remains the same when linking their changing points, while it differs to that from third floor to second floor. When checking every single floor, it can also find that every specific floor will cover a certain range of height while these ranges can differ from each other. In other words, the height range for each level is within a certain range, which can be regarded as a constant.

This finding can later be used for the estimation of the height ranges for floors. The floor height of each level can then be estimated by regarding the height range between every floor and the first floor to be within a constant range (Fig.4.4.1.2). As the change environmental factors can change the results of the transferred height, the relatively stable changes between floors may help to improve the accuracy of floor detection. In this study, the experimental site is located in PMB building, which is a four-floor building, and the floor levels are treated as four levels with three transitions areas (Fig.4.4.1.2).

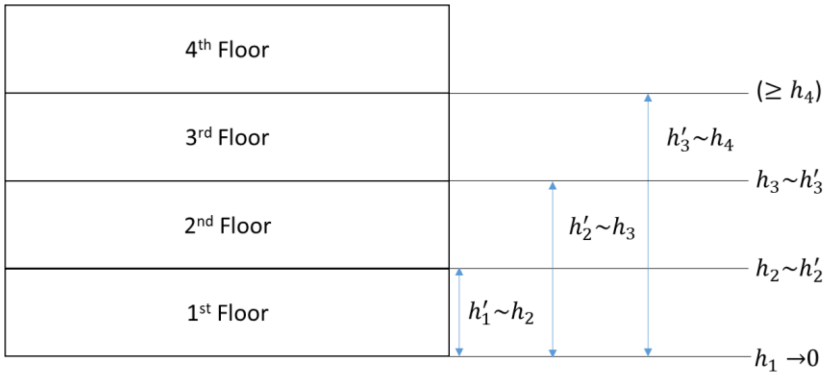

Fig.4.4.1.2. The classification of different floor levels in PMB building.

These height ranges ($h_2{\sim}h_4$) are still determined by detecting sudden changes of average heights. The next step is to treat the average height of first floor as benchmark and the height ranges of the other floors will be re-calculated to be within relative ranges after removing effect of first level. According to the calibrated result from the previously collected height information, *it also proves the hypothesis of relatively constant height changes between floors as there are no significant differences comparing estimated relative heights* with an acceptable average fluctuation of 0.072m considering the average stair's height is approximately 0.16m. The ranges for relative heights for each floor are then determined based on the integration of acquired results and can be used as references for later initial floor identification (Fig.4.4.1.3 and Table 4.4.1).

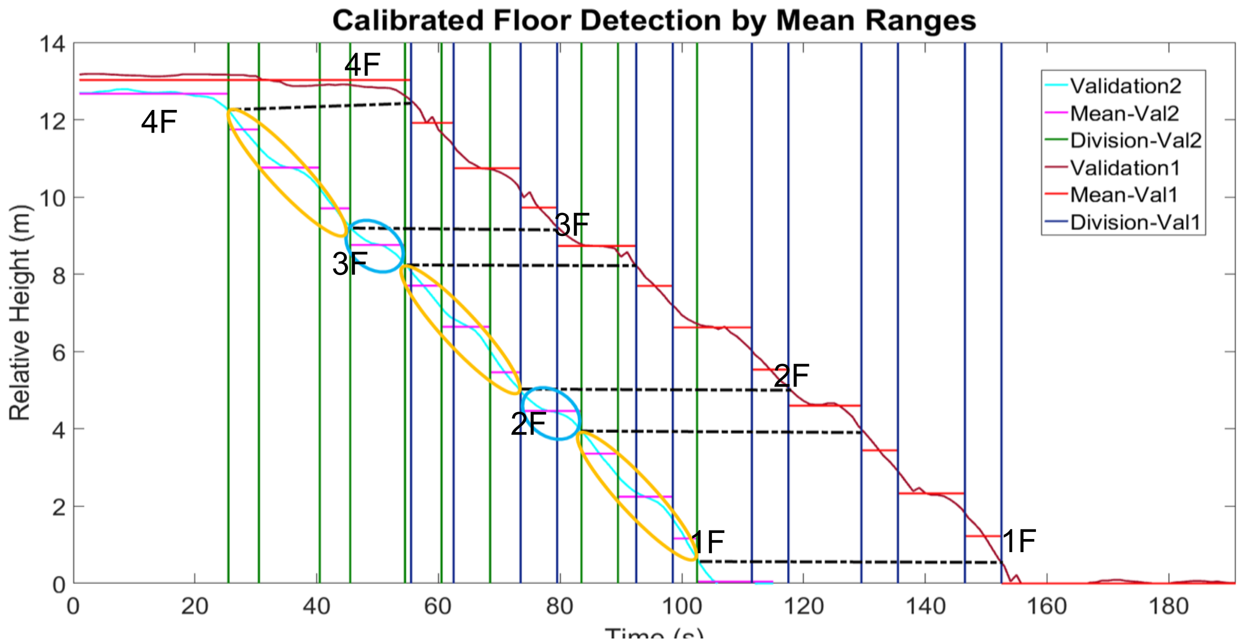

Fig.4.4.1.3. The comparison of relative height changes based on two datasets collected under different environmental conditions by mean range

determination (yellow circles for transition areas and blue circles for each floor).

These acquired ranges also needs validation from another datasets, and this study takes another random measurement five weeks later under a different weather condition with higher humidity and higher temperature to previous two measurements. The newly collected data also being processed to find height ranges for classified floor levels. When comparing the referential relative heights to new acquired height ranges, the average difference between these two sets are about 0.17m (with a range from 0.02m to 0.49m), which is significantly different than previous acquired references and is higher than the mean height of one stair. This may due to the relatively significant error for fourth floor (Fig.4.4.1.4 and Table 4.4.1) as the barometer has not been pre-calibrated by a reference device or referential reading. These errors can cause mistakes on floor detection from fourth floor to the following transition area between third and fourth floor. However, this error is already better than previous study with a range from 0.05 to 0.68m (Sabatini and Genovese, 2014).

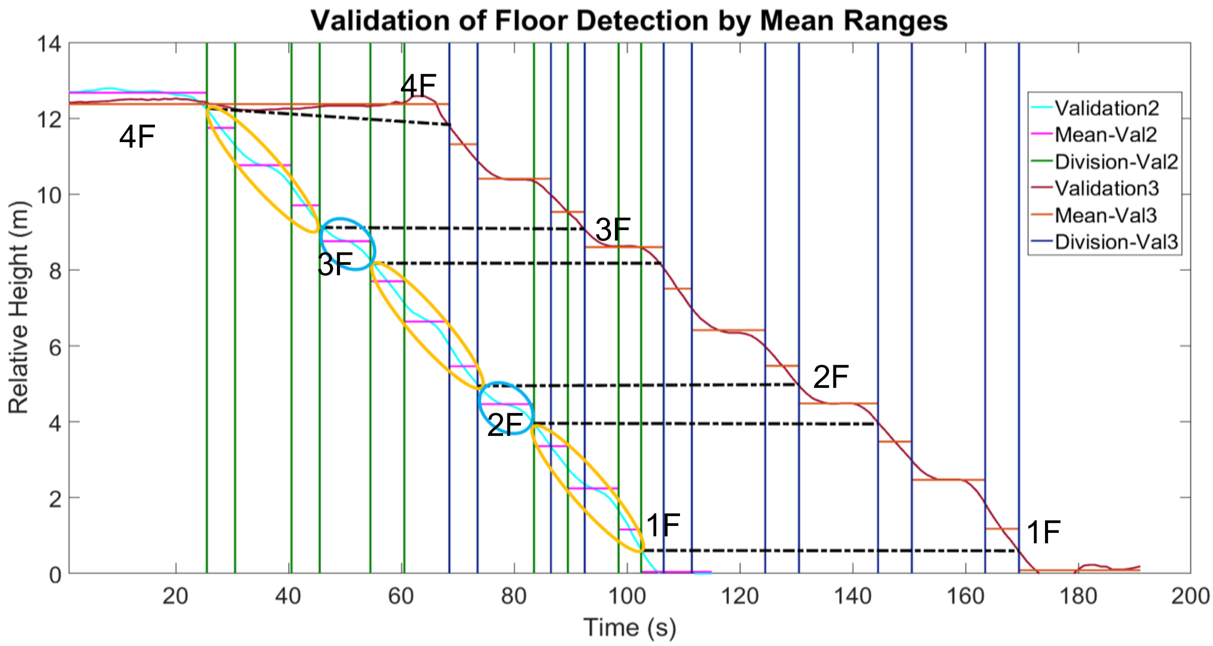

Fig.4.4.1.4. The validation of relative height ranges from new acquired dataset to one previous dataset collected under different environmental conditions by mean range determination (yellow circles for transition areas and blue circles for each floor).

Meanwhile, the late response to floor change detection remains to be a problem as it keeps using periodical changes of average height values, which lengthens the duration for every floor and may not be able to recognize some tiny but sudden changes of height information due to smoothing effect caused by averaging function. Moreover, it may also affect the precision of range determination and causing error in floor detection as the time stamps of floor changes is another important indicator for floor detection. Therefore, a new way for range determination is required to be developed for the floor detection, which should be able to respond to floor changes in time and have better accuracy on initial floor identification.

TABLE 4.4.1
RELATIVE HEIGHT RANGES COMPARISON FOR EACH FLOOR BY MEAN RANGES

Floor Number	Referential Height Range (m)	Height Range from Validation(m)	Difference (m)
4	>= 12.38	>= 11.89	0.49
3.5 [a]	9.14-12.38	9.14-11.89	0.49
3	8.33-9.14	8.15-9.14	0.18
2.5 [a]	4.93-8.33	4.87-8.15	0.24
2	3.89-4.93	3.90-4.87	0.07
1.5 [a]	0.47-3.90	0.49-3.90	0.02
1	<=0.47	<=0.49	0.02

[a] represents the transition area between every two floors and the difference here does not mean accuracy.

4.4.2. Average Function Vs Linearity Function

In order to further improve the performance of floor detection, a more effective method of both initial floor range determination and changing time recognition is required. This study tries to use linearity change based on the assumption that when passing via a specific staircase under relatively constant velocity, the changing speed of relative height, i.e. the height gradient change during this period is supposed to be similar. The data are from the previous processed relative height information with removing benchmark height acquired from the first floor. Then these data will be processed to find sudden changes of linearity, which means arriving another level. In order to distinguish the transition area and flat floor area, the slopes close to zero will be treated as flat floors and for transition area, it should pass two changes of non-zero slopes based on the certain structure of staircases in this study. The acquired results are listed below (Fig.4.4.2.1).

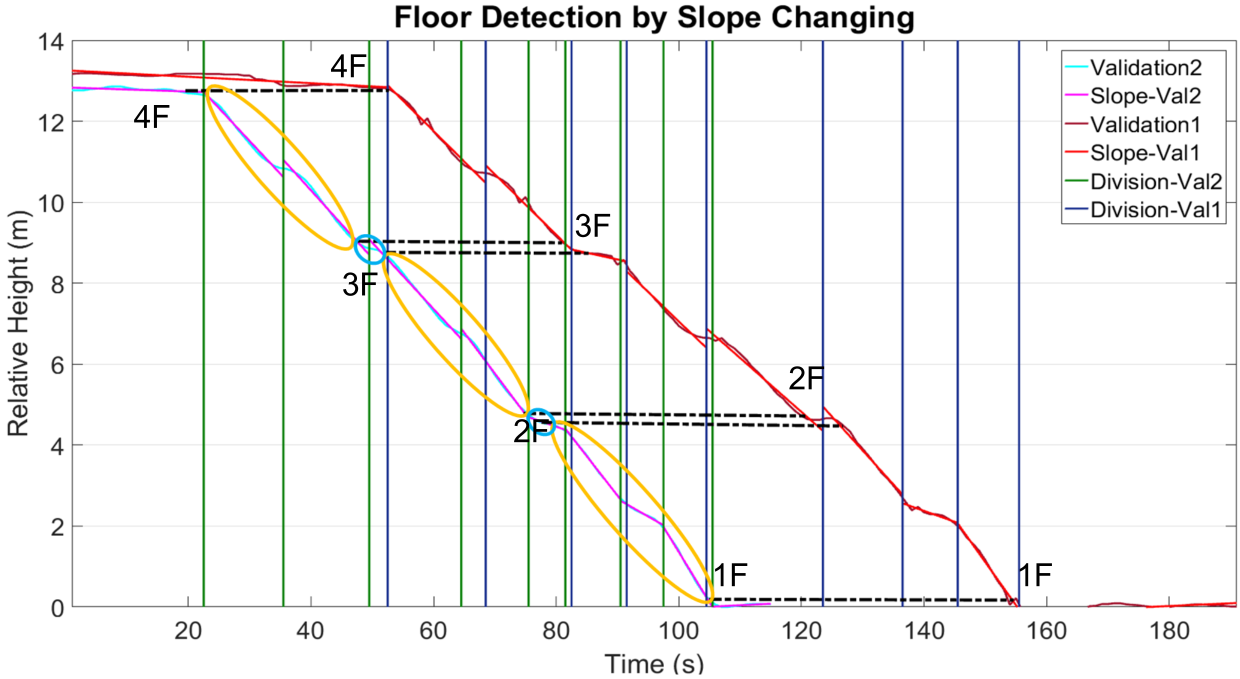

Fig.4.4.2.1. The comparison of relative height changes based on two datasets collected under different environmental conditions by slope changing (yellow circles for transition areas and blue circles for each floor).

<u>It has shown that the floor change detection based on slope changing seemed to function more sensitively, especially for transition area detection than that using averaging</u> by comparing the acquired results from Fig.4.4.2.1 and Fig. 4.4.1.3. When checking the time stamps for floor changes, the mean delay for changing floors for one to two seconds in average while comparing to using the averaging method, the average delay of detection is about three to four seconds. However, the slope detection is not good at dealing with flat floors appeared between transition areas, which happens during the movements from second to fourth floor. This is due to the collected data in these areas is not large enough and have high variations of height information. These factors are limited by the structure of staircase areas as the linkage areas between every two staircases during the whole movement from fourth to first floor are similar, making it hard to distinguish from the other moving periods and they are usually being treated as partial areas with the neighbouring transition areas. Therefore, the different floor levels are divided by the intersections of

specific linearity of each area and the transferred height information in corresponded area. However, there are still some special cases appearing during the movement between first and second floor, which are unexpected detections in the transition areas between different staircases as it passes three non-zero slopes (Fig.4.4.2.1). This makes the slope detection method unsuitable for floor identification as it does not have stable performances of dealing with the horizontal variations when moving on flat floors, though it has improved the response velocity of sudden vertical movement changing process to a large extent. *On the other hand, the averaging method has the advantage of smoothing effects, which makes it relatively more robust than slope changing detection to deal with variations during horizontal movements, though it has negative effects for vertical change detection.*

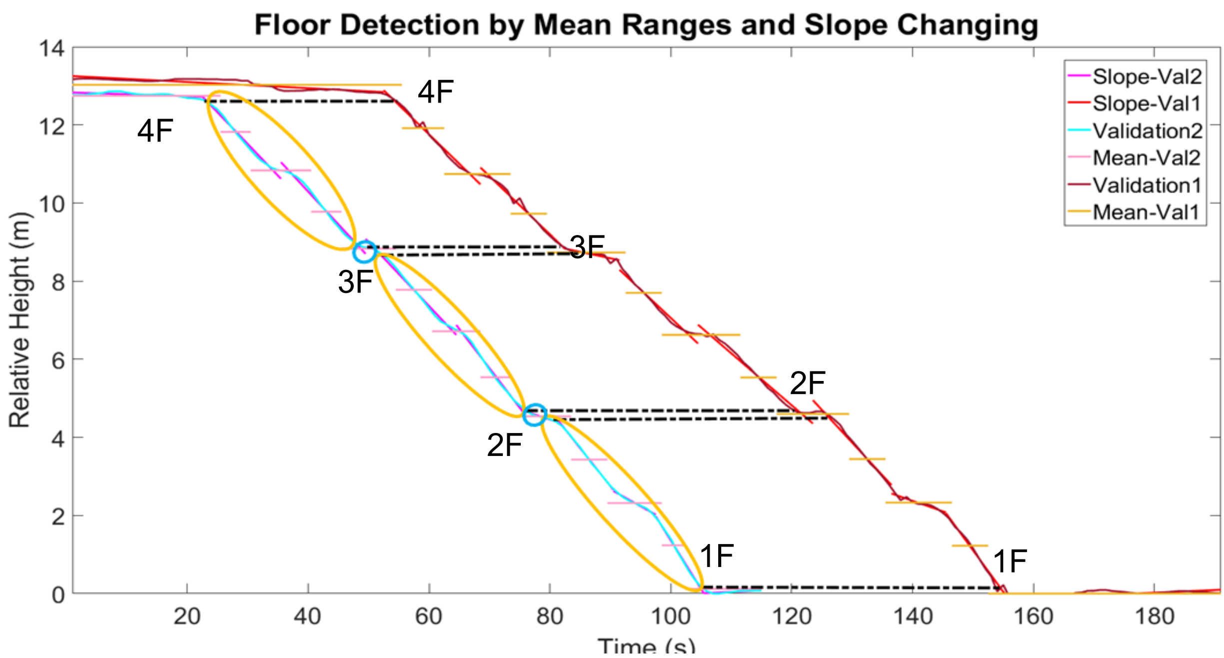

Fig.4.4.2.2. The comparison of relative height changes based on two datasets collected under different environmental conditions by slope changing and mean range determination (yellow circles for transition areas and blue circles for each floor).

<u>As both of the methods cannot handle the floor change detection individually, the new idea is to integrate these two methods together, which can keep the advantages of linearity changing detection to detect vertical changes in time and also can deal with high variations when passing through the flat places.</u> According to the moving patterns of user when passing through staircases in

this study, the user needs to pass two staircases and a linkage area between them. This needs to be treated as a whole process in floor detection. For height change, the transition area between every two floors requires to pass two changes of linearity and three different means of heights, while the flat floors between these transition areas will be treated as the following parts after passing these areas, except the initial level. The initial level will be determined by the intersection between the first change of linearity and the transferred height. The processed results based on previous data are listed in Fig.4.4.2.2.

With the processing of both mean ranges and slope changing, the performance of time stamp recognition of floor change has been improved than that using only slope changing or mean ranges, as some of undetected ranges from using only slope changes while it still keeps quick response to sudden changes in vertical direction, with a delay of only one to two seconds (Fig.4.4.2.3). However, when determining the range of relative heights for each level, there are still some extreme measurements in detected ranges due to the unstable performance of the embedded barometers in smartphones. These measurements can be smoothed by the neighbouring measurements in the range of corresponded level. Then the boundaries of ranges for each floor will be determined by the intersections between beginning and ending slopes with the transferred height in corresponding detected level. The separate series of ranges determined by two sets of data has an average fluctuations of 0.05m, which has been improved from the previous acquired results by only using mean ranges and can increase the precision for detected range. They will be integrated together by taking an average, which can be used as referential relative height range for the starting level (Table 4.4.2).

The acquired referential database still needs to be tested to see whether it can be used for other datasets and the datasets is still taken from the validation dataset used for testing the accuracy of referential heights detected by only mean ranges. The acquired results have an average difference between referential data in 0.14m (within a range from 0.01 to 0.28m), which is acceptable as it is less than one stair’s height (0.16m) with an improvement of 17.7% than using only mean-range based methods. It is also better than a recent research with an average accuracy of 0.15m (Kim et al., 2017). When checking with individual ranges, some of them are still slightly over than the range of single stair's height, which may cause about one seconds' delay even with supplementary information of changing time when shifting from one level to another (Table 4.4.2). This is limited by the capability of the linearity change detection and there is no simple solution to that problem.

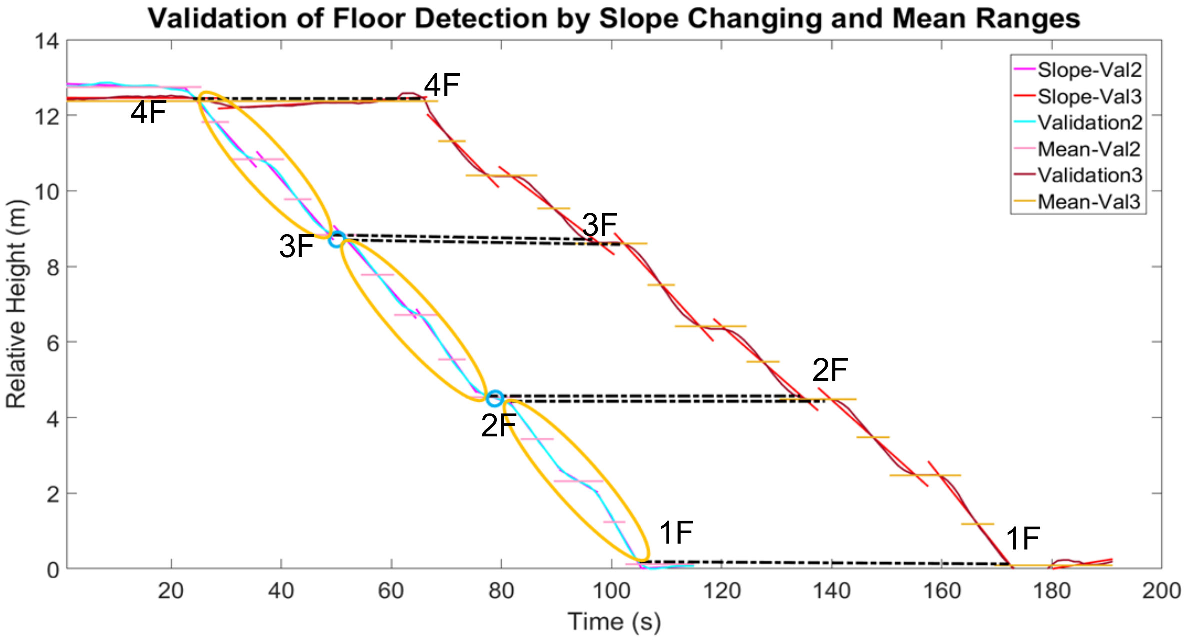

Fig.4.4.2.3. The validation of referential relative height ranges for different floors by slope changing and mean range determination (yellow circles for transition areas and blue circles for each floor).

TABLE 4.4.2

RELATIVE HEIGHT RANGES COMPARISON FOR EACH FLOOR BY SLOPE RANGING AND MEAN RANGES

Floor Number	Referential Height Range (m)	Height Range from Validation(m)	Difference (m)
4	>= 12.53	>= 12.52	0.01
3.5 [a]	8.82-12.53	8.63-12.52	0.20
3	8.69-8.82	8.60-8.63	0.28
2.5 [a]	4.67-8.69	4.55-8.60	0.21
2	4.61-4.67	4.50-4.55	0.23
1.5 [a]	0.20-4.61	0.24-4.50	0.04
1	<=0.20	<=0.24	0.04

[a] represents the transition area between every two floors and the difference here does not mean accuracy.

With this acquired referential relative heights for each level with the supporting evidence of floor changing stamps, the whole mechanism of floor detection will be an independent process based on the real measurements. The initial level of user will first be identified based on the relative height information after comparing to the referential and the user will be assumed to stay at the same level until a sudden change of floor level is detected by both mean ranges and slope changing. The time stamps of corresponded slope changing will be used as the starting point of the next floor level. The next step is to compare the following measurements with the reference height ranges. If the following measurements before the next sudden changes appears is smaller than the current height range, then these measurements will be assigned to the following lower level of the initial level, otherwise it will be assigned to a higher level than current level. The rest of measurements will also be estimated based on this process and the flow chart of this process will be described in the next section. When testing this method with other measurements for floor detection, the average accuracy of floor detection is about 95% based on 10 measurements from fourth floor to the first floor collected under different environmental conditions, which has been significantly improved (approx. 30%) by directly using pressure-height model. This makes this method a potential good solution for floor detection, though having one to two seconds' delay when displaying the results limited by sensor itself. Therefore, <u>the self-calibration of the embedded barometer before the operation is necessary</u> and this method will be further improved in the following section.

4.4.3. Design and Operation of Floor Detection Algorithm

With the above findings, the overall design of floor detection is listed below (Fig.4.4.3). Before the operation, the embedded barometer should be calibrated. The approach used in this study is to use two different barometer apps on the same smartphone: 'Barometer' and 'Barograph'. The ground level pressure will be measured as real-time readings instead of using standard atmospheric pressure, and this will be provided by 'Barometer'. 'Barometer' can provide pressure at the ground level and the current level and 'Barograph' keeps recording pressure reading during movement. Their readings will be compared initially for self-calibration before height transfer. During the operation, the indoor temperature is supposed to be measured by an indoor thermometer which needs to be pre-installed in the building, however, in this experiment the indoor temperature is controlled by an air condition system and can be regarded as a thermostatic environment and it is estimated to be 20ºC (293.15K).

The collected measurements will then be transferred to heights based on these information and be processed to relative height ranges $(\Delta H_{R_{j(Bottom)}}, \Delta H_{R_{j(Top)}})$ by removing effect of the first level, which is a reverse application of the previous reference database as the referential relative height for the first floor is supposed to be about 0.2m (Table 4.4.2). The next step is to determine what the current level of user localizes based on the comparison between processed data and reference heights. The user will be estimated staying on the same floor until a floor change is detected which requires the proof from both mean ranges and slope changes as sometimes the slope changing method is too sensitive to detect some unexpected changes. After the detection of floor change, the time stamp identified by slope changing will then be used as the starting point for the next floor. Then the following data will be compared to the reference data to see whether user is entering a higher level or a lower level, before another floor change is detected. When entering the transition areas, the reference data will identify this period and require the user to pass two changes of linearity and three changes of mean. If user are estimated to stay in transition areas in the beginning, the change to the next level will be divided into two cases. If the initial user height is higher than half of the pre-determined range, the user still need to follow the previous pattern otherwise the user only need to pass two changes of mean and one linearity change before reaching the next level and the changing time stamps will be the ending point provided by the intersection of slope change and height information.

The following measurements will follow this mode and keep tracking user's level during movements. The recognized level information will then reported back to system to help derive the corresponding floor plan. The acquired height and level information will also integrate with the 2D vision-aided system for later 3D path construction by limiting $(t(k) - t(i)) \to 0$, where $t(k)$ is the time stamps from the barometer readings. Moreover, as the 3D locations of cameras are already stored in the system before operation, the level information can be re-calibrated whenever, the user is in the visible area during movement in the building. However, there is still one weak point of this design of system, which is the requirement of an embedded barometer on smartphones, as there are some old models of the smartphones on the market do not have that kind of sensors. However, this disadvantage will be gradually counteracted by the improvement of smartphone types as almost all new versions of smartphones have embedded barometers.

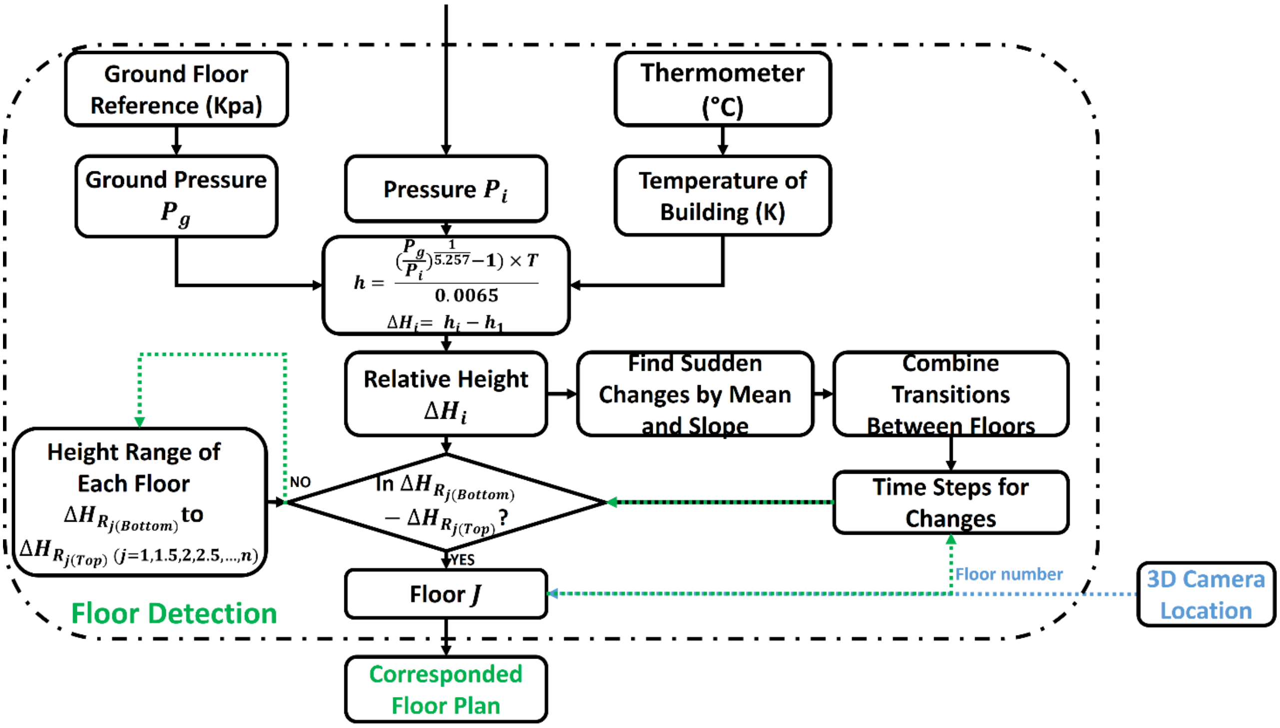

Fig.4.4.3. The workflow of processing pressure data for floor detection.

4.5. Experimental Setup

The test site in this study is still located at the four-floor PMB building at the UNNC. All data are transferred to a desktop by wireless network for post-processing by MATLAB. The reference maps in WGS84 are the digitized floor plans based on blueprints imported to ArcGIS 10.3, with assigned floor level. With the assistance of floor detection during the movement, the corresponding floor plan will be automatically selected for visualization. They are posted on a web map repository using ArcGIS Online for indoor-outdoor transition, with the simple semantic representations of indoor structures.

Along the designed walking path for horizontal moving of each floor, some distinctive markers with an inter-distance of 0.63m are marked on each floor to guide the user to follow these markers during movements. The user is asked to step over these marked referential points as strictly as possible, and the time stamp of each step point will be recorded at the same time. When passing the corners, the user does not need to turn exactly 90°, but to turn comfortably and naturally. When entering the staircase areas, each stair is counted as one step and the step length here will be adjusted to the thread length of the stairs. The experiment is then run for 10 times with the same target pedestrian, and the results are presented with one selected example and the average performances of accuracy and precision.

The overall length of the 2D referential path is about 168.0m including fifteen 90° turnings and two non-90° turnings. The total height of stairs is approx. 13.07 m. The average measured riser height of the stairs is 0.15m and the average measured thread length of the stairs is 0.29m. The total counted number of the step markers is 312 for this walking trajectory. The entire time used for walking along this path is about 311.7s under a normal walking speed about 1.0 m/s.

The cameras are located on the 4th floor in front of Room 416 (Camera #1) and 1st floor in front of elevators (Camera #5) (Fig.4.5). They are all facing directly to the corresponding corridors with the targeted user in the centre of the frame, and they are installed with a height of 3m to the floor of each level inside the test building. The detailed walking path at the 4th floor is designed as 15 steps before entering the visible area of Camera #1, 66 steps in the visible area of Camera#1, 25 steps before the non-90° turning and 12 steps before passing down the staircases. When moving in the staircase areas, every two floors has 28 steps at stairs and 12 steps at transition areas. When arriving on the 1st floor, it passes 12 steps before the non-90° turning, 40 steps before entering the visible area of Camera #5 and 22 steps in the visible area of Camera #5. The overall length of the visible path is 69.3m, which means this system is working under a situation with high amount of occlusion. This will be closer to the real applications by using existing surveillance systems in the indoor environment as there will be no visual tracking in the staircase area.

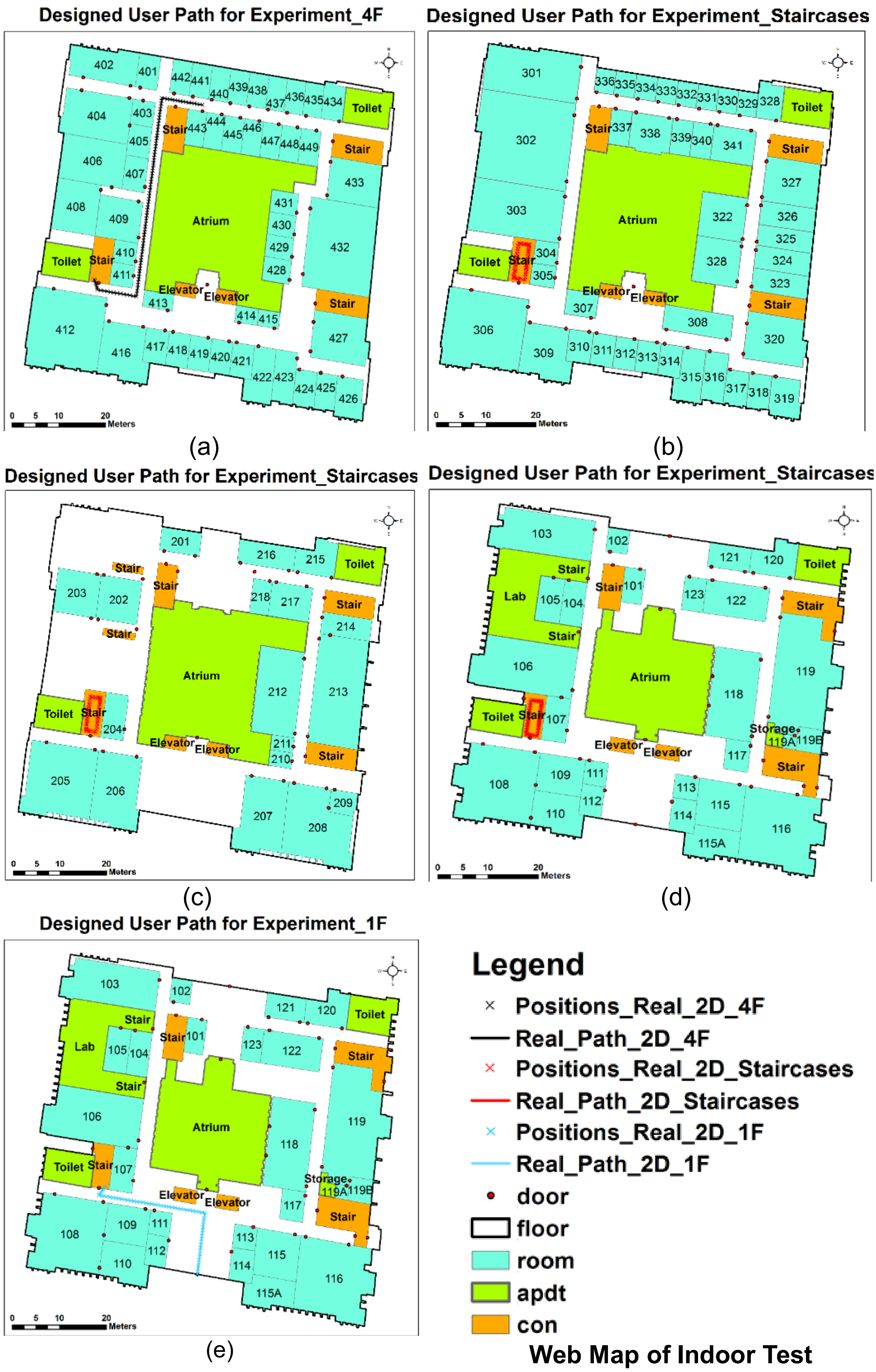

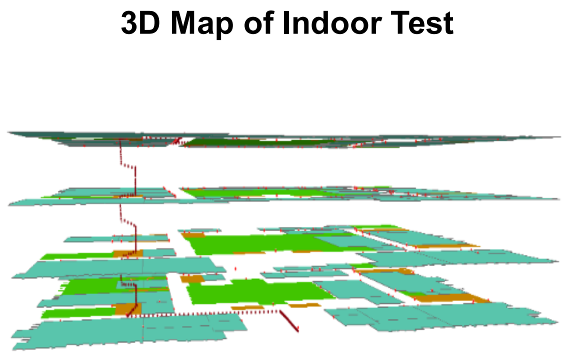

(f)

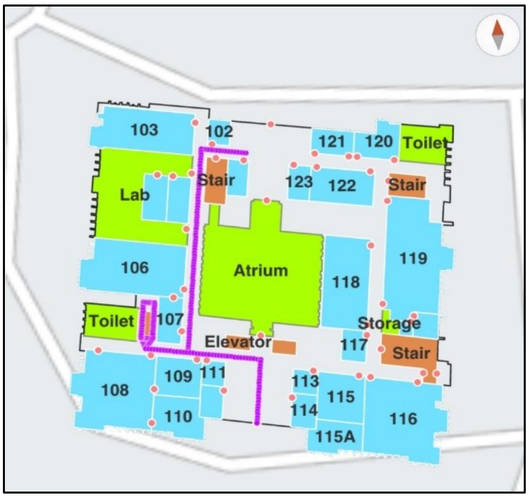

(g)

Fig.4.5. 2D reference paths visualized from different floors with positions of cameras (a)-(e), 3D view of entire indoor path (f), and the webmap with outdoor environment in ArcGIS Online (g) (where 'adpt' represents the rooms other than offices and 'con' represents stairs and elevators).

For smartphone-based PDR system, a Huawei Mate 8 (Android) and an iPhone 7 Plus (iOS) are used, which are two common models of smartphone of these two operating systems on the market with available embedded barometers. The data collection app for both smartphone-based PDR is MATLAB Mobile, which can work on both types of smartphones. The sampling frequency for two smartphones are set to be 50 Hz. During the experiment, both smartphones are held horizontally, pointing towards the walking directions. For visual tracking system, the resolution of each camera is 680×540, the vertical FOV is 27°, and so the focal pixel length is about 1.05×10^3 per inch. The frame frequency is 17 frames per second. Cameras start filming simultaneously with the initialization of smartphone-based PDR. For floor detection, the barometer apps for pressure data collection are Barometer and Barograph. The former is used for sensor self-calibration and the latter is used for continuous recording and its sampling frequency is $1s^{-1}$. Barometers are triggered before the smartphone PDR and visual tracking system for self-calibration and their timestamps will be recorded for later data fusion. On the other hand, the visual system will also help to calibrate the floor level information whenever the user are in the visible area of any of cameras.

4.6. Results and Analysis

4.6.1. 2D Visual Tracking

In this study, the overall length of visible paths is 69.3 m, which only accounts for 41.2% for the overall path. In previous studies, the non-occlusion path occupies at least 50% of the overall path when reaching decimetre-level accuracy (Jiang and Yin, 2015, Jiang and Yin, 2017, Zhang and Zhou, 2018, Yan et al., 2018b, Yan et al., 2018a), even some of them not reach completely invisible occasion but only partial occlusion (Jiang and Yin, 2015, Jiang and Yin, 2017, Zhang and Zhou, 2018). This study aims to validate whether the system can still work under this extreme condition.

The pedestrian detection accuracy of two cameras is similar at 99.8%, which is satisfactory for later processing. The way of RMSE calculation has already been described in **Section 3.8.1,** and this method is also applied in this section. The RMSE of visual tracking results is 0.06m for Camera#1 and 0.04m for Camera #5 respectively and the synthesised RMSE of two-camera-based system is 0.05m and the MAE for 10 experiments also remains a similar value, with a precision at 0.02m (Camera #1) and 0.01m (Camera #2) respectively. The OPS first provides the positions of the functioning camera, which can also help for floor detection calibration in LoS areas. As shown in Fig.4.6.1, with the mapping results from the visual tracking, two partial paths from two cameras are matched well against the reference path. However, both two paths still have a problem of unevenly distributed visual positioning points, though this phenomenon for the positioning points provided by the second camera is not distinct to be realized. This problem has been discussed in the previous chapter due to pinhole effect and long distance between target and camera (Yan et al., 2018b, Yan et al., 2018a).

Meanwhile, the filming frequency cannot match with the step frequency and the detected target positions are always in the middle of a step but cannot identify the starting and ending points of each step event. The previous visual gait detection (Jiang and Yin, 2015, Jiang and Yin, 2017, Zhang and Zhou, 2018) is not suitable for this study as: a) this study does not apply foreground masks, which is quite labour intensive and responds slowly, while using a pinhole model for distance estimation; b) the filming frequency is lower than previous studies; and c) the ratio between IMU sampling frequency and filming frequency is not in integer. This makes the results from visual positioning more time-domain based rather than gait-based, and these data are not suitable to be directly used for calibrating the PDR positioning in visible areas, though it has a Mean Average Error (MAE) of 0.05m. However, this will not affect the headings between steps and the information can be later applied for PDR calibration.

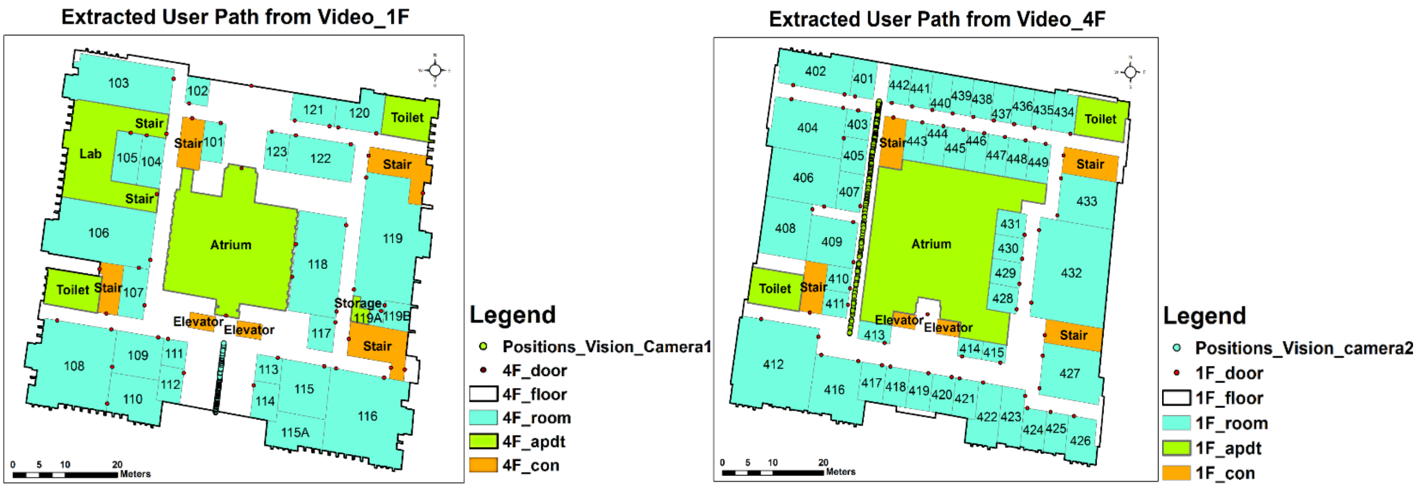

(a) (b)

Fig.4.6.1. The 2D path captured by camera on the 4th floor (a) and 1st floor (b).

4.6.2. 2D Smartphone-Based PDR

4.6.2.1. 2D Calibration

In this experiment, the user walks 312 steps in average from the fourth floor to the first floor and PDR only provides the horizontal positions to avoid imposing additional errors due to the inclusion of the third dimension. In the presented example, the Android-running phone detects 298 steps while iPhone detects 306 steps (Fig.4.6.2.1.2). After repeating for 10 times, the average detected steps do not change significantly, within 1 or 2 steps' fluctuations (Table 4.6.2.1.1). This may be caused by data logging mechanism of PDR data, as it requires the network connection for data transferring to the main control system while the signal strength of Wireless Local Area Network (WLAN) is not stable in the experimental site. This could be resolved by using 4/5G for Mobile Communications as a supplement or using an offline system for data collection. The other reason to that may be due to a relatively higher sensitivity of the accelerometers embedded in iPhone 7Plus than that of Huawei Mate 8's, providing a better step detection performance when using the iOS-based system.

TABLE 4.6.2.1.1

MEAN ACCURACY OF STEP DETECTION OF TWO TYPES OF SMARTPHONES

		Device	
	Counted Steps	Huawei Mate8	iPhone 7Plus
Detected Steps	312	296	307
Mean Accuracy	100%	94.9%	98.4%

Before the heading calibration in horizontal direction, the positional accuracies of these two types of smartphones are almost the same, i.e. the MAE is 0.31m (Android) and 0.29m (iOS) (Table 4.6.2.1.2). However, according to their CDF of error distributions, *the maximum error of iOS is higher than that of Android's while it has more positioning points with error less than 1m* (Fig.4.6.2.1.1a).This may be due to the higher noise from the embedded accelerometers in iPhone 7Plus. The precision of their positioning results is similar with iPhone 7Plus has a slightly better performance due to its higher sensitivity to the step detection by embedded accelerometers (Table 4.6.2.1.2). *However, neither performs well enough for the staircase area with the frequent turnings* (Fig. 4.6.2.1.2a). This may be improved with more accurate gyroscope in future with advancement of embedded smartphone-based inertial sensors.

This experiment also uses heading calibration, which replaces each step's heading $\psi(t(i))$ acquired from PDR by orientation decided by two consecutive frames with similar time steps. The time stamps of PDR are deduced from the detected step events and the related time stamps from the accelerometer readings, while that of the videos are inferred from the frame number and filming frequency.

$$\psi(t(i)) = \lim_{(t(j)-t(i))\to 0} \arctan_2((X_{t(j)}, D'_1 - \gamma * D'_{t(j)}), (X_{t(j+1)}, D'_1 - \gamma * D'_{t(j+1)}) \quad (4.6.2.1)$$

where $t(i)$ is the time step from the i^{th} step event, $t(j)$ and $t(j+1)$ are the time steps from j^{th} and its following frames. The 2D user positions will be recalculated based on the integration of these calibrated headings and pre-calibrated step length SL'_i (Yan et al., 2018a, Yan et al., 2019).

After the 2D heading calibration, the MAEs of both types of smartphone-based PDR have been improved to 0.16m (Table 4.6.2.1.2). 95% positioning points' error falls below 0.65m while before calibration it was 0.90m (Fig. 4.6.2.1.1b). The Android-based-PDR seems to perform better after horizontal calibration without considerations of missing detected steps (Fig.4.6.2.1.2b). It may be explained by the fact that more detected steps from iOS system will introduce more difficulties to 2D calibration as this time when LoS areas only occupied 41.3% of the entire path. Therefore, the positioning accuracy cannot be significantly improved using the heading calibration, in comparison with the previous experiments with higher proportion of LoS areas as mentioned in Chapter 3 (Yan et al., 2018b, Yan et al., 2018a), where more than 80% of positioning areas are in the view. Therefore, the positioning accuracy in this experiment cannot be significantly improved after heading calibration.

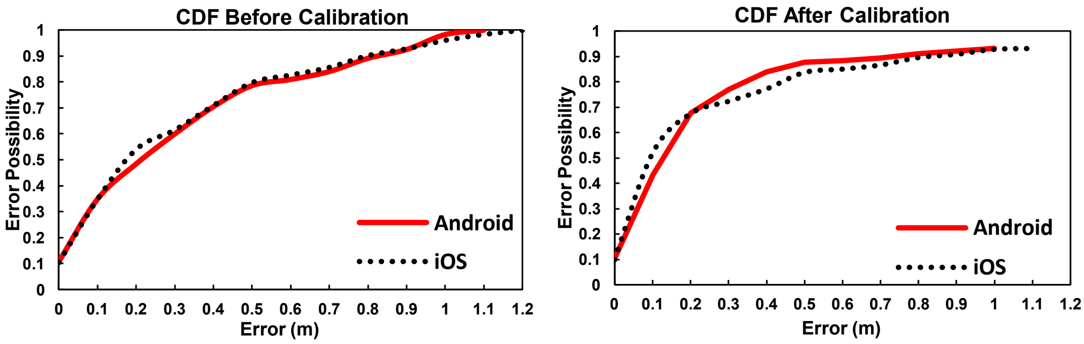

(a) (b)

Fig.4.6.2.1.1. The CDF distribution for 2D smartphone-based PDR.

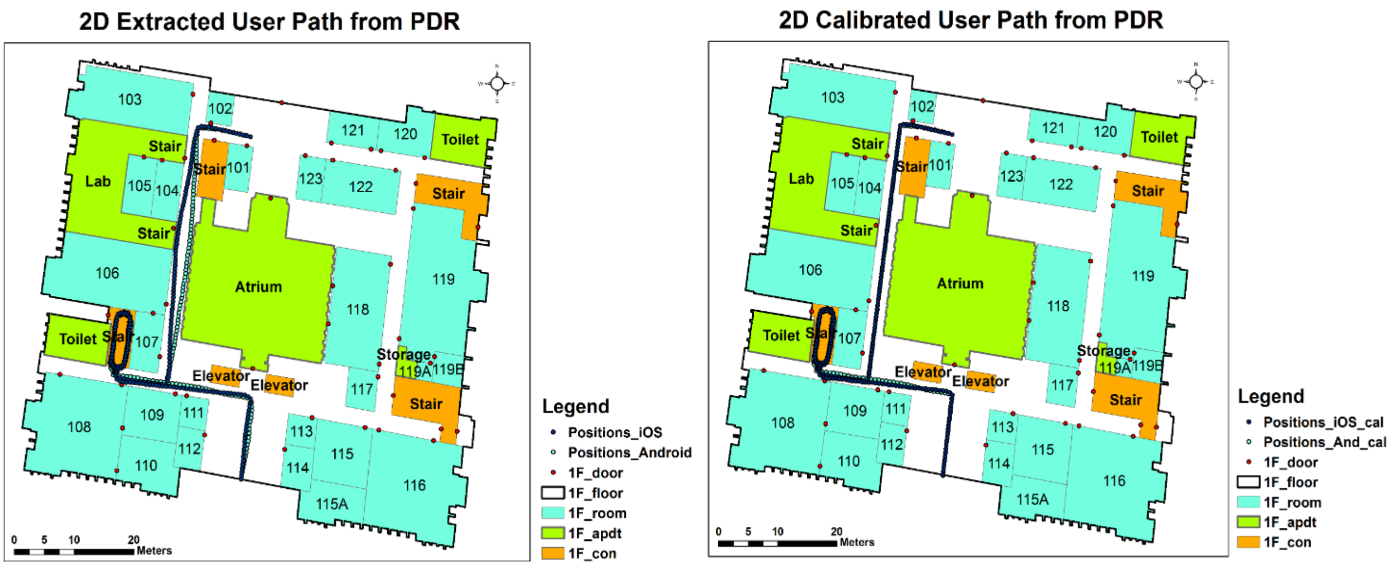

(a) (b)

Fig.4.6.2.1.2. The 2D projection of walking path on the first floor by 2D

smartphone-based PDR before calibration (a) and after calibration (b).

TABLE 4.6.2.1.2

POSITIONING ACCURACY ANALYSIS BEFORE AND AFTER CALIBRATION

Smartphone Model	HUAWEI Mate7	iPhone 7Plus
MAE Before Visual Calibration (m)	0.31	0.29
MAE After Visual Calibration (m)	0.16	0.16
Improvement	48.3%	44.8%
Precision Before Visual Calibration (m)	0.15	0.13
Precision After Visual Calibration (m)	0.10	0.08
Improvement	33.3%	38.5%

4.6.2.2. Improvements to Other Studies Using 2D PVINS

Comparing with the recent study conducted by Shanghai Technology University (Zhang and Zhou, 2018), it is understood that its minimum RMSE of PVINS can achieve an accuracy of 0.2m under the condition of partial occlusion, as it has more than 50% of positioning areas are in view during experiment. *The minimum RMSE proposed by this study can perform better, even with a simpler data fusion algorithm and a lower portion of non-occlusion areas.* The corresponding CDFs in this study also has the advantage of lower variations with about 90% of errors less than 0.4m, while this number for other studies is up to 0.5m.

The other studies conducted by Missouri University (Jiang and Yin, 2015, Jiang and Yin, 2017) have a minimum MAE of 0.5m, with a maximum improvement of 22.6%, summarizing from four tests. This is lower than the results achieved in this study when having the minimum RMSE at 0.16m with a corresponding maximum improvement of 48.3% (Table 4.6.2.2). Moreover, the designed path as ground truth has more frequent turnings of 17, which could easily introduce more errors due to the effects of noise from the embedded gyroscope in the invisible areas, while in the other studies, the maximum number of turnings is 4. This shows the potential to deal with more structurally complicated path.

Meanwhile, the ending points of both calibrated paths match well with the entrance of the building, which can keep tracking user trajectory and later be directly shifted to the outdoor positioning system when GPS signals are available. This system also has been tested on two types of smartphones while the previous studies mainly focus on Android-running systems. However, the system proposed by this study cannot provide gait-feature based visual tracking as the other studies (Jiang and Yin, 2015, Jiang and Yin, 2017, Zhang and Zhou, 2018), which makes the visual tracking results not fully compatible with step event mechanism of PDR, *making this system more single-directional calibration based, i.e. calibrating PDR by visual tracking but the other way round, and only providing data for invisible places.*

TABLE 4.6.2.2

POSITIONING ACCURACY COMPARISON BETWEEN OHTER STUDIES USING PVINS

Reference	(Jiang and Yin, 2015, Jiang and Yin, 2017)	(Zhang and Zhou, 2018)	This Study
FPS	30	20	17
Visible Area (%)	>50	51.7	41.3
Device	Samsung Galaxy S4	Huawei Honor8	Huawei Mate 8, iPhone 7 Plus
Turnings	4	3	17
Best RMSE (m)	0.50	0.20	0.16
Calibration	Bi-directional	Bi-directional	Single-directional

4.6.3. Height Estimation and Floor Detection

The common way to achieve 3D positioning is to treat the horizontal and vertical localization separately (Ye et al., 2012, Muralidharan et al., 2014, Flores and Farcy, 2014, Lin et al., 2015, Sabatini and Genovese, 2014, Shin et al., 2014). This may due to the navigation mechanism, as the horizontal positioning is more important on each floor than in the transition areas in staircases and the vertical positioning only needs to provide the correct floor. However, as this study also considers the transition areas to be individual levels, it will both provide the height accuracy and floor detection accuracy for localization. Moreover, both the initial and the final floors have additional sensor information for floor level calibration, i.e. cameras' 3D locations in the main system. This can help improve the floor detection accuracy than using only the barometer-based floor detection algorithm.

4.6.3.1. Height Estimation and Floor Detection by Barometers

After the recorded pressure data are transferred into height, the MAEs of estimated height information from both types of smartphones are about 0.5m, which is not as good as that of using two barometers with one as a reference device with an accuracy of 0.15m (Kim et al., 2017). However, it is better than the methods with a single barometer, which only achieves an accuracy of 1 to 2m (Flores and Farcy, 2014, Lin et al., 2015, Shin et al., 2014, Sagawa et al., 2000) (Table 4.6.3.1). Considering the low-cost and easy implementation, the proposed method is still a better choice than other methods with comparable accuracy. In addition, its precision is within an average value at 0.16m, suggesting a relatively stable performance while other studies have not provided corresponding data for comparison.

TABLE 4.6.3.1

ACCURACY COMPARISON BETWEEN DIFFERENT STUDIES USING BAROMETERS

Reference	(Sagawa et al., 2000)	(Flores and Farcy, 2014)	(Lin et al., 2015, Shin et al., 2014)	(Kim et al., 2017)	This Study
Methods	BPF	Relative height fingerprint	Relative height fingerprint + GNSS signals	Reference Device	Self-calibration + Mean and Slope Change Detection
No. of Barometers	1	1	1	2	1
Device	Self-created prototype	Samsung Galaxy S3	Unknown Android Phone	Samsung Galaxy Note 5, Samsung Galaxy S4	Huawei Mate 8/ iPhone 7 Plus
MAE (m)	1.20	1~2m	1~2m	0.15	0.50

After being processed using the floor detection algorithm, the results show that the barometers from both types of smartphones are sensitive enough to recognize the floors with a relatively high accuracy, i.e. 98%. These errors typically appear in the few first stairs of the movement going down from the staircases. This may be due to two major reasons as described in the previous sections. First is the imprecision of embedded barometers, which makes the errors unavoidable during processing and the previous studies also have faced the similar problem (Muralidharan et al., 2014, Ye et al., 2014, Ye et al., 2016). Although this study has improved the sensitivity of floor height change detection as it is able to detect about less than half meter's change in average, it is still over the average stair's height. This is mainly from the limitations of algorithm used for detecting sudden changing points, which will cause short delays during floor detection.

4.6.3.2. Comparison with IMU-based Height Estimation

Some studies explore the accuracy of using vertical acceleration changes based on foot-mounted INS for height estimation (Foxlin, 2005, Hsu et al., 2017). As the experimental conditions of these studies are different, the accuracy will be assessed by the ratio between estimated height error and the overall height of the staircases (Table 4.6.3.2). The results suggest that the barometer-assisted height detection is comparable to these foot-mounted sensor systems, even using lower precision of embedded hardware in smartphones.

TABLE 4.6.3.2
ACCURACY COMPARISON BETWEEN OTHER STUDIES USING ACCELEROMETERS

Reference	(Foxlin, 2005)	(Hsu et al., 2017)	This Study
Methods	ZUPT	ZUPT + Probabilistic Neutral Network Classification	Self-calibration + Mean and Slope Change Detection
Total Height (m)	3	7.84	13.07
Device	InertiaCube3	Self-created Prototype	Huawei Mate8/ iPhone7 Plus
MAE (m)	0.06	0.50	0.50

4.6.4. 3D System Validation

The above experiment described in **Section 4.6.1** to **4.6.3** is based on the data of a single user, and its accuracy is better than the targeting requirements (Rantakokko et al., 2007, Rantakokko et al., 2010). In order to validate the robustness of the designed 3D system, more variations of participants have been introduced with similar experimental setups, which can be found in Section **5.2.3.1.1** in Chapter 5 with more females and males moving between floors via the staircases. In addition, this study also has involved a group of the same number of males and females who are unfamiliar to the selected building, i.e. PMB, to participate in the experiment. The acquired results have both achieved similar accuracy and precision as listed in Table 4.6.2.1.2 and 4.6.3.1. This has suggested a relatively stable performance of the designed 2D system with various users.

In addition, similar experimental setups have also been tested in another building with similar structure at UNNC, which is used for 3D building model establishment (Chen et al., 2018). According to the achieved accuracy (Chen et al., 2018), the horizontal and vertical MAEs are also similar as those in this study. Together with the previous 2D validation in **Section 3.8.2.5**, it has suggested the reliability of the application of the designed 2D system under various environments.

4.6.5. 3D Localization and Comparison to Other Studies

A 3D path is produced after the integration with previous calibrated results of 2D PVINS by similar time stamps (Fig.4.6.4). However, as not all the steps are detected, there are some additional errors being introduced into PDR-based positioning system besides the errors from the barometer measurements, especially for Android-running system as it has more undetected steps. Moreover, as the step event frequency is not perfectly matching with that of height data, which will be another error source for the 3D localization. Thus, 3D positions estimated by Android-running system will have larger total MAE (1.55m) than that by the iOS-based system (1.52m). *The errors mainly come from the transition areas, where there is no calibration from visual positioning and the barometer cannot deal with the quick changes of insignificant changes of height by walking downstairs* (Fig.4.6.4), which has also been proved by (Ebner et al., 2015) with similar conclusions. When comparing to the other systems with precise IMU sensors (Foxlin, 2005, Zhang et al., 2015), their performances are not affected by the missing detection of steps during sensor fusion. Therefore, their previous higher accuracies in both 2D positioning and height estimation will lead to a relatively better 3D positioning accuracy, with 0.3% in (Foxlin, 2005), and 1.1% in (Zhang et al., 2015) (the accuracy here is the ratio between estimated error and the total distance of referential path). The accuracy of the proposed system is about 0.9%, which can be regarded as comparable to these studies.

Moreover, this is also better than the previous study using multi-sensor system including Wi-Fi, iBeacons, and barometer for positioning with a 3D positioning accuracy of 1.7% (Ebner et al., 2015), while having no additional cost for installation or infrastructure management. The accuracy of the proposed system may be improved in future with the PDR algorithm or the advancement of embedded IMU sensors to have higher sensitivity to detect the correct number of steps. Considering the requirements of a suitable 3D indoor positioning system, which is high precision, low-cost and offers an improved user experience, this system is a good solution, while the other precise 3D indoor positioning solutions need either a specific attachment of body sensors on the foot (Foxlin, 2005, Zhang et al., 2015) or additional installations of infrastructures (Ebner et al., 2015).

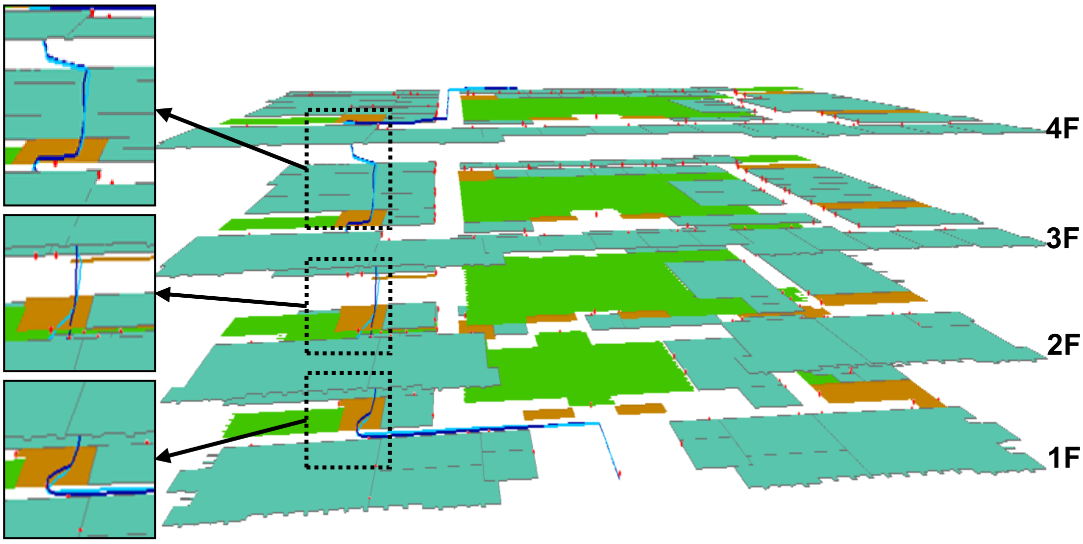

Fig.4.6.4. The 3D view of the estimated path by smartphone-based PDR (Android in light blue and iOS in dark blue) and the locations of main errors in dash boxes.

However, the requirement of 3D positioning accuracy is less important for real applications as it usually requires 2.5D positioning instead of real 3D positioning. The user positions can then be represented as $P^{*}(x_R, y_R, J)$ by providing the horizontal positions (x_R, y_R) and the correct floor number J. By integrating floor number information into the previous 2D system based similar time stamps, <u>the overall performance of the system will not be significantly affected as this time the 2D positions are more important and the floor detection accuracy is high enough to handle automatic floor plan changes.</u>

4.7. LIMITATIONS OF SYSTEM BEFORE BEING APPLIED INTO REAL PRACTICAL

According to the previously acquired results from the experiments in the selected building, it can be found out that the designed prototype can satisfy the proposed requirements in **Section 1.2.1.1**, which is low-cost, high accessibility and accuracy. However, the application of this prototype in real practical may have some other difficulties. This is because that the environmental conditions in a real fire scene can be harsher than those under the experiments, which may affect the functionality of the system. The following sections will focus on some potential effects caused by high temperature, low visibility, and power outage. It will also investigate whether the designed 3D PVINS has the potential to be transferred from the current offline-mode into a real-time processing system.

4.7.1. Tolerance to High Temperature

As this system will be applied at a fire scene, the environmental temperature could be an important factor as it is involved in the process of height estimation. As the designed system is supposed to have a remote processing centre out of the managed building for building manager, the data processing during the fire will not be significantly affected by the high temperature of the fire scene. The main threats are on the user devices and surveillance system which need to be functional at the fire scene for position identification.

According to the previous studies, the highest temperature limit for human survival during fire evacuation is about 60°C (Kenney et al., 2004, Zhang et al., 2011a, Wang et al., 2015), and a higher temperature may cause difficulty on human movements and threats to human life. Meanwhile, the safe zone of smartphone functioning and surveillance camera working is also at a similar level (65°C). This has set the upper limit temperature to the system as well for moving occupants (60°C) and trapped victims (65°C).

The impacts on the embedded barometer will be investigated first, as the identification of the floor level is the first priority for corresponding map information selection. It will focus on whether the maximum change of temperature will affect the accuracy of height estimation and whether this effect is tolerated for floor identification. According to Formula (4.4.1.6) and

Fig.4.4.3, the relative height Δh based on the pressure data can be rewritten as:

$$\Delta h = \frac{((\frac{P_0}{P})^{\frac{1}{5.257}}-1)\times T}{0.0065} - \frac{((\frac{P_0}{P_g})^{\frac{1}{5.257}}-1)\times T}{0.0065} \tag{4.7.5.1}$$

$$\Rightarrow \frac{0.0065\times\Delta h}{P_0^{\frac{1}{5.257}}\times T} = (\frac{1}{P})^{\frac{1}{5.257}} - (\frac{1}{P_g})^{\frac{1}{5.257}} \tag{4.7.5.2}$$

Meanwhile, according to the Gay-Lussac's Law (Poling et al., 2001), the relationship between pressure and temperature can be described as:

$$PV = nRT \tag{4.7.5.3}$$

where V represents the gas volume, n represents the molarity of air, and R is the gas constant ($R = 8.31kPa\cdot L/mol\cdot K$). The ratio between air pressures of different temperatures can then be written as:

$$\frac{P}{P'} = \frac{T_1}{T_2} \tag{4.7.5.4}$$

It can then be interpolated with the integration of Formula (4.7.5.2) to acquire the corresponding Δh under different temperatures as:

$$\begin{cases} \dfrac{0.0065\times\Delta h_1}{P_0^{\frac{1}{5.257}}\times T_1} = \left(\dfrac{1}{P}\right)^{\frac{1}{5.257}} - \left(\dfrac{1}{P_g}\right)^{\frac{1}{5.257}} \\ \dfrac{0.0065\times\Delta h_2}{P_0^{\frac{1}{5.257}}\times T_2} = \left(\dfrac{1}{P'}\right)^{\frac{1}{5.257}} - \left(\dfrac{1}{P'_g}\right)^{\frac{1}{5.257}} = \left(\dfrac{T_1}{P\times T_2}\right)^{\frac{1}{5.257}} - \left(\dfrac{T_1}{P_g\times T_2}\right)^{\frac{1}{5.257}} \end{cases} \tag{4.7.5.5}$$

$$\begin{aligned} \frac{\Delta h_1}{\Delta h_2} &= \frac{\left(\frac{1}{P}\right)^{\frac{1}{5.257}} - \left(\frac{1}{P_g}\right)^{\frac{1}{5.257}}}{\left(\frac{T_1}{P\times T_2}\right)^{\frac{1}{5.257}} - \left(\frac{T_1}{P_g\times T_2}\right)^{\frac{1}{5.257}}} \times \frac{T_1}{T_2} \\ &= \frac{\cancel{\left(\frac{1}{P}\right)^{\frac{1}{5.257}} - \left(\frac{1}{P_g}\right)^{\frac{1}{5.257}}}}{\left(\frac{T_1}{T_2}\right)^{\frac{1}{5.257}}\left(\cancel{\left(\frac{1}{P}\right)^{\frac{1}{5.257}} - \left(\frac{1}{P_g}\right)^{\frac{1}{5.257}}}\right)} \times \frac{T_1}{T_2} \\ &= \left(\frac{T_1}{T_2}\right)^{1-\frac{1}{5.257}} \end{aligned} \tag{4.7.5.6}$$

The maximum ratio between $\frac{\Delta h_1}{\Delta h_2}$ is then only be determined by the maximum change of the temperature, which is in the range from 20°C to 60°C, and the result of this study is about 0.90. With the integration of the previous results of accuracy of height estimation, the new error with the maximum available increasing temperature for safe human movement at a fire scene is supposed to be 0.55m, and it will not cause great difference for floor detection when applying the similar height ranges. The accuracy of floor detection is still 98%, showing a relatively high tolerance to height/floor estimation.

Moreover, the change of the temperature can also lead to the drift of IMU sensors (Aggarwal et al., 2008, Niu et al., 2013) and the failure of the surveillance cameras. The latter will be discussed later as it can be treated similarly as the result of low visibility. For the drift of the gyroscopes, it can be calibrated in the visible area. However, it will become worse if without enough heading calibration from visual tracking system due to high occlusion. However, for the drift of accelerometer, the current algorithm may need to be modified as the current threshold for step detection is more suitable for measurement under 20°C. The designed 3D PVINS needs some further works on the performances analysis of accelerometer under different temperatures from 20°C to 60°C. Moreover, the future development of system may need the integration of a thermometer for temperature recording, in order to derive the corresponding accelerometer performances.

However, if the room temperature is over 60°C, the occupants are under the risk of unsafe evacuation movements. Thus, they are suggested to stay inside the room other than moving by themselves while the designed system is supposed to record their last position before stopping functioning. However, this information may not be very reliable as people may keep moving after the crash of the system, which can cause some difficulties for later rescue when the fire brigades try to utilize the last reported information to identify the trapped victims. When the temperature is over 65°C, the entire system will stop working.

4.7.2. Tolerance to Low Visibility

The visibility condition at a fire scene also needs careful considerations as it is normal to face a situation of low visibility caused by the insufficient illumination or heavy smokes (Proulx et al., 1999, Jeon et al., 2011, Zeng et al., 2017).

This may cause difficulties for the applications of the proposed system, on both aspects of the sensors and the users.

On the aspect of the sensors, it may affect the utilization of the surveillance cameras, as it requires LoS for proper functioning. These two effects may lead to higher errors of pedestrian detection or even failure of the visual tracking. The factors which can lead to the low visibility during the operation at the fire scene can be divided into three categories based on different environmental conditions as insufficient illumination, heavy smoke, and entire failure of proper functioning. Thus, the corresponding approaches to deal with these situations are also different based on the specific factors.

For low visibility caused by the deficient illumination, it may be overcome depended on the model of the surveillance camera applied in the building. If the camera is able for IR Imaging, it may still be functional with the modification of the Faster R-CNN based pedestrian detection system into multispectral detection. It can be achieved by the combination of the Visual-Optical (VOS) and IR spectra to improve the situation of weak image contrast for pedestrian detection (Leykin et al., 2007, Hwang et al., 2015, Choi et al., 2016, Liu et al., 2016, Konig et al., 2017). However, the detection accuracy may be slightly lower than that under the situation better illumination due to the poor image quality. The heat radiation effects from the fire scene should also be realized as an unneglectable environmental factor, which may add unwanted noise to pedestrian detection.

For low visibility caused by heavy smoke, it may lead to haze effect inside the images and this effect can also be removed to some extent with the introduction of atmospheric scattering model (Ju et al., 2017) to the Faster R-CNN based pedestrian detection by the application of an additional Multi-Scale CNN (MSCNN) for medium transmission estimation (Cai et al., 2016, Ren et al., 2016, Li et al., 2017). Some recent studies have also introduced a more advanced deep network called Generative Adversarial Network (GAN) with higher accuracy and faster computation speed to deal with the heavy haze problem (Zhang et al., 2017, Suárez et al., 2018) and the de-hazed images can later be used for pedestrian detection. However, the level of the smoke should not be too high to make the targets entirely invisible, otherwise the algorithm may not function properly. In this case, the integration of Near IR can also help to remove the haze effects to improve the detection accuracy. However, there is still some future work required to deal with that situation (Suárez et al., 2018).

When the surveillance system completely fails to work, regardless due to power outage or too many people in the view with no entire detectable body, there is still a solution to deal with that situation if the temperature at the fire scene has not exceed the upper limit (60°C). As the designed system enables the independent working of the sub-systems, the smartphone-based PDR is still functional even under the situation of low visibility and provide the positioning information of the users. However, the failure of surveillance cameras does not happen at the very initial state as the fire expansion requires some time before the crash of the surveillance system. Thus, the surveillance system can still work for a short time before the final failure. After that, as without the heading calibration from the visual tracking, the accuracy of the provided results by PDR may be deteriorated depended on the specific moving path. If passing a long distance with an open loop, it may lead to larger drifts than moving across a short distance with a closed loop. For the situation of temperature within 60°C to 65°C, it may be used for trapped user localization though problematic as mentioned before, while it will stop working when over 65°C.

On the user aspect, the low visibility may also raise difficulties for pedestrians to follow the guidance services as they need to check the screens of smartphones as well as the surrounding environment to figure out their current positions and the planned path for evacuation. When the low visibility is caused by insufficient illumination, this may not cause difficulties for positioning and path reading as the screen can still be visualized with its own illumination. In addition, the screen light can help people to have a rough check of the surrounding environment. On the other hand, if the low visibility is caused by heavy smoke, it may raise difficulties of checking screens and surroundings as people may not be able to see very clearly even when they are using a bending posture. In this situation, the vocal guidance may help to resolve the problem. However, as the low visibility can cause panic of the pedestrians (Trivedi and Rao, 2018), it may raise the unwillingness of people to follow the navigation guidance, which has also been suggested in the later investigations mentioned **in Section 6.3.3**. When low visibility is caused by a power outage, this can be treated as the same situation of insufficient illumination when the temperature in the indoor environment is not over the extreme condition (60°C). When temperature is over 60°C, the system should strongly suggest people to stay inside the room via either visual or vocal guidance, in order to avoid hurt and ensure the last record of their trapped position can help the fire brigade to localize them in a short time.

4.7.3. Consequences of Power Outage

The cut-off of the electric power during a fire event can also be considered as a challenge as it will disable the functionality of both the surveillance-camera-based visual tracking and data transfer of the entire system via WLAN. For the failure of the surveillance system, it has been discussed in the previous section as it can be compensated by the smartphone-based PDR to some extent, though with lower accuracy. For the data transfer via WLAN, it may be overcome by using the alternative mobile data option (3G/4G). However, both these two solutions are limited by the temperature of fire scene, and it is only feasible when it has not exceeded 65°C. As the safe temperature for human movement is 60°C, the worst case may not happen for tracking moving occupants. However, for the trapped victims, it may raise the issue of false identification of their current locations.

4.7.4. Possibility of Transferring into Online Mode

Like other similar studies (Jiang and Yin, 2015, Jiang and Yin, 2017, Zhang and Zhou, 2018, Foxlin, 2005, Huang et al., 2010a, Zhang et al., 2015, Meng et al., 2014, Hsu et al., 2017, Fourati, 2015, Fang et al., 2005, Yun et al., 2012, Kothari et al., 2012), the data in this study is post-processed after transmission to the desktop. This is mainly limited by the visual data acquisition due to the privacy policy in the university and the visual data is not allowed to be transmitted to the desktop in real time. Meanwhile, the inertial and pressure data can be sent to desktop and processed during the movement via WLAN and the positions of the user will be stored in the system.

The current offline system can be used for low-cost 3D mobile mapping, which can provide the moving trajectories for 2D laser scanning to build 3D indoor models (Chen et al., 2018, Yang et al., 2019). It also can provide historical paths of the indoor pedestrians for security checking. In the future, one of the limitations of turning this system into an online system will be the live streaming speed of surveillance videos. This is determined by the available bandwidth of the existing WLAN in the building. For the current system, the bandwidth should be approx. 6 Mbps for each camera, while the university's WLAN bandwidth is 10 Mbps and it can fully support its live streaming. The storage of the data may be another problem. However, this system is designed for a whole building with a powerful processing centre and it is assumed to finish all processing in the mainstream and send the data back to the user's device via the network, like the idea mentioned in (Fang et al., 2005). The requirement of the computation power for real-time detection is not very high. In this study, the computer has a CPU in Intel Core i7-7700, a GPU in NVIDIA GTX 1080, and 16G RAM, which is commonly used in the field of computer vision industry. This makes the design of this system highly possible to be applied as a real-time system in real scenarios with fewer barriers to overcome for industrial applications in fire evacuations.

4.8. SUMMARY

The previous studies (Jiang and Yin, 2015, Jiang and Yin, 2017, Zhang and Zhou, 2018, Abdulrahim et al., 2011, Yan et al., 2018b, Yan et al., 2018a, Yan et al., 2018c) mentioned in Chapter 3 only provide 2D user locations, while to enable a continuous positioning service, particularly for the time the user is walking up or downstairs, a 3D (or the recognition of the floors) are required (Tanigawa et al., 2008, Shen et al., 2015, Ye et al., 2016). This chapter introduces embedded barometer from smartphone and provides the height and floor estimation using a novel floor detection algorithm with the integration of pre-stored camera locations for precise floor identification. It achieves a vertical accuracy of 0.5m with 98% accurate floor detection. However, the results are still limited by the precision of barometers and the limited capability of algorithm itself for sudden change detection.

This study has designed a novel low-cost 3D PVINS that uses multi-cameras, smartphone-based PDR and embedded barometer, and provides a comparable 3D accuracy of 0.9%. The novelty of this system is:

a) a modified Faster R-CNN based passive visual tracking, with simple implementation, high accuracy, and real-time detection;
b) a novel algorithm for multi-scene shifting with automatic PDR turning detection;
c) a novel data fusion method with simple operation and high effectiveness, achieving more than 20% 2D accuracy improvement for severe occlusion-affected areas than previous 2D PVINSs;
d) a novel algorithm for height/floor estimation with more detailed floor-level division using single embedded barometer in a smartphone;
e) the acquired results with absolute coordinates to be directly used in outdoor systems;
f) the application on both Android-running and iOS-running smartphones with better robustness than previous Android-only systems.

This system can provide 2D positions of each floor with an accuracy of 0.16m while identifying the current floor level of the users with 98% detection accuracy (0.5m vertical accuracy), which has already reached the requirement by Federal Communications Commission (FCC), with 50m horizontal accuracy and 3m vertical accuracy (FCC, 2015). Another advantage of this 3D PVINS is no special requirement of attaching instruments on user bodies or using specific sensor-suite as settlements in other self-contained systems, which makes them more accessible for future applications. However, the PDR algorithm used in this study needs further improvement, because there are more missing steps with the accumulation of distance. This may be due to the data logging mechanism, and it may be solved by temporary data storage on a user's device and resuming data transmission when having Wi-Fi connection again. This problem mainly happened in the staircase area as the RSS of WLAN is significantly weakened, while it is not a big problem in previous chapter as the WLAN RSS in the floor area is stronger and more stable. Moreover, as this system is currently designed for single user tracking, it still has the potential to be developed into a multi-user system, which needs to improve the algorithm of visual tracking. The acquisition of surveillance data may be another limitation before turning the current system into a real-time system as it will raise the issue of personal privacy and this time the permission is pre-applied for data downloading. The floor identification approach can also be more precise to identify exact user 3D locations inside buildings.

Chapter 5. AGENT-BASED INDOOR EVACUATION MODELLING OF TWO EVACUATION STRATEGIES WITH PHYSICALLY MEASURED PARAMETERS

5.1. INTRODUCTION

The preparation of the proper safety measures, e.g. the calculation of the evacuation time, have become more important for building life safety assessment (Kuligowski et al., 2010, Wagner and Agrawal, 2014). This study will provide a design of a simulation model with the integration of ABM and continuous-network based indoor environment driven from real CAD plans of a four-floor building, to simulate and analyse occupants' movement from indoor area to the outside before and after fire alarm in the venues of ordinary campus-office area with the change of available exits. It will attempt to compare the efficiency of two evacuation strategies called randomly movement and nearest exit assignment.

When using the ABMs, the occupant characteristics is one of the important human factors to accurately represent the whole process and features involved in the evacuation models (Proulx, 2002, Muhdi et al., 2006, Kady and Davis, 2009a), which is defined as the abilities or behaviours of people before and during a fire by Life Safety Code ((NFPA and Coté, 2015). Among them, the pedestrian speed and ID (Inter-Person Distance) are two important factors that require careful specification (Shi et al., 2009b). This study mainly focuses on speed and diameter change of different genders under the condition of using two different types of the stoop-walking (SW) postures with simulated scenarios of emergency and non-emergency. The corresponding setups of the parameters can then be measured based on the data collected by smartphone-based sensors following the same methods mentioned in Chapter 4, which may help to improve the reality of the simulation results. The pre-evacuation period is summarized based on the practical survey data instead of estimation (0~120s) (Daamen et al., 2007, Tang and Ren, 2008, Spearpoint and Xiang, 2011) or be ignored as previous studies (Shiwakoti and Sarvi, 2013, Wagner and Agrawal, 2014, Kasereka et al., 2018, Trivedi and Rao, 2018).

Meanwhile, a simplified and self-defined fire model is also integrated into the simulation process based on the spread of the flame, in order to predict the percentage of the population in danger during the process of evacuation and figure out possible solutions. The simulated models will help to predict the average as well as the maximum evacuation time of the occupants for the whole building and for each exit. Moreover, it will find out the potential congestion areas inside the building. Based on comparisons of simulated evacuation performances by using two evacuation strategies, it will provide an answer about which strategy is more suitable in order to improve the efficiency of future evacuation planning and guidance.

The following sections will separately describe the detailed setups of the spatial environment, the person movement, and fire expansion during simulation followed by simulated results.

5.2. DESIGN OF THE ABM AND ATTRIBUTES OF THE AGENTS

The fire evacuation simulation is a complicated system, which can be divided into three parts as the building environment, occupants and fire (Fig.5.2). This study proposes a hybrid ABM to model a four-floor campus teaching building, which is created as a GIS-based building environment and is proportional to the real world coordinates with offices, staircases, and exits. The system is designed for simulating the process of crowd movement before the fire drill and crowd evacuation after firm alarm. The movements of the individual agents are based on the mixture of SF and ABM modelling approaches. The former will provide the interactions between individuals and the environment, while the latter can support the heterogeneous individual characteristics description. The integration of these two modelling methods will provide a continuous description of the crowd evacuation process inside the building. There are two types of agents included in this model, i.e. occupants and the fire. The initial locations of the occupants will be created according to the distribution of rooms and move randomly inside the building before the fire alarm is triggered. After the fire alarm, there will be a random distribution of occupants inside the building moving to the exits based on their random decisions of the routes (i.e. behavioural model), and the number of exits will increased from two to five with the availability of emergency exits. The average time for survivals will then be estimated depended on the different exits and for the entire building. In addition, a density distribution map will be acquired during the movement in order to discover the bottlenecks inside the building. Meanwhile, a simplified fire model will be integrated into the evacuation model, in order to estimate the ASET and to evaluate the percentage of the population in danger during the process of the evacuation.

This system is implemented under the environment of AnyLogic, which is able to provide quick and high-fidelity agent-based modelling and simulation with an user-friendly interface, Java-based programming environment, and multi-purpose supportive component libraries (Borshchev, 2013). It will be helpful in the planning of the fire evacuations with the following four advantages to the emergency managers:

1) The GIS-based building environment can be modified to fit the different requirements of floor plans with similar spatial characteristics as rooms, staircases and changing number of exits. This allows the quick replication of different kinds of buildings of multi-floors (not very high building as it may require a refuge layer) with the availability of their floor plans to execute the similar simulations and acquire the results close to the reality;
2) The fire model is simplified and thus requires less computational power as previously using Fire Dynamics Simulation (FDS) model to render the expansion of flames;
3) The fire and occupant model can be specified based on different user definitions, with various spread rate, locations, ID and behavioural rules;
4) The model can be tested for multiple solutions of evacuation strategies, with a relatively low cost and risks.

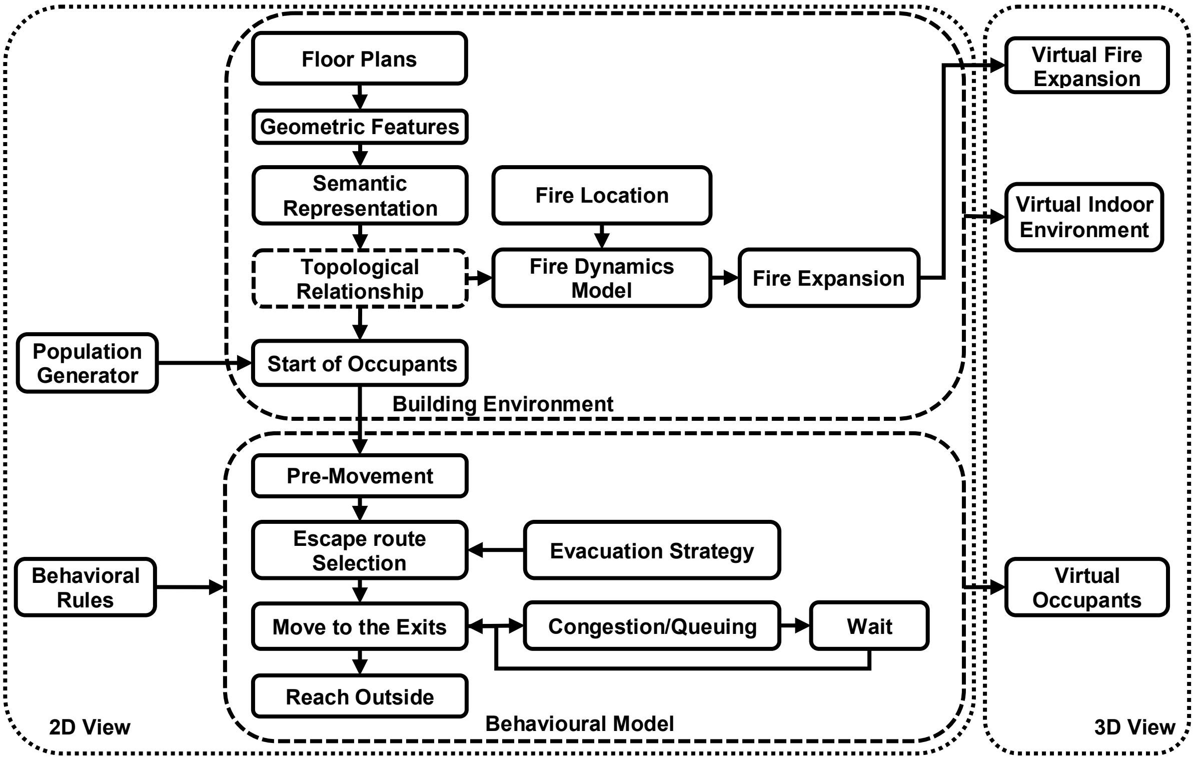

Fig.5.2. The general architecture of the ABM-based fire evacuation model.

The attributes of the agents are acquired in two ways. For the occupants, their moving attributes are acquired from the experiments, using the system called PVINS with the integration of smartphone-based IMUs, surveillance cameras, and the smartphone-based barometer. The experiments will be able to provide the moving velocity and preferences of using different postures, i.e. UW, Trunk-flexion-only SW (TSW) and Trunk-and-Knee-flexion SW (TKSW). The preference of the bending postures and the pre-movement time are depended on the survey data of occupants regularly work inside the building and then be applied to the model. For the fire dynamics, as it is simplified as a spatial-temporal model, the key parameter related with the fire simulation model is the spread rate of the fire and this data is based on the summary from the previous studies (Galea et al., 2008, Wagner and Agrawal, 2014, Niu and Song, 2016).

5.2.1. Spatial Setups

The fire evacuation is related with both the geometric/static features and the dynamic features from the fire and the pedestrian movement (Galea et al., 2008, Tang and Ren, 2008, Shi et al., 2009a, Tang and Ren, 2012, Tan et al., 2015). In this study, the establishment of the spatial environment is supported by the Space Markup Elements in Pedestrian Library in AnyLogic, which can develop a continuous graphical model in a real-scale (Borshchev, 2013). For the static features, it is represented as a GIS-based model with multiple layers established based on the floor plans imported from the GIS shapefiles (Fig.5.2.1.1). The topological relationships can then be simply acquired based on the spatial analysis, which is usually stored as the external attributes with the GIS shapefiles, in order to identify corridors, doors, rooms, staircases and exits. Meanwhile, these features can help to shape the potential routes for pedestrians, as only the opening space is allowed to pass through. For the dynamic features, such as the pedestrian distribution and flame expansion, can be represented as a temporal series, with the provision of initial locations. These can also be determined due to the spatial attributes from the static features, as the pedestrians are usually located inside the room and the fire location is user-defined. The simulation results can also be imported to the GIS model with the accumulation of the time, and the corresponding dynamic features inside the GIS models can be updated with the time stamps. The quantity of spatial statistics during the evacuation process, such as the changes of the pedestrian density distribution in different floors and the fire expansion can also be automatically acquired by analysing the corresponding variables (Fig.5.2.1.2).

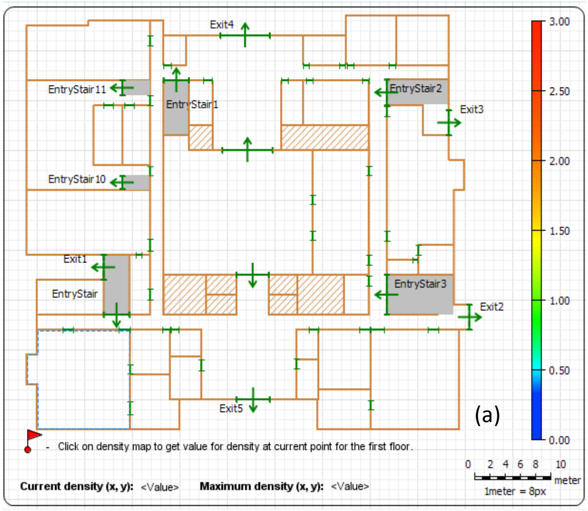

(a)

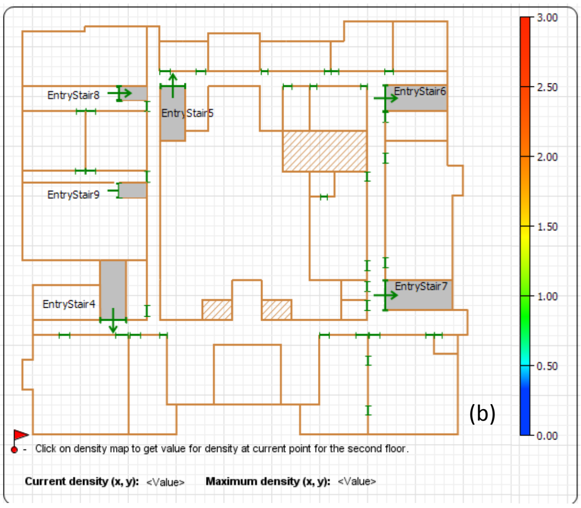

(b)

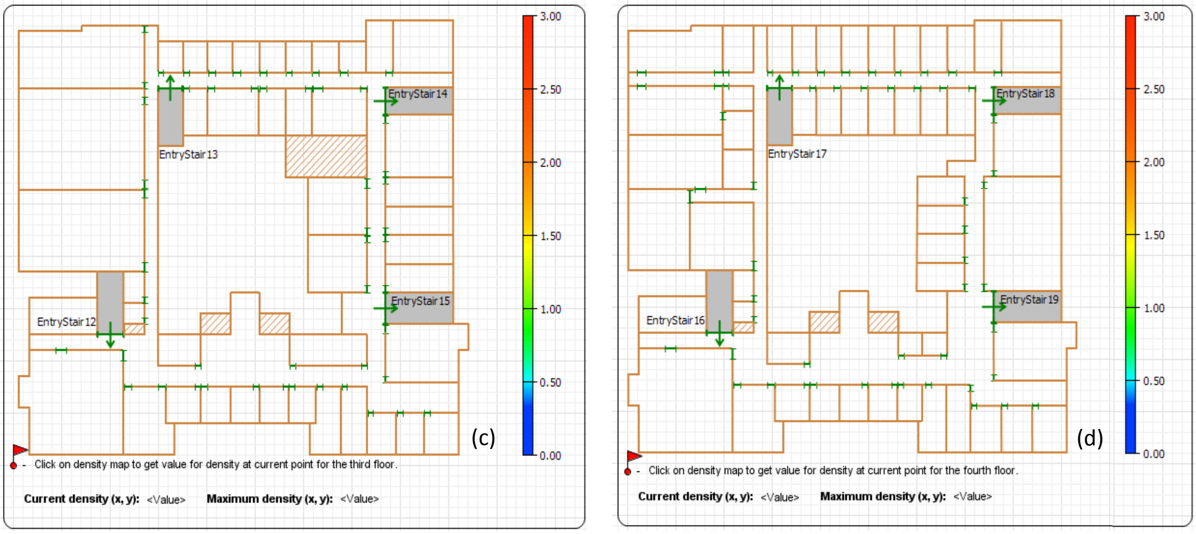

(c) (d)

Fig.5.2.1.1.The GIS-based simulation environments from 1st floor to 4th floor (a)-(d) established by AnyLogic with pedestrian density identifications (The rooms enclosed by walls are in orange, the doors and exits are in green, and the staircase areas are in grey).

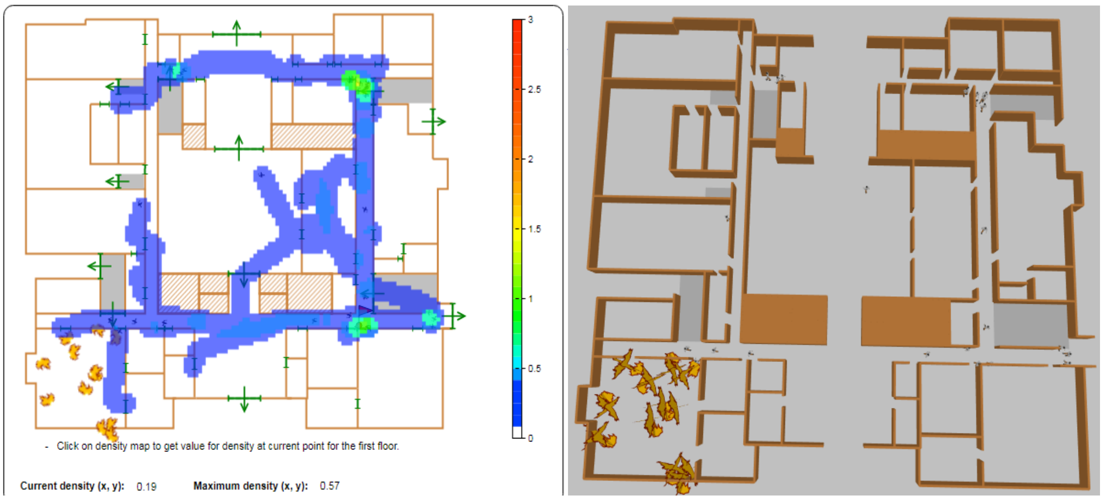

(a) (b)

Fig 5.2.1.2. An example of fire expansion and pedestrian density distribution (person/m^2) on the 1st floor of the tested building in 2D (a) and 3D (b).

5.2.2. Fire Dynamics

In previous studies, the fire data is usually represented by a Computational Fluid Dynamics (CFD) model, which can simulate the expansion of flames, smokes and other relative combustion products in relatively realistic way (Jia et al., 2006, Grandison et al., 2007, Galea et al., 2008, Tang and Ren, 2008, Shi et al., 2009a, Tang and Ren, 2012). However, this may require more computational power for rendering. As mentioned before, the fire data can be simply represented by a simplified temporal-spatial model with the linear increasing of the detrimental areas, without the considerations of characteristics of flaming materials (Wagner and Agrawal, 2014, Niu and Song, 2016). The fire will expand in a random direction from a user-defined ignition location with a specified spreading rate. In this study, the fire agents are treated as fluid-based agents as the fire event initiates inside the room and will fulfil the 'room' space first before being released into the corridors by using the 'valve' for controlling. They are first created from the 'source', and then be transferred to the fluids by using 'agentToFluid' module while randomly expanding inside using 'queue' module. When it is moving to outside of the room (also treated as the triggering of the fire alarm), it is transferred back to normal agent by using 'fluidToAgent' with a lateral spreading rate. With consideration of the fire-proof doors, the flames will only move along the corridors without the re-entering of the other rooms by using 'moveTo' module. The fire will keep expanding until it fulfil the open spaces inside the building and stopped at the exits by using the 'delay' and 'hold' modules (Table 5.2.2).

TABLE 5.2.2

THE ALGORITHM OF FIRE EXPANSION

Algorithm 1 Fire Dynamics Model

```
Initialize fire at the selected office ⊳ Using Source
Start of Event ← Current Time
Transfer fire agents into fluid-based agents ⊳ Using AgentToFluid
If room is not full then
⊳  Current room is not fulfilled  by the smoke/flame
    Fire agents accumulate in the room with specified rate
    ⊳  Using Tank
else
    Release the agents from room ⊳ Using Valve
    Transfer fluid-based agents back ⊳ Using FluidToAgent
    for each agent Є Fire do
        Exit {Exit1, …, Exit 5}← Uniform Probability
        Move to Exit ⊳ Using MoveTo
        Fire has been blocked before being released to outdoor
        ⊳ Using Hold
     End for
End if
Return Time before Alarm = Current Time – Start Time
```

The pedestrians who are located within a specified distance to the fire after being released into the corridors are treated as hurt. The smoke cannot not visualized in the GIS-based environment provided by AnyLogic but with the calculation of the production rate, due to no corresponding agent symbols. When the amount of smoke reaches the specified threshold after certain time period (i.e. the calculation of the ASET), all remaining people inside the building area are treated as trapped.

5.2.3. Pedestrian Movement

In this study, the movement of the pedestrians is supported by the Pedestrian Library in AnyLogic, which allows the modelling of pedestrian behaviours based on a SF model in a microscale with a continuous manner. The custom attributes and behaviours of the people will be assigned to the specific types of the agents, i.e. people. AnyLogic can randomly assign the initial values of the physical attributes to the agents, such as the velocity and group population, based on a certain probability distribution by the 'PedSource' function. In this study, it assigns a triangular distribution of the velocity attributes to the populations based on the survey data of preferred bending postures and the specific velocities of the corresponding postures are acquired by the experiments based on the using of the PVINS mentioned in the previous chapters.

5.2.3.1. Individual Agent Design

5.2.3.1.1. Moving Velocity of Different Postures

1) Subjects Selection

The moving velocities of different bending postures, i.e. TSW and TKSW, are collected by the PVINS with the selected subjects based on the survey data of user knowledge during indoor evacuation. The survey has been conducted among undergraduate students with 28 females and 22 males, who regularly work inside the tested building, i.e. PMB building from the UNNC. The overall height and weight distribution of anticipated female volunteers are listed below (Fig. 5.2.3.1.1).

In this survey, the majority of the anticipated female volunteers have a height in the range of 160~165cm and their weights are in the range of 50~55kg. Meanwhile, the representative height and weight of male anticipants are in the range of 175~180cm, and 65~75kg respectively. All the participated volunteers have a BMI (Body Mass Index) at a healthy stage (19.9~24.2), getting rid of the effects from the overweight and age (Grasso et al., 2000, Kobes et al., 2010a, Hora et al., 2012, Hora and Sladek, 2014, Hora et al., 2017). These physical conditions will be also applied for searching for potential representative volunteers in both genders to testify how different postures during the movement will affect the walking speed and step length. 10 subjects (5 males and 5 females) meeting the above requirements from UNNC are selected for the walking posture experiment. The study was approved by UNNC's Ethics Review Board and all attendees have signed the informed consent.

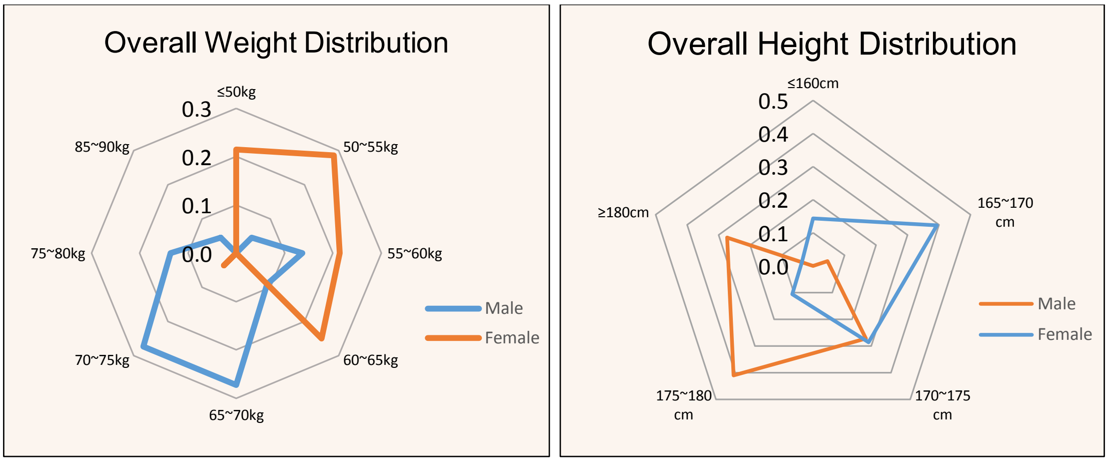

(a) (b)

Fig.5.2.3.1.1. The height (a) and weight (b) distribution of male and female participants.

2) Experimental Design for Horizontal Movement

The subjects are required to walk through a 92.75m test track, which is a corridor located at the fourth floor on the test building. The way of applying the PVINS by the users is similar to the setups as that applied in the previous studies (Yan et al., 2018a, Yan et al., 2018b, Yan et al., 2019) (Fig.5.2.3.1.2a). The subjects will be filmed by the surveillance system inside the building with the installation of the MATLAB Mobile apps to transfer their PDR data to the data-control desktop. Other than the other studies about the user velocity of different postures (Kady and Davis, 2009b, Davis, 2011b, Gallagher et al., 2010, Gallagher et al., 2011, Cao et al., 2014, Cao et al., 2018), which use a specific set of multi-camera/motion capture system with professional sensors for acquiring the walking speed during the process, the method applied in this study, which is mentioned in Chapter 3, is much simpler as it does not need a large number of professional cameras/sensors, but the existing indoor infrastructures and available user devices.

Before the test, all the subjects will have 10 minutes to learn to use the installed data collection app on smartphones and the required postures based on the designed reduction of body height (30%). The reduction limitation for the height is based on the previous findings that the maximum available height for long-term SW is 70% of the height for the females (Morrissey, 1980, Morrissey et al., 1985). During the experiment, each subject will first use a UW posture before reaching to the first camera, which accounts for 60.9m of the track. The participants are required to stop here if they are informed that the current scenario is under a relaxed state. Otherwise they will be required to finish the rest of the track, using a SW posture in the form of TSW or TKSW in a random order (Fig.5.2.3.1.2b). Meanwhile, every two subjects will be treated as a group and one people will start walking first while the other will start one-step later, in order to study the ID between people. The groups are settled as two females, two males, and a mixture of male and female, and the postures used within one group are settled as two TSWs and two TKSWs, without the mixture setting. This is due to the distance between every two people is actually decided by the second people's distance to the first people as the first moving user does not have any limitations of moving forward.

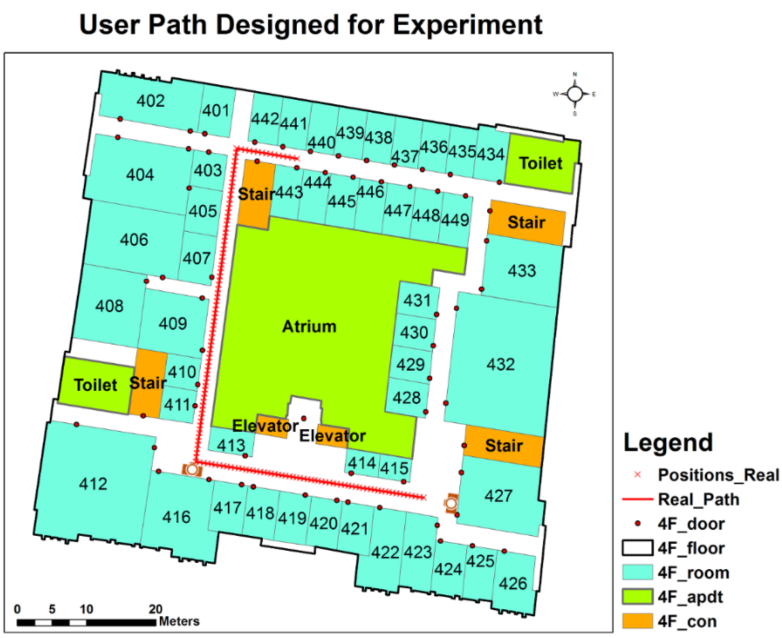

(a)

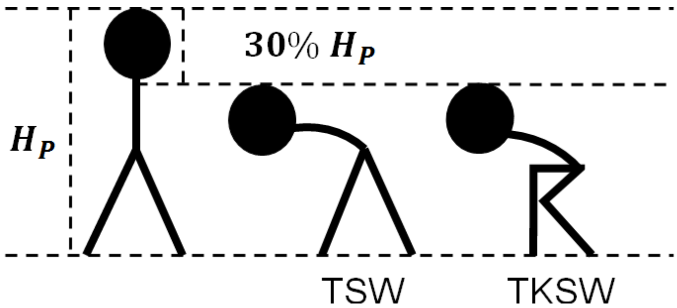

Fig.5.2.3.1.2. The test track for the horizontal walking speed changes (a) with different postures (b).

3) Results of Horizontal Movement

According to the previous studies, the comprehensive analysis and processing of acceleration data from the smartphones, especially at the vertical directions (z-axis), can help to detect different activities, such as jumping, walking, running and falls (Zhang et al., 2006, Yang, 2009, Khan et al., 2010, Lee and Carlisle, 2011, Zintus-art et al., 2011, He et al., 2012, Sucerquia et al., 2018). This study also takes the idea but to detect a certain continuous changing pattern of the speed to distinguish the different SW postures as the change of the accelerations is not as significant as in the previous studies. The acquired synthesized accelerations of the detected steps will be processed for velocity and step lengths of each subjects. These data will then be processed based on the finding the sudden changes of the average values, in order to investigate a periodical velocity changes affected by the changes of postures during the process. The patterns of speed and step length changes for different SW postures can be found in the provided examples under the simulated emergency scenarios (Fig.5.2.3.1.3 and 5.2.3.1.4).

(a)

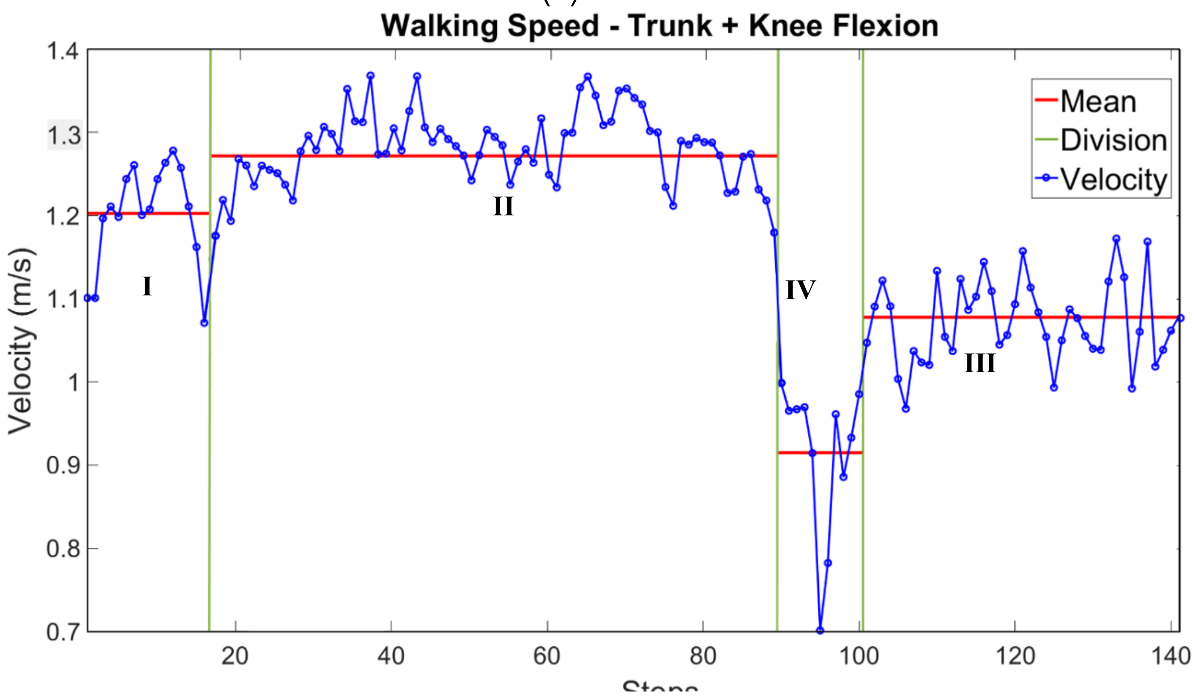

(b)

Fig.5.2.3.1.3. An example of the walking speed changing patterns for using TSW (a) and TKSW (b) (I~IV represent the different periods of the walking process).

According to the provided examples, both of the two processes for UW have experienced an initialization period and reaching a stable state of comfortable speed, represented as Phase I and II in Fig.5.2.3.1.3. The velocity changes under a relaxed scenario also experienced a similar pattern, though the average values are slightly lower. This may be caused by the effect from the panic, as it can accelerate the motions of the pedestrians during the evacuation process (Helbing et al., 2000, Shen et al., 2018, Trivedi and Rao, 2018). The speed of using either of the SW postures have reduced from the stable state, which is agreeable to the findings in the previous studies (Kady and Davis, 2009a, Gallagher et al., 2010, Cao et al., 2014, Cao et al., 2018), caused by hip and/or knee flexion (Ivanenko et al., 2000, Gard et al., 2004, Orendurff et al., 2004, Hora et al., 2017). The main difference between the two postures are in the following periods, although the velocity shows a significant decrease from the Phase II after using either of these two SW postures. The user who uses a TSW posture directly transfers to another stable state (III) with lower velocity, while for who uses a TKSW posture, it need a transition state (IV) before reaching to the second stable state (III). This may be explained by the more significant changes of accelerations at z-axis for the TKSW as the smartphone with IMU sensors are held horizontally in front of the lower chest. The bending of the trunk alone will not cause great changes of COM while the bending of the knees will lead to greater decreases of the COM. Meanwhile, the speed after using the TSW is higher than that of using TKSW. The former (TSW) is even higher than that in Phase I (initial UW), while the latter (TKSW) is lower than that in Phase I. The above patterns for the two different postures are shared by all the selected participants of the experiment and this can help for future identification for the different SW postures. This study also summarizes the average ranges of the speed of different postures for corresponding genders based on the results from the repeated experiments (Table 5.2.3.1.1& 5.2.3.1.2). It also supports the conclusion from the previous studies that the gender can also be a factor which affects the walking speed (Kady and Davis, 2009a, Cao et al., 2014, Cao et al., 2018).

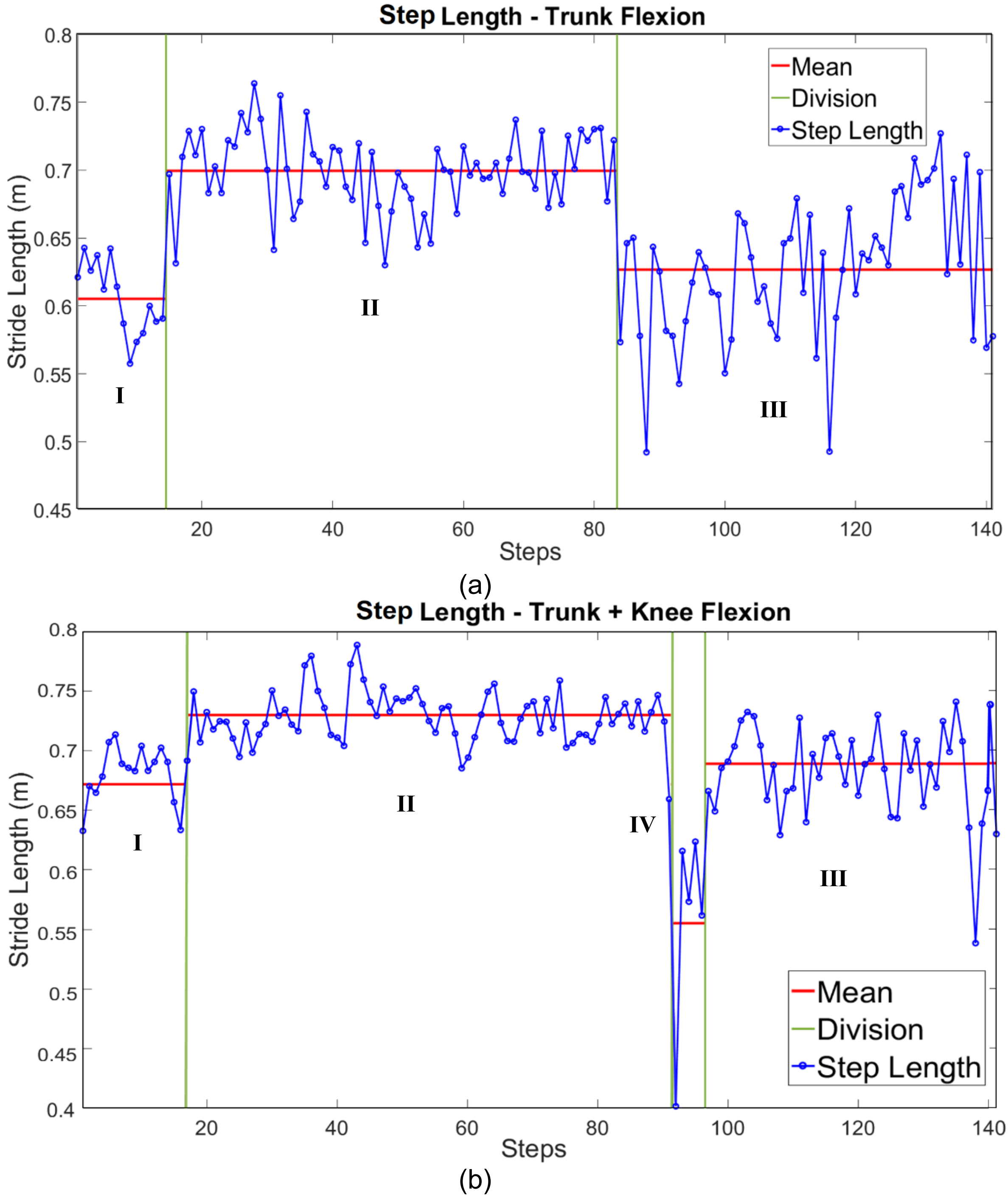

Fig.5.2.3.1.4. An example of the step length changing patterns for using TSW (a) and TKSW (b) (I~IV represent the different periods of the walking process).

The step length changes for this two SW postures follow the similar patterns (Fig.5.2.3.1.4). The users have also experienced a process of familiarization of their walking behaviours when using UW posture, from an initial state to a comfortable state under both normal and emergency scenarios. The characteristics of changing to different SW postures also follows the similar pattern of as the velocity changes, which the TSW posture does not have a transition state before reaching to a new stable state while the TKSW does. However, the average step lengths for the final stable state for the two SW postures are both lower than that of UW at Phase II due to limitations from the lower limb length (Hora et al., 2017) but still higher than that of the Phase I, which is different from the corresponding phases of the speed changes. Moreover, the step length of the TKSW are even higher than that of the TSW. This may be caused by the different attempts of keeping a relatively fast speed when people are using the TKSW posture. Some of the people tries to move a larger step though the step length are limited by the lower limb length while the others move a smaller stance in order to keep a relatively high frequency of steps. In this study, the former kind of the subjects occupy the majority of the participants. However, this requires further investigation in future studies due to the limited number of the participants in this study. Moreover, the observed patterns of velocity and step length changes can be further used for posture recognition, with increasing number of participants.

TABLE 5.2.3.1.1
THE AVERAGE VELOCITY AND STEP LENGTH (MEAN ± SD) OF DIFFERENT POSTURES FOR BOTH GENDERS UNDER EMERGENCY SCENARIO

		Posture				
			UW	TSW	TKSW	
State		Initial (I)	Comfortable (II)	TSW (III)	Transition to TKSW (IV)	TKSW (III)
Velocity (m/s)	Male	1.12±0.10	1.36±0.16	1.16±0.16	0.82±0.24	1.02±0.12
	Female	1.01±0.09	1.23±0.13	1.13±0.15	0.62±0.22	0.97±0.10
Step Length (m)	Male	0.66±0.10	0.74±0.12	0.68±0.11	0.62±0.18	0.69±0.21
	Female	0.60±0.09	0.70±0.11	0.62±0.10	0.56±0.17	0.64±0.10

TABLE 5.2.3.1.2
THE AVERAGE VELOCITY AND STEP LENGTH (MEAN ± SD) OF DIFFERENT POSTURES FOR BOTH GENDERS UNDER NORMAL SCENARIO

		Posture	
			UW
State		Initial (I)	Comfortable (II)
Velocity (m/s)	Male	0.66±0.10	1.10±0.12
	Female	0.60±0.09	1.01±0.11
Step Length (m)	Male	0.56±0.10	0.65±0.12
	Female	0.50±0.09	0.60±0.11

For the ID between every two people, there is no great differences between two genders under two scenarios. The major difference is mainly caused by applying different postures. For UW, the mean ID between people is about 0.40±0.05m. When turning to using bending postures, the mean ID for TSW is about 0.80±0.10m, while for the TKSW, the mean ID is about 0.60±0.10m. All the above information will be applied to be used in the setups of the pedestrian movement model.

4) Experimental Design for Vertical Movement

For the movements between the floors, it will be risky to require people using these two SW postures on the staircases as the SW postures may lead to falls with corresponding injuries with relatively high possibility (Campbell, 2013, Ferraz and Saba, 2017). Therefore, the walking speed of moving along the staircases are inferred from using UW. For UW, the participants are required to move downstairs from fourth floor to the first floor, passing a track about 36.12m (Fig.5.2.3.1.5). In the test site, the average riser height of the stairs is 0.15m and the average thread length of the stairs is 0.29m. This time, both the barometer and the PDR data are required to be recorded at the smartphones held by the participants. The method applied for speed measurement is based on the algorithm mentioned in Chapter 4 (Yan et al., 2019).

During the experiment, the participants are required to hold the smartphones horizontally in front of the lower chest when walking downstairs. They also move in groups with two people in each group. One people will start walking first while the other will start two-stair later, in order to study the ID between people. The groups are settled as two females, two males, and a mixture of male and female.

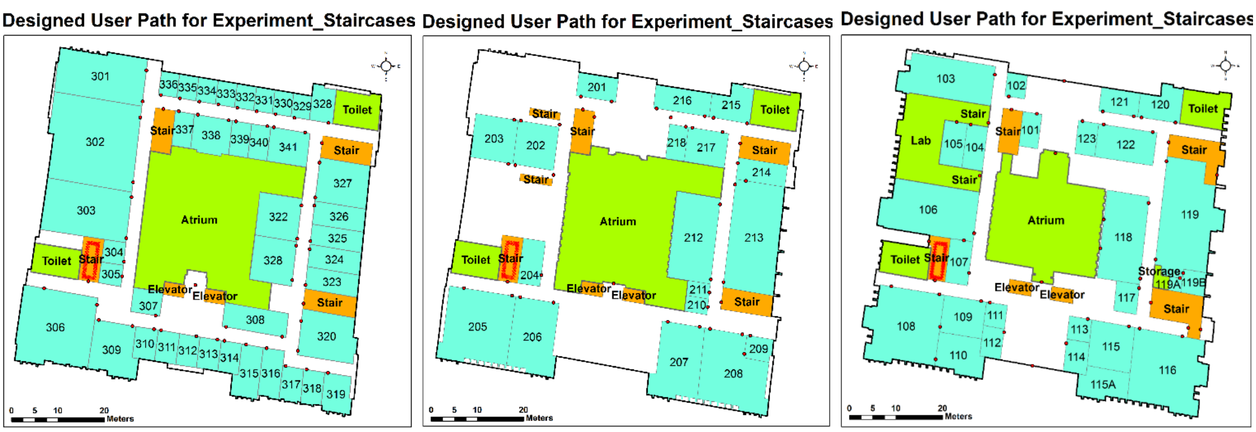

Fig.5.2.3.1.5. The test track for the vertical walking speed changes.

5) Results of Vertical Movement

The movement of the pedestrians at the staircases can be treated as repeated height change patterns based on the previous findings in Chapter 4 (Yan et al., 2019). This study considers one staircase plus one transition platform as one group of the characteristically repeated pattern, and thus it has six groups in the experiment according to the results of floor identification. In order to eliminate the effects from the initialization of the speed in the beginning, the first group will be removed during the process of speed calculation. The average UW speed for vertical movement is then calculated from the rest five groups and the value is about 0.82±0.16m/s for the males and 0.74±0.16m/s for the females. When comparing to the horizontal speed of using UW, it can be found out that the ratio between vertical speed and the horizontal speed is a constant based on the results in this study, which is about 0.6. This ratio can be applied to the model in order to infer the potential instantaneous speed in the staircases based on the actual speed of the horizontal movement during the simulation process. For the ID between two people, there is still no great differences between two genders and its value is close to that of horizontal movement (0.29m), which is about one-stair away between each other. Thus, the previous ID of other SW postures can still be applied into the evacuation model with the same value.

5.2.3.1.2. Application of the Velocity inside the Simulation

When applying the pedestrian velocity to the simulation, it needs be within a specific range which is based on the integration of experimental and survey data. This study also investigates the preferences of the TSW and the TKSW during evacuation among the students in order to determine the specific triangular model of the speed in the simulation model. According to the acquired results, 66% of the interviewees prefer to take a TKSW posture during the evacuation requiring bending. For different genders, their choices do not have a significant differences as the majority (66%) of them seems to prefer to take a TKSW posture. With the integration of the corresponding velocity and ID information, the triangular model for the parameters of the pedestrian movement can then be determined based on the formula below (Samuel, 2004):

$$f(x) = Triangular(Min,\ Max, Mode) = \begin{cases} \frac{2(x-Min)}{(Mode-Min)(Max-Min)} & x \in (Min, Mode) \\ \frac{2(Max-x)}{(Max-Mode)(Max-Min)} & x \in (Mode, Max) \end{cases} \quad (5.2.3.1.2)$$

Where the Min, Max and Mode represents the minimum, maximum and mode value of the parameters. The horizontal velocity required for the model under different scenarios can be acquired from the previous experiments. For the non-emergency scenario, the minimum is taken from female's average velocity of UW postures at both initial and comfortable states and maximum is taken from same states of males. For the emergency scenario, it varies from different postures, the minimum and maximum values will be taken from the lowest (female with TKSW) and highest speed (male with UW) for all different postures of two genders. This is due to that the average speed of the males are always higher than that of the females, regardless of the postures. For the mode value for the both postures, as there are more females inside the tested building based on the survey data and the TKSW is the preferred posture, they are acquired from the female's velocity with TKSW. For the vertical movement, as it is proportional to the horizontal speed, its range can also be determined with the above information. The ID data is also settled by following the similar rules. These data can then be applied into the designed simulation model of evacuation in each floor.

5.2.3.2. SF Model-Based Personal Interaction

The AnyLogic utilize an SF-based model to describe the interactions between agents and agent to the environment, which is affected by the panic level $L_p(t)$ updated every second. During the movement inside the building, the pedestrians tends to form small groups/crowds. The agent i inside the group of mass m_i moves with a certain desired velocity $v_i^0(t)$ in a certain direction $e_i^0(t)$, and the instantaneous speed $v_i(t)$ will be updated correspondingly within a certain characteristic time period τ_i. Meanwhile, the agent i will keep certain safe distances to other agents j and walls W due to the effects of repulsive interactions forces, which can be represented as f_{ij} and f_{iW} respectively (Helbing et al., 2000, Lin et al., 2006, Zheng et al., 2009, Xi et al., 2011). The overall dynamic model can be represented as:

$$\underbrace{m_i \frac{dv_i}{dt}}_{Acceleration} = \underbrace{m_i \frac{v_i^0(t)\, e_i^0(t) - v_i(t)}{\tau_i}}_{Driving\ Force} + \underbrace{\sum_{(j \neq i)} f_{ij} + \sum_W f_{iW}}_{Replusive\ Forces} \qquad (5.2.3.2.1)$$

$$v_i(t) = [1 - L_p(t)]v_i^0(0) + L_p(t) \cdot \max(v_i^0(t)),\ L_p(t) \in (0,1) \qquad (5.2.3.2.2)$$

$v_i^0(0)$ is the desired velocity at the initial state and the $\max(v_i^0(t))$ is the maximum desired velocity, which are already acquired from the above process of individual agent design. The repulsive forces f_{ij} and f_{iW} can be further interpreted as:

$$f_{ij} = \underbrace{A \exp\left(\frac{r_{ij} - d_{ij}}{B}\right) \boldsymbol{n}_{ij}}_{Psychological\ Force} + \underbrace{\underbrace{kg(r_{ij} - d_{ij})\boldsymbol{n}_{ij}}_{Body\ Force} + \underbrace{\kappa g(r_{ij} - d_{ij})\Delta v_{ji}^t \boldsymbol{t}_{ij}}_{Sliding\ Friction\ Force}}_{Physical\ Force} \qquad (5.2.3.2.3)$$

$$f_{iW} = \left[A \exp\left(\frac{r_i - d_{iW}}{B}\right) + kg(r_i - d_{iW})\right] \boldsymbol{n}_{iW} + \kappa g(r_i - d_{iW})(v_i \cdot \boldsymbol{t}_{iW})\boldsymbol{t}_{iW} \qquad (5.2.3.2.4)$$

$$g(x) = \begin{cases} x & x \geq 0 \\ 0 & x \leq 0 \end{cases},\ x = (r_{ij} - d_{ij})\ or\ (r_i - d_{iW}) \qquad (5.2.3.2.5)$$

where r_{ij} is the sum of radii of agent i (r_i) and agent j (r_j), d_{ij} and d_{iW} represent the physical distance between agent i and agent j (ID) and the distance between agent i and wall W respectively, $\boldsymbol{n}_{ij}$ is the unit vector pointing from agent j to i, $\boldsymbol{n}_{iW}$ is the perpendicular vector to wall W, $\boldsymbol{t}_{ij}$ and $\boldsymbol{t}_{iW}$ represent the tangential direction to agent i and wall W respectively, and Δv_{ji}^t is the velocity difference in tangential direction to agent i. The rest parameters, A, B, k, and κ are all constants and their values are 2000 N, 0.08 m, 1.2×10^5 kg/s^2, and 2.4×10^5 kg/m·s. According to previous studies, r_i is within the range of 0.25m to 0.4m according to the shoulder length (i.e. $r_{ij} \in (0.5, 0.8)$) (Helbing et al., 2000, Trivedi and Rao, 2018). As the measured ID (d_{ij}) in this study is with the range of 0.4m to 0.8m, it suggests that $r_{ij} - d_{ij}$ is always positive in formula (5.2.3.2.5), meaning all agents are touching with each other.

5.2.3.3. Behavioural Rules

5.2.3.3.1. Pre-Alarm

Before the fire alarm, the pedestrians inside the building are randomly moving around based on personal choices of the routes, starting from different rooms of each floor (Table 5.2.3.3.1). They are assumed to initially move out from the rooms, and thus the agents are created at the doors of the rooms by using 'pedSource' modules. The possibilities of pedestrians' choices of the different staircases and exits to pass through, which are represented by 'pedSelectOutput' modules, are evenly distributed as the average familiarity to the different exits are prone to the mid-high level according to the survey taken among the participants regularly working inside the building. Then, their processes of moving to the selected staircases or exits are represented by using 'pedGoTo' modules. Moreover, for people of the upper floors, i.e. not on the first floor, they need to change between floors by using 'pedChangeGround' modules. Meanwhile, their average decision time as well as the potential queuing time are also considered in the simulation, which are represented by 'PedWait' modules in the model. The amount of the people inside the building will reach to an equilibrium as people keep moving in and out.

TABLE 5.2.3.3.1.

THE ALGORITHM OF PRE-ALARM MOVEMENT

Algorithm 2 Pre-Alarm Movement

Initialize Population of each floor based on rooms with limited capacity
⊳ Using PedSource(i) ($i = 1,2,3,4$) (pedestrians of each floor)
Start of Movement ← Current Time
While (Time < Time Before Alarm)
⊳ The fire alarm has not been triggered
for each Ped Є Population **do**
if Ped Є PedSource($i > 1$) **then**
Stairs($1, \ldots, j$)_Floor(i)← Uniform Probability
Goto Stairs(j)_Floor(i) ⊳ Using PedGoto
Change to Floor($i \pm 1$) ⊳ Using PedChangeGround
else
{Stair_Floor(1), Exit1, Exit2}← Uniform Probability
If Goto Stair_Floor(1) **then** ⊳ Using PedGoto
Change to Floor($i + 1$) ⊳ Using PedChangeGround
else
Goto Exit(k) ⊳ Using PedGoto
Remove Pedestrians from Population ⊳ using PedSink
End if
End if
End for
End While

The postures applied in this period is UW and the corresponding speed and ID of the people will be all set up based on the previous data of initial and comfortable state for UW postures. All these pedestrians' activities under normal mode will be cancelled when being transferred to the evacuation mode. The fire alarm will be triggered based on the expansion of the fire/smoke when meeting the condition that fire/smoke fulfil the blocked space according to the fire dynamics model introduced in **Section 5.2.2**. Meanwhile, ASET is also calculated based on the smoke expansion inside the entire building, and in this study, the fulfilment of the smoke within an entire floor is considered to be the end of the ASET.

5.2.3.3.2. Post-Alarm

After triggering fire alarm, the goal for the people inside the building is moving to all available exits as quickly as possible based on personal choices under corresponding evacuation strategies, i.e. evacuation with and without guidance (Table 5.2.3.3.2).

TABLE 5.2.3.3.2a.

THE ALGORITHM OF EVACUATION WITHOUT GUIDANCE

Algorithm 3 Post-Alarm: Random Walking

```
Stop all pre-alarm movements
▻ Cancel PedSource, PedGoto, and PedChangeGround
Start of Evacuation ← Current Time
Response Time ← Delay{Long-Wait, Short-Wait}
While (Time < Delay) ▻ People have not decided to move
    People wait at their current locations ▻ Using PedWait
    if (Time > Delay) then ▻ Pedestrians decide to evacuate
        for each Ped Є Population do
            Floor(i)← Ped.Z
            ▻ Get pedestrians' current floor number
            if Floor(i) > 1 then ▻ pedestrians not at the 1st floor
                Stairs(1, …, j)_Floor(i)← Uniform Probability
                Goto Stairs(j)_Floor(i) ▻ Using PedGoto
                Change to Floor(i − 1) ▻ Using PedChangeGround
                i = i − 1
            else
                Exit(k) (k = 1, …,5)← Uniform Probability
                ▻ Exit number changes with fire expansion
                Goto Exit(k) ▻ Using PedGoto
                Count the number of pedestrians passing Exit(k)
                Remove Pedestrians from Population ▻ using PedSink
                RSET = Current Time – Start of Evacuation
            End if
        End for
    End if
End While
```

TABLE 5.2.3.3.2b.

THE ALGORITHM OF EVACUATION WITH GUIDANCE

Algorithm 4 Post-Alarm: Searching Nearest-Exits

```
Stop all pre-alarm movements
⊳ Cancel PedSource, PedGoto, and PedChangeGround
Start of Evacuation ← Current Time
Response Time ← Delay{Long-Wait, Short-Wait}
While (Time < Delay) ⊳ People have not decided to move
    People wait at their current locations ⊳ Using PedWait
    if (Time > Delay) then ⊳ Pedestrians decide to evacuate
        for each Ped Є Population do
            Floor(i)← Ped.Z
            ⊳ Get pedestrians' current floor number
            if Floor(i) > 1 then ⊳ pedestrians are not at the 1st floor
                Ped{X,Y}← {Ped.X, Ped.Y}
                ⊳ Get pedestrians' current 2D locations of each floor
                Stairs(j)_Floor(i)← Nearest Stair from Ped{X,Y}
                Goto Stairs(j)_Floor(i) ⊳ Using PedGoto
                Change to Floor(i − 1) ⊳ Using PedChangeGround
                i = i − 1
            else
                Exit(k) (k = 1, … ,5)←Nearest Exit from Ped{X,Y}
                ⊳ Exit number changes with fire expansion
                Goto Exit(k) ⊳ Using PedGoto
                Count the number of pedestrians passing Exit(k)
                Remove Pedestrians from Population ⊳ using PedSink
                RSET = Current Time – Start of Evacuation
            End if
        End for
    End if
End While
```

The number of available exits has increased from two to five after the alarm. However, this number will decrease with the expansion of the fire. Before evacuation, there is a pre-movement period requiring consideration, which is the response time of people after hearing the fire alarm. It will be summarized based on the survey data, which can also be described in a triangular distribution format with two different choices, i.e. 'Short-Wait' and 'Long-Wait'. The postures applied in this period is a mixture of UW, TSW and TKSW under emergency scenario. For the evacuation of pedestrians, there are two strategies being applied in this study for comparison. One strategy is that all pedestrians will be randomly assigned to the available exits of each floor, regardless of their current locations. The other strategy is that all pedestrians are assigned to the nearest available exits based on their current locations. The number of survivals in ASET and the average RSET for survivals at different exits will be compared, in order to figure out a more efficient strategy.

5.3. SIMULATION SETUPS

The above described design of ABM will be applied to simulate the fire expansion and pedestrian evacuation within the PMB building in UNNC, which is a four-floor building with multiple office rooms, staircases, entrances and exits. There are only two exits available under normal condition, and the other three exits are blocked until the fire evacuation. The whole processing is achieved by using AnyLogic 8.4, running on a computer with CPU in Inter Core i5-6500, and 16GB RAM. It can simulate pedestrian movement with an SF-based ABM algorithm, which has a continuous and more realistic description of pedestrian movement (Zheng et al., 2009, Vermuyten et al., 2016) with the integration of CAD floor plans. The specific environmental setting are already mentioned in Fig.5.2.1.1. The parameters for pedestrian movement are acquired from experiments (Table 5.3), which can help to improve the reality of the simulated results.

TABLE 5.3

THE PARAMETERS OF THE PEDESTRIAN MOVEMENT AND FIRE DYNAMICS MODEL

Parameter	Value
Population	180~230
Initial Speed (m/s)	Triangular (0.6,0.7,0.6)
Comfortable Speed before Alarm (m/s)	Triangular (1.0,1.1,1.0)
Initial Speed After Alarm (m/s)	Triangular (0.9,1.5,1.0)
Diameter of the pedestrians (m)	Triangular (0.5,0.8,0.6)
Level of Panic	0~1
Pre-evacuation Time (Short Decision) (min)	Triangular (0.0,0.8,1.0)
Pre-evacuation Time (Long Decision) (min)	Triangular (1.0,1.2,3.0)
No. of Exits before Evacuation	2 (Main Entrances)
No. of Exits before Evacuation	5 (2 Main Entrances + 3 Emergency Exits)
Fire Location	Room 118 at 1st floor Near Exit 1
Fire Spread Rate (m/s)	1
Smoke Spread Rate (m/s)	0.1~1
Evacuation Strategy #1	Randomly to the available exits
Evacuation Strategy #2	To the nearest available exits

Meanwhile, the simplified fire expansion model are integrated into the pedestrian model. The parameters for this model is summarized from the applications in previous studies under similar situations (Table 5.4.2). The ignition location of fire in this study is manually selected at the first floor, which is one of the highly risky places inside the building as it is the chemistry lab. Once the fire/smoke expands out of the room, the surrounding environment, especially the staircases nearby connected to the second floor and exits to the outdoor will be blocked. This may increase the risk of evacuation and lead to the injuries of pedestrians who need to pass through these specific places.

The pre-evacuation time is deduced from the survey answers and the results is summarized in Fig.5.3. The answers for the short decision time, which are ‘Immediately’ and ‘Wait for the 2nd round’, the latter is more popular, especially for the females. For long decision choices, which are ‘Waiting until others move’, ‘Move after being informed by security people’ and ‘Move after being informed by the security people and packing personal belongings’, the first choice are the most popular answers. According to the code for the fire alarm, one round of the alarm bells is about 36s and each bell signal of one round is about 12s. Moreover, the entire period of the fire alarm is about 180s (NFPA, 2010). According to the observations of the fire drills, most of the people will move at the first or the second strike of the bell of the 2nd round of the fire alarm and thus the range of the pre-evacuation time is about 0 to 1 min. Meanwhile, the majority of people start to move after the 2nd round of the alarm (1.2 min).

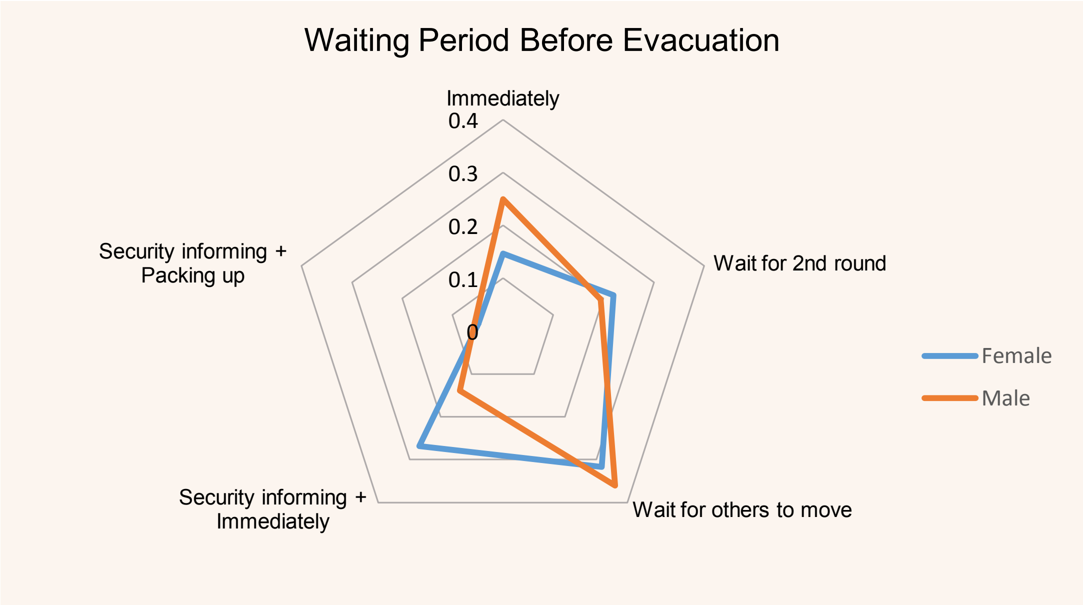

Fig.5.3. The distribution of user responses of pre-evacuation for both genders.

5.4. Simulation Results

5.4.1. Before Fire Alarm

Before the evacuation, the pedestrians are assumed to be all staying at rooms before the simulation and move randomly inside the room after the initialization of the modelling, with similar possibilities to different staircases and exits and the results can be viewed in both 2D and 3D (Fig.5.4.1). The entire time period for the free movement is around 240s, which is calculated based on the expanding rate of the fire and smoke.

During this process, the entire population inside the building tends to reach an equilibrium with a population around 180 to 230 after the simulations have been repeated for 10 times (Fig.5.4.2.3). According to the density maps of different floors, the places nearby the connection regions between the floors, i.e. the staircases, tend to higher pedestrian density than the corridors. This is due to the more frequent using of these functional places for floor transitions, especially at the peak time. According to the average results of ten simulations (Table 5.4.1), the peak-time pedestrian density of each floor gradually reduces with floor levels. The maximum pedestrian density appears at the 4th floor, while the 1st floor have the lowest peak pedestrian density. This may be due to the longest distance from the 4th floor to the 1st floor, and people from this level need a longer time before leaving the building. Moreover, the staircases to the 1st floor are more easily occupied by the pedestrians from the other lower floors, leading to longer time of queueing. For the 1st floor, people works in this level have closer distances to the exits and they are unlikely to queue at staircases. Therefore, they are less affected by the people from the upper levels, though the places nearby the staircases are still more possible to have a relatively higher density of pedestrians.

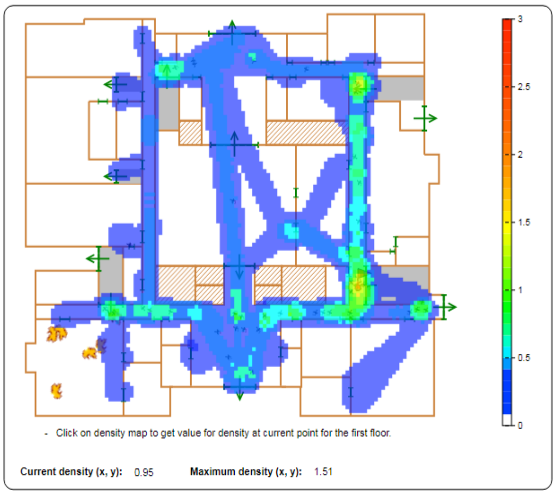

(a)

(e)

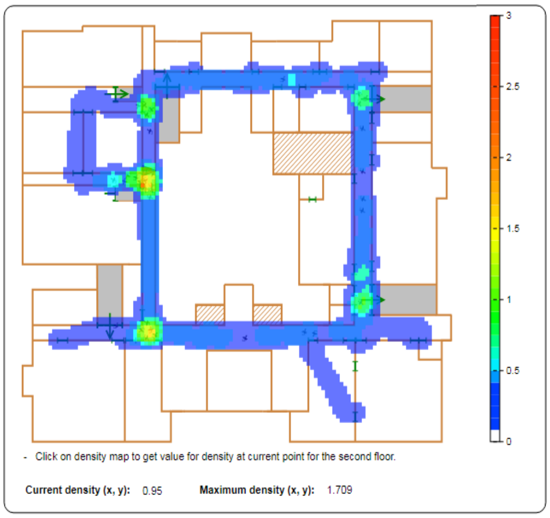

(b)

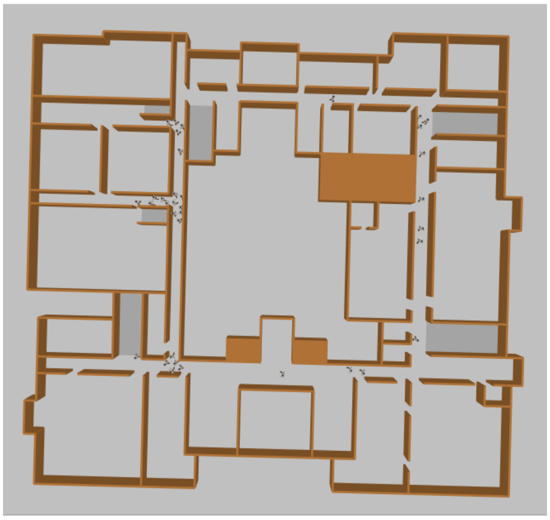

(f)

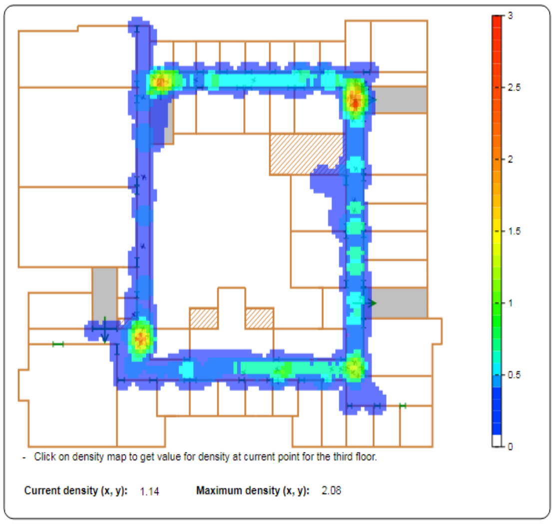

(c)

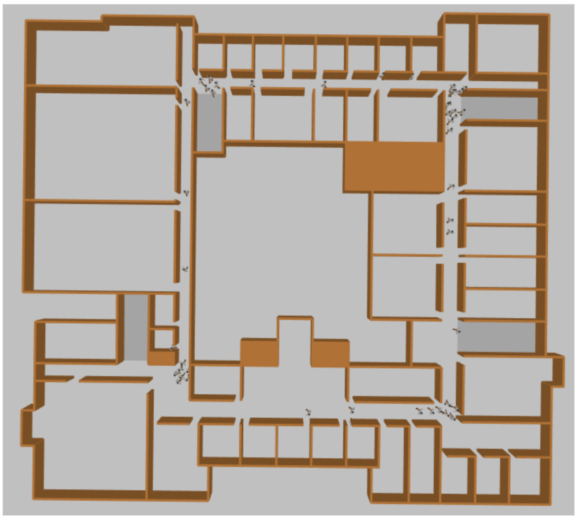

(g)

(d)

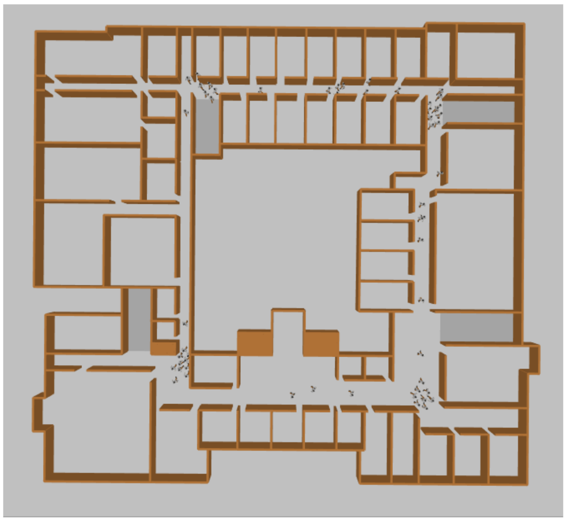

(h)

Fig.5.4.1. An example of simulation results before the fire alarm from the first floor to the fourth floor in 2D (a)-(d) and corresponding 3D visualization (e)-(h).

TABLE 5.4.1.
THE AVERAGE PEAK PEDESTRIAN DENSITY OF EACH FLOOR

Floor Number	Maximum Pedestrian Density (person/m^2)
4	2.3
3	2.0
2	1.7
1	1.5

5.4.2. After Fire Alarm

After the alarm is triggered, the fire and smokes are expanding into the indoor space. Due to evacuation code in the indoor area that all doors needs to be closed after leaving the room. The paths for fire and smoke to expand is along the corridors and other empty spaces (Fig.5.4.2.1). The ASET is calculated based on this principle and it is about 10 min for the whole building. The exit nearby the fire location, which is Exit 1, is unavailable for evacuation after about 32s. This will lead to the rest of the pedestrians to choose other exits and the staircases close to that exits will be unavailable after 171s for people from upper than 2nd floor, and 342s for people from upper then 3rd floor, and totally unavailable after 512s for all people who need to use these staircases to move to the 1st floor. Meanwhile, other exits will also become risky with the expansion of the fire. These will gradually limit the available paths for the pedestrians, regardless what strategy is taking.

Fig.5.4.2.1. An example of the simulated fire expansion.

As some of the simulation inputs are under random control, the simulation results under same environmental and parameter settings may be various for each individual run. These inputs include the people distribution after pre-alarm period and the specific pedestrian velocity and reaction time. For example, with the number of people distributed at each floor, the simulation results can still be different as people may concentrate at different exits. For pedestrian velocity and reaction time, as they are settled in ranges instead of certain values, the applied values can still be different for individual runs. In order to reduce these variations, the simulations for both two strategies have been repeated for 10 times in order to acquire their average performances (Table 5.4.2.1). The evacuation process using Strategy #1 (random walking) has also been validated to some extent by comparing to the result from a fire drill in another four-floor building with similar indoor structure and population level, but about half of the available exits. The maximum RSET of survivals estimated in this study of the building under the situation without guidance support is about 6 minutes while for that of the fire drills, it reaches 12 minutes due to fewer exits. This may help to demonstrate the effectiveness of the applied ABM used in this paper and the acquired results are more convincible.

TABLE 5.4.2.1

THE AVERAGE PERFORMANCES OF SIMULATION OF USING TWO EVACUATION STRATEGIES

Simulation Result	Strategy #1	Strategy #2
No. of Injuries	19	14
Survival Level (%)	90.95	93.33
Mean Average RSET of Survivals (s)	206.14	148.55
Mean Maximum RSET of Survivals (s)	351.39	185.25
Mean Maximum Evacuation Speed of Survivals (m/s)	1.49	1.40
Mean Travel Distance (m)	274.3	211.3

According to the simulation, when moving without navigation guidance (Strategy #1), the average level of survivals is 90.95%, with approx.19 people in average cannot escape from the indoor area within the calculated ASET. On the contrary, when moving with assistance of guidance (Strategy #2), the average level of survivals is 93.33%, with approx.14 people being trapped in danger according to calculated ASET. Moreover, both the average and maximum RSET for survivals of using Strategy #2 are significantly shorter than those of using Strategy #1. These findings suggest that moving with guidance support is more efficient than moving without guidance, due to lower level of trapped people and shorter average RSET. Moreover, it can be found that the maximum speed during evacuation is slightly faster than that of pre-alarm (Table 5.3 and 5.4.2.1), regardless of the evacuation strategies being applied. Meanwhile, it can be found that the average maximum evacuation speed of 2nd strategy are slightly lower than of the 1st strategy while the average evacuation distance of 2nd strategy is shorter than that of 1st strategy. This also suggests that the 2nd evacuation strategy have a better efficiency due to the better planning of the evacuation routes with shorter distances. It may also help to reduce the level of panic, inferring based on the less increase of the evacuation speed as there is a moderately positive relationship between evacuation distance and evacuation speed (Fig.5.4.2.2).

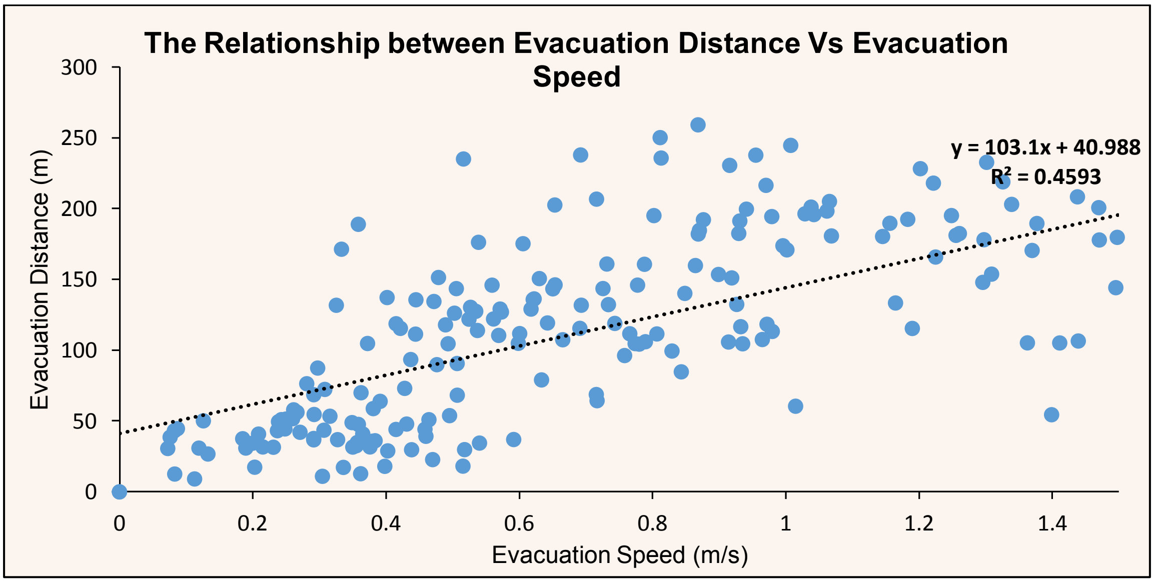

Fig.5.4.2.2. An example of the relationship between evacuation distance and evacuation speed.

An example of the changing pattern of the entire process of using two strategies are listed in Fig.5.4.2.3. It can be found out that after the beginning the evacuation, the evacuation population applying the 2nd strategy decreased more quickly than that of applying the 1st strategy. This can be explained by the reason that people may spend more time on searching for potential routes to the targeted places than being directed by the navigation system with the shortest distances. This can also be proved by the distribution of average RSET and the corresponding queuing population of different exits in Table 5.4.2.2. According to its results, when using the Strategy #1, all exits other than Exit 1 have a significantly longer average evacuation time than that of using Strategy #2. Meanwhile, their distribution of the average queuing population at all exits are only slightly different to each other. This can be regarded as an evidence of the hypothesis that the rest of the trapped people are on their way of searching for potential route to the exits rather than being blocked in the queues in front of the exits before escaping to the outside. Moreover, the width of the exits plays a more important role when applying

Strategy #1 as Exit 2 and 3 with smaller widths requires longer evacuation time than those for Exit 4 and 5.

On the other hand, the distance to the exit, both from fire and current user location, plays a more important role when using Strategy #2. It can be found out that the Exit 2 have the second shortest average evacuation time as it is close to the fire location and once the Exit 1 is blocked, the affected occupants may choose it for evacuation while it is also soon affected by the fire expansion. Exit 4 and 5 could also be the second optimal alternative choices after the blocking of the Exit 1. However, as Exit 5 is closer to the fire location, the average available evacuation time is shorter than that of Exit 4. The distance between Exit 3 and the pedestrians who located at the regions closer to Exit 1, is much farther than to the Exit 4. Thus, it is less likely to be chosen by these people. However, it has longer average evacuation time than that of Exit 4, due to the narrower gate of the Exit 3. The Exit 4 have the advantages of closer and safer distance and the larger width, leading to a relatively shorter evacuation time than using Strategy #1, but a second longest average RSET due to its higher preference among evacuees. Moreover, the queueing population at this exit is also the second largest among all exits, due to closer distances and wider exit gate. It also agrees with the hypothesis of the previous studies that people prefers the main exits/entrances during evacuations (Benthorn and Frantzich, 1999, Helbing et al., 2000, Kobes et al., 2010a, Sarshar et al., 2013, Shiwakoti and Sarvi, 2013), which are Exit 4 and Exit 5 in this study.

TABLE 5.4.2.2

THE AVERAGE EVACUATION TIME OF DIFFERENT EXITS

	Strategy #1		Strategy #2	
	Mean Evacuation Time (s)	Queuing Population	Mean Evacuation Time (s)	Queuing Population
Exit 1	31.89	0	28.08	0
Exit 2	173.53	2	46.50	1
Exit 3	174.55	2	78.19	3
Exit 4	148.34	2	73.53	2
Exit 5	126.21	1	72.77	1

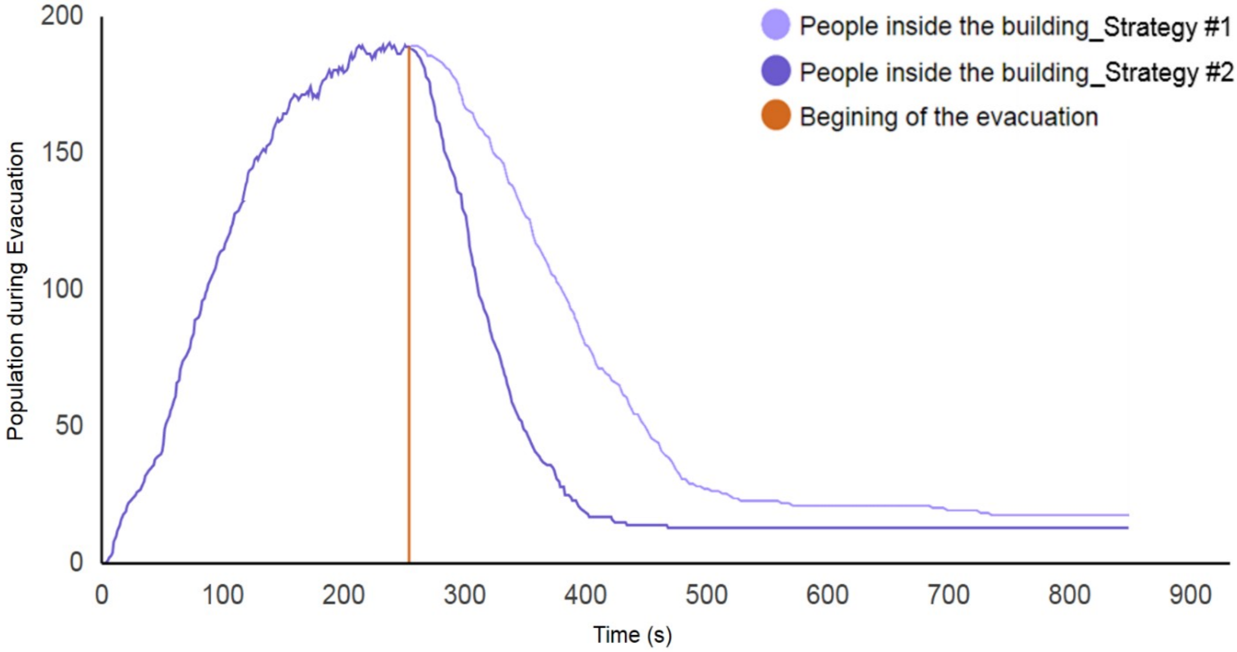

Fig.5.4.2.3. An example of the evacuation patterns for two strategies.

This can be a good example showing the advantages of using the guidance service during evacuation, as the main principle of 2nd strategy is similar to that of emergency navigation, which can efficiently support the evacuation process by helping people find the nearest available exits and avoid the risks of fire. Moreover, the final survival rate is also relatively higher than that of using randomly searching strategies. However, the acceptance of the smartphone-based navigation during fire evacuation, which is also an important factor affected by the user familiarity to the service and corresponding decision time to the orders, have not been integrated into this model due to the simplification purpose. Moreover, the approaches of displaying guidance information is also worth investigation in future research.

5.5. SUMMARY

This chapter has proposed a design of SF-based ABM in order to simulate pedestrian movements in a four-floor campus teaching building in University of Nottingham Ningbo China before and after the fire alarm with lower risk and cost. The developed ABM system has integrated with a self-designed simplified temporal-spatial model of fire expansion, in order to improve the reality of the ABM-based simulation, which is usually not included in the previous studies using ABM. It is created in a GIS-based building environment with pre-defined behavioural rules by using a quick-processing software with relatively low requirement of computation power called AnyLogic. The application of this model can help identify potential bottlenecks of the test building by providing the pedestrian density maps of different floors under the normal conditions. Moreover, it has compared the efficiency of two evacuation strategies, i.e. random-walking and nearest-exits. The latter can be treated as the evacuation process with the support of the previously developed smartphone-based indoor navigation system while the former is regarded as the evacuation process without navigation assistance. This study will find a more efficient solution by comparing the survival rate within the calculated ASET as well as the average evacuation time and evacuation distances for the survivals. During the evacuation process, the developed model has adopted the mixture of two SW postures during the evacuation period. The parameters applied for this model are acquired from the physical experiments with self-developed user-friendly and effective sensing system as well as the field survey data, which will help to improve the accuracy of the simulated results. After repeating the simulations of 10 times for using each evacuation strategy, the results suggest that assigning pedestrians to the closest exits/staircases is better than allowing them moving randomly inside the building with higher survival rate within ASET, the shorter average and maximum evacuation RSET as well as the average evacuation distance for survivals. The hypothesis that navigation can help to improve evacuation efficiency is then proved in this case. The results also suggest the width and distribution of the exits can be important factors for user selections of the evacuation routes and efficiency. According to the acquired results, the pedestrians prefer exits with wider door gate and closer distance to their current locations.

Moreover, the model applied in this study can be easily replicated in the environments with similar indoor structures, which is beneficial to building managers for easier operations. Meanwhile, the simulation process is able to be viewed both in 2D and 3D, which is more direct for visualization of different purposes and preferences. It can also help for further investigation of the evacuation procedure under different time stamps.

In future, this can be further integrated with the investigation of the guidance service provided by the smartphone-based navigation. However, the effects from other potential parameters, such as the physical body parameters (e.g. height), personalized indoor familiarities, potential sources of the panic level, the effects from the personal sensation, familiarity to smartphone guidance, and the potential supportive information for guidance, have not been integrated into this model. They need to be further investigated and quantified when integrating with the results provided by the above model to give a thorough evaluation of the application of the smartphone-based indoor fire evacuation guidance. The following chapter will focus on these parameters and their potential effects on the application of navigation services during indoor fire emergency.

Chapter 6. INVESTIGATION OF COGNITION FACTORS OF FIRE RESPONSE PERFORMANCES BASED ON SURVEY

6.1. INTRODUCTION

The design of an indoor navigation system for fire evacuation support requires not only the physical feasibility but also a relatively thorough consideration of the human factors of cognition. The previous chapters have already tested the physical feasibility of the designed indoor navigation system, by conducting a simulation model based on the physical parameters of the pedestrians and fire. However, the evacuation capability is not only based on the physical mobility of people, their response performance to the fire, i.e. Fire Response Performance (FRP) also merits consideration (Kobes et al., 2010a). The factors which affect the FRP can be divided into three categories from fire, human and building environments (Kobes, 2008, Kobes et al., 2010a, Xiong et al., 2014). This study will first focus on the more detailed influences from human and environments, and the impacts from the fire and pedestrian mobility have already been simulated in Chapter 5.

In order to assess the responses of participants in an environment that they are accustomed to, this study selected the PMB building and students in the faculty of Science and Engineering as the test site and volunteers in the survey. This is because this building is the common workplace for these students in daily campus life and they are supposed to have more knowledge about the indoor infrastructures of the environment, which are very important during the evacuation process. This study also tries to understand the relationship between participants' familiarity with the indoor environments and their intuitive psychological conditions with different walking postures. It also gauges users' potential attitudes to the smartphone-based guidance, and potential causes of decision making during movement.

6.2. FACTORS OF FIRE RESPONSE PERFORMANCE (FRP)

6.2.1. Indoor Familiarity

For the environmental factor of FRP, this study mainly focuses on the wayfinding aspect of situational factors, which can be divided into five classes as visibility, the directionality of indoor structures, the complexity of layouts, the familiarity with the building and the implementation locations of path markings (Raubal and Egenhofer, 1998, Kobes et al., 2010a). Among these classes, this study is more interested in investigating the effects of the indoor familiarity and the locations of existing indoor signs based on the collected answers from the interviewed participants, as the other factors are all fixed by using the same building for the survey. The reason for treating the familiarity to the indoor environments as an important factor for fire evacuation is due to the unfamiliarity with the building context is also considered as a special vulnerable group of disability (Aedo et al., 2012, Koo et al., 2012, Manley and Kim, 2012, Trivedi and Rao, 2018). Meanwhile, the decision making during the fire evacuation, which is time consuming due to floor plan discovery and escape route formulation (Kuligowski, 2016, Mohan et al., 2016), is quite related to the familiarity with the indoor layouts as people prefer using familiar paths/exits for evacuation (Graham and Roberts, 2000, Shi et al., 2009a).

This survey takes three aspects to evaluate the degree of indoor familiarity of participants, which are the familiarity to the evacuation exits, risky places and the clearance of guiding signs. According to the collected answers, the majority of both participated males (54%) and females (61%) have at least mid-level knowledge (‘3 to 4’) of the locations of all exits in their daily working indoor environment. Among them, the male has a higher average familiarity (2.77) with the exits than the female (2.64) (Fig. 6.2.1.1a). There is one male participant has the full confidence of familiarity with all the exits while there is none for female. Meanwhile, for the familiarity of indoor risky places, the participants from both genders have less knowledge of these areas, and more male participants (50%) have a relatively higher degree of the familiarity (‘3 to 5’) than females (46%) (Fig.6.2.1.1b). These may be partially explained by the satisfaction of indoor signs, as about half of the interviewed male students are relatively satisfied with the current setups of the indoor evacuation signs (with the high score as ‘4’), while for the female participants, they tend to have fewer people with similar degree of satisfaction (Fig.6.2.1.1c).

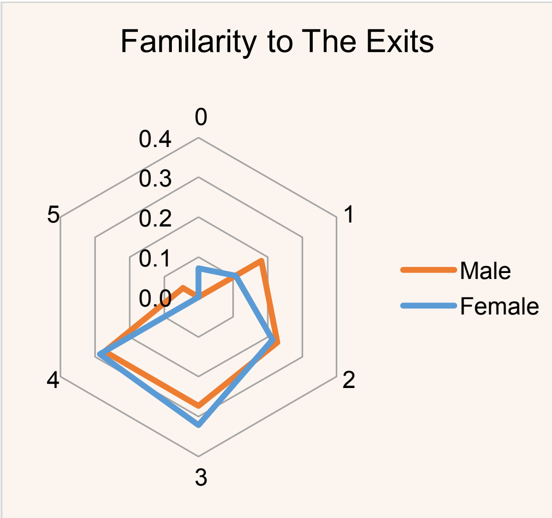

(a)

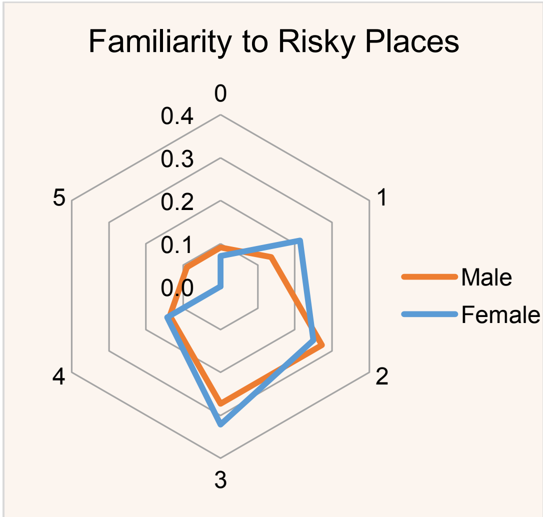

(b)

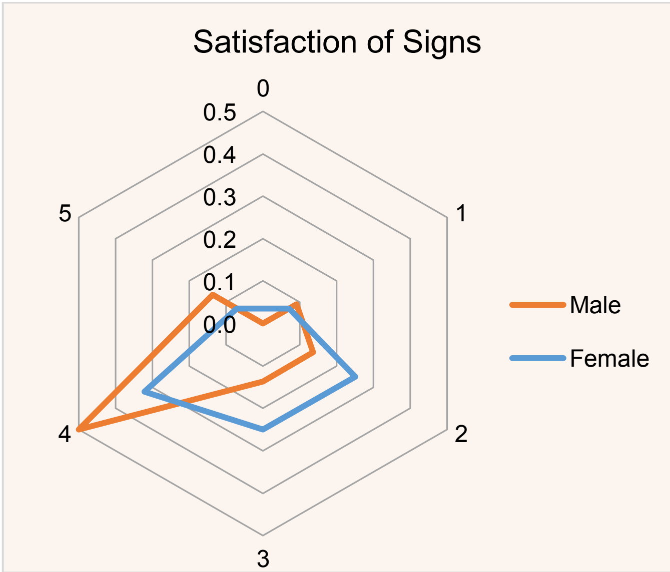

(c)

Fig.6.2.1.1. The distribution of the feedback of the familiarity to the indoor exits (a), risky places (b), and satisfaction of Indoor signs (c) from lowest (0) to Highest (5).

The problem of the current installation of the indoor guidance signs may be related to the height of the installed signs. According to the analysis of the relationship between user height and satisfaction degree of indoor signs, they are positively related to each other with at least medium strength of the correlation, which is about 0.311 for female and 0.559 for the male. The overall pattern of satisfaction keeps growing with height except for the '170~175cm' group and this trend is more significant based on the male's data than the female's (Fig.6.2.1.2). This also suggests that height can slightly affect the satisfaction of indoor signs as male participants have higher average heights than the female participants, which may help them more easily to recognize the existence of the indoor signs.

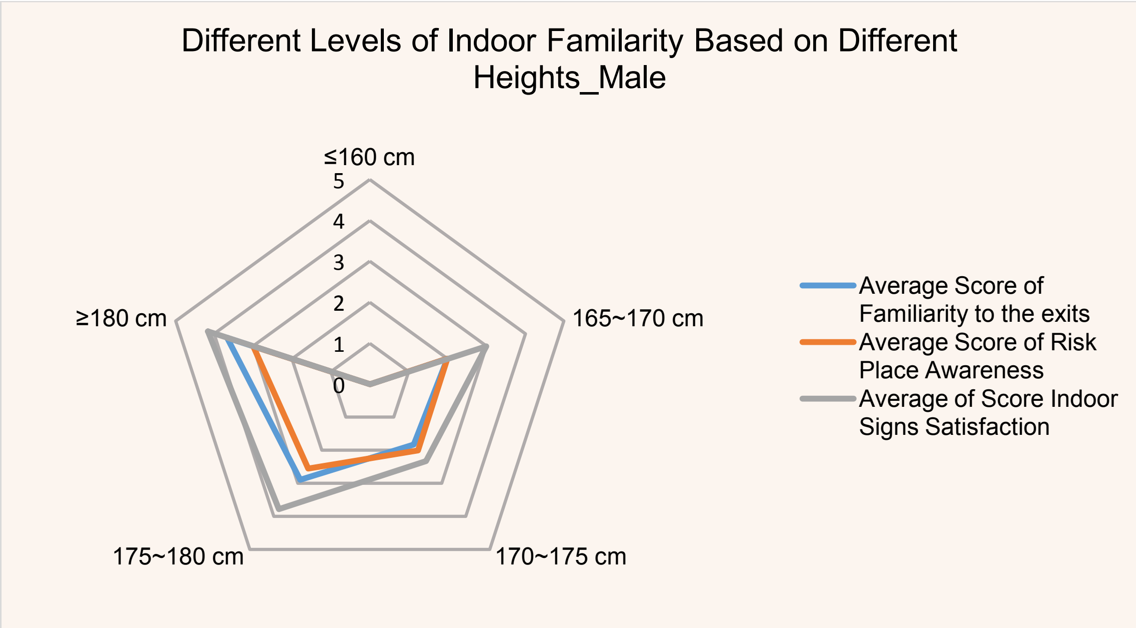

(a)

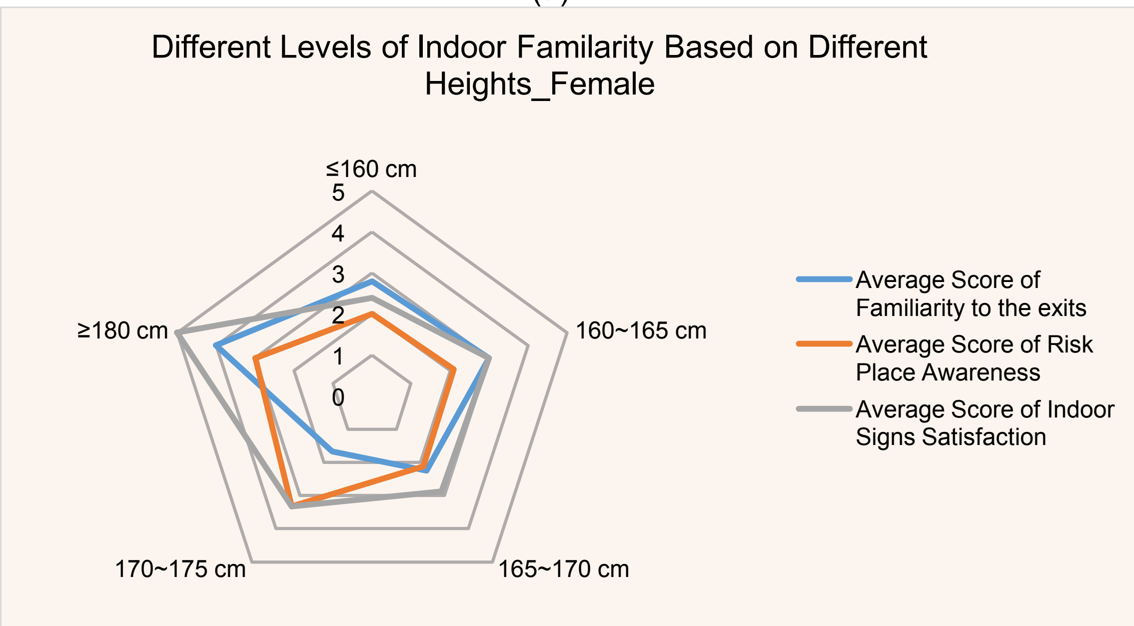

(b)

Fig.6.2.1.2. The comparison of indoor familiarity based on different heights of male (a) and female (b).

Meanwhile, the correlation analysis between heights and familiarity to exits also suggests similar conclusions as males' data shows a stronger positive relationship (0.561) between these two factors while the females' showing a weak correlation (-0.145) (Table 2.1.1 and Table 2.1.2). According to the changing pattern shown in Fig 2.1.2, the males have a similar growing trend of familiarity to exits based on the heights as the satisfaction of the indoor signs, while for the females, this trend is affected with the majority of the people in different height groups with similar average level of familiarity to exits. On the other hand, it also implies the current height of the indoor signs may not be ideal for all populations, especially for people with lower body heights. This finding is also supported by a previous study that occupants during the evacuation are less likely to realize the existence of guidance signs at the ceiling level, and their choices of evacuation path are less dependent on them (Johnson, 2005). However, the growth of heights does not significantly affect the familiarity with the risky places for both genders, suggesting people's ubiquitous lower awareness of that information.

In addition, people's knowledge of indoor exits and risky places are also positively correlated with the satisfaction levels of indoor signs (Table 6.2.1.1 and Table 6.2.1.2). Between these two factors, the familiarity to the exits has stronger impacts on the sign satisfaction, with 0.532 for the female and 0.414 for the male than 0.31 for indoor risky place awareness of both genders. According to the previous findings, there are more females have higher familiarity with the indoor risky places. However, it does not affect their correlation to the indoor sign satisfaction as there is no great difference between the two genders. This implies that the current indoor signs do not give a very clear direction to the risky places. On the other hand, the increasing familiarity with the indoor exits signs can lead the growth of the satisfaction with at least moderate possibility. This suggests that people are more interested in the sign for exit guidance rather than the guidance to the risky places, which also agrees to the findings from the relationship analysis between height data. This hypothesis is supported by the correlation between the familiarity between exits and risky places. Before the survey, it is assumed that people with higher familiarity with the exits may also highly familiar with risky places. However, after calculating their correlation efficient, the positive relationship seems to be weak with approx. 0.27 for the female and 0.21 for the male (Table 6.2.1.1 and Table 6.2.1.2).

TABLE 6.2.1.1
CORRELATION BETWEEN HEIGHT AND OTHER INDOOR FAMILIARITY FACTORS FOR MALES

	Height (cm)	Familiarity with the Exits	Risk Place Awareness
Familiarity with the Exits	0.561	1	
Risk Place Awareness	0.265	0.213	1
Indoor Signs Satisfaction	0.559	0.414	0.315

TABLE 6.2.1.2
CORRELATION BETWEEN HEIGHT AND OTHER INDOOR FAMILIARITY FACTORS FOR FEMALES

	Height (cm)	Familiarity with the Exits	Risk Place Awareness
Familiarity with the exits	-0.145	1	
Risk Place Awareness	0.284	0.271	1
Indoor Signs Satisfaction	0.311	0.532	0.314

When integrating the effects from the familiarity of exits and indoor risky places from both genders, their correlation coefficients can achieve 0.471 (male) and 0.556 (female), reflecting a strong bonding relationship between the integrated factors. In other words, *people who are more familiar with the current indoor environment may be potentially more satisfied with the current installation of the indoor environment.* However, the familiarity with the selected factors for this experiment is only about the exits and risky places, this may be limited as other indoor infrastructures (e.g. temporary shelters for blocked people) may also be important for the evacuation process. Integrating with the factor from the height to the indoor familiarity, the correlations with the indoor sign satisfaction of both genders are stronger than only considering the effects from familiarity to the exits and risky places, with 0.562 for the female and 0.479 for the male. When comparing to the previous results, the height has higher effect for the male as it has a 1.49% improvement of correlation while the female only has 1.08% (Table 6.2.1.3). On the contrary, the height factor integrated with the satisfaction to the signs may also help people to familiarize their surrounding environments, supported by the increasing correlation with the exit and risky places for both genders (Table 6.2.1.4).

TABLE 6.2.1.3
CORRELATION BETWEEN INDOOR SATISFACTION AND OTHER INDOOR FAMILIARITY FACTORS WITH AND WITHOUT THE EFFECT OF THE HEIGHT

	Indoor Signs Satisfaction	
	Male	Female
Familiarity with the exits+ Risk Place Awareness	0.471	0.556
Height+ Familiarity to the exits+ Risk Place Awareness	0.479	0.562

TABLE 6.2.1.4
CORRELATION BETWEEN DIFFERENT INDOOR FAMILIARITY FACTORS WITH AND WITHOUT THE EFFECT OF THE HEIGHT

	Male		Female	
Factors	Familiarity with exits	Familiarity with risky places	Familiarity with exits	Familiarity with risky places
Satisfaction to the signs	0.41	0.31	0.53	0.31
Height + Satisfaction to the signs	0.43	0.32	0.54	0.32

6.2.2. Psychological Stress

The level of psychological stress is one of the most important personal characteristics for consideration during the evacuation, as it can impede people's cognition and response process, leading to irrational and uncontrolled behaviours (Aguirre, 2005, Kobes et al., 2010a, Drury et al., 2013, Sarshar et al., 2013, Trivedi and Rao, 2018), such as stampede, leading to casualties or great loss (Helbing et al., 2000, Saloma et al., 2003, Heide, 2004, Fahy et al., 2012, Shi and Wang, 2013, Cocking and Drury, 2014, Kasereka et al., 2018). This section mainly concentrates on the psychological effects on the individual level, which is about the evacuation knowledge and experience, the capability of observation and decision-making, and evacuation mobility (Kobes et al., 2010a, Xiong et al., 2014).

The level of panic during the evacuation can be affected by the human's psychology characteristics, such as gender, age, and the level of experience (Sarshar et al., 2013, Shen et al., 2018), and specific environmental conditions (Sarshar et al., 2013). This study aims to investigate the possible reactions of people of different genders during their movements under a special case of using bending posture due to smoke expansion. It wants to discover whether the utilization of bending posture will cause some increase in psychological stress during people's movements. It evaluates the user responses based on their cognition of the moving difficulty, the nervousness, and change of moving speed when forcing to move under a bending posture. The reason to set up that special situation for the participants is due to the potential threats from the smoke inhalation in both the physical and psychological aspects and the possible panic caused by the growing fall risk by using the bending posture (Campbell, 2013, Brown, 2017). In this section, it aims to find out whether the posture can be regarded as a physical force which is highly related with psychological stress, as a previous study suggests that the actions can affect the psychological stress level (Sillem, 2005).

According to the collected data, the psychological hardness of using a bending structure is more polarized for male participants as the majority of their responses are concentrated on the '0~1' (36%) and '3~4' (46%); while the female participants' responses are more prone to a moderate level in the range of 2 to 3 (54%) (Fig.6.2.2.1a). However, their average levels of hardness sensing are similar, with 2.27 for males and 2.25 for females. Meanwhile, for the aspect of nervousness, about 41% of male participants are considered vulnerable population of experiencing such stress by using bending movements with a score of level from '4-5', while only about 36% of the female have scored in the same range (Fig 6.2.2.1b). However, the females still have a slightly higher average level of nervousness during movement with bending (3.11) than male participants (2.86). This may be explained by the fact that there are still more female participants who have a moderate level of nervousness (score '3') when using stoop-walking posture to move while the responses from the male participants tend to more evenly distributed. This finding is also supported by the previous suggestion that man is more prone to maintain calm during the evacuation (Shen et al., 2018). Under the physical pressure of using bending posture, about half of the male interviewees have scored '4' for speed reduction sensation with an average level of 3.5, while only about 29% of female participants have same responses with an average score of 3.29 (Fig.2.2.1c). This may be explained by that the females' responses to the speed reduction are more evenly distributed while the males' responses are more concentrated at '4', showing a greater capability of the male participants to control the reduction of the moving velocity during fire emergency than the females.

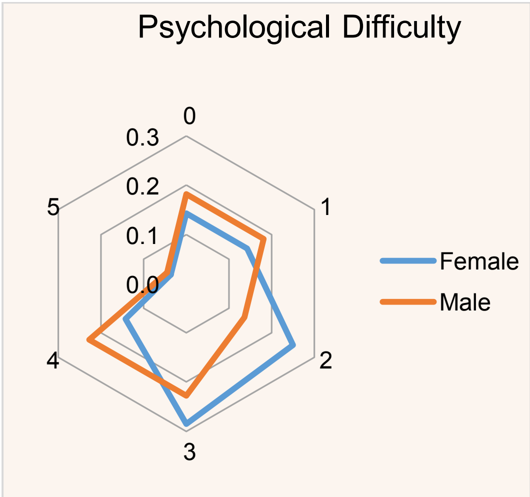

(a)

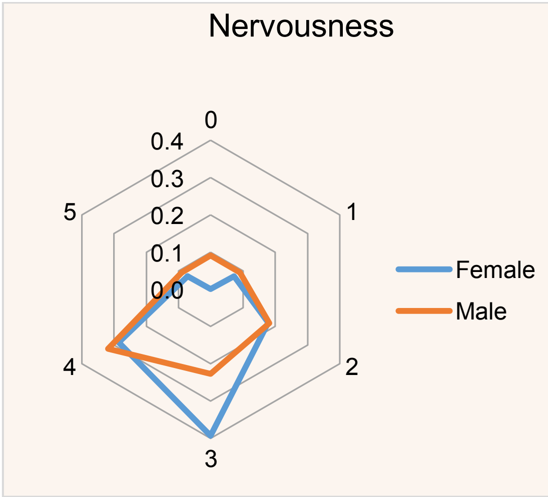

(b)

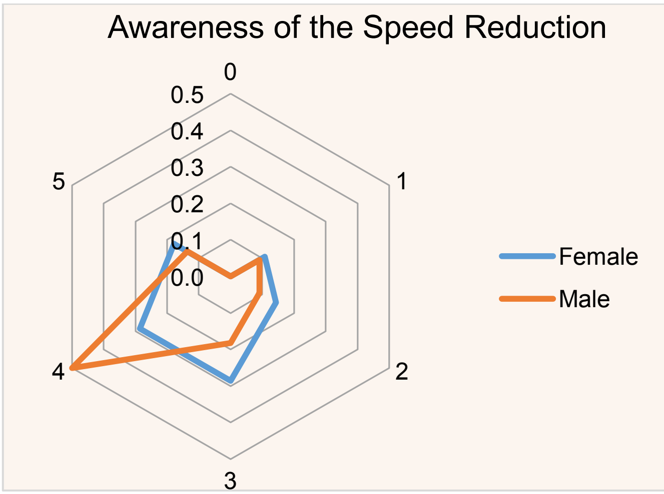

(c)

Fig.6.2.2.1. The distribution of the feedback of the psychological difficulty (a), nervousness (b) and the awareness feeling of speed (c).

Among these three factors of psychological stress, they have a positive correlation between each other from mid-level to high-level (Table 6.2.2.1 and 6.2.2.2). According to the acquired results, the correlation between psychological difficulty and nervousness are much stronger for male participants (0.74) than that of females (0.45). This may be explained by the influence from the height factor, as the height has a stronger negative impact on males' nervousness (-0.427) of using stoop-walking posture than females (-0.133) and the average height of the males are also higher than that of the females based on the above acquired results. This hypothesis is supported by integrating the height factor and psychological feeling of difficulty, as the correlation coefficient for both genders have slightly increased and the improvement for the males (0.54%) are more significant than that of females (0.22%) (Table 6.2.2.1).

TABLE 6.2.2.1

HEIGHT EFFECTS ON CORRELATION BETWEEN NERVOUSNESS AND PSYCHOLOGICAL DIFFICULTY

	Nervousness	
	Male	Female
Psychological Difficulty	0.741	0.450
Height + Psychological Difficulty	0.745	0.451
Improvement	0.54%	0.22%

TABLE 6.2.2.2

CORRELATION AMONG THREE PSYCHOLOGICAL FACTORS

	Awareness of Speed Reduction	
	Male	Female
Psychological Difficulty	0.448	0.476
Nervousness	0.557	0.640
Psychological Difficulty + Nervousness	0.542	0.656
Height + Psychological Difficulty + Nervousness	0.543	0.656

The awareness of speed reduction is more positively correlated with the level of nervousness, especially for the female participants (0.64). This may be due to that psychological stress can affect the cognition of the changing speed (Kobes et al., 2010a). With the growth of the nervousness level, it will be easier to feel the reduction of the moving velocity, though it may not be as significant as that in reality.

On the other hand, panicking people will try to move faster than at the normal state, in order to evacuate from the danger as soon as possible (Helbing et al., 2000, Shen et al., 2018, Trivedi and Rao, 2018). This may lead to a vicious circle as the adage goes *'Faster is slower'*, because the behaviours such as jamming and stampede may also occur with blocking sights and narrowing paths (Helbing et al., 2000, Mawson, 2005, Hu et al., 2007b, Hu et al., 2007a, Parisi and Dorso, 2007, Soria et al., 2012, Suzuno et al., 2013, Shahhoseini et al., 2018). Based on the findings from this study, it may be due to their exaggeration of the speed reduction, leading to lower control of their decision process and action execution. Meanwhile, the level of difficulty perception of using a bending posture also has a moderate impact on the cognition of the velocity reduction, and this impact is more significant for the females. It is understandable as the perception of difficulty may raise the feelings of diffidence and discomfort, exaggerating people's feelings on the speed reductions.

When integrating the impacts from both the psychological difficulty and nervousness level, it can be found that the correlation to the awareness of speed reduction has become stronger for the females while for the males, it has become slightly weaker. This may be due to the lower level of nervousness from the male participants, which may weaken the effects of the nervousness.

According to the previous results in **Section 6.2.1**, the height factor may also affect the perception of the difficulty. Thus, this study has put forward a hypotheis that the height factor may also affect the level of speed reduction perception. However, after integrating the effects from the heights and the other two psychological stresses, the strength of the correlation does not change significantly, especially for the females. It can be inferred that the current level of the height does not have great impacts on speed reduction recognition.

The impacts from the indoor familiarity can be treated as a critical and comprehensive factor for the psychological stress, especially for the level of the nervousness. According to the previous study, one reason for panic is due to the non-efficient using or ignorance of the alternative exits (Helbing et al., 2000, Sarshar et al., 2013, Shiwakoti and Sarvi, 2013, Benthorn and Frantzich, 1999, Kobes et al., 2010a). On the other hand, the occupants with better indoor familiarity may not be limited to using the shortest routes as people tend to use their familiar routes for evacuation (Graham and Roberts, 2000, Shi et al., 2009a, Tan et al., 2015). This study also evaluates the correlations between the factors of different indoor familiarity and psychological stress and the results are shown in Table 6.2.2.3 and 6.2.2.4.

TABLE 6.2.2.3
CORRELATION BETWEEN FACTORS OF INDOOR FAMILIARITY AND PSYCHOLOGICAL STRESS FOR MALES

	Familiarity with the Exits	Risk Place Awareness	Indoor Signs Satisfaction	Indoor Familiarity
Psychological Difficulty	-0.395	-0.064	-0.477	-0.509
Nervousness	-0.293	-0.151	-0.431	-0.432
Awareness of Speed Reduction	0.262	-0.015	-0.176	**0.401**

TABLE 6.2.2.4
CORRELATION BETWEEN FACTORS OF INDOOR FAMILIARITY AND PSYCHOLOGICAL STRESS FOR FEMALES

	Familiarity with the Exits	Risk Place Awareness	Indoor Signs Satisfaction	Indoor Familiarity
Psychological Difficulty	0.187	0.074	0.049	0.172
Nervousness	0.355	-0.054	-0.084	0.436
Awareness of Speed Reduction	0.264	0.152	0.104	**0.256**

According to the acquired results, the hypothesis that the growing familiarity to the exits can help reduce the nervousness is strenghtened by the results to some extent due to the moderately negative correlation based on the males' responses. However, the situation for the females is reverse, as their level of nervousness has a moderately positive relationship between the familiarity to the exits. This may be due to the higher average level of indoor familiarity and composure of the male participants as well as different decision process from two genders.

Similar findings can also be found for the sensation of the difficulty as the familiarity to the exits has a moderately negative effect for the males, while having a weakly positive effect for the females. This may be due to the physical limitations of different genders as the females are more easily getting tired using an energy-consuming posture. However, there is no great difference in the impacts on the speed reduction awareness, which is positively related to the familiarity to the exits at a mid-level. This can be explained by the aspiration of escaping from the danger (Helbing et al., 2000, Shen et al., 2018, Trivedi and Rao, 2018), which may also increase when approaching to the known exits regardless the effects from the gender.

As the prior knowledge to the risk places for both genders is at a low level, its correlation between all different psychological stresses is all relatively weak. Meanwhile, the satisfaction level of the indoor signs has a mid-level negative effect on both the level of the sensation of difficulty and the nervousness feelings for the males, while for the females, the strength of the correlation is nearly neglectable. This may be due to the relatively higher level of satisfaction to the indoor signs based on the replies from the males. It can be helpful during the evacuation process as the males can better utilize the guidance provided by these signs than the females, leading to a decrease of cognition of difficulty and nervousness.

When integrating all indoor-familiarity-based factors together to investigate the relationships between each psychological factors, it can be found out that that males' psychological stresses, such as difficulty and nervousness sensation, may be moderately released with the increasing indoor familiarity, except for the speed reduction awareness. This may be due to the effects from the familiarity to the exits and satisfaction of indoor signs, as males have higher average levels of these two items and a better level of physical abilities. The increasing possibility of speed reduction awareness can be explained by the similar reason mentioned before, i.e. the growing desire of escaping to the outside, which may be affected by the increasing indoor familiarity during the process of moving to the exits. While for the females, their psychological stresses do not follow a similar pattern as the males. All the psychological factors are likely to increase with the growing indoor familiarity, though the correlation coefficients are relatively lower than those for the males. This may be due to the overall higher average levels of psychological stresses and less knowledge of the indoor environments, as well as their physical limitations comparing to the males. Moreover, males have a higher average sensitivity of the speed reduction, showing greater controllability of their own moving velocity and lower vulnerability from the other potential factors. Meanwhile, the previous choices of each factor between the two genders have no significant differences ($p > 0.05$), however, when integrating them together into a comprehensive factor, there are significant differences between the choices made by the two genders ($p < 0.01$). It indicates that the effects from indoor familiarity need to be treated as an entirety before analysing their correlations to the psychological effects.

With the above analyses, it suggests that factors from indoor familiarity are correlated with the psychological effects to some extent, especially from the aspects of the familiarity to all building exits and the satisfaction to the indoor guidance signs. Thus, it suggests that when integrating effects from all the indoor familiarity factors together with the impacts from the cognition of difficulty and nervousness, it may have a comprehensive effect on the perception of the speed reduction. The reason of concentrating on the effects to the people's moving velocity is due to that the moving velocity is one of the decisive factors for the establishment of the evacuation models, and it is usually used to evaluate the capability of moving out of the indoor area (Sime, 2001, Kobes, 2005, Oomes, 2006, Kobes et al., 2010a). If the occupants are subject to less than ideal conditions, regardless of the physical or the psychological aspects, this kind of the evacuees can be treated as in a mode with temporarily reduced mobility (Oomes, 2006, Kobes et al., 2010a), which can affect the process of evacuation to some extent.

When integrating the indoor familiarities with the other two psychological effects, it can be found out that these factors have a slightly greater impact on the awareness of the speed reduction for the female participants (0.655) than that for the males (0.617). This is consistent with the previous findings that the male participants have higher controllability of their speed than the females, although they may still be affected by the effects of the indoor environments. Moreover, the psychological factors have a higher overall impact on the speed reduction awareness than that on the males, while the males' activities are more affected by the indoor environments based on results from Table 6.2.2.5.

TABLE 6.2.2.5

CORRELATION BETWEEN FACTORS FROM SPEED REDUCTION AWARENESS AND INDOOR FAMILIARITIES PLUS PSYCHOLOGICAL STRESSES

	Awareness of Speed Reduction	
	Male	Female
Indoor Familiarity	0.401	0.256
Psychological Difficulty + Nervousness	0.542	0.656
Indoor Familiarity + Psychological Difficulty + Nervousness	0.617	0.655

With the above information, it has proved in this case the hypothesis that the awareness of moving speed reduction during the evacuation will be affected by both environmental and psychological stresses, with a moderately positive relationship. The increase of the environmental familiarity and psychological relief can be achieved by using a personalized and supportive navigation system. This information needs to be considered into the future applications of the smartphone-based emergency guidance as it will affect the user's current psychological state, leading to the variations of the performances of the evacuation strategies.

6.3. THE ACCEPTANCE DEGREE TO THE SMARTPHONE-BASED EMERGENCY GUIDANCE

In addition to the above analysis of the effects from the FRP, the attitude of the users to the smartphone-based navigation also plays an important role in future applications of an indoor fire evacuation. It is considered one of the major challenges to the promotion of the previously designed system to be applied to a wide range of the population. This study has investigated the user attitudes to emergency navigation from four main aspects:

1) the familiarity to the existing smartphone-based navigation service;
2) the willingness of following guidance service during the evacuation;
3) the obedience to the directions provided by the navigation system under some extreme cases;
4) the decision time for the corresponding situations

These factors will help pinpoint potential problems based on the user responses to the emergency navigation, which needs to be considered and helps to provide corresponding suggestions in the future improvements before providing customizable navigation services to the users.

6.3.1. The Familiarity with the Smartphone-based Navigation Service

Navigation services have been widely used by people around the world (Bao et al., 2015, Bentley et al., 2015), which is affected by the popularization of smart devices (Duggan and Smith, 2013, Yun et al., 2013). Thus, this study has proposed an assumption that the current smartphone users should be familiar to the smartphone-based navigation services as it is widely used in daily life.

However, according to the results from the survey data of this study (Fig.6.3.1), the average level of the familiarity (2.64) is not as high as expected before the survey, which is only slightly higher than the mid-level. This may suggest that the participants for the survey may have experienced the navigation services but still not be very familiar with the mechanism of how it works. This may be also due to the sense of direction as well as the guidance services provided by the navigation systems still require people to have the capability of spatial cognition, which is based on interaction between human and environment (Darken et al., 1998, Geary et al., 2000, Jones and Healy, 2006, de Goede, 2009).

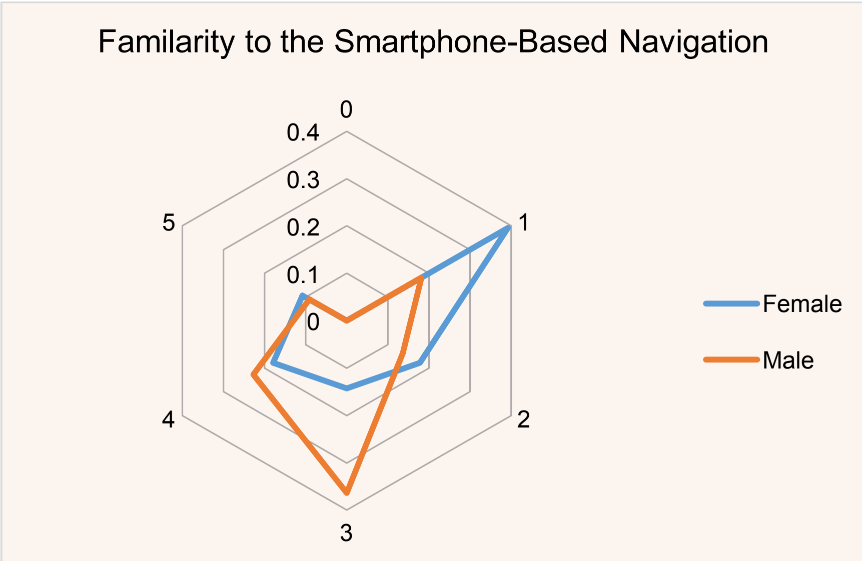

Fig. 6.3.1. The familiarity with the smartphone-based navigation of two genders.

When comparing the differences between the two genders, it can be found out that the male participants have a slightly higher average level (2.91) of the familiarity to the smartphone-based navigation services than the females (2.43). This finding also agrees with the findings from the previous studies that males usually outperform females on navigation-based tasks (Geary et al., 2000, Jones and Healy, 2006, de Goede, 2009). This may be due to the different cues utilized by two genders for spatial tasks, as the males prefer identifying the geometric properties and cardinal directions while the females are good at landmark memorization (Jones and Healy, 2006, de Goede, 2009, He et al., 2015b). It suggests that the future applications of the smartphone-based emergency navigation may still need some training, especially for the female users before providing navigation services to the users.

6.3.2. The willingness of Following Smartphone-Based Guidance during Evacuation

This factor is to test whether the users are willing to have a smartphone-based app to assist their movement during the evacuation, which is also regarded as the premise of the other following questions. *According to the results, the participants of both genders show a positive attitude to the future emergency navigation app,* as none of them shows an attitude of rejection to this service ('0') (Fig. 6.3.2). This shows a relatively good acceptance from the users to this kind of service, which can help to reduce the difficulty from the promotions of this service in future applications.

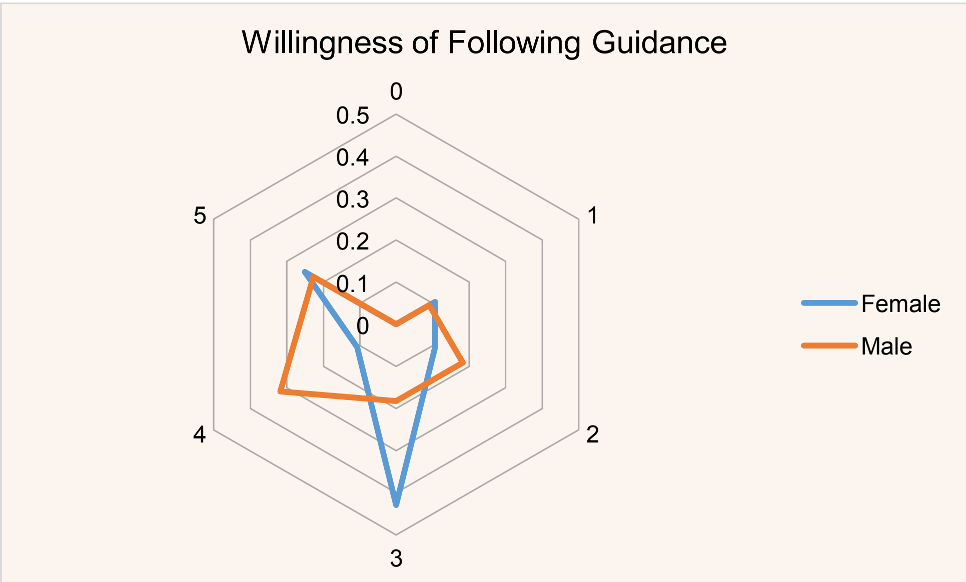

Fig.6.3.2. The willingness of following the guidance service provided by the smartphone app.

The average score of the males (3.41) is still higher than that of the females (3.29), which may be related to the higher familiarity of the male users to the existing smartphone-based navigation. Moreover, the majority of the females (79%) tend to have an at least mid-level positive attitude ('3-5') to the acceptance of the guidance service, while the choices for the rest of them are more evenly distributed. Meanwhile, about 73% of the males have an at least mid-level of positive acceptance of using a longer route, with more population having a relatively higher score ('4-5') of the willingness of following the guidance, and the overall distribution of their acceptance level to the navigation is more uniform than that of the females.

6.3.3. The Obedience to the Guidance under Two Extreme Cases

The familiarity and the willingness of following guidance can be integrated together as a comprehensive index of the user attitude to the smartphone-based navigation during evacuation. Although the selected participants show a positive attitude of following the guidance during the evacuation, it does not mean that they will still follow that guidance under some extreme conditions. The navigation service without the threats from the fire expansion will provide the shortest route based on the current location of the users (Fahy et al., 2012), which has been simulated in the previous chapter. This survey is interested in the responses of the users when they are required by the navigation system to change from the original planned path when facing the dangers. The two extreme cases selected for this study are the willingness of using a longer path due to risk assessment and changing to an alternative exit during the movement with the original plan. The aim of testing these two cases is to find out the degree of the confidence of users to the potential guidance under the fire evacuation.

For the first case, i.e. the navigation system provides a longer path instead of the shortest path due to the higher risk of the latter, the majority of the participants are willing to follow the provided directions. Comparing the responses from two genders, the majority of females (86%) show a positive attitude while there are only 55% of the males having the confidence of trusting the guidance provided by the smartphones (Fig.6.3.3.a). The effects of the above differences may come from three aspects, i.e. indoor familiarity, psychological stress and attitude to the smartphone-based navigation (Table 6.3.3.1). For indoor familiarity, people who are more familiar with indoor structures are more willing to use an alternative but safer path, while the people with the opposite situation may prefer a shorter path (Graham and Roberts, 2000, Shi et al., 2009a, Tan et al., 2015). When comparing the correlations between different factors, it can be inferred that psychological stress plays a more important role in the decision of using a longer but safer route, especially for the males. With the increase of psychological stress, people are less likely to use a longer route rather than the shortest route. This may be due to that the psychological stress will affect the decision making during evacuation (Kobes et al., 2010a, Xiong et al., 2014), and the average level of the psychological stress of the males is lower than that of the females. The integrated effect from the above two factors moderately contributes to the decision of following a longer but safer route, and this impact is more evident on the males (0.413) than that on the females (0.350). The effect from the acceptance of the smartphone-based navigation is more correlated with the decision of using a longer route for the females, which may be related to males' better performances on geometry identification and lower willingness to use a longer path (Jones and Healy, 2006, de Goede, 2009).

TABLE 6.3.3.1

CORRELATION BETWEEN FACTORS FROM WILLINGNESS OF USING A LONGER ROUTE AND INDOOR FAMILIARITIES, PSYCHOLOGICAL STRESSES, AND ATTITUDE TO NAVIGATION

	The willingness of Using A Longer but Safer Path	
	Male	Female
Indoor Familiarity	0.276	0.256
Psychological Stress	-0.376	-0.288
Attitude to Navigation	0.187	0.269
Indoor Familiarity + Psychological Stress	0.413	0.350
Indoor Familiarity + Psychological Stress + Attitude to Navigation	0.428	0.389

For the situation of changing to an alternative exit during the process of the evacuation, most of the participants keep showing the confidence in the guidance provided by the app. When comparing the responses from two genders, the percentage of the population, who shows a positive attitude, of the females (79%) are not significantly higher than that of the males (73%) (Fig.6.3.3b). For the male participants, their decision is more related with the indoor familiarity while for the female participants, their decision is more affected by the acceptance of the navigation services. This may also due to males' better performances on geometry identification and sensation of the cardinal directions (Jones and Healy, 2006, de Goede, 2009). This leads to the integrated effects from the indoor familiarity and psychological stress are more correlated with the males' decision of the using an alternative exit (0.377) than females (0.352). After integrating with the effect from attitude to the navigation services, the overall comprehensive effects from the three factors shows a greater correlation with the females' decisions (0.515) rather than the males (0.406) (Table 6.3.3.2).

TABLE 6.3.3.2

CORRELATION BETWEEN FACTORS FROM WILLINGNESS OF USING AN ALTERNATIVE EXIT AND INDOOR FAMILIARITIES, PSYCHOLOGICAL STRESSES, AND ACCEPTANCE OF NAVIGATION

	The willingness of Using An Alternative Exit	
	Male	Female
Indoor Familiarity	0.311	0.265
Psychological Stress	-0.301	-0.243
Attitude to Navigation	0.206	0.393
Indoor Familiarity + Psychological Stress	0.377	0.352
Indoor Familiarity + Psychological Stress + Attitude to Navigation	0.406	0.515

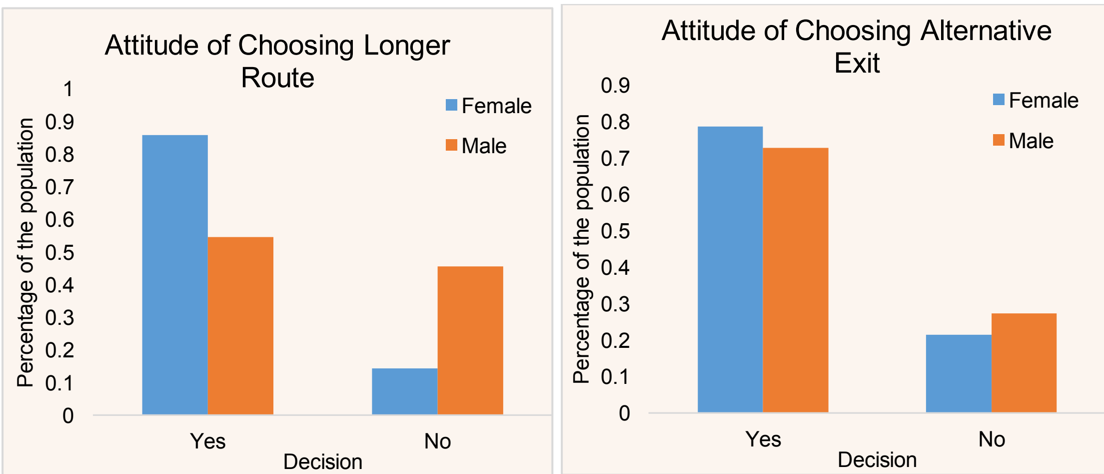

(a) (b)

Fig.6.3.3. The attitude of choosing a longer route (a) and alternative exit (b) from two genders.

6.3.4. The Decision Time for the Corresponding Situations

The decision time for different cases is also an important factor to evaluate people's confidence to the provided navigation services. This time period needs be reduced in order to improve the efficiency of the evacuation.

According to the acquired results, the females tend to have a longer decision time, regardless of the situations of extreme cases (Fig.6.3.4). <u>It suggests that the females are more hesitant to make decisions under extreme cases.</u> This may be related with their relatively higher level of the psychological stress than the males, leading to the increase of the difficulty of decision making especially for complicated situations. Thus, females may need some additional comforting service to persuade them keep trusting the guidance. Meanwhile, the average time for choosing an alternative exit during evacuation other than the original planning is longer than that of choosing a longer route in the beginning of planning, regardless of the gender. *It suggests that changing the direction during the movement is more difficult than making decisions in the beginning and people have the tendency to keep the original guidance during the evacuation movement.* This problem needs to considered in the approach design of providing navigation services to people, making the provided information more acceptable to people.

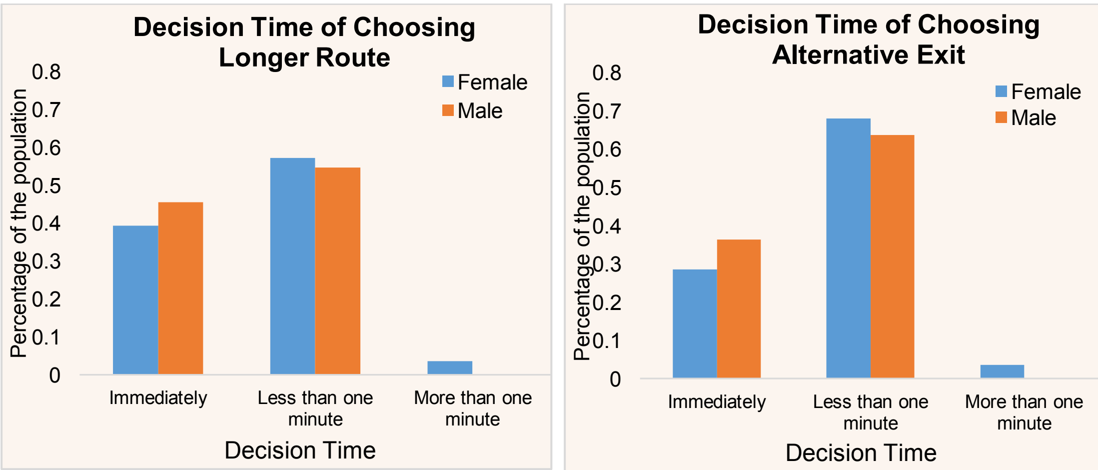

(a) (b)

Fig.6.3.4. The decision time of two genders for choosing longer route (a) and alternative exit (b).

6.4. The Service for Trapped People during Evacuation

Based on the simulation model, the evacuation system designed for this study should be able to provide the location of the fire, the potential expansion of the fire, and the nearest exits. However, according to the simulated results in the previous chapter, not all people can evacuate outside the building in the limited evacuation time. For these people, the navigation system should be able to help people to stay calm in their original locations rather than movement (Fahy et al., 2012).

This study has first investigate whether people can stay calm after being trapped inside the building. The responses from the two genders are significantly different (Fig.6.4.1). The majority of the females (68%) cannot stay calm after being trapped while the males are prone to staying in a calm state (55%). This finding is in agreement to the previous results that the males have a lower average level of psychological stress during the process of evacuation.

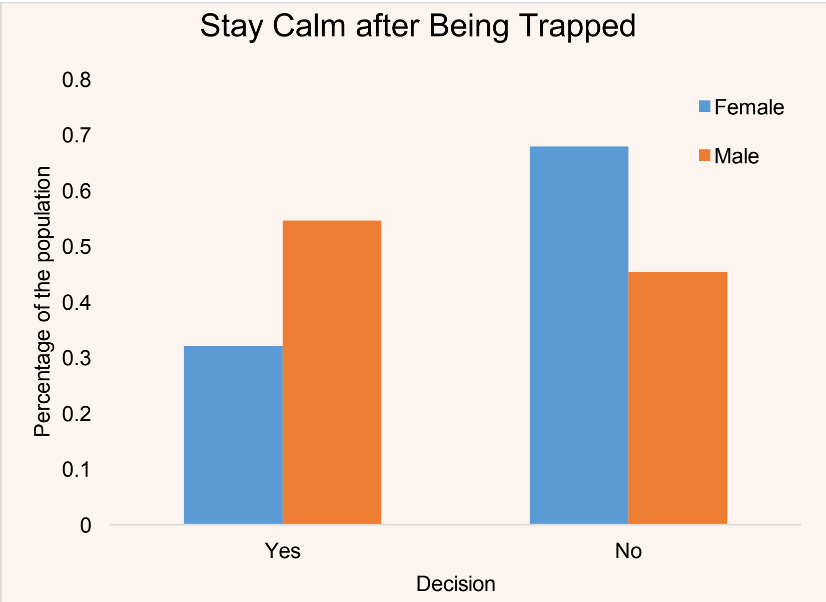

Fig.6.4.1. The psychological state of people after being trapped inside the building.

In order to help people stay calm and stay in the original locations before being rescued by the firefighters, this study has also provided some options to the interviewees and investigated their preferences of these factors to help them stay calm after being trapped (Fig.6.4.2). The responses from different genders both psychologically prefer the factor of “distances to the nearest firefighters” as the top option to help them stay calm during the evacuation. This suggest that the future design of the navigation app should be able provide the positions of the nearest firefighters based on the current user locations. Meanwhile, their considerations of the top three least helpful information of calming assistance are also the same, which is related with the situations of other trapped pedestrians inside the building. This may be due to that people are more self-concerned in a situation of high risks. The future development of the app can remove these kinds of information to help people more concentrated on key notifications.

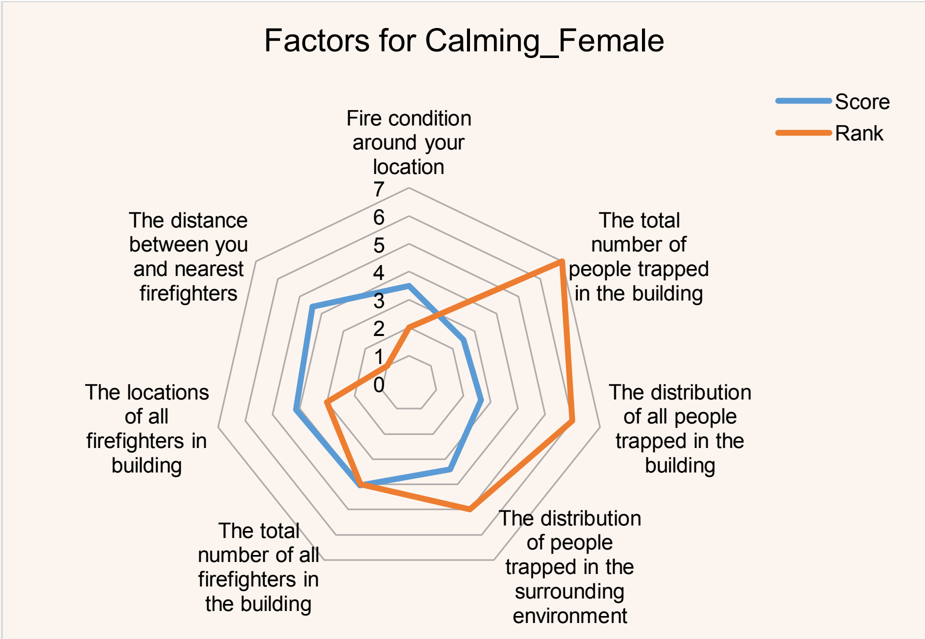

(a)

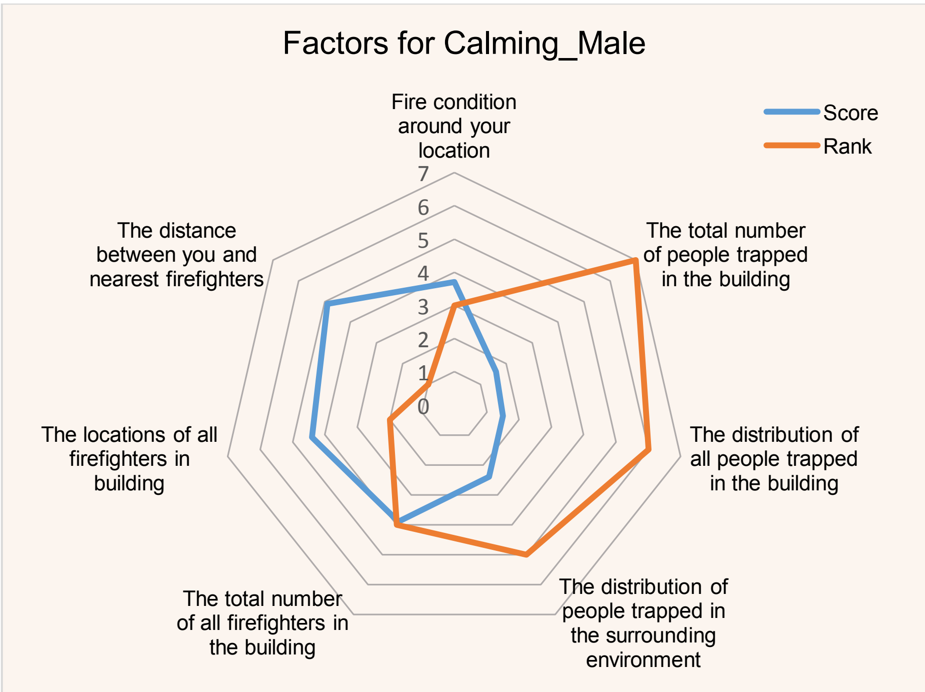

(b)

Fig.6.4.2. The factors help people to stay calm after being trapped in fire for different genders.

For the second and third options for calming assistance, both of the genders have chosen the options of **"the current conditions of the fire"** in the surrounding environment and the "**locations of all the firefighters"**. However, among these two factors, the male participants are more interested in the locations of the rest firefighters while the females are more concentrated on the current status of the fire expansion around their locations. This suggest that the condition of the fire plays an more important role on threatening for females and this may be a possible reason of their higher level of the psychological stress than males during evacaution. Meanwhile, the males' better spatial cognition may also plays an important role and they have a higher level of the indoor familiarity, which may help them have more confidence on their current situation of the indoor risks. However, the expansion of the fire is also regarded as an important information for the males as they have selected as the third important factor for calming down. The above acquired information can be used to customize personalized navigation for indoor fire evacuation and they can help to ease the psychological burden while waiting for the rescue. It can also help persuade people to stay in the orignial shelters rather than irrationally rushing into danger under a relatively high level of panic.

6.5. SUMMARY

The design of an indoor navigation system for fire evacuation support requires not only the physical feasibility but also a relatively thorough consideration of the human factors of cognition. This study has taken a survey to investigate the FRP of the indoor occupants with a median age of 22 in a virtual environment for their routine life, focusing on the aspects of indoor familiarity (spatial cognition), psychological stress, and decision making. For indoor familiarity, it focused on three factors, i.e. *the familiarity to the exits, familiarity to risky places, and the satisfaction degree of the current indoor sign installation*. According to the analysis, males have a higher average familiarity to the indoor exits while both genders have a relatively low level of risky place awareness. These two factors are positively correlated with satisfaction degree of the current installation of the indoor signs, and this correlation is more evident for exit familiarity. To explain this correlation, the height can be regarded as an important factor as it has shown a positive relationship to the indoor sign satisfaction, especially for the males with an average higher level of height. After integrating with the effects from the indoor sign satisfaction, their correlations to the familiarity with either exits or risky places are strengthened, though this phenomenon is not very significant for the familiarity to the risky places, being affected by the generally low awareness of the risky places. On the other hand, the integration of the height factor with the other two indoor familiarity factors can also improve the degree of the indoor sign satisfaction. This also suggests that future installations of the indoor signs require a pre-survey of the height information of indoor occupants, which may better help for their indoor evacuation processes.

For psychological stress, this study concentrates on the situated cognition of moving difficulty, nervousness, and speed reduction when using a bending posture during the fire evacuation to avoid smoke inhalation. The results have shown that both genders have a similar mid-level of hardness sensation. Meanwhile, the females have a higher average level of nervousness while males have a higher average level of speed reduction sensation. Moreover, there is at least a mid-level positive correlation between the sensation of moving difficulty and nervousness when using a bending posture, and this correlation will be strengthened after integrating the impacts from the height, especially for the males. The sensation of speed reduction is more closely correlated with nervousness, especially for the females who have an average level of that factor. This time, the impact from the height is not significant to affect the speed reduction awareness. When analysing the relationships between the factors of indoor familiarity and psychological stress, the increasing familiarity with the indoor areas can help to improve the sensation to the changes in speed. This study has assumed that the growing level of the indoor familiarity can help ease the psychological hardness and nervousness. However, it only seems to be true after reaching a certain threshold, otherwise it will lead to a unexpected reverse effect. When integrating the effects from indoor familiarity and the other two psychological factors, the sensation of speed change can be strengthened, based on a stronger positive correlation with the integrated factors. This has raised the importance of increasing indoor familiarity and psychological relief, and the development of a personalized supportive indoor navigation can help with these situations.

This study has also investigated the participants' attitude to navigation support during evacuation. All the participants have shown positive attitudes to the guidance support that can be applied in indoor fire evacuation while the females may need some more training before using this service. For following the guidance under duress, i.e. changing to a longer path and to an alternative exit other than the originally planned one, the majority of the people have shown trust in the real-time guidance. Moreover, these decisions are both affected by the combined influences from indoor familiarity, psychological stress, and attitude of using navigation services. For the decision time of the selected extreme cases, it costs more time in average for deciding to use an alternative exit than to use a longer route, and this situation is more evident for the female participants. This requires further considerations when designing a personalized smartphone-based app. This study has also investigated the calming factors for people being trapped. According to the results, the top consideration is the distance to the nearest firefighters, and the other important considerations are the current fire conditions in the surrounding environment and the locations of all firefighters. The ranking of the latter two considerations are very gender-dependent according to the results. All these investigated cognition factors should be carefully considered in future design of navigation support for indoor fire evacuations.

Chapter 7. CONCLUSIONS AND THE FUTURE WORKS

7.1. CONCLUSIONS

This study has tested the hypothesis whether the application of a self-developed intelligent indoor navigation system with acceptable positioning accuracy can help to improve the efficiency of indoor fire evacuation process in the period before the arrival of firefighters, which the evacuation movements are entirely depended on the self-decision and mobility.

During the process, it has first developed a prototype of a self-adaptive indoor evacuation system, with the advantages of:

1) Real-time tracking of indoor 3D pedestrian locations with seamless transition between indoor and outdoor environment;
2) Constantly identifying pedestrian postures from upright walking, stoop-walking with and without knee flexion;
3) Dynamic route planning during a fire event based on real-time user locations with changing of exit number and path closure;
4) Spatial visualization of indoor environment in both 2D and 3D;
5) Information updating during the fire event via user devices for decision making;
6) Bottleneck identification based on pedestrian density;
7) Trapped people reporting for later rescue;

The developed self-adaptive system will be applied to run the simulations based on a self-established hybrid ABM system, with the user velocity and inter-person distance provided by a real-time and accurate self-developed novel 3D indoor tracking system. The hypothesis of this study is that the indoor fire evacuation process with the support of the navigation system to find nearest exits is more efficient than moving randomly inside the building for evacuation. This hypothesis can be treated as the comparison of two different evacuation strategies and it is tested by the simulation results provided by the ABM system designed in this research. Moreover, the designed system is able to handle the changing environments, such as the changing of the exit number, the expansion of the fire and availability of certain paths.

According to the above requirements, the development of an accurate, reliable and flexible 3D indoor positioning system is one of the most important and novel components of this study. The development of such system is achieved with the following steps.

First, it has designed a low-cost, highly accurate, intuitive and user friendly advanced 2D indoor positioning system with highly stable performances to the occlusions. This is achieved based on the integration of smartphone-based PDR and surveillance-based visual tracking. The rationale for choosing these two technologies are the higher accessibility of the sensors required for using these two technologies, which are native to the user devices and the existing indoor surveillance system, based on the comparison to the other infrastructure-based indoor positioning technologies. The smartphone-based PDR can continuously provide the relative user positions in indoor area by using embedded accelerometers and gyroscopes for step detection as well as step length and heading estimation, with a novel algorithm for automatic turning detection and step-length calibration. Meanwhile, the visual tracking system is used to calibrate the user positions in the visible areas, by using the estimated user positions from the synthesized results acquired from a modified Faster R-CNN based pedestrian detection and a novel algorithm of depth information transformation, with a relatively higher accuracy. This research has also shown the robustness of system from handling only single camera to multiple cameras, with the development of a novel automatic scene shifting algorithm.

Both sub-systems can work independently and their results are required to be transformed into absolute coordinates before further integration, with the support from GIS-based digital map information in WGS84. These maps are pre-stored in the system and can be integrated into the 2D PVINS results by automatic selection based on the current floor. During the movement, the smartphones are held horizontally and pointing forward. Meanwhile, the video recording is triggered once the user starts moving. Once entering the LoS area of each camera and a significant change is detected from the estimated PDR headings, the 2D visual positions will be calculated based on BBs' positions by pedestrian detection and the estimated depth information in corresponding frames. This study has proposed two methods for integrating the data from two sub-systems: position replacement based on time synchronization and heading calibration for PDR with corresponding step lengths. The latter has been selected due to its better positioning performance based on the experimental results. The 2D visual headings are then determined by visual positions in every two consecutive frames. The system in the 2D PVINS aspect provides a calibrated 2D path in WGS84, with a relatively higher accuracy (0.08m) than other 2D positioning systems investigated in this study under similar conditions of environmental occlusion and complexity, but having the advantage of simpler implementation and higher flexibility. The acquired results, for the first time, can be directly used in outdoor systems and visualized in corresponding floor plan, while none of the other investigated studies has achieved that.

This study also compares the performances between two types of common smartphone models, other than the previous studies using only Android-running smartphones, which has improved the ubiquity of the system for different kinds of smartphones. The operating systems of the smartphones applied in this experiment are in Android 6 and iOS 11, respectively.

The 2D system is then upgraded into a 3D version, with the integration of a self-designed novel algorithm for height estimation and floor identification by using a single smartphone-based barometer, with the advantages of simple operation and fewer requirements of sensor. The algorithm is developed from the fingerprint based pressure-height transformation model and finally it uses a linearity-average model, by detecting certain patterns during vertical movements. This algorithm, for the first time, is even able to detect transition areas between floors, by following the pattern of two changes of linearity and three different means of the height, while none of the other studies has achieved that. Moreover, it has first introduced a self-calibration mechanism of using two smartphone apps other than using two barometers. The acquired height estimation accuracy (0.5m) with 98% floor identification is more accurate than other studies and is then used for later integration with 2D PVINS for 3D positioning.

The height estimation with floor identification is synthesized with the previous 2D PVINS by finding similar time stamps and this 3D system is tested in a severe-occlusion environment with fewer visible areas. The acquired 2D accuracy (0.16m) is highly comparable to the other studies with less occlusion, regardless of using 2D PVINS or alternative foot-mounted systems. After integration with the height estimation data, the acquired 3D positioning accuracy is still comparable to other foot-mounted or signal-based approaches, with the advantage of more accessible sensors, lower cost and better user experiences than other studies. It has also satisfied the requirements by the Federal Communications Commission (FCC) for fire emergency with 50m horizontal accuracy and 3m vertical accuracy.

With the above novel and accurate 3D indoor positioning system, this study is able to measure the user velocity and inter-person distance by taking experiments in the building of case study, with advantages of simpler operation than previous studies using more dense distribution of professional cameras. The measured parameters are important to describe the social force model between pedestrians for the establishment of the hybrid ABM-based simulation. Meanwhile, the previously acquired GIS-based floor plans can also be used in the ABM-based simulation, as the software applied in this study, AnyLogic, requires a GIS-based simulation environment.

The established ABM is used to simulate two scenarios as pre-alarm and post-alarm, with a combination with a novel fire expansion model. The fire expansion model is usually ignored in previous ABM-based simulations, as the pedestrian movement is a continuous process while the fire expansion is more matrix-based. However, this study has simplified it as a spatial-temporal process, and it has first enabled the integration of fire expansion model with ABM. The pre-alarm scenario is used for identification of the bottlenecks inside the building. The post-alarm scenario aims to compare the efficiency of two evacuation strategies, the evacuation with or without navigation assistance, by comparing the number of survivals, the mean and maximum RSET of survivals, and their average evacuation distance. The overall hypothesis of this thesis is supported by the acquired results from the ABM simulations. Moreover, it has suggested the effects from the exit width and distribution for evacuation route selection.

This study also suggested more cognition factors worth investigating for the fire response performances of people, before the further development and adoption of an intelligent and personalized fire evacuation support system. In this study, these factors are classified into three aspects as indoor spatial cognition, the psychological stress and the decision making for different situations. This study has first conducted a survey of these factors among the occupants with a median age of 22 inside the building for the case study, under a virtual situation of using bending posture during evacuation. There are some interesting findings being discovered after analysing the results:

For indoor spatial cognition, the study is interested in familiarity to exits and risky places as well as the satisfaction to the current indoor sign installation. The acquired results are gender-dependent to some extent and the familiarity to the indoor exits and the risky places are positively correlated with satisfaction degree of the current installation of indoor signs. The height factor can also affect these correlations.

For psychological stress, this study concentrates on the situated cognition of moving difficulty, nervousness, and speed reduction when using a bending posture to avoid smoke inhalation. The results are also gender-dependent. After reaching certain levels, the growing indoor spatial cognition can help ease the psychological hardness and nervousness conditions. Moreover, it can help strengthen the sensation of speed reduction, with the integration of the other factors of psychological stress.

For decision making aspect, the majority of the participants all have shown a positive altitude to the future navigation guidance during evacuation, even under some extreme situations, i.e. using a longer route or an alternative exit. The decision time of different situations are also different and gender-depended to some extent.

Meanwhile, people tend to stay in a state of high psychological stress when being trapped inside the building during a fire event. This study has first discovered that the knowledge of the provision of distance to the nearest firefighters, the current fire condition in users' surrounding environment, as well as the distributions of all firefighters inside the building induces people to stay calm. These factors are useful information for future development of a personalized indoor navigation system for indoor fire evacuation. This study has achieved the first step of the development of a customizable system with much future work to be done based on the findings.

7.2. FUTURE WORKS

Some of the potential developments from this work are listed below:

1) Improve the current indoor 3D positioning from single-person to multi-person tracking;
2) Improve the current system from offline processing to online tracking by achieving video live streaming;
3) Validation of the designed 3D indoor positioning system in different types of the buildings;
4) Increase the number of participants for velocity and inter-person distance measurement;
5) Increase the diversity of participants for the above experiment, with different groups of age, height, weight and availabilities;
6) Improve the ABM design with more factors for considerations, e.g. different levels of indoor familiarity, psychological stress and attitude to the navigation support;
7) More repentance for ABM-based simulations with more stable performances of simulated results;
8) More evacuation strategies testing for ABM-based simulations, e.g. the timely arrangement for different floors with different starting time with or without navigation support;
9) More environmental scenarios for the ABM-based simulations, e.g. different fire locations, different number of fire events, and different types and buildings;
10) Development of real-time fire expansion monitoring by sensors to validate and improve the current fire expansion model;

11) The development of a smartphone-based app for indoor fire evacuation and user feedback collection for that specific app for further improvement.

REFERENCES

ABDULRAHIM, K., HIDE, C., MOORE, T. & HILL, C. 2011. Aiding low cost inertial navigation with building heading for pedestrian navigation. *Journal of Navigation,* 64**,** 219-233.

ADLER, S., SCHMITT, S., WOLTER, K. & KYAS, M. A survey of experimental evaluation in indoor localization research. 2015 International Conference on Indoor Positioning and Indoor Navigation (IPIN), 2015. IEEE, 1-10.

AEDO, I., YU, S., D AZ, P., ACU A, P. & ONORATI, T. 2012. Personalized alert notifications and evacuation routes in indoor environments. *Sensors,* 12**,** 7804-7827.

AGGARWAL, P., SYED, Z., NIU, X. & EL-SHEIMY, N. 2008. A standard testing and calibration procedure for low cost MEMS inertial sensors and units. *The Journal of Navigation,* 61**,** 323-336.

AGUIRRE, B. E. 2005. Emergency evacuations, panic, and social psychology. *Psychiatry: Interpersonal and Biological Processes,* 68**,** 121-129.

AL-AHMADI, A. S. M., OMER, A. I., KAMARUDIN, M. R. & RAHMAN, T. A. 2010. Multi-floor indoor positioning system using bayesian graphical models. *Progress In Electromagnetics Research,* 25**,** 241-259.

ALSEHLY, F., ARSLAN, T. & SEVAK, Z. Indoor positioning with floor determination in multi story buildings. 2011 International Conference on Indoor Positioning and Indoor Navigation (IPIN), 2011. IEEE, 1-7.

ALZANTOT, M. & YOUSSEF, M. Crowdinside: automatic construction of indoor floorplans. Proceedings of the 20th International Conference on Advances in Geographic Information Systems, 2012. ACM, 99-108.

ALZANTOT, M. & YOUSSEF, M. Demonstrating CrowdInside: A system for the automatic construction of indoor floor-plans. 2013 IEEE International Conference on Pervasive Computing and Communications Workshops (PERCOM Workshops), 2013. IEEE, 321-323.

ARTIM, N. 1999. An Introduction to Fire Detection, Alarm, and Automatic Fire Sprinklers. *Northeast Document Conservation Center*.

ATILA, U., KARAS, I., TURAN, M. & RAHMAN, A. 2013. Design of an intelligent individual evacuation model for high rise building fires based on neural network within the scope of 3d GIS. *ISPRS Annals of Photogrammetry, Remote Sensing and Spatial Information Sciences,* 1**,** 13-24.

AVERILL, J. 2011. Five grand challenges in pedestrian and evacuation dynamics. *Pedestrian and Evacuation Dynamics.* Springer, 1-11.

AZIMI, E., DOSWELL, J. & KAZANZIDES, P. Augmented reality goggles with an integrated tracking system for navigation in neurosurgery. Virtual Reality Short Papers and Posters (VRW), 2012 IEEE, 2012. IEEE, 123-124.

BAI, Y., JIA, W., ZHANG, H., MAO, Z.-H. & SUN, M. Helping the blind to find the floor of destination in multistory buildings using a barometer. 2013 35th Annual International Conference of the IEEE Engineering in Medicine and Biology Society (EMBC), , 2013. IEEE, 4738-4741.

BAKAR, N. A. A., ADAM, K., MAJID, M. A. & ALLEGRA, M. A simulation model for crowd evacuation of fire emergency scenario. 2017 8th International Conference on Information Technology (ICIT), 2017. IEEE, 361-368.

BAO, J., ZHENG, Y., WILKIE, D. & MOKBEL, M. 2015. Recommendations in location-based social networks: A survey. *GeoInformatica,* 19**,** 525-565.

BASIRI, A., LOHAN, E. S., MOORE, T., WINSTANLEY, A., PELTOLA, P., HILL, C., AMIRIAN, P. & E. SILVA, P. F. 2017. Indoor location based services challenges, requirements and usability of current solutions. *Computer Science Review.* 24, 1-12.

BASTOS, A. S., VIEIRA, V. & APOLINARIO JR, A. L. Indoor location systems in emergency scenarios-A Survey. Proceedings of the annual conference on Brazilian Symposium on Information Systems: A Computer Socio-Technical Perspective, 2015. Brazilian Computer Society, 251-258.

BAUS, J., KR GER, A. & WAHLSTER, W. A resource-adaptive mobile navigation system. Proceedings of the 7th international conference on Intelligent user interfaces, 2002. ACM, 15-22.

BECKER, T., NAGEL, C. & KOLBE, T. H. 2009. A multilayered space-event model for navigation in indoor spaces. *3D geo-information sciences.* Springer, 61-77.

BENTHORN, L. & FRANTZICH, H. 1999. Fire alarm in a public building: How do people evaluate information and choose an evacuation exit? *Fire and Materials,* 23**,** 311-315.

BENTLEY, F., CRAMER, H. & M LLER, J. 2015. Beyond the bar: The places where location-based services are used in the city. *Personal and Ubiquitous Computing,* 19, 217-223.

BONENBERG, L. K., HANCOCK, C. M. & ROBERTS, G. W. 2010. Indoor multipath effect study on the Locata system. *Journal of Applied Geodesy,* 4, 137-143.

BONOMI, A., MANZONI, S., PISANO, A. & VIZZARI, G. Experimenting situated cellular agents in indoor scenario: pedestrian dynamics during lecture hall evacuation. 2009 IEEE/WIC/ACM International Joint Conference on Web Intelligence and Intelligent Agent Technology, 2009. IEEE, 591-594.

BORONOWSKY, M., HERZOG, O., KNACKFU , P. & LAWO, M. wearIT@ work-Empowering the Mobile Worker by Wearable Computing–the First Results. Proceedings AMI@ work forum day, Munich, 2005. 38-45.

BORSHCHEV, A. 2013. *The big book of simulation modeling: multimethod modeling with AnyLogic 6*, Chicago, North America, AnyLogic.

BORSHCHEV, A. & FILIPPOV, A. From system dynamics and discrete event to practical agent based modeling: reasons, techniques, tools. Proceedings of the 22nd International Conference of the System Dynamics Society, 2004. Citeseer.

BRAUER, S. G., BURNS, Y. R. & GALLEY, P. 2000. A prospective study of laboratory and clinical measures of postural stability to predict community-dwelling fallers. *The Journals of Gerontology Series A: Biological Sciences and Medical Sciences,* 55, 469-476.

BRAUN, A., BODMANN, B. E. & MUSSE, S. R. Simulating virtual crowds in emergency situations. Proceedings of the ACM Symposium on Virtual Reality Software and Technology, 2005. ACM, 244-252.

BROWN, J. D. 2017. *Significance of Posture in Relation to Falls in the Elderly.* Master Thesis. Ashland University.

BRYAN, J. L. 2002a. Behavioral response to fire and smoke. *SFPE handbook of fire protection engineering,* 2, 42.

BRYAN, J. L. 2002b. A Selected Historical Review of Human Behaviour in Fire. *Journal of Fire Protection Engineering,* 16, 4-10.

BRYNER, N., MADRZYKOWSKI, D. & GROSSHANDLER, W. Reconstructing the station nightclub fire-computer modelling of the fire growth and spread. 11th International Conference of Interflam, 2007. 1181-1192.

BURNS, E. R., STEVENS, J. A. & LEE, R. 2016. The direct costs of fatal and non-fatal falls among older adults—United States. *Journal of safety research,* 58**,** 99-103.

BUTLER, M. 2011. Android: Changing the mobile landscape. *IEEE Pervasive Computing,* 10**,** 4-7.

CAI, B., XU, X., JIA, K., QING, C. & TAO, D. 2016. Dehazenet: An end-to-end system for single image haze removal. *IEEE Transactions on Image Processing,* 25**,** 5187-5198.

CAI, Y. & TAN, X. Weakly supervised human body detection under arbitrary poses. 2016 IEEE International Conference on Image Processing (ICIP), 2016. IEEE, 599-603.

CAMILLEN, F., CAPR , S., GAROFALO, C., IGNACCOLO, M., INTURRI, G., PLUCHINO, A., RAPISARDA, A. & TUDISCO, S. Multi agent simulation of pedestrian behavior in closed spatial environments. 2009 IEEE Toronto International Conference Science and Technology for Humanity (TIC-STH), 2009. IEEE, 375-380.

CAMPBELL, W. W. 2013. *DeJong's The neurologic examination, 7th Edition,* Philadelphia, Lippincott Williams & Wilkins.

CAO, L., DAVIS, G. A., GALLAGHER, S., SCHALL, M. C. & SESEK, R. F. 2018. Characterizing posture and associated physiological demand during evacuation. *Safety science,* 104**,** 1-9.

CAO, L., DAVIS, J. & GALLAGHER, S. The impact of posture on evacuation speed. Proceedings of the 2nd International Tall Building Fire Safety Conference, 2014. 111-121.

CARREIRA, J. & SMINCHISESCU, C. 2012. Cpmc: Automatic object segmentation using constrained parametric min-cuts. *IEEE Transactions on Pattern Analysis and Machine Intelligence,* 34**,** 1312-1328.

CFPA 2009. Fire safety engineering concerning evacuation from buildings, Technical report, CFPA-E. The Confederation of Fire Protection Associations in Europe.

CHATFIELD, K., SIMONYAN, K., VEDALDI, A. & ZISSERMAN, A. Return of the devil in the details: Delving deep into convolutional nets. Proceedings of the British Machine Vision Conference, 2014. Nottingham, UK. BMVA Press.

CHATTARAJ, U., SEYFRIED, A. & CHAKROBORTY, P. 2009. Comparison of pedestrian fundamental diagram across cultures. *Advances in complex systems,* 12**,** 393-405.

CHEN, C., TANG, L., HANCOCK, C. M., YAN, J., DE LIGT, H. & ZHANG, P. 2D-based indoor mobile laser scanning for construction digital mapping application. FIG Congress, 2018. Istanbul, Turkey.

CHITTARO, L. & NADALUTTI, D. Presenting evacuation instructions on mobile devices by means of location-aware 3D virtual environments. 10th international conference on Human computer interaction with mobile devices and services. 2008 Amsterdam, The Netherlands. ACM, 395–398.

CHITTARO, L. & NADALUTTI, D. A mobile RFID-based system for supporting evacuation of buildings. International Workshop on Mobile Information Technology for Emergency Response, 2009 Berlin, Heidelberg. Springer, 22-31.

CHOI, H., KIM, S., PARK, K. & SOHN, K. Multi-spectral pedestrian detection based on accumulated object proposal with fully convolutional networks. 23rd International Conference on Pattern Recognition (ICPR), 2016. IEEE, 621-626.

CHU, L. A RFID-based hybrid building fire evacuation system on mobile phone. Sixth International Conference on Intelligent Information Hiding and Multimedia Signal Processing (IIH-MSP), 2010. IEEE, 155-158.

COCKING, C. & DRURY, J. 2014. Talking about Hillsborough:'Panic'as discourse in survivors' accounts of the 1989 football stadium disaster. *Journal of Community & Applied Social Psychology,* 24**,** 86-99.

COLLINS, R. T., LIPTON, A. J., KANADE, T., FUJIYOSHI, H., DUGGINS, D., TSIN, Y., TOLLIVER, D., ENOMOTO, N., HASEGAWA, O. & BURT, P. 2000. A system for video surveillance and monitoring. *VSAM Final Report by Robotics Institute of CMU*, Pittsburgh PA: The Robotics Institute, Carnegie Mellon University. 1456-1471.

CONSTANDACHE, I., BAO, X., AZIZYAN, M. & CHOUDHURY, R. R. Did you see bob?: Human localization using mobile phones. Proceedings of the 16th Annual International Conference on Mobile Computing and Networking, 2010a. ACM, 149-160.

CONSTANDACHE, I., CHOUDHURY, R. R. & RHEE, I. Towards mobile phone localization without war-driving. Proceedings of IEEE Infocom, 2010b. IEEE, 1-9.

CUTTER, S. L. 2003. GI science, disasters, and emergency management. *Transactions in GIS,* 7**,** 439-446.

DAAMEN, W. & HOOGENDOORN, S. P. 2007. Flow-density relations for pedestrian traffic. *Traffic and granular flow'05,* 315-322.

DAAMEN, W., HOOGENDOORN, S. P. & LUNDGREN, N. Passengers Evacuating in Rail Tunnels: A Simulation Study to Predict Evacuation Times. 11th World Conference on Transport ResearchWorld Conference on Transport Research Society, 2007.

DANION, F., VARRAINE, E., BONNARD, M. & PAILHOUS, J. 2003. Stride variability in human gait: the effect of stride frequency and stride length. *Gait and Posture,* 18**,** 69-77.

DARKEN, R. P., ALLARD, T. & ACHILLE, L. B. 1998. Spatial orientation and wayfinding in large-scale virtual spaces: An introduction. *Presence: Teleoperators and Virtual Environments,* 7**,** 101-107.

DAVIS, R. A. 2011a. *A Comparison of Physiological Effects of Traditional Walking Locomotion to Crawling.* Master Thesis, East Stroudsburg University of Pennsylvania.

DAVIS, R. A. 2011b. *Physiological Characterization of Crawling Activity.* Master Thesis, East Stroudsburg University.

DE GOEDE, M. 2009. *Gender differences in spatial cognition*, PhD Thesis, Utrecht University.

DE VILLIERS, B., CLARKE, W. & ROBINSON, P. Mean shift object tracking with occlusion handling. 21st Conference of the International Association for Pattern Recognition (IAPR), 2012. IAPR.

DENG, Z., YU, Y., YUAN, X., WAN, N. & YANG, L. 2013. Situation and development tendency of indoor positioning. *China Communications,* 10**,** 42-55.

DOLLAR, P., WOJEK, C., SCHIELE, B. & PERONA, P. 2012. Pedestrian detection: An evaluation of the state of the art. *IEEE Transactions on Pattern Analysis and Machine Intelligence,* 34**,** 743-761.

DONAHUE, J., JIA, Y., VINYALS, O., HOFFMAN, J., ZHANG, N., TZENG, E. & DARRELL, T. Decaf: A deep convolutional activation feature for generic visual recognition. International conference on machine learning, 2014. 647-655.

DONG-SI, T. C. & MOURIKIS, A. I. Estimator initialization in vision-aided inertial navigation with unknown camera-IMU calibration. IEEE/RSJ International Conference on Intelligent Robots and Systems, 2012. 1064-1071.

DRURY, J., NOVELLI, D. & STOTT, C. 2013. Psychological disaster myths in the perception and management of mass emergencies. *Journal of Applied Social Psychology,* 43**,** 2259-2270.

DUGGAN, M. & SMITH, A. 2013. Social media update 2013. *Pew Internet and American Life Project*.

EBNER, F., FETZER, T., DEINZER, F., K PING, L. & GRZEGORZEK, M. Multi-sensor 3D indoor localisation. 2015 International Conference on Indoor Positioning and Indoor Navigation (IPIN), 2015. IEEE, 1-11.

ELLOUMI, W., LATOUI, A., CANALS, R., CHETOUANI, A. & TREUILLET, S. 2016. Indoor pedestrian localization with a smartphone: a comparison of inertial and vision-based methods. *IEEE Sensors Journal,* 16**,** 5376-5388.

ENZWEILER, M. & GAVRILA, D. M. 2008. Monocular pedestrian detection: Survey and experiments. *IEEE Trans.Pattern Analysis and Machine Intelligence***,** 2179-2195.

FAHY, R. F. Available Data and Input Into Models. *In:* KULIGOWSKI, E. D. & PEACOCK, R. D., eds. Workshop on Building Occupant Movement During Fire Emergencies, 2005 Gaithersburg, MD. National Institute of Standardsand Technology (NIST) , 62-67.

FAHY, R. F., PROULX, G. & AIMAN, L. 2012. Panic or not in fire: Clarifying the misconception. *Fire and materials,* 36**,** 328-338.

FANG, L., ANTSAKLIS, P. J., MONTESTRUQUE, L. A., MCMICKELL, M. B., LEMMON, M., SUN, Y., FANG, H., KOUTROULIS, I., HAENGGI, M. & XIE, M. 2005. Design of a wireless assisted pedestrian dead reckoning system-the NavMote experience. *IEEE Transactions on Instrumentation and Measurement,* 54**,** 2342-2358.

FARAGHER, R., SARNO, C. & NEWMAN, M. Opportunistic radio SLAM for indoor navigation using smartphone sensors. Position Location and Navigation Symposium (PLANS), 2012 IEEE/ION, 2012. IEEE, 120-128.

FCC 2015. Fourth Report and Order in PS Docket No. 07-114. Federal

Communications Commission (FCC).

FERRAZ, H. B. & SABA, R. A. 2017. Clinical Aspects of Movement Disorders: Effects on Walking and Posture. *Locomotion and Posture in Older Adults.* Springer, 21-31.

FILIPPOUPOLITIS, A., HEY, L., LOUKAS, G., GELENBE, E. & TIMOTHEOU, S. Emergency response simulation using wireless sensor networks. Proceedings of the 1st international conference on Ambient media and systems, 2008. ICST (Institute for Computer Sciences, Social-Informatics and Telecommunications Engineering, 21.

FILONENKO, V., CULLEN, C. & CARSWELL, J. Investigating ultrasonic positioning on mobile phones. 2010 International Conference on Indoor Positioning and Indoor Navigation (IPIN) 2010. IEEE, 1-8.

FIRE-SERVICE-BUREAU 2017. The Distribution of Fire Based on Action Scene in 2015. Beijing: Fire Service Bureau, Ministry of Public Security, China fire services.

FLORES, J. Z. & FARCY, R. Indoor navigation system for the visually impaired using one inertial measurement unit (IMU) and barometer to guide in the subway stations and commercial centers. International Conference on Computers for Handicapped Persons, 2014. Springer, 411-418.

FOURATI, H. 2015. Heterogeneous data fusion algorithm for pedestrian navigation via foot-mounted inertial measurement unit and complementary filter. *IEEE Transactions on Instrumentation and Measurement,* 64**,** 221-229.

FOXLIN, E. 2005. Pedestrian tracking with shoe-mounted inertial sensors. *IEEE Computer Graphics and Applications,* 25**,** 38-46.

FUCHS, C., ASCHENBRUCK, N., MARTINI, P. & WIENEKE, M. 2011. Indoor tracking for mission critical scenarios: A survey. *Pervasive and Mobile Computing,* 7**,** 1-15.

GALEA, E. R., WANG, Z., VEERASWAMY, A., JIA, F., LAWRENCE, P. J. & EWER, J. 2008. Coupled fire/evacuation analysis of the station nightclub fire. *Fire Safety Science,* 9**,** 465-476.

GALLAGHER, S., POLLARD, J. & PORTER, W. L. Characteristics of Gait in Restricted Vertical Space Versus Unrestricted Walking. Proceedings of the Human Factors and Ergonomics Society Annual Meeting, 2010, Los

Angeles, CA. SAGE Publications,1149-1153.

GALLAGHER, S., POLLARD, J. & PORTER, W. L. 2011. Locomotion in restricted space: Kinematic and electromyographic analysis of stoopwalking and crawling. *Gait & posture,* 33**,** 71-76.

GARD, S. A., MIFF, S. C. & KUO, A. D. 2004. Comparison of kinematic and kinetic methods for computing the vertical motion of the body center of mass during walking. *Human movement science,* 22**,** 597-610.

GARTNER, G., FRANK, A. U. & RETSCHER, G. *Pedestrian navigation system in mixed indoor/outdoor environment-the NAVIO project*, 9th International Symposion on Planning & IT, 2004. 165-171.

GEARY, D. C., SAULTS, S. J., LIU, F. & HOARD, M. K. 2000. Sex differences in spatial cognition, computational fluency, and arithmetical reasoning. *Journal of Experimental Child Psychology,* 77**,** 337-353.

GILLI RON, P.-Y., B CHEL, D., SPASSOV, I. & MERMINOD, B. Indoor navigation performance analysis. Proceedings of the 8th European Navigation Conference GNSS, 2004. 30.

GIRSHICK, R. Fast R-CNN. Proceedings of the IEEE International Conference on Computer Vision, 2015. 1440-1448.

GIRSHICK, R., DONAHUE, J., DARRELL, T. & MALIK, J. Rich feature hierarchies for accurate object detection and semantic segmentation. Proceedings of the IEEE Conference on Computer Vision and Pattern Recognition, 2014. 580-587.

GOLDSTONE, R. L. & JANSSEN, M. A. 2005. Computational models of collective behavior. *Trends in cognitive sciences,* 9**,** 424-430.

GOYAL, P., RIBEIRO, V. J., SARAN, H. & KUMAR, A. Strap-down pedestrian dead-reckoning system. 2011 International Conference on Indoor Positioning and Indoor Navigation (IPIN), 2011. IEEE, 1-7.

GRAHAM, T. & ROBERTS, D. 2000. Qualitative overview of some important factors affecting the egress of people in hotel fires. *International Journal of Hospitality Management,* 19**,** 79-87.

GRANDISON, A. J., GALEA, E. R., PATEL, M. K. & EWER, J. 2007. Parallel CFD fire modelling on office PCs with dynamic load balancing. *International Journal for Numerical Methods in Fluids,* 55**,** 29-39.

GRASSO, R., ZAGO, M. & LACQUANITI, F. 2000. Interactions between posture and locomotion: motor patterns in humans walking with bent posture versus erect posture. *Journal of Neurophysiology,* 83**,** 288-300.

GRAUMAN, K. & DARRELL, T. The pyramid match kernel: Discriminative classification with sets of image features. Tenth IEEE International Conference on Computer Vision (ICCV), 2005. IEEE, 1458-1465.

GRIESBACH, D., BAUMBACH, D. & ZUEV, S. 2014. Stereo-vision-aided inertial navigation for unknown indoor and outdoor environments. *International Journal of Cultural Policy,* 20**,** 281-295.

GROSSHANDLER, W., BRYNER, N., MADRZYKOWSKI, D. & KUNTZ, K. 2005. A report of the technical investigation of the station nightclub fire. *NIST NCSTAR 2.* Gaitherburg, MD., USA,: National Institute of Standard and Technology (NIST).

GSA 2015. GNSS market report, issue 4. European GNSS Agency (GSA).

GU, C., LIM, J. J., ARBEL EZ, P. & MALIK, J. Recognition using regions. IEEE Conference on Computer Vision and Pattern Recognition (CVPR), 2009. IEEE, 1030-1037.

GUO, R. A network-based method for modeling pedestrian evacuation in indoor areas. Third International Joint Conference on Computational Science and Optimization (CSO), 2010. IEEE, 495-498.

GUPTA, A. & YADAV, P. K. 2004. SAFE-R: a new model to study the evacuation profile of a building. *Fire Safety Journal,* 39**,** 539-556.

GWYNNE, S., GALEA, E., LAWRENCE, P. J. & FILIPPIDIS, L. 2001. Modelling occupant interaction with fire conditions using the buildingEXODUS evacuation model. *Fire Safety Journal,* 36**,** 327-357.

HA, V. & LYKOTRAFITIS, G. 2012. Agent-based modeling of a multi-room multi-floor building emergency evacuation. *Physica A: Statistical Mechanics and its Applications,* 391**,** 2740-2751.

HAJIBABAI, L., DELAVAR, M., MALEK, M. & FRANK, A. 2007. Agent-based simulation of spatial cognition and wayfinding in building fire emergency evacuation. *Geomatics solutions for disaster management.* Springer.

HARDEGGER, M., ROGGEN, D. & TR STER, G. 2015. 3D ActionSLAM: wearable person tracking in multi-floor environments. *Personal and Ubiquitous computing,* 19**,** 123-141.

HARITAOGLU, I., HANRWOOD, D. & DAVIS, L. 2010. Real-time surveillance of people and their activilies. *IEEE Transactions on Pattern Analysis and Machine Intlligence,* 22**,** 809-830.

HARLE, R. 2013. A survey of indoor inertial positioning systems for pedestrians. *IEEE Communications Surveys and Tutorials,* 15**,** 1281-1293.

HARTMANN, B., LINK, N. & TROMMER, G. F. Indoor 3D position estimation using low-cost inertial sensors and marker-based video-tracking. IEEE/ION Position Location and Navigation Symposium (PLANS), 2010. IEEE, 319-326.

HE, C., KAZANZIDES, P., SEN, H. T., KIM, S. & LIU, Y. 2015a. An inertial and optical sensor fusion approach for six degree-of-freedom pose estimation. *Sensors,* 15**,** 16448-16465.

HE, D. & ZHAO, S. Emergency evacuation model based on multi-agent system. 2010 International Symposium on Computational Intelligence and Design, 2010. IEEE, 164-166.

HE, G.-Q., YANG, Y., CHEN, Z.-H., GU, C.-H. & PAN, Z.-G. 2013. A review of behavior mechanisms and crowd evacuation animation in emergency exercises. *Journal of Zhejiang University SCIENCE C,* 14**,** 477-485.

HE, G., ISHIKAWA, T. & TAKEMIYA, M. 2015b. Collaborative Navigation in an Unfamiliar Environment with People Having Different Spatial Aptitudes. *Spatial Cognition & Computation,* 15**,** 285-307.

HE, K., ZHANG, X., REN, S. & SUN, J. Spatial pyramid pooling in deep convolutional networks for visual recognition. European Conference on Computer Vision, 2014. Springer, 346-361.

HE, Y., LI, Y. & BAO, S.-D. Fall detection by built-in tri-accelerometer of smartphone. Proceedings of 2012 IEEE-EMBS International Conference on Biomedical and Health Informatics, 2012. IEEE, 184-187.

HEIDE, E. A. 2004. Common misconceptions about disasters: Panic, the disaster syndrome, and looting. *The first 72 hours: A community approach to disaster preparedness,* 337.

HELBING, D., FARKAS, I. & VICSEK, T. 2000. Simulating dynamical features of escape panic. *Nature,* 407(6803)**,** 487-490.

HIDE, C., BOTTERILL, T. & ANDREOTTI, M. Low cost vision-aided IMU for pedestrian navigation. Ubiquitous Positioning Indoor Navigation and Location Based Service (UPINLBS), 2010a. IEEE, 1-7.

HIDE, C., BOTTERILL, T. & ANDREOTTI, M. Vision-aided IMU for handheld pedestrian navigation. GNSS 2010 Conference Proceedings of the Institute of Navigation, 2010b Portland, Oregon.

HORA, M., SL DEK, V., SOUMAR, L. & MICH LEK, T. 2012. Influence of body mass and lower limb length on knee flexion angle during walking in humans. *Folia Zoologica,* 61**,** 330-340.

HORA, M. & SLADEK, V. 2014. Influence of lower limb configuration on walking cost in Late Pleistocene humans. *Journal of human evolution,* 67**,** 19-32.

HORA, M., SOUMAR, L., PONTZER, H. & SL DEK, V. 2017. Body size and lower limb posture during walking in humans. *PloS ONE,* 12(2), 1-26.

HSU, Y.-L., WANG, J.-S. & CHANG, C.-W. 2017. A wearable inertial pedestrian navigation system with quaternion-based extended Kalman filter for pedestrian localization. *IEEE Sensors Journal,* 17**,** 3193-3206.

HU, M.-B., JIANG, R., WU, Q.-S. & WU, Y.-H. 2007a. Simulating the wealth distribution with a Richest-Following strategy on scale-free network. *Physica A: Statistical Mechanics and its Applications,* 381**,** 467-472.

HU, M.-B., WANG, W.-X., JIANG, R., WU, Q.-S. & WU, Y.-H. 2007b. The effect of bandwidth in scale-free network traffic. *EPL (Europhysics Letters),* 79**,** 14003.

HUA, Y., ALAHARI, K. & SCHMID, C. Occlusion and motion reasoning for long-term tracking. European Conference on Computer Vision, 2014. Springer, 172-187.

HUANG, C., LIAO, Z. & ZHAO, L. 2010a. Synergism of INS and PDR in self-contained pedestrian tracking with a miniature sensor module. *IEEE Sensors Journal,* 10**,** 1349-1359.

HUANG, H., GARTNER, G., SCHMIDT, M. & LI, Y. Smart environment for ubiquitous indoor navigation. International Conference on New Trends in Information and Service Science (NISS), 2009. IEEE, 176-180.

HUANG, Y., MEIJER, O. G., LIN, J., BRUIJN, S. M., WU, W., LIN, X., HU, H., HUANG, C., SHI, L. & VAN DIE N, J. H. 2010b. The effects of stride length and stride frequency on trunk coordination in human walking. *Gait and Posture,* 31**,** 444-449.

HUNG, T. N. & SUH, Y. S. 2013. Inertial sensor-based two feet motion tracking for gait analysis. *Sensors,* 13**,** 5614-5629.

HWANG, S., PARK, J., KIM, N., CHOI, Y. & SO KWEON, I. Multispectral pedestrian detection: Benchmark dataset and baseline. Proceedings of the IEEE Conference on Computer Vision and Pattern Recognition, 2015. 1037-1045.

ICC 2015. International Building Code. International Code Council (ICC).

INOUE, Y., SASHIMA, A., IKEDA, T. & KURUMATANI, K. Indoor emergency evacuation service on autonomous navigation system using mobile phone. Second International Symposium on Universal Communication (ISUC), 2008. IEEE, 79-85.

IVANENKO, Y., GRASSO, R. & LACQUANITI, F. 2000. Influence of leg muscle vibration on human walking. *Journal of Neurophysiology,* 84**,** 1737-1747.

JAIN, S. & MCLEAN, C. R. 2008. Components of an incident management simulation and gaming framework and related developments. *Simulation,* 84**,** 3-25.

JENSEN, C. S., LU, H. & YANG, B. Graph model based indoor tracking. Tenth International Conference on Mobile Data Management: Systems, Services and Middleware (MDM), 2009. IEEE, 122-131.

JEON, G.-Y., KIM, J.-Y., HONG, W.-H. & AUGENBROE, G. 2011. Evacuation performance of individuals in different visibility conditions. *Building and Environment,* 46**,** 1094-1103.

JEON, J.-S., KONG, Y., NAM, Y. & YIM, K. An indoor positioning system using bluetooth RSSI with an accelerometer and a barometer on a smartphone. 2015 10th International Conference on Broadband and Wireless Computing, Communication and Applications (BWCCA), 2015. IEEE, 528-531.

JIA, F., PATEL, M. K., GALEA, E. R., GRANDISON, A. & EWER, J. 2006. CFD fire simulation of the Swissair Flight 111 in-flight fire–Part II: fire spread analysis. *The Aeronautical Journal,* 110**,** 303-314.

JIANG, G., MA, F., SHANG, J. & CHAU, P. Y. 2014. Evolution of knowledge sharing behavior in social commerce: an agent-based computational approach. *Information Sciences,* 278**,** 250-266.

JIANG, L., HOE, L. N. & LOON, L. L. Integrated UWB and GPS location sensing system in hospital environment. 2010 5th IEEE Conference on Industrial Electronics and Applications, 2010. IEEE, 286-289.

JIANG, W. & YIN, Z. Combining passive visual cameras and active IMU sensors to track cooperative people. 18th International Conference on Information Fusion (FUSION), 2015. IEEE, 1338-1345.

JIANG, W. & YIN, Z. 2017. Combining passive visual cameras and active IMU sensors for persistent pedestrian tracking. *Journal of Visual Communication and Image Representation,* 48**,** 419-431.

JIANG, X., CHEN, N. Y., HONG, J. I., WANG, K., TAKAYAMA, L. & LANDAY, J. A. Siren: Context-aware computing for firefighting. International Conference on Pervasive Computing, 2004. Springer, 87-105.

JOHNSON, C. 2005. Lessons from the evacuation of the world trade centre, 9/11 2001 for the development of computer-based simulations. *Cognition, Technology & Work,* 7**,** 214-240.

JONES, C. M. & HEALY, S. D. 2006. Differences in cue use and spatial memory in men and women. *Proceedings of the Royal Society B: Biological Sciences,* 273**,** 2241-2247.

JOSH. 2010. *The 4 Stages of a Fire*. Journey to Firefighter. Available: http://journeytofirefighter.com/4-stages-of-a-fire/ [Accessed Feb, 15th 2017].

JU, M., ZHANG, D. & WANG, X. 2017. Single image dehazing via an improved atmospheric scattering model. *The Visual Computer,* 33**,** 1613-1625.

JUN, C. & KIM, H. 2009. An indoor crowd simulation using a 2D-3D hybrid data model. *Computational Science and Its Applications–ICCSA 2009***,** 397-412.

JUN, C., KIM, H. & KIM, G. 2009. Developing an indoor evacuation simulator using a hybrid 3D model. *3D Geo-Information Science.* 173-178.

KADY, R. A. & DAVIS, J. 2009a. The effect of occupant characteristics on crawling speed in evacuation. *Fire Safety Journal,* 44**,** 451-457.

KADY, R. A. & DAVIS, J. 2009b. The impact of exit route designs on evacuation time for crawling occupants. *Journal of Fire Sciences,* 27**,** 481-493.

KANG, W., NAM, S., HAN, Y. & LEE, S. Improved heading estimation for smartphone-based indoor positioning systems. 2012 IEEE 23rd International Symposium on Personal Indoor and Mobile Radio Communications (PIMRC), 2012. IEEE, 2449-2453.

KARAS, I. R., BATUK, F., AKAY, A. E. & BAZ, I. 2006. Automatically extracting 3D models and network analysis for indoors. *Innovations in 3D Geo*

Information Systems. 395-404.
KASEREKA, S., KASORO, N., KYAMAKYA, K., GOUFO, E.-F. D., CHOKKI, A. P. & YENGO, M. V. 2018. Agent-Based Modelling and Simulation for evacuation of people from a building in case of fire. *Procedia Computer Science,* 130**,** 10-17.
KENNEY, W. L., DEGROOT, D. W. & HOLOWATZ, L. A. 2004. Extremes of human heat tolerance: life at the precipice of thermoregulatory failure. *Journal of Thermal Biology,* 29**,** 479-485.
KHAN, A. M., LEE, Y.-K., LEE, S. & KIM, T.-S. 2010. Accelerometer's position independent physical activity recognition system for long-term activity monitoring in the elderly. *Medical & biological engineering & computing,* 48**,** 1271-1279.
KIM, S.-S., KIM, J.-W. & HAN, D.-S. Floor detection using a barometer sensor in a smartphone. 2017 International Conference on Indoor Positioning and Indoor Navigation (IPIN), 2017. IEEE.
KINATEDER, M. T., KULIGOWSKI, E. D., RENEKE, P. A. & PEACOCK, R. D. 2014. A review of risk perception in building fire evacuation, National Institute of Standards and Technology (NIST).
KJÆRGAARD, M. B., BLUNCK, H., GODSK, T., TOFTKJ R, T., CHRISTENSEN, D. L. & GR NB K, K. Indoor positioning using GPS revisited. International Conference on Pervasive Computing, 2010. Springer, 38-56.
KLANN, M. 2009. Tactical navigation support for firefighters: The LifeNet ad-hoc sensor-network and wearable system. International Workshop on Mobile Information Technology for Emergency Response, 2009. Springer, 41-56.
KLEPEIS, N. E., NELSON, W. C., OTT, W. R., ROBINSON, J. P., TSANG, A. M., SWITZER, P., BEHAR, J. V., HERN, S. C. & ENGELMANN, W. H. 2001. The national human activity pattern survey (NHAPS): a resource for assessing exposure to environmental pollutants. *Journal of Exposure Science and Environmental Epidemiology,* 11**,** 231.
KLUGER, D., MAJOR, M. J., FATONE, S. & GARD, S. A. 2014. The effect of trunk flexion on lower-limb kinetics of able-bodied gait. *Human Movement Science,* 33**,** 395-403.
KOBES, M. 2005. Een bouwkundig perspectief op evacuatie uit gebouwen [An architectural perspective on building evacuation]. *In:* VAN DEN BRAND, R.,

DUYVIS, M. & KOBES, M. (eds.) *Zelfredzaamheid en fysieke veiligheid van burgers: verkenningen [Resillience and physical safety of citizens: explorations].* Nibra, Arnhem: Nibra Publicatiereeks.

KOBES, M. 2008. *Zelfredzaamheid bij brand: Kritische factoren voor het veilig vluchten uit gebouwen [Fire response performance: the critical factors for a safe escape out of buildings].* Den Haag,The Netherlands, Boom Juridische Uitgevers.

KOBES, M., HELSLOOT, I., DE VRIES, B. & POST, J. G. 2010a. Building safety and human behaviour in fire: A literature review. *Fire Safety Journal,* 45**,** 1-11.

KOBES, M., HELSLOOT, I., DE VRIES, B., POST, J. G., OBERIJ , N. & GROENEWEGEN, K. 2010b. Way-finding during fire evacuation: an analysis of unannounced fire drills in a hotel at night. *Building and Environment,* 45**,** 537-548.

KOLBE, T. H. 2009. Representing and exchanging 3D city models with CityGML. *3D Geo-Information Sciences.* 15-31.

KONIG, D., ADAM, M., JARVERS, C., LAYHER, G., NEUMANN, H. & TEUTSCH, M. Fully convolutional region proposal networks for multispectral person detection. Proceedings of the IEEE Conference on Computer Vision and Pattern Recognition Workshops, 2017. 49-56.

KOO, J., KIM, Y. S. & KIM, B.-I. 2012. Estimating the impact of residents with disabilities on the evacuation in a high-rise building: A simulation study. *Simulation Modelling Practice and Theory,* 24**,** 71-83.

KOTHARI, N., KANNAN, B., GLASGWOW, E. D. & DIAS, M. B. 2012. Robust indoor localization on a commercial smart phone. *Procedia Computer Science,* 10**,** 1114-1120.

KOUROGI, M., SAKATA, N., OKUMA, T. & KURATA, T. 2006. Indoor/outdoor pedestrian navigation with an embedded GPS/RFID/self-contained sensor system. *Advances in Artificial Reality and Tele-Existence.* 1310-1321.

KRIZHEVSKY, A., SUTSKEVER, I. & HINTON, G. E. 2012. Imagenet classification with deep convolutional neural networks. *Advances in Neural Information Processing Systems*, 1097-1105.

KULIGOWSKI, E. D. 2009. The process of human behavior in fires, US Department of Commerce, National Institute of Standards and Technology

(NIST).

KULIGOWSKI, E. D. 2016. Human behavior in fire. *SFPE Handbook of Fire Protection Engineering.* Springer.

KULIGOWSKI, E. D., PEACOCK, R. D. & HOSKINS, B. L. 2005. *A review of building evacuation models*, Gaithersburg, MD: US Department of Commerce, National Institute of Standards and Technology (NIST).

KULIGOWSKI, E. D., PEACOCK, R. D. & HOSKINS, B. L. 2010. *A review of building evacuation models, 2nd Edition,* Washington, US Department of Commerce, National Institute of Standards and Technology (NIST) Technical Note 1680.

KWAN, M.-P. & LEE, J. 2005. Emergency response after 9/11: the potential of real-time 3D GIS for quick emergency response in micro-spatial environments. *Computers, Environment and Urban Systems,* 29**,** 93-113.

LAMARCA, A., CHAWATHE, Y., CONSOLVO, S., HIGHTOWER, J., SMITH, I., SCOTT, J., SOHN, T., HOWARD, J., HUGHES, J. & POTTER, F. Place lab: Device positioning using radio beacons in the wild. International Conference on Pervasive Computing, 2005. Springer, 116-133.

LAZEBNIK, S., SCHMID, C. & PONCE, J. Beyond bags of features: Spatial pyramid matching for recognizing natural scene categories. IEEE Computer Society Conference on Computer Vision and Pattern Recognition, 2006. IEEE, 2169-2178.

LEE, J. A 3D data model for representing topological relations of urban features. Proceedings of the 21st Annual ESRI International User Conference, San Diego, CA, USA, 2001.

LEE, J. 3D GIS for geo-coding human activity in micro-scale urban environments. International Conference on Geographic Information Science, 2004a. Springer, 162-178.

LEE, J. 2004b. A spatial access-oriented implementation of a 3-D GIS topological data model for urban entities. *GeoInformatica,* 8**,** 237-264.

LEE, J. 2007. A three-dimensional navigable data model to support emergency response in microspatial built-environments. *Annals of the Association of American Geographers,* 97**,** 512-529.

LEE, J. & ZLATANOVA, S. 2008. A 3D data model and topological analyses for emergency response in urban areas. *Geospatial Information Technology* *for Emergency Response.* 143-165.

LEE, R. Y. & CARLISLE, A. J. 2011. Detection of falls using accelerometers and mobile phone technology. *Age and Ageing,* 40**,** 690-696.

LEYKIN, A., RAN, Y. & HAMMOUD, R. Thermal-visible video fusion for moving target tracking and pedestrian classification. 2007 IEEE Conference on Computer Vision and Pattern Recognition, 2007. IEEE, 1-8.

LI, B., HARVEY, B. & GALLAGHER, T. Using barometers to determine the height for indoor positioning. 2013 International Conference on Indoor Positioning and Indoor Navigation (IPIN), 2013a. IEEE, 1-7.

LI, B., PENG, X., WANG, Z., XU, J. & FENG, D. Aod-net: All-in-one dehazing network. Proceedings of the IEEE International Conference on Computer Vision, 2017. 4770-4778.

LI, M., KIM, B. H. & MOURIKIS, A. I. Real-time motion tracking on a cellphone using inertial sensing and a rolling-shutter camera. 2013 IEEE International Conference on Robotics and Automation (ICRA), 2013b. IEEE, 4712-4719.

LI, N., BECERIK-GERBER, B., KRISHNAMACHARI, B. & SOIBELMAN, L. 2014. A BIM centered indoor localization algorithm to support building fire emergency response operations. *Automation in Construction,* 42**,** 78-89.

LIN, P. C., LU, J. C., TSAI, C. H. & HO, C. W. 2012. Design and implementation of a nine-axis inertial measurement unit. *IEEE/ASME Transactions on Mechatronics,* 17**,** 657-668.

LIN, Q., JI, Q. & GONG, S. A crowd evacuation system in emergency situation based on dynamics model. International Conference on Virtual Systems and Multimedia, 2006. Springer, 269-280.

LIN, T., LI, L. & LACHAPELLE, G. Multiple sensors integration for pedestrian indoor navigation. 2015 International Conference on Indoor Positioning and Indoor Navigation (IPIN), 2015. IEEE, 1-9.

LINK, J. A. B., SMITH, P., VIOL, N. & WEHRLE, K. FootPath: Accurate map-based indoor navigation using smartphones. International Conference on Indoor Positioning and Indoor Navigation (IPIN), 2011. Citeseer, 1-8.

LIU, H., DARABI, H., BANERJEE, P. & LIU, J. 2007. Survey of wireless indoor positioning techniques and systems. *IEEE Transactions on Systems, Man, and Cybernetics, Part C (Applications and Reviews),* 37**,** 1067-1080.

LIU, J., CHEN, R., CHEN, Y., PEI, L. & CHEN, L. 2012a. iParking: An intelligent indoor location-based smartphone parking service. *Sensors,* 12**,** 14612-14629.

LIU, J., CHEN, R., PEI, L., GUINNESS, R. & KUUSNIEMI, H. 2012b. A hybrid smartphone indoor positioning solution for mobile LBS. *Sensors,* 12**,** 17208-17233.

LIU, J., ZHANG, S., WANG, S. & METAXAS, D. N. Multispectral deep neural networks for pedestrian detection. British Machine Vision Conference. 2016.

LIU, T., CARLBERG, M., CHEN, G., CHEN, J., KUA, J. & ZAKHOR, A. Indoor localization and visualization using a human-operated backpack system. 2010 International Conference on Indoor Positioning and Indoor Navigation (IPIN) 2010. IEEE, 1-10.

LONG, J., SHELHAMER, E. & DARRELL, T. Fully convolutional networks for semantic segmentation. Proceedings of the IEEE Conference on Computer Vision and Pattern Recognition, 2015. 3431-3440.

LORD, J., MEACHAM, B., MOORE, A., FAHY, R. & PROULX, G. 2005. Guide for evaluating the predictive capabilities of computer egress models. *NIST GCR 06-886*.

MAGHDID, H. S., LAMI, I. A., GHAFOOR, K. Z. & LLORET, J. 2016. Seamless outdoors-indoors localization solutions on smartphones: implementation and challenges. *ACM Computing Surveys (CSUR),* 48**,** 53.

MAHMOOD, I., HARIS, M. & SARJOUGHIAN, H. Analyzing emergency evacuation strategies for mass gatherings using crowd simulation and analysis framework: Hajj scenario. Proceedings of the 2017 ACM SIGSIM Conference on Principles of Advanced Discrete Simulation, 2017. ACM, 231-240.

MANLEY, M. & KIM, Y. S. 2012. Exitus: Agent-based evacuation simulation for individuals with disabilities in a densely populated sports arena. *International Journal of Intelligent Information Technologies (IJIIT),* 8**,** 1-13.

MARTIN, E., LIU, L., COVINGTON, M., PESTI, P. & WEBER, M. 2010. Positioning Technologies in Location-Based Services. *Location-Based Services Handbook: Applications, Technologies, and Security.* CRC Press.

MASON, S. J., LEGGE, G. E. & KALLIE, C. S. 2005. Variability in the length and frequency of steps of sighted and visually impaired walkers. *Journal of Visual Impairment and Blindness,* 99, 741-754.

MASSAGUER, D., BALASUBRAMANIAN, V., MEHROTRA, S. & VENKATASUBRAMANIAN, N. Synthetic humans in emergency response drills. Proceedings of the Fifth International Joint Conference on Autonomous Agents and Multiagent Systems, 2006. ACM, 1469-1470.

MAUTZ, R. & TILCH, S. Survey of optical indoor positioning systems. 2011 International Conference on Indoor Positioning and Indoor Navigation (IPIN), 2011. IEEE, 1-7.

MAWSON, A. R. 2005. Understanding mass panic and other collective responses to threat and disaster. *Psychiatry: Interpersonal and biological processes,* 68, 95-113.

MEIJERS, M., ZLATANOVA, S. & PFEIFER, N. 3D geoinformation indoors: structuring for evacuation. Proceedings of Next generation 3D city models, 2005. 21-22.

MENG, X., ZHANG, Z.-Q., WU, J.-K., WONG, W.-C. & YU, H. 2014. Self-contained pedestrian tracking during normal walking using an inertial/magnetic sensor module. *IEEE Transactions on Biomedical Engineering,* 61, 892-899.

MILLER, H. J. & SHAW, S.-L. 2001. *Geographic information systems for transportation: principles and applications*, Oxford University Press.

MIRABI, M. & JAVADI, S. People tracking in outdoor environment using Kalman filter. 2012 Third International Conference on Intelligent Systems Modelling and Simulation, 2012. IEEE, 303-307.

MISRA, P. & ENGE, P. 2006. Global Positioning System: *Signals, Measurements and Performance, Second Edition.* Massachusetts, Ganga-Jamuna Press.

MOESLUND, T. B., HILTON, A. & KR GER, V. 2006. A survey of advances in vision-based human motion capture and analysis. *Computer Vision and Image Understanding,* 104, 90-126.

MOHAN, M., SRIDHAR, P. & SRINATH, S. 2016. SMART Evacuation System. *International Journal for Research in Applied Science & Engineering Technology (IJRASET),* 4, 681-685.

MORRISSEY, S., GEORGE, C. & AYOUB, M. 1985. Metabolic costs of stoopwalking and crawling. *Applied Ergonomics,* 16, 99-102.

MORRISSEY, S. J. 1980. *A simulation of selected low coal mining tasks.* Texas Tech University.

MOURIKIS, A. I. & ROUMELIOTIS, S. I. A multi-state constraint Kalman filter for vision-aided inertial navigation. 2007 IEEE International Conference on Robotics and Automation, 10-14 April 2007 Roma, Italy. 3565-3572.

MUHDI, R., DAVIS, J. & BLACKBURN, T. Improving occupant characteristics in performance-based evacuation modeling. Proceedings of the Human Factors and Ergonomics Society Annual Meeting, 2006 Los Angeles, CA. Sage Publications, 1199-1203.

MUNOZ-SALINAS, R., MEDINA-CARNICER, R., MADRID-CUEVAS, F. J. & CARMONA-POYATO, A. 2009. Multi-camera people tracking using evidential filters. *International Journal of Approximate Reasoning,* 50**,** 732-749.

MURALIDHARAN, K., KHAN, A. J., MISRA, A., BALAN, R. K. & AGARWAL, S. Barometric phone sensors: More hype than hope! Proceedings of the 15th Workshop on Mobile Computing Systems and Applications, 2014. ACM, 1-6.

MUSLIMAN, I. A., RAHMAN, A. A. & COORS, V. 2008. Implementing 3D network analysis in 3D-GIS. *International archives of ISPRS,* 37.

NAGAI, R., FUKAMACHI, M. & NAGATANI, T. 2006. Evacuation of crawlers and walkers from corridor through an exit. *Physica A: Statistical Mechanics and its Applications,* 367**,** 449-460.

NFPA 2010. NFPA 72: national fire alarm and signaling code. National Fire Protection Association (NFPA).

NFPA & COTÉ, R. 2015. Life Safety Code Handbook: With the Complete Text of the 2015 Edition of NFPA 101, Life Safety Code. Quincy, Mass.: National Fire Protection Association (NFPA).

NIU, L. A survey of wireless indoor positioning technology for fire emergency routing. IOP Conference Series: Earth and Environmental Science, 2014. IOP Publishing, 1-6.

NIU, L. & SONG, Y. 2016. A simulation model fusing space and agent for indoor dynamic fire evacuation analysis. *Simulation,* 92**,** 215-232.

NIU, X., LI, Y., ZHANG, H., WANG, Q. & BAN, Y. 2013. Fast thermal calibration of low-grade inertial sensors and inertial measurement units. *Sensors,* 13**,**

12192-12217.
O CONNOR, D. J. 2005. Integrating Human Behavior Factors Into Design An examination of behaviors that increase or reduce harm from fires. *Fire Protection Engineering,* 28**,** 8.
OFSTAD, A., NICHOLAS, E., SZCODRONSKI, R. & CHOUDHURY, R. R. Aampl: Accelerometer augmented mobile phone localization. Proceedings of the first ACM international workshop on Mobile entity localization and tracking in GPS-less environments, 2008. ACM, 13-18.
OKAYA, M. & TAKAHASHI, T. Human relationship modeling in agent-based crowd evacuation simulation. International Conference on Principles and Practice of Multi-Agent Systems, 2011. Springer, 496-507.
OOMES, E. 2006. Mobiliteit [Mobility]. Article in*:'Ome Ed' ,* December 2006*.*
OPASANON, S. & MILLER-HOOKS, E. 2009. The safest escape problem. *Journal of the Operational Research Society,* 60**,** 1749-1758.
ORENDURFF, M. S., SEGAL, A. D., KLUTE, G. K., BERGE, J. S., ROHR, E. S. & KADEL, N. J. 2004. The effect of walking speed on center of mass displacement. *Journal of Rehabilitation Research & Development,* 41.
ORTAKCI, Y., KARAS, I. R., ATILA, U. & DEMIRAL, E. 2016. Intelligent mobile indoor navigation system for fire evacuation based on artificial neural network. *International Journal of Computer Science and Information Security,* 14**,** 980.
OSHA. 2015. *Occupational Safety and Health Administration (OSHA) – Elaws – Employment laws assistance for workers and small businesses* [Online]. Available: https://webapps.dol.gov/elaws/osha/lead/glossary.asp.
OTSASON, V., VARSHAVSKY, A., LAMARCA, A. & DE LARA, E. Accurate GSM indoor localization. International Conference on Ubiquitous Computing, 2005. Springer, 141-158.
PAI, C.-J., TYAN, H.-R., LIANG, Y.-M., LIAO, H.-Y. M. & CHEN, S.-W. 2004. Pedestrian detection and tracking at crossroads. *Pattern Recognition,* 37**,** 1025-1034.
PAN, X., HAN, C. S., DAUBER, K. & LAW, K. H. 2006. Human and social behavior in computational modeling and analysis of egress. *Automation in Construction,* 15, 448-461.
PAN, X., HAN, C. S., DAUBER, K. & LAW, K. H. 2007. A multi-agent based

framework for the simulation of human and social behaviors during emergency evacuations. *AI & Society,* 22, 113-132.

PANAHANDEH, G. & JANSSON, M. 2014. Vision-aided inertial navigation based on ground plane feature detection. *IEEE/ASME Transactions on Mechatronics,* 19, 1206-1215.

PANNURAT, N., THIEMJARUS, S. & NANTAJEEWARAWAT, E. 2014. Automatic fall monitoring: a review. *Sensors,* 14, 12900-12936.

PARISI, D. R. & DORSO, C. O. 2007. Morphological and dynamical aspects of the room evacuation process. *Physica A: Statistical Mechanics and Its Applications,* 385, 343-355.

PARK, I., KIM, H. & JUN, C. 2D-3D Hybrid Data Modeling for Fire Evacuation Simulation. ESRI User Conference, 2007.

PARNIAN, N. & GOLNARAGHI, F. 2010. Integration of a multi-camera vision system and strapdown inertial navigation system (SDINS) with a modified Kalman filter. *Sensors,* 10, 5378-5394.

PELECHANO, N., ALLBECK, J. M. & BADLER, N. I. Controlling individual agents in high-density crowd simulation. Proceedings of the 2007 ACM SIGGRAPH/Eurographics Symposium on Computer Animation, 2007. Eurographics Association, 99-108.

PELECHANO, N. & BADLER, N. I. 2006. Modeling crowd and trained leader behavior during building evacuation. *IEEE Computer Graphics and Applications,* 26, 80-86.

PELECHANO, N. & MALKAWI, A. 2008. Evacuation simulation models: Challenges in modeling high rise building evacuation with cellular automata approaches. *Automation in Construction,* 17, 377-385.

PEREZ, P., BANOS, A. & PETTIT, C. Agent-based modelling for urban planning current limitations and future trends. Agent Based Modelling of Urban Systems, 2017 Cham, Switzerland. Springer 60-69.

PETRUSHIN, V. A., WEI, G. & GERSHMAN, A. V. 2006. Multiple-camera people localization in an indoor environment. *Knowledge and Information Systems,* 10, 229-241.

PICASCIA, S. & YORKESMITH, N. Towards an agent-based simulation of housing in urban beirut. International Workshop on Agent Based Modelling of Urban Systems, 2016. Springer International Publishing.

PINCHIN, J., HIDE, C. & MOORE, T. A particle filter approach to indoor navigation using a foot mounted inertial navigation system and heuristic heading information. 2012 International Conference on Indoor Positioning and Indoor Navigation (IPIN), 2012a. IEEE, 1-10.

PINCHIN, J., HIDE, C. & MOORE, T. The use of high sensitivity gps for initialisation of a foot mounted inertial navigation system. 2012 IEEE/ION Position Location and Navigation Symposium (PLANS), 2012b. IEEE, 998-1007.

PIRES, T. T. 2005. An approach for modeling human cognitive behavior in evacuation models. *Fire Safety Journal,* 40**,** 177-189.

PISCATAWAY, N. Multi-camera multi-person tracking for Easy Living. 3rd IEEE Int'l Workshop on Visual Surveillance, 2000. 3-10.

PLUCHINO, S., TRIBULATO, C. M. G., CAVERZAN, A., MC QUILLAN, A., CIMELLARO, G. P. & MAHIN, S. Agent-based model for pedestrians' evacuation after a blast integrated with a human behavior model. Proceedings of the 2015 Structures Congress, 2015. American Society of Civil Engineers (ASCE), 1506-1517.

POLING, B. E., PRAUSNITZ, J. M. & O'CONNELL, J. P. 2001. *The properties of gases and liquids (Fifth Edition)*, New York, Mcgraw-hill.

PROULX, G. Occupant behaviour and evacuation. Proceedings of the 9th International Fire Protection Symposium, 2001. 219-232.

PROULX, G. 2002. Cool under fire. *Fire Protection Engineering***,** 33-35.

PROULX, G. 2008. Movement of people: The evacuation timing. *In:* DINENNO, P. J. (ed.) *SFPE Handbook of Fire Protection Engineering, 4th Edition.* Quincy: National Fire Protection Association (NFPA).

PROULX, G., TILLER, D., KYLE, B. & CREAK, J. 1999. Assessment of photoluminescent material during office occupant evacuation. *Internal Report.* Canada: Institute for Research in Construction, National Research Council.

PU, S. & ZLATANOVA, S. 2005. Evacuation route calculation of inner buildings. *Geo-Information for Disaster Management.* 1143-1161.

PURSER, D. A. & BENSILUM, M. 2001. Quantification of behaviour for engineering design standards and escape time calculations. *Safety Science,* 38**,** 157-182.

RÜETSCHI, U.-J. & TIMPF, S. Modelling wayfinding in public transport: Network space and scene space. International Conference on Spatial Cognition, 2004a. Springer, 24-41.

RÜETSCHI, U.-J. & TIMPF, S. 2004b. Schematic geometry of public transport spaces for wayfinding. *Geoinformation und Mobilität,* 40**,** 191-203.

RACKO, J., BRIDA, P., PERTTULA, A., PARVIAINEN, J. & COLLIN, J. Pedestrian dead reckoning with particle filter for handheld smartphone. 2016 International Conference on Indoor Positioning and Indoor Navigation (IPIN), 2016. IEEE, 1-7.

RAJAGOPAL, S. 2008. *Personal dead reckoning system with shoe mounted inertial sensors.* Master's Degree Project, Royal Institute of Technology (KTH).

RAMANANDAN, A., CHEN, A. & FARRELL, J. A. 2012. Inertial navigation aiding by stationary updates. *IEEE Trans. Intelligent Transportation Systems,* 13**,** 235-248.

RAMIREZ, L., DENEF, S. & DYRKS, T. Towards human-centered support for indoor navigation. Proceedings of the SIGCHI Conference on Human Factors in Computing Systems, 2009.1279-1282.

RANTAKOKKO, J., H NDEL, P., EKL F, F., BOBERG, B., JUNERED, M., AKOS, D., SKOG, I., BOHLIN, H., NEREG RD, F. & HOFFMANN, F. 2007. Positioning of emergency personnel in rescue operations. *Technical Report TRITA-EE 2007.* Stockholm, Sweden: Royal Institute of Technology.

RANTAKOKKO, J., H NDEL, P., FREDHOLM, M. & MARSTEN-EKL F, F. User requirements for localization and tracking technology: A survey of mission-specific needs and constraints. 2010 International Conference on Indoor Positioning and Indoor Navigation (IPIN), 2010. IEEE, 1-9.

RAUBAL, M. & EGENHOFER, M. J. 1998. Comparing the complexity of wayfinding tasks in built environments. *Environment and Planning B: Planning and Design,* 25**,** 895-913.

REHRL, K., G LL, N., LEITINGER, S. & BRUNTSCH, S. Combined indoor/outdoor Smartphone navigation for public transport travellers, Proceedings of the 3rd Symposium on Location Based Services & Telecartography, 2005 Vienna, Austria. 235-239..

REN, S., HE, K., GIRSHICK, R. & SUN, J. Faster R-CNN: Towards real-time object detection with region proposal networks. Advances in Neural Information Processing Systems, 2015. 91-99.

REN, W., LIU, S., ZHANG, H., PAN, J., CAO, X. & YANG, M.-H. Single image dehazing via multi-scale convolutional neural networks. European conference on Computer Vision, 2016. Springer, 154-169.

RETSCHER, G. & THIENELT, M. 2004. NAVIO–a navigation and guidance service for pedestrians. *Journal of Global Positioning Systems,* 1, 208-217.

RONCHI, E. & NILSSON, D. 2013. Fire evacuation in high-rise buildings: a review of human behaviour and modelling research. *Fire Science Reviews,* 2, 1-21.

ROY, A., CHATTOPADHYAY, P., SURAL, S., MUKHERJEE, J. & RIGOLL, G. 2015. Modelling, synthesis and characterisation of occlusion in videos. *IET Computer Vision,* 9, 821-830.

SABATINI, A. M. & GENOVESE, V. 2014. A sensor fusion method for tracking vertical velocity and height based on inertial and barometric altimeter measurements. *Sensors,* 14, 13324-13347.

SADDA, P., AZIMI, E., JALLO, G., DOSWELL, J. & KAZANZIDES, P. 2013. Surgical navigation with a head-mounted tracking system and display. *Studies in Health Technology and Informatics.* IOS Press.

SAGAWA, K., INOOKA, H. & SATOH, Y. Non-restricted measurement of walking distance. 2000 IEEE International Conference on Systems, Man, and Cybernetics, 2000. IEEE, 1847-1852.

SALOMA, C., PEREZ, G. J., TAPANG, G., LIM, M. & PALMES-SALOMA, C. 2003. Self-organized queuing and scale-free behavior in real escape panic. *Proceedings of the National Academy of Sciences,* 100, 11947-11952.

SAMUEL, K. 2004. *Beyond beta: other continuous families of distributions with bounded support and applications*, World Scientific.

SANTOS, G. & AGUIRRE, B. E. A critical review of emergency evacuation simulation models. Proceedings of Building Occupant Movement during Fire Emergencies, 2004 Gaithersburg, Maryland.

SARSHAR, P., RADIANTI, J. & GONZALEZ, J. J. Modeling panic in ship fire evacuation using dynamic Bayesian network. Third International Conference on Innovative Computing Technology (INTECH), 2013. IEEE, 301-307.

SASHIMA, A., INOUE, Y. & KURUMATANI, K. Spatio-temporal sensor data management for context-aware services: designing sensor-event driven service coordination middleware. Proceedings of the 1st international workshop on Advanced data processing in ubiquitous computing (ADPUC 2006), 2006. ACM, 4.

SCHOLZ, M., RIEDEL, T. & DECKER, C. A flexible architecture for a robust indoor navigation support device for firefighters. Seventh International Conference on Networked Sensing Systems (INSS), 2010. IEEE, 227-232.

SCHUT, M. C. 2010. On model design for simulation of collective intelligence. *Information Sciences,* 180**,** 132-155.

SERMANET, P., EIGEN, D., ZHANG, X., MATHIEU, M., FERGUS, R. & LECUN, Y. Overfeat: Integrated recognition, localization and detection using convolutional networks. International Conference on Learning Representations, 2013a Banff, Canada..

SERMANET, P., KAVUKCUOGLU, K., CHINTALA, S. & LECUN, Y. Pedestrian detection with unsupervised multi-stage feature learning. Proceedings of the IEEE Conference on Computer Vision and Pattern Recognition, 2013b. 3626-3633.

SEYFRIED, A., STEFFEN, B., KLINGSCH, W. & BOLTES, M. 2005. The fundamental diagram of pedestrian movement revisited. *Journal of Statistical Mechanics: Theory and Experiment,* 2005, 10002-10014.

SHA, K., SHI, W. & WATKINS, O. Using wireless sensor networks for fire rescue applications: Requirements and challenges. 2006 IEEE International Conference on Electro/Information Technology, 2006. IEEE, 239-244.

SHAHHOSEINI, Z., SARVI, M. & SABERI, M. 2018. Pedestrian crowd dynamics in merging sections: Revisiting the “faster-is-slower” phenomenon. *Physica A: Statistical Mechanics and its Applications,* 491**,** 101-111.

SHEN, J.-Q., WANG, X.-W. & JIANG, L.-L. 2018. The influence of panic on the efficiency of escape. *Physica A: Statistical Mechanics and its Applications,* 491**,** 613-618.

SHEN, X., CHEN, Y., ZHANG, J., WANG, L., DAI, G. & HE, T. BarFi: Barometer-aided Wi-Fi floor localization using crowdsourcing. IEEE 12th International Conference on Mobile Ad Hoc and Sensor Systems, Oct, 19-22 2015. 416-424.

SHEN, X., XU, K., SUN, X., WU, J. & LIN, J. Optimized indoor wireless propagation model in WiFi-RoF network architecture for RSS-based localization in the Internet of Things. 2011 International Topical Meeting on Asia-Pacific Microwave Photonics & Microwave Photonics Conference (MWP/APMP), 2011. IEEE, 274-277.

SHI, D.-M. & WANG, B.-H. 2013. Evacuation of pedestrians from a single room by using snowdrift game theories. *Physical Review E,* 87**,** 22802.

SHI, J., REN, A. & CHEN, C. 2009a. Agent-based evacuation model of large public buildings under fire conditions. *Automation in Construction,* 18**,** 338-347.

SHI, L., XIE, Q., CHENG, X., CHEN, L., ZHOU, Y. & ZHANG, R. 2009b. Developing a database for emergency evacuation model. *Building and Environment,* 44**,** 1724-1729.

SHIN, B., LEE, S., KIM, C., KIM, J., LEE, T., KEE, C., HEO, S. & RHEE, H. Implementation and performance analysis of smartphone-based 3D PDR system with hybrid motion and heading classifier. 2014 IEEE/ION Position, Location and Navigation Symposium-PLANS, 2014. IEEE, 201-204.

SHIWAKOTI, N. & SARVI, M. 2013. Understanding pedestrian crowd panic: a review on model organisms approach. *Journal of Transport Geography,* 26**,** 12-17.

SILLEM, S. 2005. Een psychologisch perspectief op evacuatie uit gebouwen. *In:* VAN DEN BRAND, R., DUYVIS, M. & KOBES, M. (eds.) *Zelfredzaamheid en fysieke veiligheid van burgers: verkenningen [A psychological perspective on building evacuation, in:Resillience and physical safety of citizens:explorations].* Nibra, Arnhem: Nibra Publicatiereeks.

SIME, J. 1999. An occupant response shelter escape time (ORSET), model: research and practice. *Fire and Explosions: Recent Advances in Modelling and Analysis, London, Bury St. Edmunds*, Professional Engineering Publishing Ltd., 23-33.

SIME, J. D. 2001. An occupant response shelter escape time (ORSET) model. *Safety Science,* 38**,** 109-125.

SIVIC, J. & ZISSERMAN, A. Video Google: A text retrieval approach to object matching in videos. Proceedings Ninth IEEE International Conference on Computer Vision, 2003. IEEE, 1470-1477.

SKOG, I., HANDEL, P., NILSSON, J. O. & RANTAKOKKO, J. 2010. Zero-Velocity Detection—An Algorithm Evaluation. *IEEE Transactions on Bio-Medical Engineering,* 57**,** 2657-2666.

SONG, X., SENEVIRATNE, L. D. & ALTHOEFER, K. 2011. A Kalman filter-integrated optical flow method for velocity sensing of mobile robots. *IEEE/ASME Transactions on Mechatronics,* 16**,** 551-563.

SORIA, S. A., JOSENS, R. & PARISI, D. R. 2012. Experimental evidence of the "Faster is Slower" effect in the evacuation of ants. *Safety Science,* 50**,** 1584-1588.

SPEARPOINT, M. & XIANG, X. 2011. Calculating evacuation times from lecture theatre type rooms using a network model. *Fire Safety Science,* 10**,** 599-612.

STEINHOFF, U. & SCHIELE, B. Dead reckoning from the pocket-an experimental study. IEEE International Conference on Pervasive Computing and Communications (PerCom), 2010. IEEE, 162-170.

SU REZ, P. L., SAPPA, A. D., VINTIMILLA, B. X. & HAMMOUD, R. I. Deep learning based single image dehazing. Proceedings of the IEEE Conference on Computer Vision and Pattern Recognition Workshops, 2018. 1169-1176.

SUCERQUIA, A., L PEZ, J. & VARGAS-BONILLA, J. 2018. Real-life/real-time elderly fall detection with a triaxial accelerometer. *Sensors,* 18**,** 1101.

SUN, Y., ZHAO, Y. & SCHILLER, J. An autonomic indoor positioning application based on smartphone. IEEE Wireless Communications and Networking Conference (WCNC), 2014. IEEE, 3326-3331.

SUZUNO, K., TOMOEDA, A. & UEYAMA, D. 2013. Analytical investigation of the faster-is-slower effect with a simplified phenomenological model. *Physical Review E,* 88**,** 052813.

SZEGEDY, C., LIU, W., JIA, Y., SERMANET, P., REED, S., ANGUELOV, D., ERHAN, D., VANHOUCKE, V. & RABINOVICH, A. Going deeper with convolutions. IEEE Conference on Computer Vision and Pattern Recognition (CVPR), 2015. IEEE, 1-9.

SZWEDKO, J., SHAW, C., G. CONNOR, A., LABRINIDIS, A. & CHRYSANTHIS, P. Demonstrating an evacuation algorithm with mobile devices using an e-scavenger hunt game. Eighth ACM International Workshop on Data

Engineering for Wireless and Mobile Access, 2009 Rhode Island, USA. 49-52.

TAN, L., HU, M. & LIN, H. 2015. Agent-based simulation of building evacuation: Combining human behavior with predictable spatial accessibility in a fire emergency. *Information Sciences,* 295**,** 53-66.

TANG, F. & REN, A. 2008. Agent-based evacuation model incorporating fire scene and building geometry. *Tsinghua Science and Technology,* 13**,** 708-714.

TANG, F. & REN, A. 2012. GIS-based 3D evacuation simulation for indoor fire. *Building and Environment,* 49**,** 193-202.

TANIGAWA, M., LUINGE, H., SCHIPPER, L. & SLYCKE, P. Drift-free dynamic height sensor using MEMS IMU aided by MEMS pressure sensor. 5th Workshop on Positioning, Navigation and Communication, 2008. IEEE, 191-196.

TARDIF, J. P., GEORGE, M., LAVERNE, M. & KELLY, A. A new approach to vision-aided inertial navigation. IEEE/RSJ International Conference on Intelligent Robots and Systems, 2010. 4161-4168.

THOMPSON, K. 2016. Fire Dynamics. *Pain,* 3**,** 5.

TIAN, Q., SALCIC, Z., KEVIN, I., WANG, K. & PAN, Y. An enhanced pedestrian dead reckoning approach for pedestrian tracking using smartphones. 2015 IEEE Tenth International Conference on Intelligent Sensors, Sensor Networks and Information Processing (ISSNIP), 2015. IEEE, 1-6.

TING, S., KWOK, S. K., TSANG, A. H. & HO, G. T. 2011. The study on using passive RFID tags for indoor positioning. *International Journal of Engineering Business Management,* 3**,** 8.

TORRES-SOLIS, J., FALK, T. H. & CHAU, T. 2010. A review of indoor localization technologies: towards navigational assistance for topographical disorientation, *Ambient Intelligence.* INTECH Open Access Publisher.

TORRES-SOSPEDRA, J., JIM NEZ, A. R., KNAUTH, S., MOREIRA, A., BEER, Y., FETZER, T., TA, V.-C., MONTOLIU, R., SECO, F. & MENDOZA-SILVA, G. M. 2017. The smartphone-based offline indoor location competition at IPIN 2016: Analysis and future work. *Sensors,* 17**,** 557.

TRIVEDI, A. & RAO, S. 2018. Agent-based modeling of emergency evacuations considering human panic behavior. *IEEE Transactions on Computational*

Social Systems, 5, 277-288.

TSAI, T.-H., CHANG, C.-H. & CHEN, S.-W. Vision based indoor positioning for intelligent buildings. 2016 2nd International Conference on Intelligent Green Building and Smart Grid (IGBSG), 2016. IEEE, 1-4.

UEHARA, S. & TOMOMATSU, K. 2003. Evacuation Simulation System Considering Evacuee Profiles and Spatial Characteristics. *Fire Safety Science,* 7, 963-974.

UIJLINGS, J. R., VAN DE SANDE, K. E., GEVERS, T. & SMEULDERS, A. W. 2013. Selective search for object recognition. *International Journal of Computer Vision,* 104, 154-171.

VAN DIGGELEN, F. & ABRAHAM, C. 2001. Indoor GPS technology. *CTIA Wireless-Agenda,* Dallas.

VANCLOOSTER, A., DE MAEYER, P. & FACK, V. On the way of integrating evacuation approaches. 5th International Conference on 3D Geoinformation (3D GeoInfo Conference), 2010. International Society for Photogrammetry and Remote Sensing (ISPRS). Commission IV. Working Group 8, 169-172.

VARSHAVSKY, A., LAMARCA, A., HIGHTOWER, J. & DE LARA, E. The skyloc floor localization system. Fifth Annual IEEE International Conference on Pervasive Computing and Communications (PerCom), 2007. IEEE, 125-134.

VERMUYTEN, H., BELI N, J., DE BOECK, L., RENIERS, G. & WAUTERS, T. 2016. A review of optimisation models for pedestrian evacuation and design problems. *Safety Science,* 87, 167-178.

VU, A., RAMANANDAN, A., CHEN, A., FARRELL, J. A. & BARTH, M. 2012. Real-time computer vision/DGPS-aided inertial navigation system for lane-level vehicle navigation. *IEEE Transactions on Intelligent Transportation Systems,* 13, 899-913.

WAGNER, N. & AGRAWAL, V. 2014. An agent-based simulation system for concert venue crowd evacuation modeling in the presence of a fire disaster. *Expert Systems with Applications,* 41, 2807-2815.

WANG, H., LENZ, H., SZABO, A., HANEBECK, U. D. & BAMBERGER, J. Fusion of barometric sensors, wlan signals and building information for 3D indoor/campus localization. Proceedings of International Conference on

Multisensor Fusion and Integration for Intelligent Systems (MFI), 2006. 426-432.

WANG, H., SEN, S., ELGOHARY, A., FARID, M., YOUSSEF, M. & CHOUDHURY, R. R. No need to war-drive: Unsupervised indoor localization. Proceedings of the 10th International Cconference on Mobile Systems, Applications, and Services, 2012. ACM, 197-210.

WANG, S.-H., WANG, W.-C., WANG, K.-C. & SHIH, S.-Y. 2015. Applying building information modeling to support fire safety management. *Automation in Construction,* 59**,** 158-167.

WANG, X. & WANG, S. 2007. Collaborative signal processing for target tracking in distributed wireless sensor networks. *Journal of Parallel and Distributed Computing,* 67**,** 501-515.

WEINBERG, H. 2002. Using the ADXL202 in pedometer and personal navigation applications. *Analog Devices AN-602 Application Note,* 2**,** 1-6.

WOODMAN, O. J. 2007. *An introduction to inertial navigation.* PhD Thesis, Computer Laboratory, University of Cambridge.

WU, C., YANG, Z., LIU, Y. & XI, W. 2013. WILL: Wireless indoor localization without site survey. *IEEE Transactions on Parallel and Distributed Systems,* 24**,** 839-848.

XI, H., LEE, S. & SON, Y.-J. An integrated pedestrian behavior model based on extended decision field theory and social force model. Human-in-the-Loop Simulations, 2011. Springer, 69-95.

XIA, H., WANG, X., QIAO, Y., JIAN, J. & CHANG, Y. 2015. Using multiple barometers to detect the floor location of smart phones with built-in barometric sensors for indoor positioning. *Sensors,* 15**,** 7857-7877.

XIN, J. & HUANG, C. 2013. Fire risk analysis of residential buildings based on scenario clusters and its application in fire risk management. *Fire Safety Journal,* 62**,** 72-78.

XIONG, L., BRUCK, D. & BALL, M. 2014. Utilization of the Haddon Matrix to organize factors of survived accidental residential fires: frequencies for human, agent, and environment-related variables. *Fire Safety Science,* 11**,** 1049-1062.

YAMAMOTO, F. Investigation of an agent-based modeling on crowd evacuation and its application to real buildings. International Conference on Digital

Human Modeling and Applications in Health, Safety, Ergonomics and Risk Management, 2013. Springer, 373-382.

YAN, J., HE, G., BASIRI, A. & HANCOCK, C. Indoor pedestrian dead reckoning calibration by visual tracking and map information. Ubiquitous Positioning, Indoor Navigation and Location-Based Services (UPINLBS), 2018a. IEEE, 40-49.

YAN, J., HE, G., BASIRI, A. & HANCOCK, C. Vision-aided indoor pedestrian dead reckoning. 2018 IEEE International Instrumentation & Measurement Technology Conference, 2018b Houston, USA. IEEE, 1-6.

YAN, J., HE, G., BASIRI, A. & HANCOCK, C. 2019. 3D Passive-Vision-Aided Pedestrian Dead Reckoning for Indoor Positioning. *IEEE Transactions on Instrumentation and Measurement*, 1370-1386.

YAN, J., HE, G. & HANCOCK, C. Low-cost vision-based positioning system. Adjunct Proceedings of the 14th International Conference on Location Based Services, 2018c. ETH Zurich, 44-49.

YAN, J., LING, Q., ZHANG, Y., LI, F. & ZHAO, F. A novel occlusion-adaptive multi-object tracking method for road surveillance applications. 2013 32nd Chinese Control Conference (CCC), 2013. IEEE, 3547-3551.

YANG, Y., HANCOCK, C., KAPOGIANNIS, G., JIN, R., DE LIGT, H., YAN, J., CHEN, C. & LI, C. Integrating Indoor Positioning Techniques with Mobile Laser Scanner to Create Indoor Laser Scanning Models. FIG Congress, 2019. Hanoi, Vietnam.

YANG, J. Toward physical activity diary: motion recognition using simple acceleration features with mobile phones. Proceedings of the 1st International Workshop on Interactive Multimedia for Consumer Electronics, 2009. ACM, 1-10.

YANG, P., LI, C. & CHEN, D. 2013. Fire emergency evacuation simulation based on integrated fire–evacuation model with discrete design method. *Advances in Engineering Software,* 65, 101-111.

YANG, Z., WU, C. & LIU, Y. Locating in fingerprint space: wireless indoor localization with little human intervention. Proceedings of the 18th Annual International Conference on Mobile Computing and Networking, 2012. ACM, 269-280.

YE, H., GU, T., TAO, X. & LU, J. B-Loc: Scalable floor localization using barometer on smartphone. 2014 IEEE 11th International Conference on Mobile Ad Hoc and Sensor Systems (MASS), 2014. IEEE, 127-135.

YE, H., GU, T., TAO, X. & LU, J. 2016. Scalable floor localization using barometer on smartphone. *Wireless Communications and Mobile Computing,* 16**,** 2557-2571.

YE, H., GU, T., ZHU, X., XU, J., TAO, X., LU, J. & JIN, N. FTrack: Infrastructure-free floor localization via mobile phone sensing. 2012 IEEE International Conference on Pervasive Computing and Communications (PerCom), 2012. IEEE, 2-10.

YUAN, B. H., ZHANG, D. X., FU, K. & ZHANG, L. J. 2013. Video tracking of human with occlusion based on Meanshift and Kalman filter. *Applied Mechanics and Materials*, 3672-3677.

YUN, H., HAN, D. & LEE, C. C. 2013. Understanding the use of location-based service applications: do privacy concerns matter? *Journal of Electronic Commerce Research,* 14**,** 215.

YUN, X., CALUSDIAN, J., BACHMANN, E. R. & MCGHEE, R. B. 2012. Estimation of human foot motion during normal walking using inertial and magnetic sensor measurements. *IEEE Transactions on Instrumentation and Measurement,* 61**,** 2059-2072.

YUNG, D. & BENICHOU, N. 2003. Concepts of Fire Risk Assessment. *Report No. NRCC-46393.* Ottawa, ON: National Research Council Canada.

ZAMPELLA, F., JIM NEZ, A. R. & SECO, F. 2017. *LOPSI repository: GetSensorData application* [Online]. Available: http://lopsi.weebly.com/downloads.html.

ZEILER, M. D. & FERGUS, R. Visualizing and understanding convolutional networks. European Conference on Computer Vision, 2014. Springer, 818-833.

ZENG, Y., SONG, W., JIN, S., YE, R. & LIU, X. 2017. Experimental study on walking preference during high-rise stair evacuation under different ground illuminations. *Physica A: Statistical Mechanics and its Applications,* 479**,** 26-37.

ZHANG, H., SINDAGI, V. & PATEL, V. M. 2017. Joint transmission map estimation and dehazing using deep networks. *IEEE Transactions on Circuits and Systems for Video Technology*.

ZHANG, H., YUAN, W., SHEN, Q., LI, T. & CHANG, H. 2015. A handheld inertial pedestrian navigation system with accurate step modes and device poses recognition. *IEEE Sensors Journal,* 15**,** 1421-1429.

ZHANG, J. & ZHOU, P. Integrating low-resolution surveillance camera and smartphone inertial sensors for indoor positioning. 2018 IEEE/ION Position, Location and Navigation Symposium (PLANS), 2018. IEEE, 410-416.

ZHANG, J., ZHU, G., LI, H. & ZHANG, L. 2011a. The evaluation of personnel evacuate safely in commercial pedestrian street. *Procedia Engineering,* 11**,** 675-681.

ZHANG, M., HOL, J. D., SLOT, L. & LUINGE, H. Second order nonlinear uncertainty modeling in strapdown integration using MEMS IMUs. 2011 Proceedings of the 14th International Conference on Information Fusion (FUSION), 2011b. IEEE, 1-7.

ZHANG, M., VYDHYANATHAN, A., YOUNG, A. & LUINGE, H. Robust height tracking by proper accounting of nonlinearities in an integrated UWB/MEMS-based-IMU/baro system. 2012 IEEE/ION Position Location and Navigation Symposium (PLANS), 2012. IEEE, 414-421.

ZHANG, T., WANG, J., LIU, P. & HOU, J. 2006. Fall detection by embedding an accelerometer in cellphone and using KFD algorithm. *International Journal of Computer Science and Network Security,* 6**,** 277-284.

ZHAO, C., LO, S., LU, J. & FANG, Z. 2004. A simulation approach for ranking of fire safety attributes of existing buildings. *Fire Safety Journal,* 39**,** 557-579.

ZHENG, X., ZHONG, T. & LIU, M. 2009. Modeling crowd evacuation of a building based on seven methodological approaches. *Building and Environment,* 44**,** 437-445.

ZHOU, B., LI, Q., MAO, Q., TU, W. & ZHANG, X. 2015. Activity sequence-based indoor pedestrian localization using smartphones. *IEEE Transactions on Human-Machine Systems,* 45**,** 562-574.

ZHOU, S., CHEN, D., CAI, W., LUO, L., LOW, M. Y. H., TIAN, F., TAY, V. S.-H., ONG, D. W. S. & HAMILTON, B. D. 2010. Crowd modeling and simulation technologies. *ACM Transactions on Modeling and Computer Simulation (TOMACS),* 20**,** 20.

ZHOU, Y., ZLATANOVA, S., WANG, Z., ZHANG, Y. & LIU, L. 2016. Moving human path tracking based on video surveillance in 3D indoor scenarios. *ISPRS Annals of the Photogrammetry, Remote Sensing and Spatial Information Sciences,* 3**,** 97-101.

ZINTUS-ART, K., SAETIA, S., PONGPARNICH, V. & THIEMJARUS, S. 2011. Dogsperate Escape: A demonstration of real-time BSN-based game control with e-AR sensor. *Knowledge, Information, and Creativity Support Systems***,** 253-262.

ZLATANOVA, S. & HOLWEG, D. 3D Geo-information in emergency response: a framework. Proceedings of the Fourth International Symposium on Mobile Mapping Technology, Kunming, China, 2004. 29-31.

APPENDIX A: QUESTIONNAIRE OF INDOOR EVACUATION KNOWLEDGE AND BEHAVIOURS

This survey is a part of my PhD study of Indoor Guidance for Public Evacuation. It aims to test your knowledge and responses under certain situations of indoor evacuation. This survey only costs you 3 minutes to answer all the questions.

1. What is your gender? *

○Male

○Female

2. What is you approximate height? *

○≤160 cm

○160~165cm

○165cm~170cm

○170cm~175cm

○175cm~180cm

○≥180cm

3. What is your approximate weight? *

○≤50kg

○50~55kg

○55~60kg

○60~65kg

○65~70kg

○70~75kg

○75~80kg

○80~85kg

○85~90kg

○90~95kg

○95~100kg

○≥100kg

4. Are you familiar with all emergency exits in PMB building? Please mark out the degree from 0 (none) to 5 (very well known). *

○0 ○1 ○2 ○3 ○4 ○5

5. Are you aware of the risk places inside the PMB building (e.g. chemical labs, mechanical labs with high voltage electrical machines, biological labs, etc.). Please mark out the degree from 0 (none) to 5 (very well known). *

○0 ○1 ○2 ○3 ○4 ○5

6. Would you agree that the current indoor signs are clear and useful during your movement to the emergency exits? Please mark out the degree from 0 (none) to 5 (very clear). *

○0 ○1 ○2 ○3 ○4 ○5

7. When you hear a fire alarm, how long will it take you to respond (stand up and start moving outside)? Please select the top two choices. *

□Immediately

□Wait until it rings for the second round

□Wait until other people start to move

□Wait until being informed by security people/broadcast and move immediately

□Being informed by security people/broadcast and move after packing up your belongings

8. During your movement, there may be smog or smokes in the air, requiring you to walk in a bending pose. Will you feel it hard to walk in a bending pose than in upright pose? Please mark out the degree from 0 (none) to 5 (very hard).*

○0 ○1 ○2 ○3 ○4 ○5

9. When you have to walk in a bending pose during evacuation, will you feel a bit nervous/panic than walking in erected pose? Please mark out the degree from 0 (none) to 5 (definitely). *

○0 ○1 ○2 ○3 ○4 ○5

10. When you have to walk in a bending pose during evacuation, will you feel that you are moving more slowly than walking erectly? Please mark out the degree from 0 (strongly disagree) to 5 (strongly agree). *

○0 ○1 ○2 ○3 ○4 ○5

11. Under some extreme conditions, you have to bend and keep your head close to your pelvis. Which bending posture will you prefer? *

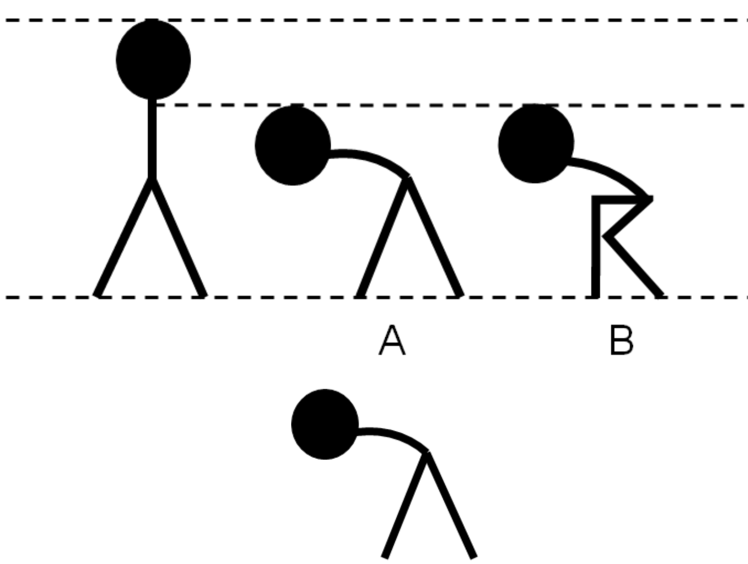

○A. Bending without knee flexion but more trunk flexion

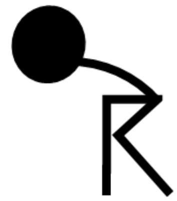

○B. Bending with knee flexion but less trunk flexion

12. Are you familiar with smartphone-based guidance? Please mark out the degree from 1 (least) to 5 (very well known). *

○1 ○2 ○3 ○4 ○5

13. If you have an app on smartphone which can help you move outside during evacuation, will you be happy to use it and follow its guidance? Please mark out the degree from 0 (none) to 5 (definitely). *

○0 (Go to 18) ○1 (→ 14) ○2 (→ 14) ○3 (→ 14) ○4 (→ 14) ○5 (→ 14)

14. When you find out the app not giving you the shortest way to move outside because the shortest way may be risky, will you still trust its guidance? *

○Yes

○No

15. For the last question, how long will it take you to make your decision under this evacuation condition? *

○Immediately

○Less than one minute

○More than one minute

16. During your movement to the outside following the mobile guidance, it suddenly asks you to change to another exit because the planned exit is blocked, will you still follow its guidance? *

○Yes

○No

17. For the last question, how long will it take you to make your decision under this evacuation condition? *

○Immediately

○Less than one minute

○More than one minute

18. If you are trapped in the indoor area during evacuation, can you still stay calm before the firefighters coming? *

○Yes (Jump to finish)

○No (Go to 19)

19. If you cannot stay calm when trapped, will the following information help you to calm down? Please mark the following choices from 0 (strongly disagree) to 5 (strongly agree). *

	0	1	2	3	4	5
Fire condition around your location	○	○	○	○	○	○
The total number of people trapped in the building	○	○	○	○	○	○
The distribution of all people trapped in the building	○	○	○	○	○	○
The distribution of people trapped in the surrounding environment	○	○	○	○	○	○
The total number of all firefighters in the building	○	○	○	○	○	○
The locations of all firefighters in building	○	○	○	○	○	○
The distance between you and nearest firefighters	○	○	○	○	○	○

20. Please rank the previous options from most important (1) to least important (7) *

[ ]Fire condition around your location

[ ]The total number of people trapped in the building

[ ]The distribution of all people trapped in the building

[ ]The distribution of people trapped in the surrounding environment

[ ]The total number of all firefighters in the building

[ ]The locations of all firefighters in building

[ ]The distance between you and nearest firefighters

END

APPENDIX B: 2D POSITIONING ACCURACY COMPARISON TO OTHER STUDIES USING MAGNETOMETER-BASED HEADING CALIBRATION

This study also compares its 2D positioning performance under the both conditions with and without severe occlusions to some other studies, who investigate alternative approaches to improve the performances of Dead Reckoning (DR) based Indoor Inertial Systems (Foxlin, 2005, Huang et al., 2010a, Zhang et al., 2015, Meng et al., 2014, Hsu et al., 2017, Fourati, 2015, Fang et al., 2005, Yun et al., 2012, Kothari et al., 2012). They use magnetometers for heading calibration instead of passive OPS. The majority of these studies apply self-developed hardware-suite without support from additional sensing system for precise positioning. Their preferred position for sensor wearing is on the foot, such as (Fourati, 2015, Hsu et al., 2017, Huang et al., 2010a, Meng et al., 2014, Yun et al., 2012, Foxlin, 2005). Their algorithms are mainly based on Zero-Velocity Updates (ZUPT), with data fusion and error control based on EKF (Foxlin, 2005, Hsu et al., 2017) or Complimentary Filter (CF) (Yun et al., 2012, Fourati, 2015). Some of the studies even integrate ZUPT and Step-and-Heading System (SHS) together for position estimation (Meng et al., 2014, Huang et al., 2010a). Others hold the device in hand (Kothari et al., 2012, Zhang et al., 2015) or put it on the waist (Fang et al., 2005). These studies apply SHS for position estimations, with either Peak-Detection-based (PDT) or Zero-Detection-based (ZDT) algorithm for step detection. Among these methods, the accuracy and experimental conditions of these studies are shown in Table B. As almost all path types in other studies are close-loops and their accuracies are evaluated as Start-to-End radial distance, <u>thus the positioning accuracy for this study is treated</u>

as the ratio between the largest error during estimation and total walking distance for reference. The distance error is also treated as the ratio between the overall length of the predicted distance and the ground truth, due to the different lengths of the designed paths. However, as the testing conditions and the application scenarios for these studies are not very similar as mentioned in this study, the comparison of their positioning accuracies may not be very convincible. This is partially due to that different environmental factors, such as the indoor structures and the design of the moving paths. Meanwhile, the constraints from the human aspects, such as the accuracy validation of their referential paths and the requirement of the positioning accuracy under certain scenarios, can also have affect the final achieved 2D positioning accuracy. Thus, the following comparisons are just showing rough idea about the potential superiority of the designed system proposed in this study.

When comparing the positioning accuracy, the performance of the system is superior than these relatively precise foot-mounted INS systems with commercial IMU sensors under limited-occlusion conditions, such as 0.3% in Foxlin (2005) and 0.4% in Fourati (2015). This makes this method very competitive in the future development. However, *when under the conditions of severe occlusions, its performance is not as good as these relatively precise foot-mounted INS systems, though they are still comparable.* This can be explained by the following reasons. First, this system is only calibrated in LoS areas while the accuracy listed in Table V is the overall performance of both the visible and the invisible areas. The positioning accuracy in the LoS areas is 0.06%, which is much better than that in previous studies (Fourati, 2015, Foxlin, 2005). The largest error actually appears in the invisible areas with frequent turnings, by only using smartphone-based PDR. This can be affected by the precision of applied hardware. The precision of the IMU sensors embedded in smartphones is not comparable to that of commercial foot-mounted sensors (Harle, 2013). Moreover, as this system is tested on an open-loop path when having severe occlusions, it cannot have reverse-calibration as testing on a close-loop path (Harle, 2013). Meanwhile, the foot-mounted systems have higher accuracy of step detection due to the position of sensor installation and the mechanism of ZUPT. However, this system has an advantage of higher accessibility as it only requires having a specific smartphone app for data collection and transfer, while the foot-mounted systems with comparable accuracies (Fourati, 2015, Foxlin, 2005) require the wearing of specific body-attached sensors, cables, or batteries. Meanwhile, considering the user experience, it can be hard to persuade the users to wear specific sensor suites on body as in (Fourati, 2015, Foxlin, 2005) while this system only requires current buildings to install a surveillance system. Although it also needs the potential costs of camera installation and calibration for the application, it may not be a problem as the installation of surveillance cameras is necessary not only for the tracking but also for the security purpose and the calibration is required only once. In addition, the surveillance system installation will be a ubiquitous requirement for the future buildings, which shows potential market for this system. Moreover, it shows a relatively higher accuracy of total distance estimation than the previous studies by using the camera calibration (0.1%). For processing algorithm, the computation cost for deep learning is higher than that for EKF, however, this will be compensated by its higher accuracy in the LoS areas (0.06%).

When compared to Zhang et al.'s study with better overall performance among SHS-based systems (Zhang et al., 2015), the system in this study has comparable performance on positioning accuracy. However, for the step detection, the accuracy of this system (98.4%) is slightly lower than that of (Zhang et al., 2015) (98.67%) when having vertical movements on the stairs. This may be also partially due to the hardware precision as mentioned above. Moreover, Zhang et al.'s study divides the steps modes into four classes by SVM classification and introduces a Band-Pass Filter (BPF) for step detection under different walking modes (Zhang et al., 2015). This may require more manual preparations before the test. However, this system does not have this process and just treats the whole process with one mixed class. Moreover, the difference between step-detection accuracies is not significant and the performance of this system is acceptable for positioning. Another advantage of this handheld system is the deployed sensor suite is already available in daily life and will be more easily accepted by users.

TABLE B

POSITIONING ACCURACY COMPARISON BETWEEN MAGNETOMETER-BASED STUDIES

Reference	Foxlin (2005)	Hsu et al. (2017)	Yun et al. (2012)	Fourati (2015)	Huang et al. (2010a)	Meng et al. (2014)	Fang et al. (2005)	Kothari et al. (2012)	Zhang et al. (2015)	This Study without Severe Occlusion	This Study with Severe Occlusion
Algorithm	ZUPT-EKF	ZUPT-EKF	ZUPT-CF	ZUPT-CF	ZUPT-SHS	ZUPT-SHS	SHS-PDT	SHS-ZDT	SHS-(BPF)PDT	SHS-ZDT	SHS-ZDT
PDR Data Collection Devices	Inertia-Cube3	Self-created prototype	MicroStrain 3DM-GX1	MTi & MTi-G	NanoIMU	ADIS16405	NavMote	Nexus S	Self-created prototype	Huawei Mate7/ iPhone7 Plus	Huawei Mate8/ iPhone7 Plus
Device Positions	On Foot	On Foot	On Foot	On Foot	On Foot	On Foot	On Waist	Hand-held	Handheld	Handheld	Handheld
Path Type	Close loop	Close loop	Close loop	Close loop	Close loop	Close loop	Close loop	Close loop	Close loop	Close loop	Open loop
Total Distance (m)	118.5	239.9	437.50	80	60	132	400	120	400	178.29	168.0
Positioning Accuracy (%)	0.3	2.01	1.0	0.4	2.0	3.26	3.0	4.2	1.8	0.07	0.6
2D Distance Error (%)	/	3.47	0.27	/	2.0	/	3.0	1.7-6.7	1.9	0.06	0.1
Data Transfer	Radio Frequency-Receiver	Bluetooth	Sony UXP- 180 Mini-computer	USB	Data Cable	Bluetooth	NetMote	USB	ARM Processor	WLAN	WLAN